



UNIVERSITÀ DEGLI STUDI DI VERONA

DIPARTIMENTO DI
BIOTECNOLOGIE

*SCUOLA DI DOTTORATO DI
SCIENZE NATURALI E INGEGNERISTICHE*

*DOTTORATO DI RICERCA IN
BIOTECNOLOGIE*

XXXI CICLO

Identification of key regulators for grapevine ripening by integrated genetic approaches

S.S.D. AGR/07

Coordinatore: Prof. Matteo Ballottari

Firma _____

Tutor: Prof.ssa Diana Bellin


Firma _____

Dottorando: Dott. Pietro Delfino

Firma _____

Quest'opera è stata rilasciata con licenza Creative Commons Attribuzione – non commerciale
Non opere derivate 3.0 Italia . Per leggere una copia della licenza visita il sito web:

<http://creativecommons.org/licenses/by-nc-nd/3.0/it/>

 **Attribuzione** Devi riconoscere una menzione di paternità adeguata, fornire un link alla licenza e indicare se sono state effettuate delle modifiche. Puoi fare ciò in qualsiasi maniera ragionevole possibile, ma non con modalità tali da suggerire che il licenziante avalli te o il tuo utilizzo del materiale.



NonCommerciale Non puoi usare il materiale per scopi commerciali.



Non opere derivate —Se remixi, trasformi il materiale o ti basi su di esso, non puoi distribuire il materiale così modificato.

Identification of key regulators for grapevine ripening by integrated genetic approaches

Pietro Delfino
Tesi di Dottorato
Verona, 17 Maggio 2019

**Identification of key
regulators for grapevine
ripening by integrated
genetic approaches**

Table of contents

Summary

Background

Vitis vinifera L.

The genome of Vitis vinifera

The reproductive developmental cycle of grapevine

Grapevine veraison

Impact of climate change on viticulture

Chapter 1

Integration of meta-QTL analysis and transcriptomic data identifies candidate genes controlling veraison time in grapevine

Chapter 2

Exploit the genetic diversity of a grapevine collection for genetic association studies

Conclusions

Acronyms

Appendix

Acknowledgments

Summary

Grapevine is one of the most economically relevant fruit crops in the world. In the past few years climate change and in particular global warming have started to significantly impact agriculture and viticulture as well. Indeed, higher temperatures occurring early during the growing season may advance the date of the phenological stages like bud burst, flowering and veraison. As a consequence, the shift in veraison to earlier dates causes ripening to occur under higher temperatures which impairs wine quality. It is of great interest for viticulture to investigate the timing of veraison and disentangle its genetic control. Genetic variation between cultivars leads to differences in the expression of phenotypic traits such as veraison time. A deeper knowledge of the genes involved in the phenology processes is critical to select varieties that are well adapted for current and future climatic conditions.

The aim of this thesis was to identify the most promising candidate genes for the regulation of the transition to grapevine berry ripening through complementary genetic study. The thesis is divided in two chapters: in the first chapter an approach based on the integration of data from QTL studies has been developed, in order to narrow down the number of candidate genes that may be related with berry ripening. Meta-QTL analysis integrated with transcriptomic data led to the identification of 61 candidate genes related to veraison, including well known transcription factors and genes related to carbohydrate metabolism.

In the second part, we have characterized a wide germplasm collection of different grapevine accessions (from CREA-VIT Conegliano collection) with the aim to identify the best panels of grapevine varieties, representing the most diverse genotypes and phenotypes for the traits of interest, to be exploited to test the genotype-phenotype association. The Conegliano collection has been previously phenotyped for flowering time and veraison time in the last 50 years; our work focused on the phenotypic data of the last 13 years (data kindly made available by our partners). These phenotypic data have been firstly used to assist the construction of a core collection, including the most genetic diverse accessions and individuals with contrasting phenotypes. Approximately 600 CREA-VIT accessions were previously genotyped (Cipriani et al., 2010) using 45 microsatellite markers. The

genotypic data have been used to assess the genetic diversity and population structure of the Conegliano collection. The end of the second part was dedicated to performing the association analysis itself with two different approaches, firstly using the GrapeReSeq 18K Vitis genotyping chip, then with an innovative approach called XP-GWAS (Yang et al., 2015) where pool of individuals displaying extreme phenotypes are whole-genome resequenced and allele frequencies compared to a random pool are screened for enrichment.

The findings of this study provide indications of the genetic factors controlling or influencing veraison time in grapevine. The elucidation of the genetic network underlying the beginning of the berry ripening phase is of fundamental importance for the need to breed new grapevine varieties adapted to changing climatic conditions.

Background

Vitis vinifera L.

Grapevine belongs to the family *Vitaceae*, a family of fourteen genera and about 910 known species (Christenhusz and Byng, 2016), covering mainly woody or herbaceous lianas (Mullins et al., 1992). *Vitis* is the most common genus of the family and contains 79 species. *Vitis* species are mainly spread in temperate zones of the Northern hemisphere and the same number of species is almost found between America and Asia. Only one *Vitis* species is native to Europe, *Vitis vinifera* L., which consists of two subspecies, *Vitis vinifera* L. subspecies *sylvestris*, the wild grapevine, and *Vitis vinifera* L. subspecies *vinifera*, the cultivated grapevine (Boss et al., 2003). The wild species *Vitis vinifera sylvestris* is the progenitor of the cultivated one, characterized by many large, sweet berries (Duchene, 2016). As a result, *Vitis vinifera vinifera* (*Vitis vinifera* from now on) is hermaphroditic while *Vitis vinifera sylvestris* is dioecious. Considering cultivation area (about 7.5 million ha in 2014) and economic value, grapevine is one of the major fruit crops of the world. The centre of domestication for grapevine is considered the near East between the Black Sea and Iran (Terral et al., 2010). From there, the first cultivated forms were diffused by humans probably throughout the middle and near East up to central Europe. To date, all the most known grapevine varieties, such as *Pinot*, *Cabernet Sauvignon* or *Sangiovese*, derives from *Vitis vinifera*. More than 74 million tons of grapes are produced annually, with the greatest portion in Europe. The usages of the grapes are various (fresh as table grapes, dried as raisins, juice, jelly, jam, ethanol, vinegar, grape seed oil, tartaric acid, and fertilizer), however, the most common product is wine (53% of the world's yield of grape). *Vitis vinifera* is hence one of the most important cultivated plants of the whole world.

The genome of *Vitis vinifera*

Vitis vinifera is a diploid plant with 38 chromosomes ($n = 19$). It has a genome size of approximately 475–500 Mb (Jaillon et al., 2007) and about 32,000 genes (Vitulo et al., 2014). Since fertilization is occurring mainly by means of wind and insect

pollination, all grapevine varieties are highly heterozygous. Inbreeding depression is also a particular feature of grapevine, with sterility occurring often from the first to third generation of selfing. A reference genome sequence is available since 2007 from Jaillon et al.; this sequence is derived from a cultivated clone of *Vitis vinifera* Pinot Noir (PN40024), which from recurrent selfings has reached about a 93% of homozygosity. The *Vitis* genome sequence was firstly created from a Sanger sequencing assembly at an average 8-fold coverage of the genome, later updated with a 12X assembly in 2010 when additional sequences were added to the pool (<http://www.genoscope.cns.fr/externe/GenomeBrowser/Vitis/>). The PN40024-12Xv0 assembly, available on the website of the international Grape Genome Browser Genoscope, was improved and updated to the 12Xv2 assembly by the French-Italian Public Consortium (Canaguier et al., 2017) but the sequences of contigs and scaffolds remained unchanged compared to version 12Xv0. Several different gene annotations derived from different gene predictions are available at present. One gene set derived from PN40024-12Xv0 is available since 2009 and can be found on the Genoscope website. The gene prediction 12Xv1 is the result of the union of v0 and a gene prediction performed at the Centro di Ricerca Interdipartimentale per le Biotecnologie Innovative (CRIBI) in Padova, Italy and is available on the CRIBI website (<http://genomes.cribi.unipd.it/grape/>). In 2014 an improved gene annotation, called v2 was established on the 12Xv0 assembly version at the CRIBI (Vitulo et al., 2014). Recently, with the advent of new sequencing technologies based on the so-called “long reads”, the area of the plant genomics has started to take advantage of these new approaches, and few grapevine genome announcements based on it have been made (Chin et al., 2016; Roach et al., 2018).

The reproductive developmental cycle of grapevine

Vitis vinifera is a polycarpic perennial plant that cycles between periods of flowering and vegetative growth. Its entire reproductive developmental cycle is completed over two consecutive growing seasons, separated by dormancy (Carmona et al., 2008). Both vegetative and reproductive tissues are formed simultaneously on the same shoot by the shoot apical meristem. During the spring

of the first season, lateral meristems, called uncommitted primordia, are formed within latent buds in the axis of grapevine leaves, and do not burst until the second year after formation. These will develop into inflorescence primordia, while other uncommitted primordia formed on rapidly growing shoots will develop into tendrils. Inflorescence primordia enter dormancy in autumn of the first year when day length decreases then stay dormant throughout winter (Fennell et al., 2015). Bud growth is halted during bud dormancy to better tolerate low temperatures and frost. The second season is initiated in spring with bud burst when environmental conditions become permissive. Shortly before and during bud burst, flower initials are formed and flower parts become distinct. The conversion from inflorescence primordia to inflorescences begins in the spring. Inflorescence formation is regulated at the level of formation of uncommitted primordia and at the level of differentiation. Flowering occurs around May - June in the Northern hemisphere, after which berry formation and berry ripening take place.

Grapevine veraison

Veraison is the phenological stage that marks the beginning of ripening of the grapes. Several events are initiated during this phase, for example the change in skin colour, berry softening, sugar accumulation, and organic acid decline (Coombe and Bishop, 1980; Uhlir and Clingeleffer, 1998). Grapevine berry ripening follows a biphasic growth, resembling a double sigmoid curve. In the first phase, fruit set is occurring, and little hard green berries develop to a medium size; then growth interrupts for a lag phase and starts again with a second stage of maturation where softening of the berries, sugar accumulation, acid decline and colour changes of the pericarp occur. During ripening, the berries develop the properties specific to the cultivar, and then complex physical and chemical processes take place gradually from veraison to physiological maturity. The polyphenolic compounds, in particular anthocyanins, are the group subject to the main changes during berry ripening; anthocyanins accumulate rapidly, while phenolic acids levels are lower than those of anthocyanins and show different alteration during ripening (Giovanelli and Brenna, 2007). Sugar and organic acid content also undergo significantly changes during berry ripening; while the concentration of glucose and

fructose increase rapidly, organic acids decline (Sadras and Mccarthy, 2007). Each of the compounds that is subject to variation during the ripening stage may differ among genotypes and may be different according to the stage of development of the berry. Veraison is usually evaluated by checking the berries for the beginning of softening or the start of anthocyanin pigmentation, the latter process that results more difficult for white-berried cultivars, that instead of depositing anthocyanins in the skin, lose chlorophyll and start to brighten. In the internationally recognized system of descriptors for grapevine phenotypic traits developed by OIV (Organisation Internationale de la Vigne et du Vin, OIV), veraison time is described by five classes 1, 3, 5, 7 and 9 (OIV descriptor 303), with class 1 representing cultivars displaying an early veraison time and class 9 represents the very late ones. Grapevine phenology stages are also defined with the BBCH code (Lorenz et al., 1994) (stage 81), or in the E-L System (Coombe, 1995) (stage 35). Veraison time is strictly correlated to the other phenological stages and is considered a predictor of maturity and harvest time (Sadras and Petrie, 2011). It may differ significantly between cultivars and has a strong genetic determination (from this thesis, broad sense heritability estimated is 0.424). Several QTL studies have identified unique and common genetic loci explaining variable portion of the phenotypic variance, for example on chromosome 16 (Costantini et al., 2008; Duchêne et al., 2012; Fischer et al., 2004; Zyprian et al., 2016). Grapevine breeders have recently started to apply marker-assisted selection, approach that will reveal helpful especially for phenotypic traits where manual evaluation is complex and automated scoring is still lacking, such as phenology traits. Genetic markers associated to veraison time would unveil useful tools for marker-assisted breeding of new cultivars adapted to climate change.

Impact of climate change on viticulture

It is a truth universally acknowledged that climate change is occurring and is shaping the future of agriculture. Viticulture is one of the niches of agriculture that is suffering the most, given the tremendous differences in terms of wine quality that can result from even light variations in terms of precipitations and temperature during a single season, especially in cool-climate viticulture (Vasconcelos et al.,

2009). In fact, with respect to the weather conditions, yield can vary up to 32.5% between seasons, which makes grapevine by far the crop with the highest seasonal variation in yield (Boss et al., 2003; Lebon et al., 2008). Yields and quality are not only affected by events mediated all over the season, but also by extreme and precise damages occurring during key phenological stages like budburst and flowering. The major and more evident effect of climate change is global warming, that is leading to a tendency to higher temperatures at earlier dates during the growing season. This obviously results in an advancement of bud burst, flowering and veraison stages. The predicted shift in veraison to earlier dates may cause ripening to occur under higher temperatures (Delrot et al., 2013), thus affecting grape composition and wine quality, in particular by impairing the accumulation of anthocyanins in the berries, a condition that is thought unfavourable for wine quality (Duchene, 2016). Moreover, with earlier ripening a compressed time window for many grapes is observed, leading to a compressed harvesting period. Stronger temperatures or frost damage can also affect the number of flowers and thus the number of berries per plant. Few studies have shown that the higher the temperatures around bud burst, the lower the number of flowers per inflorescence (Keller et al., 2010; Petrie and Clingeleffer, 2005). Furthermore, increased temperatures lead to longer drought periods and water stress which also poses a strain to viticulture; water deficit during floral initiation can lead to a decreased number of inflorescences and can have a negative influence on berry weight, especially when applied after veraison (Niculcea et al., 2014). On the other hand, cold, rain and frost conditions are other problems affecting berries development; in particular cold or rainy weather around flowering can reduce the number of grape clusters formed; frost conditions if occurring during late spring can cause significant crop loss when showing up after bud burst (Mosedale et al., 2015; Mullins et al., 1992).

Among all the possible options that we have to contrast the negative effects of climate change in viticulture, in this thesis we discuss the genetic approach; that is, the possibility of studying and understanding the genetic of the berry ripening process in order to exploit the source of natural variation coming from different grapevine varieties and breed new cultivars adapted to a changing climate.

Chapter 1

Integration of meta-QTL analysis and transcriptomic data identifies candidate genes controlling veraison time in grapevine

Abstract

High temperature impairs the quality of grapes and wines. Understanding the genetic control of grapevine phenology-related processes is crucial to successfully breed varieties more adapted to a changing climate. Veraison time, in particular, is a key factor for determining climatic conditions during ripening, in a sense that, depending on the period of the season when occurring, it will impact the time of the season when ripening time will occur. Quantitative trait loci (QTL) studies attempting to elucidate the genetic determinism of developmental stages in grapevine have identified genomic regions including large number of genes. Broad scale transcriptomic studies, by identifying sets of genes modulated along berry development and ripening, have also highlighted a huge number of putative candidates. With the final aim of providing a functional and integrated genomic overview for the genetic control of grapevine veraison time, and of prioritizing possible main genetic regulators, we have applied a meta-QTL analysis for grapevine phenology-related traits and checked for co-localization of transcriptional candidates. Twelve QTL studies were considered, including 174 QTLs related to phenology. By using the software BioMercator v4.2 a consensus genetic map including 3130 markers was compiled. QTLs were projected onto the consensus map and clustered into meta-QTLs. Anchoring to the grapevine genome assembly 12X.v2 allowed us to select positional candidates. We generated 17 meta-QTLs from 69 QTLs for the traits flowering, veraison and ripening among which 4 specifically related to veraison time. Moreover 11 meta-QTLs for genomic regions generically affecting phenology were revealed. This approach allowed reducing the number of positional candidates by almost 4-fold. Expression data generated by transcriptomic studies during berry development performed on several grape varieties were mined with different approaches to select, among positional candidates, genes significantly modulated at veraison time.

Introduction

High temperature impairs the quality of grapes and wines. Understanding the genetic control of grapevine phenology-related processes is crucial to successfully breed varieties more adapted to a changing climate. Veraison time, in particular, is a key factor for determining climatic conditions during ripening. Understanding the genetic control of phenological developmental stages (i.e. flowering, veraison, ripening, etc) would be helpful for the adaptation of local varieties to changing climate. In particular, delaying berry veraison and ripening is a desirable breeding target, since ripening occurring under very hot summer strongly affect and uncouple berry quality traits. By applying QTL analysis, segments of the genome carrying with higher probability genes involved in the traits of interest, and thus with a potential for breeding applications, can be identified. QTL studies allow to define the genetic control of phenotypic traits dissecting the phenotypic variation and determining the contribution of each QTLs. QTLs studies in grapevine have focused on different phenotypic traits. Quantitative trait loci (QTL) studies attempting to elucidate the genetic determinism of developmental stages in grapevine have identified genomic regions including large number of genes. According to these QTL studies, a complex inheritance would control phenology traits, with low contributions scarcely reproducible among studies, even though few reproducible contributions were found. An interesting opportunity to rationalize and interpret the plethora of QTL information, especially to the aim of providing relevant trait candidates, comes from QTL meta-analysis (Goffinet and Gerber, 2000; Veyrieras et al., 2007) a statistical framework to project QTLs on a consensus map which allows to identify and mine co-localizing QTLs among independent experiments. Indeed, QTLs detected independently and located in a given region of a chromosome could possibly represent several estimations of the position of one single QTL. This hypothesis can be tested by appropriate statistical tools which indicate the most likely number of ‘real’ QTLs underlying a pool of QTLs from independent experiments, providing alongside consensus positions for these narrowing down the QTLs confidence intervals. The resulting meta-QTLs are expected to better define the boundaries of the causative genomic intervals by integrating information from different studies. QTL meta-analyses have become

popular in literature where they are used both to summarize QTL information about one trait as well as to locally verify the co-location of QTLs between different populations as a first step towards QTL validation and/or prioritization of candidates. Chardon et al. (Chardon et al., 2004) first applied this approach to study flowering time in maize by summarizing several QTLs from different mapping populations into meta-QTLs. Subsequent positional cloning and association mapping analysis found in meta-QTL intervals two genes effectively involved in modulating flowering time (Ananiev et al., 2007; Salvi et al., 2011). These successful examples confirmed meta-analysis as very useful method for predicting candidate genes and for developing molecular markers for breeding. Lately, meta-analysis has been successfully used in studying QTL in different species like rice (Khowaja et al., 2009), cotton (Said et al., 2015), potato (Danan et al., 2011) and many others. So far, this approach has not been applied in grapevine.

Given this, it must be also noted that the meta-analysis of QTLs is a methodology that does not necessarily imply causation; that is, a newly defined meta-QTL may arise from different original input QTLs that share a common genetic determinant, but may also arise from a simple “physical” co-localization or proximity. Especially in not so dense genetic maps, QTL often spans several cM, resulting in easy overlapping of QTLs that do not have a real biological common meaning. Also when different “rounds” of meta-analysis are conducted with QTLs identified from different phenotypic traits (Danan et al., 2011), the risk of obtaining meta-QTLs that do not share the same genetic background is higher. Indeed, QTL co-localization can be due to tight-linkage of QTL/genes playing different functions, but could also arise from pleiotropy; when pleiotropy is likely, it would also justify meta-analysis across traits, to further reduce the number of candidates. Such a risk of “fake” co-localization may be contained if input QTLs are manually selected and curated, and maybe also if genes contained in the original QTLs intervals are screened in advance and checked for congruence. A great advancement in the meta-QTL analysis would also come from the integration of original genotypic data instead of genetic maps markers’ distance and name; operation that is limited by the lack of resources and standards to deposit original genotyping data. Indeed, by using original data to create consensus map, this will reflect more precisely the real

position and distance of the different markers, then the QTLs projection would be more accurate, avoiding false overlappings and moreover the information of the alleles of the parents would be available thus making it fundamental in the view of selecting the favourable allele for new breeding programs.

Transcriptomic experiments in grapevine identified a number of genes as candidates for phenology in particular for the transition from immature to mature stage, the so-called veraison (Fasoli et al., 2012; Massonnet et al., 2017; Palumbo et al., 2014). The number of this transcriptomic candidates and QTL positional candidates is very large. To prioritize candidate genes it would be useful to integrate meta-QTL results, in particular meta-QTL positional genes, with transcriptomic candidate genes to identify most important genes. Broad scale transcriptomic studies, by identifying sets of genes modulated along berry development and ripening, have also highlighted a huge number of putative candidates. With the final aim of providing a functional and integrated genomic overview for the genetic control of grapevine veraison time, and of prioritizing possible main genetic regulators, we have applied a meta-QTL analysis for grapevine phenology-related traits and checked for co-localization of transcriptional candidates. We have created the first grapevine consensus map, performed the first meta-QTL analysis in grapevine, anchored the consensus map to the updated assembly of grapevine genome, integrated data from transcriptomic studies and prioritized candidate genes for veraison control in grapevine. In this study, we report a candidate-genes prioritization approach based on two steps: in the first step we perform a meta-analysis of QTLs associated to grapevine phenology; in the second step we integrate the information of grapevine phenology-related hub-genes pinpointed in transcriptomic studies with the results of the QTL meta-analysis, in order to identify genes to be considered as key regulators for the veraison stage of grapevine. The meta-QTL analysis was conducted creating the first grapevine genetic consensus map, integrating 39 different mapping populations. The consensus map was then anchored to the grapevine genome using 1055 markers. To our knowledge, this is the first meta-QTL analysis conducted in grapevine.

Methods

Grapevine consensus map construction

The process of consensus map creation started with the collection of individual genetic linkage maps with information on marker names and position in cM. To make it possible to combine the individual maps into a consensus map, marker names must be consistent. We manually checked and curated the name of the markers in order to correct misspellings and find synonyms. The files were input in BioMercator V4.2 (input files available upon request) and the linkage groups were oriented according to the reference map of Doligez (Doligez et al., 2006). Linkage groups that did not share at least two markers with the corresponding linkage groups of other maps were removed from the analysis, leading to a different number of input maps in the construction of the consensus linkage groups. The command InfoMap was used to evaluate markers order and consistency between each pair of input maps; in case of inversions in markers order between maps, the occurrence of the inverted markers in all the maps was evaluated and only the marker less represented across all the maps was removed. After all the inversions were corrected, the command ConsMap was used to construct the consensus map in a single step, without using any map as reference.

In silico mapping of GCM markers and anchoring to the grapevine genome

Sequences of the GCM markers were downloaded from the publications where they originally appeared and were blasted against the 12X.v2 assembly of the grapevine genome using the website <https://urgi.versailles.inra.fr/blast/>. An anchor map was thus created composed of the univocally mapping GCM markers and corresponding position in base pairs. The anchor map was uploaded to BioMercator and the option “New genome version” was used to anchor the GCM to the new structural annotation of the grapevine genome as a .gff3 file (<https://urgi.versailles.inra.fr/Species/Vitis/Annotations>). Physical positions of QTLs, meta-QTLs and candidate genes located in confidence intervals were then automatically calculated by BioMercator using an internal formula (Yannick De Oliveira, personal communication) and downloaded to be reported in the tables.

QTL projection and meta-analysis

Before performing the meta-analysis, specific information of QTL data were collected, in particular start and end position of the confidence interval and peak of the QTL, its associated variance explained value (R^2), and the size of the population that was used for mapping the QTL. These information were input in BioMercator and each QTL was associated to the genetic map where it was originally mapped. The command QTLProj was then applied in order to project the QTLs of the component maps to the consensus map; the command performs a homothetic projection of the original QTL to the consensus map only when flanking markers are found where the ratio of the distance of these markers to the confidence interval of the QTL that is being projected is not reduced by a factor greater than 0.25. In our case default options were kept. The meta-analysis itself was then executed; we used the Veyrieras algorithm (Veyrieras et al., 2007) which in BioMercator is divided in two steps, the QTLClust and MQTLView. The QTLClust performs the clustering of the input QTLs belonging to the same trait and finds the real number of meta-QTLs, calculating as many models as the number of the input QTLs and five different criterion values, AIC (Akaike information criterion), AICc, AIC3, BIC (Bayesian information criterion) and AWE (average weight of evidence), for each one of the models. The best model was then selected as the model minimizing the criterion value. The second step, MQTLView, was then used to graphically represent the meta-QTLs identified according to the selected model.

Transcriptomic data integration

RNA-Seq gene expression data (Fasoli et al., 2018) from 99 berry RNA samples from the cultivars Pinot Noir collected in triplicates in the years 2012, 2013 and 2014 around the time of veraison were analysed. To identify the most significant genes modulated across veraison, we developed a strategy that takes into account the entity of the modulation in the comparison of the time-point before veraison. We used a recently published dataset (Fasoli et al., 2018) reporting the results of the differential expression analysis between different time-points of the berry samples from the cultivars Pinot Noir and Cabernet Sauvignon, sampled in triplicated in the years 2012, 2013 and 2014. We selected the genes that, between

the time-point -T1 and veraison (T0), were significantly differentially expressed and displayed an absolute value of \log_2 of the fold change ($|\log_2FC|$) greater than all the other comparisons.

Results and discussion

Collection of grape QTLs studies for QTLs data integration

With the final aim of integrating available information about grapevine QTLs emerging from independent studies/populations, and especially QTLs related to veraison time control, literature was mined to identify all published grapevine QTL studies up to October 2018. Studies relying on genetic maps without enough shared markers with other maps (i.e. genetic maps including only AFLP or SNPs), or not providing information about genetic map version used as reference or all genetic information about detected QTLs, were not considered. This resulted in the selection of 42 publications, reporting 47 different QTL maps. A list of all these, including reference and information about the related genetic map, is provided in Table 1. These QTL studies exploited overall 24 different cross populations, constituted on average by 157 offsprings (number of offsprings ranging from 74 to 265). Cross population were mainly F1, with the only exception of two populations obtained by self-pollination and one obtained by selfing an F1 (Blasi et al., 2011; Duchêne et al., 2009; Fennell et al., 2019). Large number of cross populations (14) were derived by crossing *Vitis vinifera* with hybrids or other *Vitis* species, but a number of intra-*vinifera* cross was also represented. The selected QTL studies included 2093 QTLs for 354 different phenotypes scored. For each QTL study we focused on QTLs detected in the consensus map, when this was provided. QTLs mapped on parental maps were included only if genetic data for consensus maps were not available (see Table 1). All QTLs were considered, independently of their score thresholds, LOD/variance values or years of observation. A detailed list of all scored phenotypes, grouped for each study and including the QTL short name used in the relative reference as well as a short description, is provided as Table S1 (external file). More details about the phenotypic scoring for each QTL can be found in the original reference. Each measured phenotype/QTL was manually attributed to its most related trait, for which the score was considered to be a

descriptor, and traits were arbitrarily grouped in nine main trait categories. An overview about currently more characterized plant traits in grape, grouped according to the nine different trait categories, is given in Figure 1.

Table 1. List of QTL studies

<i>QTL study reference</i>	<i>Genetic map reference</i>	<i>Cross</i>	<i>Female Parent</i>	<i>Male Parent</i>	<i>Pop Type</i>	<i>Pop Size</i>	<i>QTL categories</i>	<i>Total number of used QTLs</i>
<i>Azuma et al. 2015</i>	<i>Ban et al. 2014</i>	line 693	626-84	Iku82	F1	74	berry metabolites	31
<i>Ban et al. 2014</i>	<i>Ban et al. 2014</i>	line 693	626-84	Iku82	F1	98	berry metabolites	10
<i>Ban et al. 2016</i>	<i>Ban et al. 2014</i>	line 693	626-84	Iku82	F1	98	berry morphology, phenology	24
<i>Bayo Canha, PhD thesis 2015</i>	<i>Bayo Canha, PhD thesis 2015</i>	MN x SY	Vv Monastrell	Vv Syrah	F1	229	phenology, berry morphology, cluster related traits, berry metabolites	40
<i>Bellin et al. 2009</i>	<i>Bellin et al. 2009 (parental maps)</i>	CH x BI	Vv Chardonnay	Bianca	F1	116	pathogen resistance	18
<i>Bert et al. 2013</i>	<i>Bert et al. 2013</i>	CS x RGM1995-1	Vv Cabernet Sauvignon	Vr Gloire de Montpellier	F1	138	vegetative traits, abiotic stress response	129
<i>Blasi et al. 2011</i>	<i>Blasi et al. 2011</i>	<i>V. amurensis</i> ‘Ruprecht’ S1	Va ‘Ruprecht’	Va ‘Ruprecht’	S1	232	pathogen resistance	8
<i>Cabezas et al. 2006</i>	<i>Cabezas et al. 2006</i>	D x AS	Vv Dominga	Vv Autumn Seedless	F1	118	berry morphology, seeds related traits	20
<i>Carreño Ruiz, PhD thesis 2012</i>	<i>Carreño Ruiz, PhD thesis 2012</i>	RS x M	Vv Ruby Seedless	Vv Moscatuel	F1	78	phenology, cluster related traits, berry morphology, berry metabolites, seeds related traits	72
<i>Correa et al. 2014</i>	<i>Correa et al. 2014</i>	RS x S	Vv Ruby Seedless	Vv Thompson Seedless	F1	137	cluster related traits	19
<i>Correa et al. 2015</i>	<i>Correa et al. 2015</i>	RS x S	Vv Ruby Seedless	Vv Thompson Seedless	F1	137	berry morphology, seeds related traits	40
<i>Correa et al. 2016</i>	<i>Correa et al. 2016</i>	RS x S	Vv Ruby Seedless	Vv Thompson Seedless	F1	137	berry morphology	6
<i>Costantini et al. 2008</i>	<i>Costantini et al. 2008</i>	I x BP	Vv Italia	Vv Big Perlon	F1	163	berry morphology, seeds related traits, phenology	25
<i>Costantini et al. 2015</i>	<i>Costantini et al. 2015</i>	SY x PN	Vv Syrah	Vv Pinot Noir	F1	170	berry metabolites	554
<i>CoupeL-Ledru et al. 2014</i>	<i>CoupeL-Ledru et al. 2014</i>	S x G (and reverse)	Vv Syrah	Vv Grenache	F1	186	vegetative traits, abiotic stress response	29
<i>CoupeL-Ledru et al. 2016</i>	<i>CoupeL-Ledru et al. 2014</i>	S x G (and reverse)	Vv Syrah	Vv Grenache	F1	186	vegetative traits, abiotic stress response	100
<i>Doligez et al. 2010</i>	<i>Doligez et al. 2010</i>	MTP3140	Vv MTP2223-27	Vv MTP2121-30	F1	139	cluster related traits	2
<i>Doligez et al. 2013</i>	<i>Doligez et al. 2010</i>	MTP3140	Vv MTP2223-27	Vv MTP2121-30	F1	139	berry morphology, seeds related traits	55
<i>Doligez et al. 2013</i>	<i>CoupeL-Ledru et al. 2014</i>	S x G (and reverse)	Vv Syrah	Vv Grenache	F1	191	berry morphology, seeds related traits	77
<i>Duchêne et al. 2009</i>	<i>Duchêne et al. 2009</i>	S1 MO	Vv Muscat Ottonel	Vv Muscat Ottonel	S1	121	berry metabolites	7
<i>Duchêne et al. 2012</i>	<i>Duchêne et al. 2012</i>	RI x GW	Vv Riesling	Vv Gewürztraminer	F1	188	phenology	22
<i>Fechter et al. 2014</i>	<i>Fechter et al. 2014</i>	V3125 x Börner	Vv V3125	Börner	F1	202	phenology	22
<i>Fechter et al. 2014</i>	<i>Zyprian et al. 2016</i>	Gf.Ga-47-42 x Villard blanc	Gf.Ga-47-42	Villard blanc	F1	151	phenology	9
<i>Garris et al. 2009</i>	<i>Garris et al. 2009</i>	<i>Vitis riparia</i> x <i>Vitis</i> hybrid Seyval	Vr PI 588289	Seyve Villard 5-276	F2	119	vegetative traits	17

<i>Grzeskowiak et al. 2013</i>	<i>Costantini et al. 2015</i>	SY x PN	Vv Syrah	Vv Pinot Noir	F1	170	phenology, cluster related traits	27
<i>Guo et al. 2015</i>	<i>Guo et al. 2015</i>	'87-1' x '9-22'	87-1	9-22	F1	149	berry metabolites	30
<i>Herzog et al., 2015</i>	<i>Zyprian et al. 2016</i>	Gf.Ga-47-42 x Villard blanc	Gf.Ga-47-42	Villard blanc	F1	151	pathogen resistance	1
<i>Huang et al. 2012</i>	<i>Huang et al. 2012</i>	S x G (and reverse)	Vv Syrah	Vv Grenache	F1	191	berry metabolites	114
<i>Huang et al. 2014</i>	<i>Huang et al. 2012</i>	S x G (and reverse)	Vv Syrah	Vv Grenache	F1	191	berry metabolites	29
<i>Malacarne et al. 2015</i>	<i>Costantini et al. 2015</i>	SY x PN	Vv Syrah	Vv Pinot Noir	F1	170	berry metabolites	200
<i>Marguerit et al. 2012</i>	<i>Marguerit et al. 2012</i> (parental maps)	CS x RGM1995-1	Vv Cabernet Sauvignon	Vr Gloire de Montpellier	F1	138	vegetative traits, abiotic stress response	22
<i>Mejía et al. 2007</i>	<i>Mejía et al. 2007</i>	RS x S	Vv Ruby Seedless	Vv Thompson Seedless	F1	144	berry morphology, phenology, seeds related traits	26
<i>Mejía et al. 2011</i>	<i>Mejía et al. 2011</i>	RS x S	Vv Ruby Seedless	Vv Thompson Seedless	F1	139	berry morphology, seeds related traits	6
<i>Moreira et al. 2011</i>	<i>Moreira et al. 2011</i>	VN x RP	Vv White Muscat	Vr Wr 63	F1	174	pathogen resistance	26
<i>Moreira et al. 2011</i>	<i>Moreira et al. 2011</i>	RT x AM	VRH3082 1-42	SK77 5/3	F1	94	pathogen resistance	6
<i>Ochssner et al. 2016</i>	<i>Ochssner et al. 2016</i>	V3125 x Börner	Vv V3125	Börner	F1	202	pathogen resistance	7
<i>Rex et al. 2014</i>	<i>Zhang et al. 2009</i>	V3125 x Börner	Vv V3125	Börner	F1	188	pathogen resistance	20
<i>Schwander et al. 2012</i>	<i>Schwander et al. 2012</i>	Gf.Ga-52-42 x Solaris	Gf.Ga-52-42	Solaris	F1	265	pathogen resistance	5
<i>VanHeerden et al. 2014</i>	<i>VanHeerden et al. 2014</i> (Regent parental map)	Regent x Red Globe	Regent	Vv Red Globe	F1	186	pathogen resistance	7
<i>Viana et al. 2013</i>	<i>Viana et al. 2013</i>	AT0023	D8909-15	Vv B90-116	F1	203	vegetative traits, phenology, cluster related traits, berry morphology, berry metabolites, seeds related traits	41
<i>Welter et al. 2007</i>	<i>Welter et al. 2007</i>	R x L	Regent	Vv Lemberger	F1	144	pathogen resistance	21
<i>Zhang et al. 2009</i>	<i>Zhang et al. 2009</i>	V3125 x Börner	Vv V3125	Börner	F1	188	pathogen resistance	2
<i>Zhao et al. 2015</i>	<i>Zhao et al. 2015</i>	'87-1' x '9-22'	87-1	9-22	F1	149	berry morphology, phenology, berry metabolites	5
<i>Zhao et al. 2016</i>	<i>Zhao et al. 2015</i>	'87-1' x '9-22'	87-1	9-22	F1	149	phenology	5
<i>Zyprian et al. 2016</i>	<i>Zyprian et al. 2016</i>	Gf.Ga-47-42 x Villard blanc	Gf.Ga-47-42	Villard blanc	F1	151	phenology, pathogen resistance	157

Number of QTLs for each trait as well as number of studies considering each trait are shown. The trait for which the highest number of QTLs is currently available in the literature is berry metabolites content. This is expected since high throughput metabolomic approaches can easily release large datasets. However, the overall most scored trait across independent studies was berry weight (scored in 12 independent studies), while categories most addressed by QTL studies so far have been phenology and pathogen resistance.

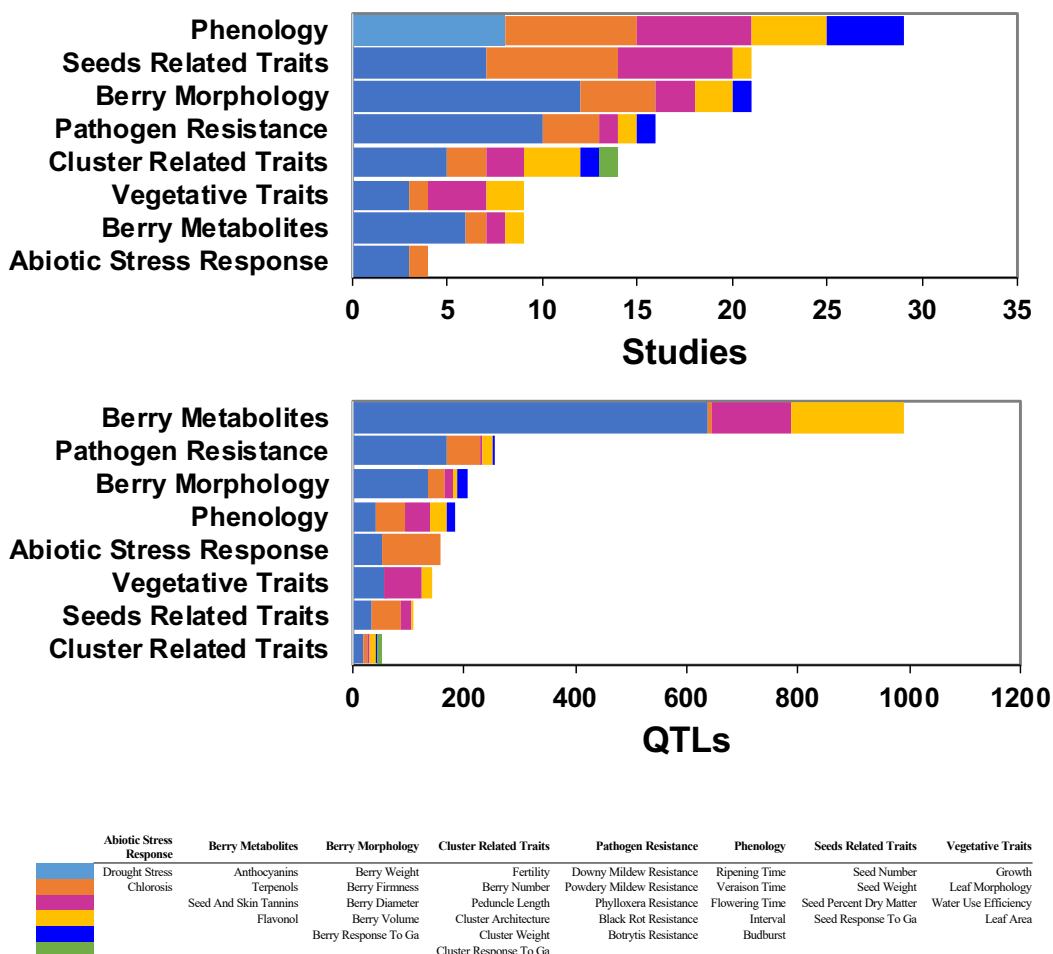


Figure 1. Summary of phenology QTL studies

Building a grapevine consensus genetic map

All the 35 reference genetic maps for the QTL studies were used as input for the construction of a consensus map in BioMercator 4.2 software (Sosnowski et al., 2012). Moreover a grapevine reference map, developed from the integration of 5 different genetic maps (Doligez et al., 2006), was also included, as well as few other available grapevine genetic maps (Costantini et al., 2008; Venuti et al., 2013). Common markers made it possible the construction of a consensus for each of the 19 grapevine chromosomes with no residual conflicts. The consensus map consisted of 19 linkage groups, corresponding to the 19 grapevine chromosomes, including 3130 markers with a total length of 1922 cM and an average number of markers and length per linkage group of 164 and 101 cM respectively. The number of markers shared by at least two maps was 1209, corresponding to 38.63% of the total markers, with an average of 63 shared markers per linkage group (Table 2). The full map file and a graphical overview are provided as Table S2 and Figure S1. The number of maps used for the construction of each linkage group varied from 26 (LG 11) to 39 (LGs 1, 2, 4, 5, 10, 12, 17, 18), due to the different number of markers shared among maps (Table 2, Table S3 [external file]).

Table 2. Consensus genetic map features

LG	N° of markers	N° unique markers	N° markers in at least two maps	Length (cM)	N° of individual maps integrated
I	214	130	84	95.68	39
II	130	71	59	89.73	39
III	135	92	43	92.03	37
IV	161	101	60	93.36	39
V	206	150	56	70.64	39
VI	139	93	46	90.72	38
VII	204	124	80	82.09	38
VIII	167	88	79	95.72	37
IX	128	77	51	85.01	35
X	168	93	75	141.87	39
XI	90	38	52	72.64	26
XII	211	153	58	143.13	39
XIII	156	89	67	113	37
XIV	202	118	84	94.79	37
XV	128	86	42	93.44	37
XVI	126	74	52	68.7	35
XVII	130	76	54	104.47	39
XVIII	275	172	103	148.93	39
XIX	160	96	64	146.03	37
Total	3130	1921	1209	1921.98	

Marker density was not equally distributed along the consensus, with peaks in putative centromeric positions similarly as found in original maps and in agreement with the expected suppression of recombination rate in such regions. However, comparison of markers order between the single component maps and the consensus map revealed a high level of correlation. Spearman's rank correlation values of pairwise comparisons were significantly high for all maps but two, possibly due to the low number of shared markers (Figure S2). The consensus genetic map was connected to the reference genome through the use of an anchor file. Markers physical position was recovered as explained in the methods section. Upon removal of markers showing incongruent or not unique physical position, 713 markers (on average of 38 markers per LG) were finally physically mapped on the 12X.v2 assembly of the grapevine genome (Canaguier et al., 2017). Their physical coordinates are also included in the map file Table S3. Among these markers, 480 (67%) were shared by at least two original maps, and the majority (513, 72%) were microsatellite markers.

Distribution of grapevine QTLs on the consensus genetic map

All QTLs from the 47 QTL studies (Table 1) were projected onto the consensus map to identify possible overlaps across populations. In total 1899 QTLs (91%) could be successfully plotted while 194 QTLs could not be projected to the consensus map due to the lack of anchoring markers. QTLs reduction was comparable across the different QTL categories, ranging from 87% of successfully plotted QTLs for berry metabolism to 98% for abiotic stress. Only for the trait category "cluster related trait" the number of plotted QTLs was lower (79%). Summary plots with distribution of projected QTLs for each trait category are provided as Figure 2. For each QTL consensus map, hotspots of overlapping QTLs across studies relying on independent populations have been highlighted. In summary we found independent overlapping QTLs for all the traits related to berry morphology (LG 1, 15, 18) and seeds related traits (LG 1, 10, 14 and 18), with only exception of traits measured in response to GA, for all vegetative traits (1, 4, 10, 13, 18) and for all phenology related traits (LG 1, 2, 3, 6, 7, 14, 16, 18) except bud burst. Moreover, we also found overlapping QTLs for anthocyanins (LG 2), and

downy (LG 1, 4, 5, 6, 7, 12, 17, 18) or powdery mildew resistance (LG 15). No overlapping QTLs were found instead for traits belonging to the category abiotic stress and for traits related to clusters.

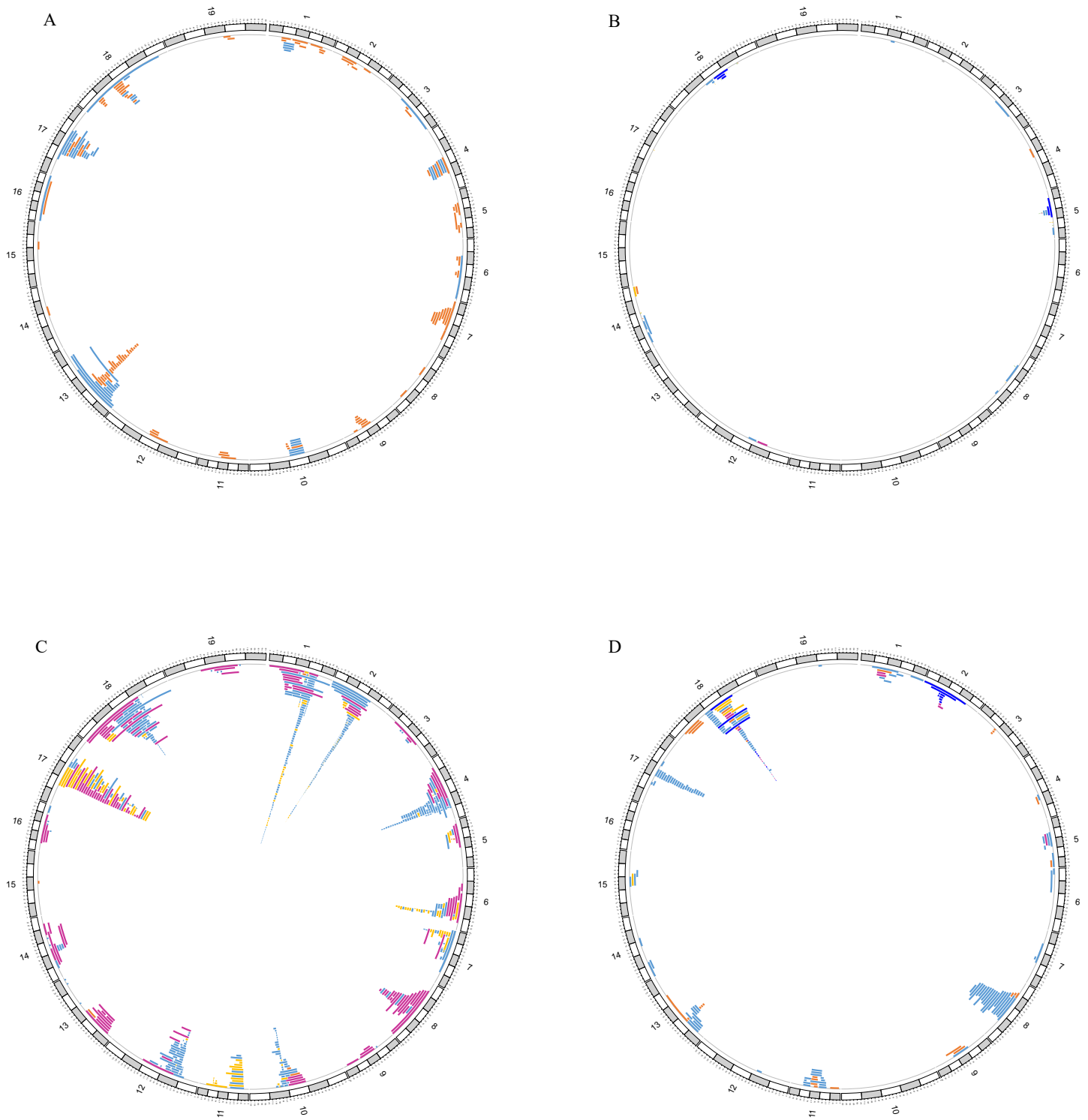


Figure 2. Summary graphic plots with distribution of projected QTLs for each trait category. Clockwise, from top left: abiotic stress response, cluster related traits, berry metabolites, berry morphology (Continue)

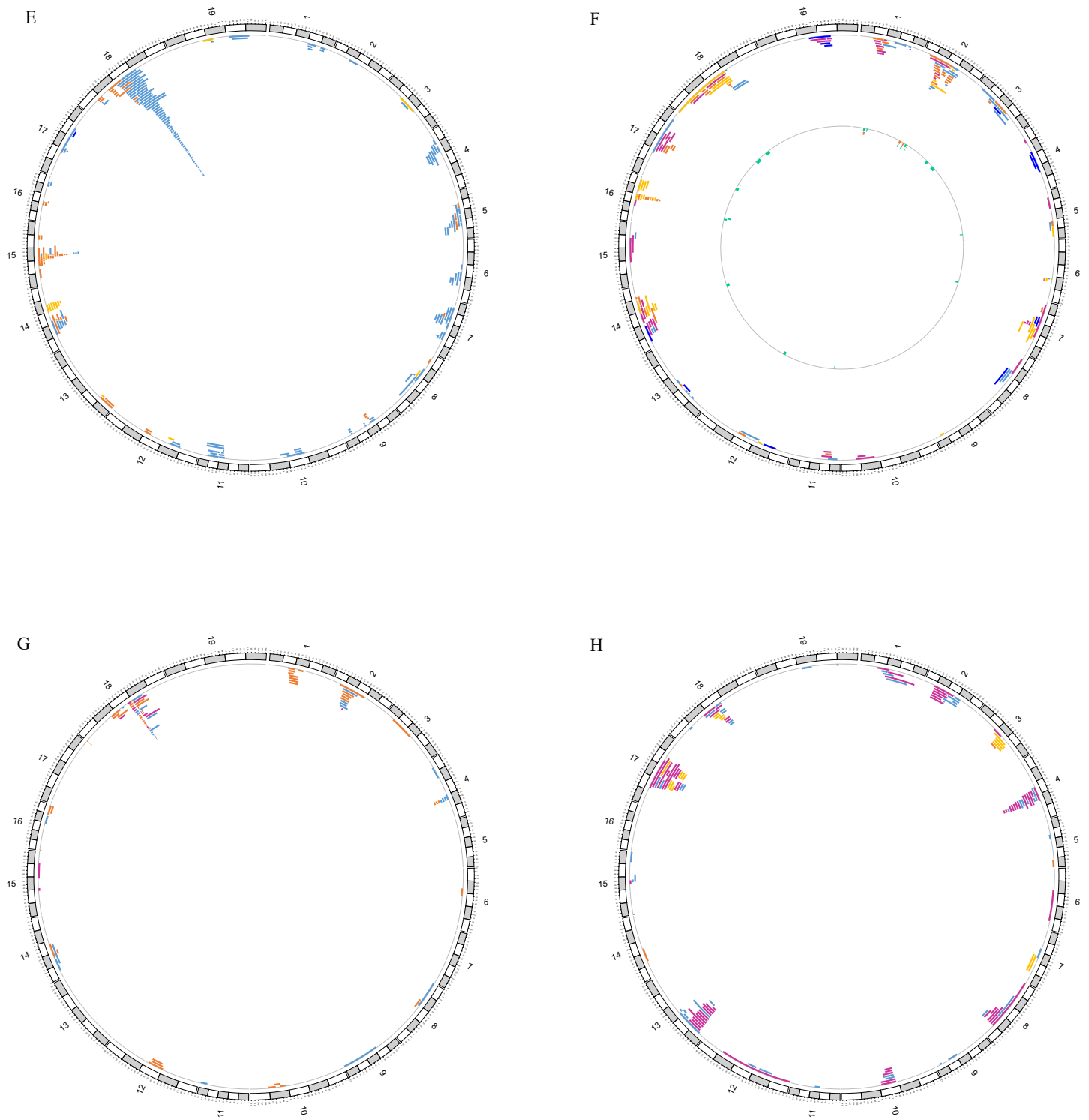


Figure 2. Continued. Summary graphic plots with distribution of projected QTLs for each trait category. Clockwise, from top left: pathogen resistance, phenology, including meta-QTLs on the inner circle, seed related traits, vegetative traits.

Interestingly, overlapping QTLs across different traits or categories possibly involved in the expression of more complex traits can also be scored in this dataset. As an example, overlapping QTLs from independent studies were found in LG 18 both for seed fresh weight and berry weight traits. Since berry weight is known to be also dependent on seed content (Doligez et al., 2013) these overlaps could hide a common genetic basis and could thus be exploited in a meta-analysis aiming to reduce, based on QTL co-locations, the number of underlying positional candidate genes. In the following we provide a detailed meta-analysis on phenology related traits aiming to identify candidate genes for veraison time.

Narrow down of candidates for veraison time by meta QTL-analyses

The list of phenology related QTLs projected onto the consensus map (141 QTLs from 13 studies) was manually curated for the purpose of performing a meta-analysis on overlapping QTLs from independent studies. Redundant QTLs, that is, QTLs with same peak position from the same study, which could overestimate the effect of that QTL in the analysis (Danan et al., 2011), were pruned as explained in the material and methods section. For the meta-analysis we considered 35 veraison related QTLs derived from six studies (Bayo Canha, 2016; Carreño Ruiz, 2012; Costantini et al., 2008; Emanuelli et al., 2013; Fechter et al., 2014; Zyprian et al., 2016). Meta-analysis was performed if at least two QTLs from independent experiments were overlapping. For veraison, overlapping QTLs from independent studies were found on LG1 and LG2 (from two studies and three studies respectively). The optimal number of meta-QTLs explaining overlapping QTLs was statistically determined by choosing the most likely model, as computed by BioMercator V4.2 software by five different tests. Our meta-analysis resulted in the identification of 4 veraison meta-QTLs located respectively on LG1 (one meta QTL) and on LG2 (three meta QTLs) (Table 3, Figure 2F). More in detail veraison meta-QTLs on LG2 resulted by integration of at least five original co-located QTLs, while *ver_1_1* on LG1 was derived from two original co-located QTLs. Average CI was 3.5 cM ranging from 1.2 cM for *ver_2_3* to 5.1 cM per *ver_2_1*, which was the largest one. On LG1 the original CI covered by QTLs was reduced from 23.9 cM to 4.3 cM (5.6 times) by the meta-analysis. On LG2 the reduction of CI by meta-

analysis was overall of five times, with a strongest effect on the *ver_2_3* meta QTL. R^2 values of meta QTLs were all higher than 10%. In particular *ver_2_2* was the most relevant, explaining up to 34% of total variance. A similar meta-QTL analysis was applied to overlapping QTLs for berry colour on LG2 to validate our procedure. Indeed, berry colour genetic control has been already elucidated and linked to a transposon insertion in the promoter region of the *MybA1* gene located on Chr 2 (Fournier-Level et al., 2009; Kobayashi et al., 2004; Walker et al., 2007). The meta-QTL analysis on 28 overlapping QTLs derived from five independent studies identified 7 meta-QTLs (Table S5). Interestingly the *MybA1* gene was included in the list of the 125 genes underlying these meta-QTLs (Table S6). Given such a high number and considering the high percentage of variance explained by many of these original QTLs, the meta-analysis resulted in a high number of very small meta-QTLs, which eventually can be considered as a single meta-QTL spanning a wider area. Here is a limitation of the meta-QTL approach when dealing with situations where the number of QTLs is high and the peaks of the original QTLs are very close to each other but not overlapping.

Inspection of the phenology QTL consensus map revealed extensive co-localization across traits for different developmental stages (i.e. co-location of veraison and ripening QTLs). Co-location of veraison QTLs with other phenology QTLs was indeed highly significant compared to a random distribution (χ^2 -test, $p < 0.01$). Overlapping phenology QTLs could represent several estimates of a single QTL affecting more developmental stages, which would justify the attempt to identify consensus QTLs across different phenology traits (Bancroft et al., 2009). In agreement with such option a meta-analysis for veraison QTLs including overlapping QTLs for other phenology traits on LG1 and LG2 identified meta-QTLs (pheno-QTLs) largely overlapping with previously reported meta-QTLs regions (Table S7). Therefore, with the final aim of reducing the number of candidate genes underlying veraison QTLs, we decided to apply also meta-analysis on veraison QTLs when overlapping QTLs from other phenological traits could be found in independent studies; then we have identified 13 further indicative meta-QTLs regions (pheno-QTLs) (Table 4, Figure 2H). Among these, two meta-QTLs on LG16 were particularly relevant, explaining on average up to 35% and 38% of

total phenotypic variance. In conclusion, the number of candidate genes underlying original veraison QTLs was narrowed down by applying meta-analysis of veraison QTLs, by a factor of 3.7. Meta-QTL analysis including alternative phenology related traits allowed also to reduce (2.2 times) the number of positional candidates (Figure 3), however this should be considered cautiously since relevant candidates might be skipped. Lists of candidate genes in veraison meta-QTLs and pheno meta-QTLs intervals, with the corresponding CRIBiv1 annotation (Vitulo et al., 2014), are given in Table S8 and Table S9 respectively.

Table 3. Results of the meta-QTL analysis on overlapping veraison QTLs. **LG** Linkage Group, **Meta-QTL** The name assigned to the meta-QTL identified, **Peak Position (cM)** Position in cM of the peak of the meta-QTL, **R²** Proportion of variance explained by the meta-QTL, **Start (cM)** Start position in cM of the meta-QTL, **End (cM)** End position in cM of the meta-QTL, **Start (bp)** Start position in bp of the meta-QTL, **End (bp)** End position in bp of the meta-QTL, **Meta-QTL Positional Candidates** The number of positional candidate genes within the meta-QTL interval, **Original QTLs co-located** The number of input QTLs that produced the meta-QTL, **QTL Studies (Populations)** The number of grapevine populations that produced the cross where QTLs were identified, **Traits** Phenotypic traits studied for the original QTL analysis, **Reference** Citation of the original publication where QTLs were originally reported.

LG	Meta-QTL	Peak Position (cM)	R ²	Start (cM)	End (cM)	Start (bp)	End (bp)	Meta-QTL Positional Candidates	Original QTLs co-located	QTL Studies (Populations)	Traits	Reference
I	ver_1_1	31.29	0.11	29.15	33.43	2510506	3254952	78	2	2	VT	Fechter et al 2014, Zyprian et al 2016
II	ver_2_1	31.34	0.17	28.79	33.89	4029921	5344816	147	7	2	VB, Vr	Bayo Canha 2015, Grzeskowiak et al 2013
	ver_2_2	41.55	0.13	40.00	43.30	5717649	7154894	96	5	3	Vr, VB, VE, VT	Costantini et al 2008, Bayo Canha 2015, Grzeskowiak et al 2013
	ver_2_3	53.47	0.34	52.88	54.07	13336750	16677137	94	5	3	Vr, VE, VP	Costantini et al 2008, Bayo Canha 2015, Grzeskowiak et al 2013

Table 4. Results of the meta-QTL analysis on veraison QTLs overlapping with other phenology QTLs. **LG** Linkage Group, **Meta-QTL** The name assigned to the meta-QTL identified, **Peak Position (cM)** Position in cM of the peak of the meta-QTL, **R²** Proportion of variance explained by the meta-QTL, **Start (cM)** Start position in cM of the meta-QTL, **End (cM)** End position in cM of the meta-QTL, **Start (bp)** Start position in bp of the meta-QTL, **End (bp)** End position in bp of the meta-QTL, **Meta-QTL Positional Candidates** The number of positional candidate genes within the meta-QTL interval, **Original QTLs co-located** The number of input QTLs that produced the meta-QTL, **QTL Studies (Populations)** The number of grapevine populations that produced the cross where QTLs were identified, **Traits** Phenotypic traits studied for the original QTL analysis, **Reference** Citation of the original publication where QTLs were originally reported.

LG	Meta-QTL	Peak Position (cM)	R ²	Start (cM)	End (cM)	Start (bp)	End (bp)	Meta-QTL Positional Candidates	Original QTLs co-located	QTL Studies (Populations)	Traits	Reference
III	<i>pheno_3_1</i>	27.67	0.15	24.43	30.92	560404	1647064	138	5	3	VT, SSC, Bpc	<i>Carreño Ruiz 2012, Viana et al 2013, Zhao et al 2015</i>
	<i>pheno_3_2</i>	50.42	0.14	45.30	55.54	5903464	10894193	288	4	3	VT, SSC, Bpc, BB	<i>Carreño Ruiz 2012, Viana et al 2013, Zhao et al 2015</i>
V	<i>pheno_5_1</i>	50.97	0.09	49.77	52.18	16799689	19536797	111	3	2	VT,F-V, Ma	Zyprian et al 2016, Bayo Canha 2015
VII	<i>pheno_7_1</i>	9.59	0.16	7.58	11.60	1087707	1552842	59	2	2	VT, Fw	<i>Carreño Ruiz 2012, Bayo Canha 2015</i>
XI	<i>pheno_11_1</i>	16.15	0.11	15.01	17.30	2934932	3356851	50	4	2	FBL, FS, Tar/Ma, VT	Bayo Canha 2015, Fechter et al 2014
XII	<i>pheno_12_1</i>	77.85	0.19	74.31	81.40	23793458	24155112	27	2	2	VT, RT	<i>Carreño Ruiz 2012, Zyprian et al 2016</i>
XIV	<i>pheno_14_1</i>	55.03	0.22	51.45	58.62	22441297	24645689	157	7	4	B-F, FS, FT, VT	<i>Carreño Ruiz 2012, Zyprian et al 2016, Fechter et al 2014, Duchêne et al 2012</i>

XVI	<i>pheno_16_1</i>	34.70	0.31	32.53	36.88	14012548	16583139	126	4	2	F-V, VT	<i>Costantini et al 2008, Zyprian et al 2016</i>
	<i>pheno_16_2</i>	38.49	0.38	36.49	40.50	16503904	17318604	51	5	2	F-V, VT	<i>Zyprian et al 2016, Duchêne et al 2012</i>
XVII	<i>pheno_17_1</i>	48.83	0.13	45.12	52.54	4969509	6401642	113	6	3	FBL, FS, RDA, VB	<i>Fechter et al 2014, Grzeskowiak et al 2013, Mejía et al 2007</i>
	<i>pheno_17_2</i>	61.83	0.11	61.46	62.20	8920888	9063993	12	7	4	FBL, FS, RDA, VB , F-V	<i>Fechter et al 2014, Grzeskowiak et al 2013, Mejía et al 2007, Zyprian et al 2016</i>
XVIII	<i>pheno_18_1</i>	34.68	0.17	28.21	41.15	1836848	5349350	322	2	2	VT , FT	<i>Carreño Ruiz 2012, Zyprian et al 2016</i>
	<i>pheno_18_2</i>	66.33	0.13	60.57	72.10	10927035	15526564	330	4	3	VT , FT, F-V	<i>Carreño Ruiz 2012, Zyprian et al 2016, Duchêne et al 2012</i>

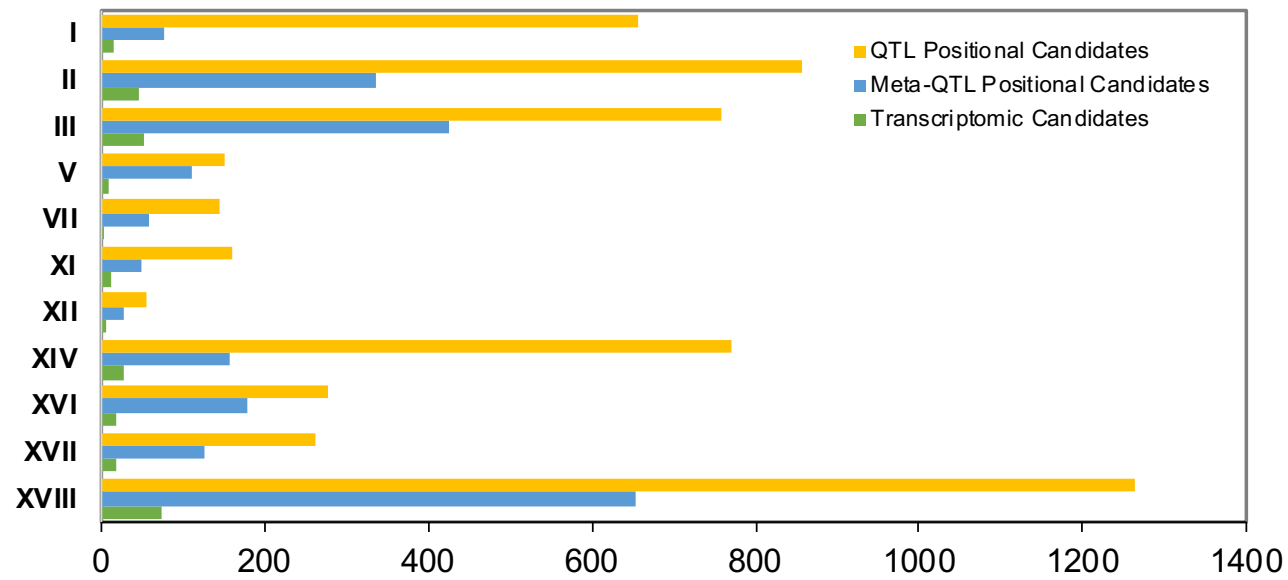


Figure 3. Bar plot showing for each linkage group where meta-QTLs were identified, the magnitude of positional and transcriptional candidate genes reduction in terms of the absolute number of candidate genes for each linkage group and each class.

Prioritization of candidates by transcriptomic data integration

Positional candidates underlying meta-QTLs were explored for their expression in different organs according to the grapevine expression atlas (Fasoli et al., 2012). Sixty-three genes among the positional candidates underlying veraison meta-QTLs (15.2% of the positional candidates) were never expressed either in berry, rachis or seed and were thus excluded from our candidate list. In a similar way 350 never expressed genes (19.6% of the positional candidates) were excluded from candidates underlying pheno meta-QTLs. Transcriptomic changes in berries along development and in particular across veraison have previously been widely explored, revealing that a massive transcriptomic change is associated to the veraison (Palumbo et al., 2014). More in detail, by comparing the expression profiles at four different berry developmental stages in 10 different grapevine varieties a first list of shared genes differentially expressed across veraison was found (Massonnet et al., 2017; Palumbo et al., 2014). Moreover, a recent RNA-Seq study has characterized weekly gene expression in Pinot Noir berries along development in the three years 2012, 2013 and 2014 (Fasoli et al., 2018). With the final aim of selecting genes putatively involved in veraison control based on their expression profile we decided to exploit such transcriptomic information. RNA-Seq data were inspected to spot in each year the expected massive transcriptional remodulation associated to the veraison transition (Table S10). The transition across which the highest number of genes was differentially expressed was considered as “molecular veraison”. Genes which were mainly modulated in their profiles across this transition in at least two of the three years have been selected also as transcriptional candidates. Altogether a list of 2850 transcriptomic candidates was selected, among which 494 have been previously suggested as veraison main regulators according to profile or network analyses (Palumbo et al., 2014). Under veraison meta-QTLs (Chr 1 and 2) we found 61 of these transcriptomic candidates. These represent the genes most likely involved in the veraison genetic control mapped at these locations (Table 5). Heatmaps showing their expression along berry development are shown (Figure 4). Moreover, 12 of these were among the genes proposed as main regulators of berry veraison transition. Among the most notable candidate genes, comprised in the *ver_2_1* and

ver_2_2 meta-QTL intervals, two pectin methylesterase inhibitor (PMEI) genes, previously reported to control pectin methylesterase activity in tomato (Di Matteo et al., 2005). Their function is supposedly to inhibit pectin methylesterase activity and then a premature berry softening related to pectin degradation (Lionetti et al., 2015). They may play a central role in the beginning of ripening by regulating some initial events at veraison, such as softening and loss of turgor (Gambetta et al., 2015). Another interesting candidate gene, again located within *ver_2_2* meta-QTL interval, is the NAC (VvNAC13) transcription factor. This gene is believed to play an important role in the transition from the immature to the mature stage of grapevine; its role in development has been demonstrated in various plant species including grapevine (Wang et al., 2013). NAC transcription factors have been shown to regulate vegetative and reproductive development in Arabidopsis (Raman et al., 2008), tomato (Hendelman et al., 2013) and papaya, suggesting a significant role as hub genes for fruit ripening. Finally, a cluster of Myb genes within *ver_2_3* meta-QTL interval, *MYBA1*, *MYBA2*, and *MYBA3*, support our approach; indeed, these genes have been previously extensively characterized for their role in the transition to berry ripening, by regulating the accumulation of anthocyanins in the berry skin (Kobayashi et al., 2004; Walker et al., 2007). Finally, a similar approach was also applied in order to try to prioritize genes located under veraison QTLs at other genetic locations. By applying the same strategy, the total number of original candidates underlying veraison QTLs was further reduced (8.2 times) allowing to build a priority list including 217 candidate genes (Figure 3, Table S11).

Table 5. Transcriptomic candidates underlying veraison meta QTLs. **Meta-QTL** The name assigned to the meta-QTL identified, **Gene ID** ID of the gene according to V1 annotation, **Chr** Chromosome, **Start (bp)** Start position in bp of the meta-QTL, **End (bp)** End position in bp of the meta-QTL, **Annotation_V1** Gene description according to V1 annotation, **Transcriptomic candidate** Citation of the original publication where transcriptomic data were taken to use for integration.

Meta-QTL	Gene ID	Chr	Start (bp)	End (bp)	Annotation_V1	Transcriptomic candidate
<i>ver_1_1</i>	VIT_01s0011g02840	1	2525946	2527902	Cytochrome B561	<i>Palumbo et al 2014, Massonet et al 2017</i>
	VIT_01s0011g02880	1	2546007	2547946	Cationic amino acid transporter 8	<i>Fasoli et al 2018</i>
	VIT_01s0011g02950	1	2618690	2632669	Zinc finger (C3HC4-type ring finger)	<i>Fasoli et al 2018</i>
	VIT_01s0011g03000	1	2688188	2688578	No hit	<i>Palumbo et al 2014, Massonet et al 2017</i>
	VIT_01s0011g03050	1	2717642	2719224	Unknown protein	<i>Palumbo et al 2014, Massonet et al 2017</i>
	VIT_01s0011g03070	1	2751566	2753036	ERF/AP2 Gene Family (VvRAV1)	<i>Palumbo et al 2014, Massonet et al 2017</i>
	VIT_01s0011g03180	1	2879352	2882108	Lysine and histidine specific transporter	<i>Palumbo et al 2014, Massonet et al 2017</i>
	VIT_01s0011g03210	1	2924829	2926924	Aspartic Protease (VvAP1)	<i>Palumbo et al 2014, Massonet et al 2017</i>
	VIT_01s0011g03360	1	3044557	3045849	Unknown	<i>Palumbo et al 2014, Massonet et al 2017, Fasoli et al 2018</i>
VIT_01s0011g03400	1	3076982	3080343	Proton-dependent oligopeptide transport (POT) family protein	<i>Palumbo et al 2014, Massonet et al 2017</i>	

	VIT_01s0011g03450	1	3127812	3132261	Alpha-glucosidase	<i>Palumbo et al 2014, Massonet et al 2017, Fasoli et al 2018</i>
	VIT_01s0011g03480	1	3147476	3149151	Cinnamoyl CoA reductase	<i>Fasoli et al 2018</i>
	VIT_01s0011g03520	1	3190826	3192777	Constans-like 16	<i>Palumbo et al 2014, Massonet et al 2017</i>
	VIT_01s0011g03550	1	3217781	3218222	Unknown	<i>Palumbo et al 2014, Massonet et al 2017</i>
	VIT_02s0025g04660	2	4037933	4039464	Senescence-inducible chloroplast stay-green protein 1	<i>Palumbo et al 2014, Massonet et al 2017, Fasoli et al 2018</i>
ver_2_1	VIT_02s0025g04730	2	4100066	4103095	Glyoxylate reductase	<i>Palumbo et al 2014, Massonet et al 2017</i>
	VIT_02s0025g04860	2	4193239	4194582	CYP76B1	<i>Fasoli et al 2018</i>
	VIT_02s0025g04880	2	4212083	4213721	Geraniol 10-hydroxylase	<i>Palumbo et al 2014, Massonet et al 2017</i>
	VIT_02s0025g04920	2	4236968	4238438	Phosphate translocator protein2, Plastidic	<i>Fasoli et al 2018</i>
	VIT_02s0025g05120	2	4410051	4413324	ACT domain-containing protein (ACR8)	<i>Fasoli et al 2018</i>
	VIT_00s2563g00010	2	4456792	4458501	Glycogenin glucosyltransferase	<i>Fasoli et al 2018</i>
	VIT_02s0241g00050	2	4516706	4519215	Unknown protein	<i>Palumbo et al 2014, Massonet et al 2017, Fasoli et al 2018</i>
	VIT_00s0323g00050	2	4703890	4704749	Invertase/pectin methylesterase inhibitor	<i>Fasoli et al 2018</i>
	VIT_00s0323g00070	2	4716445	4717351	Pectin methylesterase inhibitor	<i>Palumbo et al 2014, Massonet et al 2017, Fasoli et al 2018</i>
	VIT_02s0154g00070	2	4804832	4807460	Abnormal floral organs	<i>Palumbo et al 2014, Massonet et al 2017</i>

	VIT_02s0154g00080	2	4813347	4818031	Multi-copper oxidase (SKU5)	<i>Palumbo et al 2014, Massonet et al 2017</i>
	VIT_02s0154g00090	2	4824906	4827102	Vacuolar invertase 2, GIN2	<i>Palumbo et al 2014, Massonet et al 2017</i>
	VIT_02s0154g00260	2	5048952	5052974	Nitrate transporter	<i>Palumbo et al 2014, Massonet et al 2017</i>
	VIT_02s0154g00310	2	5077143	5078172	Protease inhibitor/seed storage/lipid transfer protein (LTP)	<i>Palumbo et al 2014, Massonet et al 2017</i>
	VIT_02s0154g00320	2	5084359	5085114	Protease inhibitor/seed storage/lipid transfer protein (LTP)	<i>Palumbo et al 2014, Massonet et al 2017, Fasoli et al 2018</i>
	VIT_02s0154g00500	2	5201356	5203907	VAP27-1 (VAMP/synaptobrevin-associated protein 27-1)	<i>Palumbo et al 2014, Massonet et al 2017</i>
	VIT_02s0154g00520	2	5216152	5221223	Aspartyl protease	<i>Palumbo et al 2014, Massonet et al 2017, Fasoli et al 2018</i>
	VIT_02s0154g00590	2	5308401	5308985	Unknown	<i>Palumbo et al 2014, Massonet et al 2017</i>
	VIT_00s1338g00020	2	5343106	5344525	Protein transport protein Sec61 subunit alpha	<i>Fasoli et al 2018</i>
ver_2_2	VIT_02s0012g00170	2	5916093	5918986	1,4-alpha-D-glucan maltohydrolase	<i>Palumbo et al 2014, Massonet et al 2017</i>
	VIT_02s0012g00310	2	6204735	6223899	Lon protease	<i>Fasoli et al 2018</i>
	VIT_02s0012g00400	2	6296189	6299377	1-aminocyclopropane-1-carboxylate oxidase	<i>Palumbo et al 2014, Massonet et al 2017</i>
	VIT_02s0012g00450	2	6323850	6325555	1-aminocyclopropane-1-carboxylate oxidase	<i>Palumbo et al 2014, Massonet et al 2017</i>

	VIT_02s0012g00500	2	6449814	6450360	Invertase/pectin methylesterase inhibitor	<i>Palumbo et al 2014, Massonet et al 2017, Fasoli et al 2018</i>
	VIT_02s0012g00550	2	6518911	6526733	Inositol polyphosphate 5-phosphatase II	<i>Palumbo et al 2014, Massonet et al 2017</i>
	VIT_02s0012g00570	2	6554241	6560259	Pseudo-response regulator 2 (APRR2) (TOC2)	<i>Palumbo et al 2014, Massonet et al 2017</i>
	VIT_02s0012g00590	2	6600611	6610281	Unknown protein	<i>Fasoli et al 2018</i>
	VIT_02s0012g00660	2	6660229	6660825	Calcium-binding EF-hand	<i>Palumbo et al 2014, Massonet et al 2017</i>
	VIT_02s0012g00990	2	7043508	7046965	LOL1 (LSD ONE like 1)	<i>Palumbo et al 2014, Massonet et al 2017</i>
	VIT_02s0012g01010	2	7087110	7089452	Leucine-rich repeat	<i>Fasoli et al 2018</i>
	VIT_02s0012g01040	2	7120118	7122681	NAC domain-containing protein (VvNAC13)	<i>Palumbo et al 2014, Massonet et al 2017, Fasoli et al 2018</i>
ver_2_3	VIT_02s0033g00030	2	13506518	13511727	No hit	<i>Fasoli et al 2018</i>
	VIT_02s0033g00180	2	13880089	13881941	Phenylpropanoid:glucosyltransferase 2	<i>Fasoli et al 2018</i>
	VIT_02s0033g00290	2	14139881	14141542	Pinoresinol-lariciresinol reductase	<i>Palumbo et al 2014, Massonet et al 2017</i>
	VIT_02s0033g00300	2	14144838	14148929	myb family	<i>Palumbo et al 2014, Massonet et al 2017</i>
	VIT_02s0033g00380	2	14291438	14291683	VvMybA2 (C-term)	<i>Palumbo et al 2014, Massonet et al 2017</i>
	VIT_02s0033g00390	2	14291727	14292732	VvMybA2	<i>Palumbo et al 2014, Massonet et al 2017</i>
	VIT_02s0033g00410	2	14351791	14352807	VvMybA1	<i>Palumbo et al 2014, Massonet et al 2017</i>

VIT_02s0033g00450	2	14420525	14421283	VvMybA3	<i>Palumbo et al 2014, Massonet et al 2017, Fasoli et al 2018</i>
VIT_02s0033g00700	2	15436012	15438008	Nitrilase	<i>Palumbo et al 2014, Massonet et al 2017</i>
VIT_02s0033g00800	2	15606321	15608743	Nitrilase 4 (NIT4)	<i>Palumbo et al 2014, Massonet et al 2017, Fasoli et al 2018</i>
VIT_02s0033g01000	2	16093114	16095441	Anthraniloyal-CoA: methanol anthraniloyal transferase	<i>Palumbo et al 2014, Massonet et al 2017</i>
VIT_02s0033g01020	2	16190948	16193334	Anthraniloyal-CoA: methanol anthraniloyal transferase	<i>Palumbo et al 2014, Massonet et al 2017</i>
VIT_02s0033g01030	2	16252684	16254941	Anthraniloyal-CoA: methanol anthraniloyal transferase	<i>Palumbo et al 2014, Massonet et al 2017</i>
VIT_02s0033g01050	2	16299329	16301080	Anthraniloyal-CoA: methanol anthraniloyal transferase	<i>Palumbo et al 2014, Massonet et al 2017</i>
VIT_02s0033g01120	2	16515095	16520470	Dehydration-responsive protein	<i>Fasoli et al 2018</i>

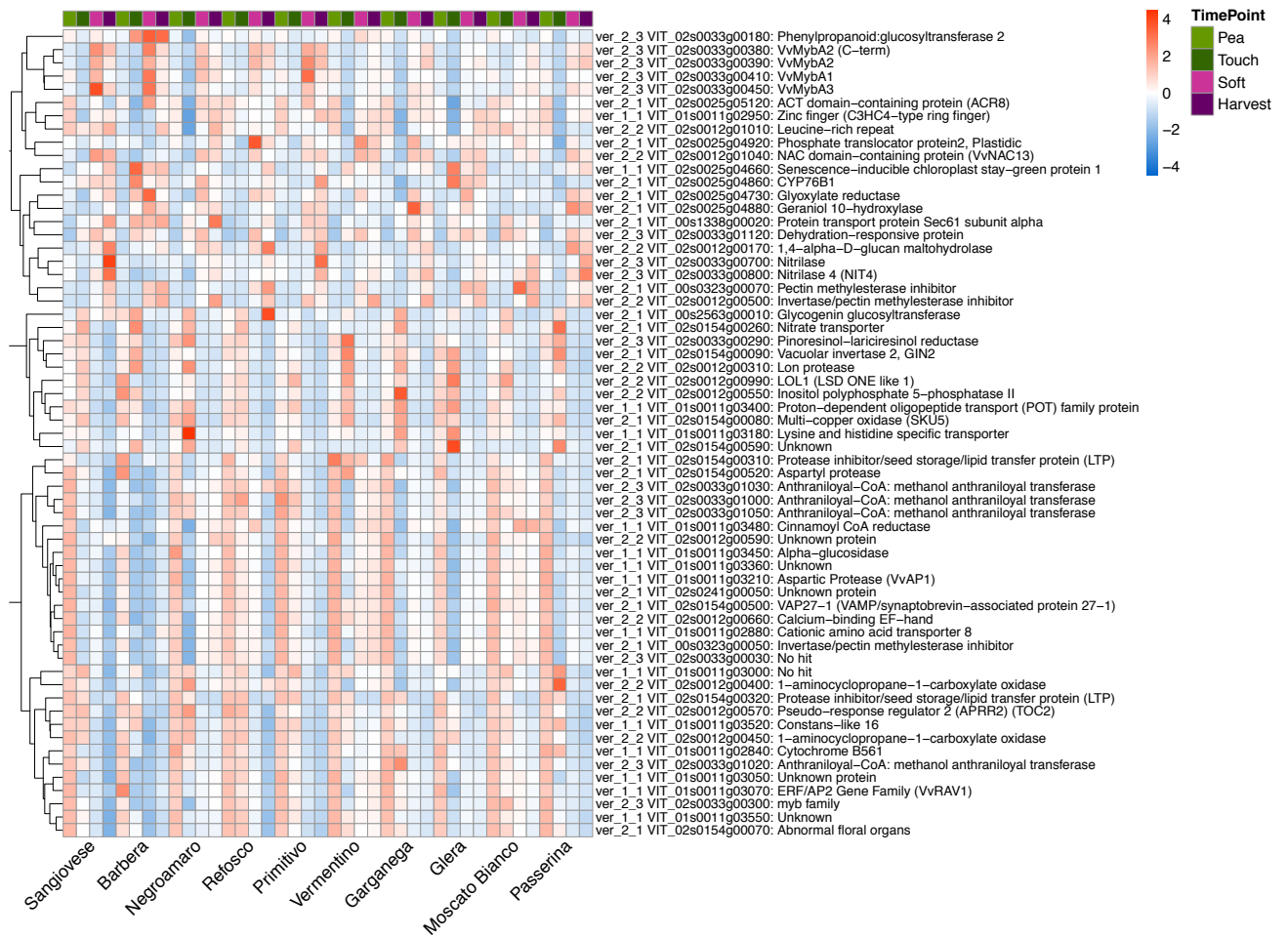


Figure 4. Heatmaps of gene expression levels of the transcriptomics candidates included in the veraison and phenology meta-QTLs from the RNA-Seq datasets of Massonnet 2017 and Palumbo 2014. In this panel the veraison transcriptomic candidates in the Massonnet dataset.

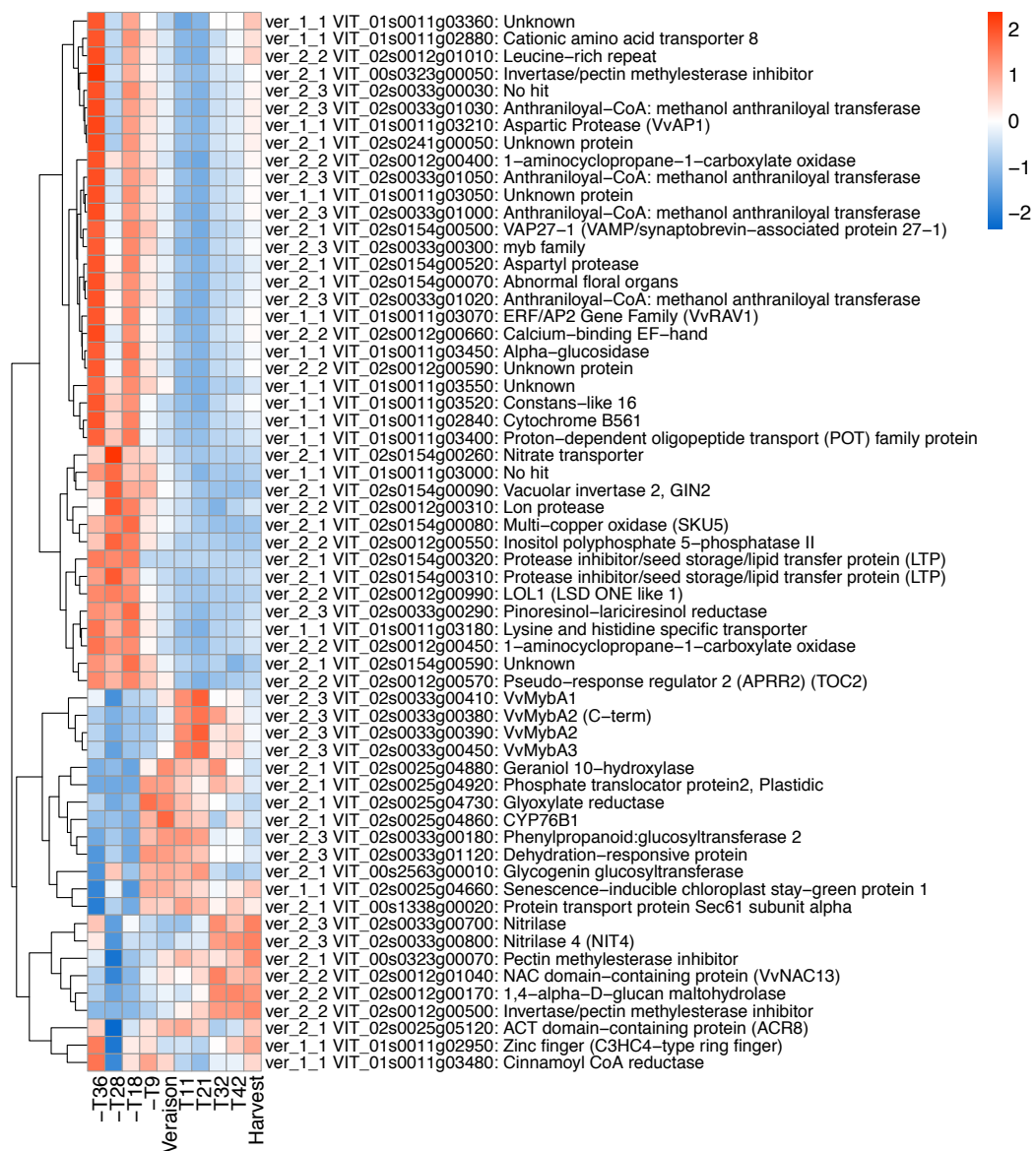


Figure 4. Continued. Heatmaps of gene expression levels of the transcriptomics candidates included in the veraison and phenology meta-QTLs from the RNA-Seq datasets of Massonnet 2017 and Palumbo 2014. In this panel the veraison transcriptomic candidates in the Palumbo dataset.

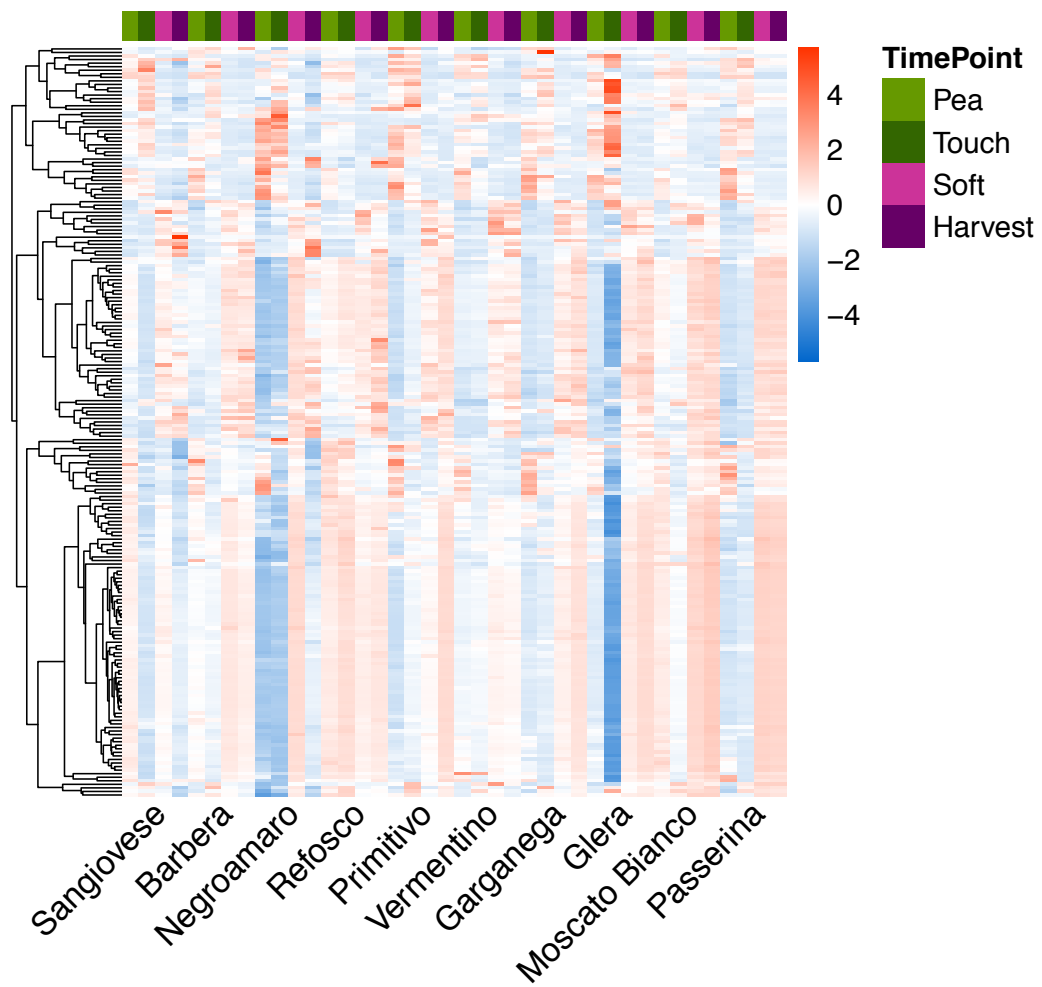


Figure 4. Heatmaps of gene expression levels of the transcriptomics candidates included in the veraison and phenology meta-QTLs from the RNA-Seq datasets of Massonnet 2017 and Palumbo 2014. In this panel the phenology transcriptomic candidates in the Massonnet dataset.

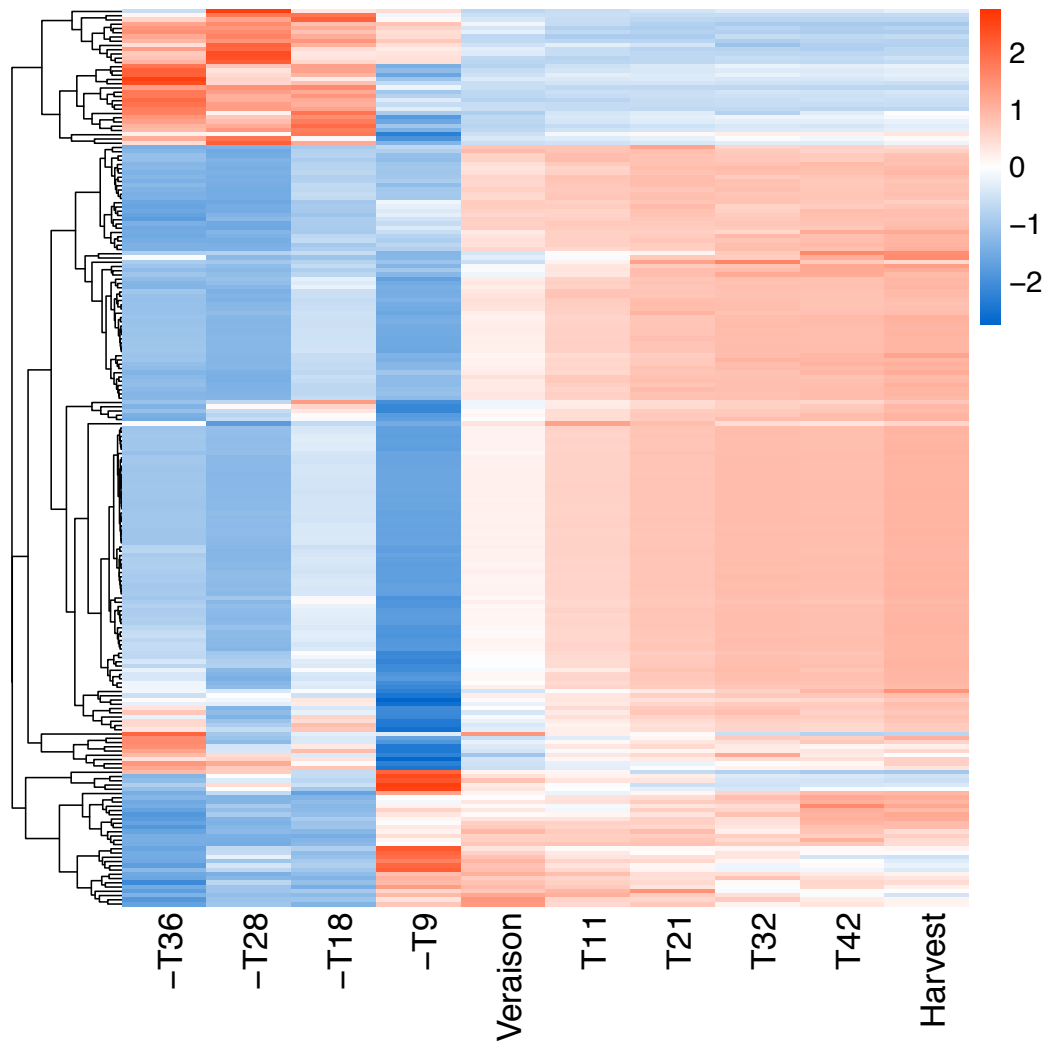


Figure 4. Heatmaps of gene expression levels of the transcriptomics candidates included in the veraison and phenology meta-QTLs from the RNA-Seq datasets of Massonnet 2017 and Palumbo 2014. In this panel the phenology transcriptomic candidates in the Palumbo dataset.

Discussion

A classical way to dissect the genetic determinism of grape phenology has been QTL studies. However, QTLs mapping often provides inconsistent results among studies, and huge genomic locations. A big advantage can derive from meta-analysis, which offers stronger evidence than individual studies, by revealing regions robustly associated with traits in multiple environments and genetic backgrounds. This approach has been already successfully exploited to improve and validate QTLs in several species, allowing insights into the genetic architecture of complex traits and paving the way for fine mapping and gene cloning. With this aim a genetic consensus map was built from 39 available SSR maps, including 3130 markers. By looking at marker distribution we observed they were not regularly spread along the chromosomes, but tended to concentrate in the middle regions, even though a good correlation was found with original maps. This is not surprising, reflecting a similar trend to original maps, due to suppression of recombination in centromeric regions. Other consensus maps already reported this drawback. Moreover, genetic positions of marker on the consensus arose from positions of shared markers according to the Biomecator software procedure, and were not based on recombination, since original genetic data are unfortunately not available from original maps. We fully agree that QTL meta-analysis would gain power and precision if raw genotypic and phenotypic data were made available. Recent advances in markers technology, with development of the NGS-based GBS technology in particular, have given a strong impulse to plant genotyping, and QTL studies now rely more on dense SNP maps. However, unshared markers do not allow for a direct genetic comparison of mapped QTLs, but require an indirect comparison through anchoring to the genome assembly. The distribution pattern of QTLs on chromosomes differs strongly between genetic and physical maps. Therefore, integration directly at genetic level could aid the improving of QTL location through co-location and meta-analysis, when feasible. Further comparisons can be then undertaken to newly generated QTLs relying on high throughput SNP maps, following anchoring to the genome assembly. Taking all this into account, we concluded that the consensus map we built constitutes a valuable reference, especially to the aim of integrating available genetic information, from

related QTL studies. Moreover, it will also provide a valuable instrument to enquire co-location with newly generated QTLs relying on dense SNP maps.

Taking advantage of this tool we have provided a compendium of all available QTL information that can be integrated at genetic level. Interestingly QTLs plotting revealed extensive co-locations across studies for each of the phenology related traits, besides downy mildew resistance, powdery mildew resistance, anthocyanin, drought stress, fertility, water use efficiency and growth, as well as for some berry and seeds related traits. However, studies addressing phenology are still few, negatively affecting the number of studies supporting each of the co-located QTLs. R^2 values of plotted QTLs, beside their distribution, suggest a highly polygenic nature for phenology related traits, with several QTLs involved, each of small effect, differently from other traits like pathogen resistance, seeds related traits and colour, all showing a more oligogenic architecture. More in detail, concerning veraison time four main regions located on LG1 and 2 have so far emerged consistently. Interestingly, plotting on a unique consensus map of QTLs also allows inspection of co-location across traits and categories, which is especially relevant for complex traits. In this way QTL meta-analysis also allows genetic correlation among traits to be investigated. In a previous work a second round meta-QTL analysis was proposed for seed yield QTLs and co-located yield associated QTLs in rapeseed, which allowed “indicator” meta-QTLs contributing to the complex trait crop yield to be defined. Indeed, QTL co-localization can be due to tight-linkage of QTL/genes playing different functions, but could also arise from pleiotropism. When pleiotropy is likely, it would also justify meta-analysis across traits, to further reduce the number of candidates. Veraison time is expected to be strictly related to other phenological stages. Accordingly, tests on the previously mentioned regions on LG1 and LG2 confirmed that, at least in some cases, comparable results are achieved when only veraison or all co-located phenology related traits are considered for the meta-analysis (see *ver_2_1/pheno_2_1* as an example). We therefore also attempted a similar approach for veraison QTLs co-located with other phenology QTLs, finally identifying a number of regions, of which the most relevant were those located on LGs 14, 16 and 18. However, we are aware that these

rely on the pleiotropic assumption, which could be not always satisfied. A recent QTL study based on a GBS SNP map also addressed the mapping of veraison time. That study mainly aimed to discover and map stable QTLs across environments. A veraison QTL mapping on LG16 between 5 and 24cM, which corresponded to the region between 2 and 16 Mbp, was found, but was not consistent across environments. Interestingly, it partially overlapped the *pheno_16_2* meta-QTL we derived here starting from a veraison meta-QTL and its co-location to a flowering-veraison interval QTL. Beside the detailed analysis of phenology traits, we have undertaken, our compendium now provides a useful tool for the inspection of co-location and meta-analysis for further traits in a similar way.

Transcriptomic studies have been also widely applied to characterize molecular changes associated to the onset of ripening, revealing, first of all, a massive transcriptomic rearrangement at veraison time. Among others, genes triggering such transition are expected to modulate their expression at this stage, although alternative regulative mechanisms cannot be excluded. We thus mined available transcriptomic profiles to i) identify the timing of such massive change, ii) select genes differentially expressed during this time in more varieties. Then, beside inspection of positional candidates underlying meta-QTLs, we propose to also integrate information about differential expression at veraison time, in order to prioritize candidates.

On LG1 a veraison time QTL was previously mapped. A more recent study also mapped a QTL for veraison at this location, which allowed us to define the *ver_1_1* meta-QTL. Flowering QTLs consistently overlapped at same location suggesting a possible control of veraison time through regulation of flowering time. Accordingly, candidates for the flowering time control mapped under this meta-QTL, like the *PFT1* (*phytochrome and flowering time 1*) gene or a *CONSTANS-like* gene both controlling the photoperiodic flowering pathway in *A. thaliana*. However, integration of transcriptomic data allowed to pinpoint 14 candidates, among which the VvRAV1 transcription factor, belonging to the plant-specific *RAV* (*RELATED TO ABI3 AND VPI*) family, was included. In *Arabidopsis* RAV1 was shown to act as negative regulator of both development and flowering, probably in

complexes with other co-repressors. Interestingly, some members of this gene family were shown to modulate developmental transitions, especially in response to temperature. Moreover RAV1 was also shown to be negatively regulated by brassinosteroid and abscisic acid, both hormones modulated at the onset of veraison time.

On LG2 meta-QTL analysis of overlapping veraison QTLs allowed 3 main regions to be spotted. In the first of these regions flowering QTLs were also plotted, again supporting a possible regulation of veraison time through flowering, even though no genes controlling flowering time were found under this locus. Interestingly, the orthologous of the Arabidopsis YABBY1/FIL transcription factor, which directly activates the AtMYB75, a key regulator of anthocyanin biosynthesis, was found among candidates selected by the integration of expression data. Moreover, by looking at other functional categories possibly related to veraison time, a gene encoding for a vacuolar invertase 2, key enzyme of sugar metabolism in fruits during ripening, a stay-green protein 1 gene related to a gene shown to be involved in ripening in tomato, beside two pectin methylesterase inhibitor (PMEI) genes, were found as differentially expressed. These last belong to a gene family previously characterized in grape. Their function is supposed to inhibit pectin methylesterase activity in pectin degradation and may play a role in the beginning of ripening by regulating initial events such as softening and loss of turgor. Interestingly, network analysis of gene expression profiles during berry ripening revealed PMEI among genes likely involved in triggering the major transcriptome reprogramming that occurs at veraison. Within *ver_2_2* meta-QTL, the most notable candidate considering both positional and expression data was the VvNAC13 transcription factor. This gene belongs to a wide family of transcription factors in grapevine. Interestingly members of this family in tomato are involved in ethylene biosynthesis, reception and signalling during ripening. Moreover, they were also already suggested as playing a crucial role in berry transcriptome modulation associated to veraison, according to network analysis of berry expression profiles. However, in the same region, a gene encoding an atypical pseudo-response regulator (APRR2), involved in the circadian clock mechanism and contributing to fruit pigmentation and ripening in tomato, as well as two 1-

aminocyclopropane-1-carboxylate oxidases, taking part in ethylene biosynthesis and ripening were also selected by our approach and represent promising candidates. Lastly, a cluster of Myb genes locates within *ver_2_3* meta-QTL interval. These genes have previously been extensively characterized for their involvement in the transition to berry ripening, by regulating the accumulation of anthocyanins in the berry skin. This finding, thus, supports our approach, even though these genes are unlikely to be themselves the early trigger of ripening onset. Other genomic regions were also proposed by previous studies for the genetic control of veraison time, among which the most relevant were mapping on LG 14, 16 and 18. By considering overlapping with other phenology related QTLs, followed by integration of transcriptomic data, we also selected candidates for these regions. The *pheno_14_3* meta-QTL was computed from overlapping veraison QTL and flowering QTLs, and was accordingly highly enriched in candidates playing a role in the flowering transition control or fruit ripening, among which the most notable are Constans 2 (COL2), the feronia receptor-like kinase, a gene encoding a Brassinosteroid-6 oxidase, a gene encoding a COBRA protein and the putative MADS-box FRUITFULL 2. Interestingly this last gene was recently shown to also contribute to modulate the onset of ripening in tomato at early fruit development, beside its involvement at later ripening stages. Instead, a QTL previously mapped on LG 16, and explaining a large part of the genetic variance in the corresponding mapping population, partially co-localized to QTLs for the derived trait flowering-veraison interval, and with the genomic region involved in veraison recently identified by a SNP map and previously discussed. According to our strategy, the original interval was reduced to two regions of about 3.3Mbp overall, including 15 transcriptomic candidates. Interestingly, more recently, the SSR marker UDV052, mapping under the *pheno_16_3* meta-QTL close to the two candidates ABC transporter and an ERF transcription factor (19.1Kbp and 56.9Kbp respectively), was shown to be significantly associated to the early phenotype in a collection of different varieties, thus supporting our approach (Zyprian et al., 2018). Lastly, three different veraison QTLs were mapped on LG18. Two of them partially co-located with flowering QTLs from an independent study, and one of them was overlapping also with a QTL for the flowering-veraison interval. Under the derived

meta-QTLs, *pheno_18_1* and *pheno_18_2*, spanning a still large region, we selected 74 transcriptomic candidates among which 19 were encoding proteins involved in regulation of gene expression, signalling or development. Candidates involved in carbohydrate metabolism, including especially a hexose (HT2) and a sucrose transporter (SUT2-2), putatively modulating sucrose signalling, or candidates encoding for genes for cell wall degradation (like a glucanase and a galactosidase, as examples), were also among those selected.

Conclusions

By building a grape consensus genetic map anchored to the genome assembly a comprehensive overview about genomic distribution of several QTLs from published studies and their co-location both inside traits as well as across related traits was provided. Extensive co-localization was evident especially for phenology related traits. Four veraison meta-QTLs located on LG1 and 2, and several phenology meta-QTLs among which most relevant on LG 14, 16 and 18 were derived from 141 phenology related QTLs. Integration of meta-QTLs with expression data from prior transcriptomic studies allowed to select a set of 272 candidate genes for the genetic control of the veraison transition, reducing by about 20 and 10 times the genes proposed so far by either only genetic or transcriptomic approaches. Among these candidates 78 genes were involved in regulation of gene expression, signal transduction or development. Specific relevant candidates according to their annotation have been discussed. Further studies will now test and eventually validate the putative involvement of these candidates in the genetic control of the veraison transition during berry development.

Chapter 2

Exploit the genetic diversity of a grapevine collection for genetic association studies

Abstract

In plant organisms, genetic association studies still represent a valuable tool to uncover the genetic loci underlying specific quantitative traits. For grapevine phenology, such studies are still poor because of different reasons: the complex genetic architecture of the trait, the high levels of heterozygosity of the species, and its genomic characteristics (i.e. extent of linkage disequilibrium). By performing two complementary GWAS approaches on a grapevine germplasm collection, and by comparing the results with the results of the meta-analysis approach, we were able to identify and prioritize with high confidence genomic regions that could be regions of interest carrying the genes responsible for the beginning of the berry ripening, the veraison stage. In the first part of the chapter, we describe the genetic and phenotypic characterization of a wide germplasm collection of different grapevine accessions (CREA-VIT Conegliano collection) with the aim to identify the best panels of grapevine varieties, representing the most diverse genotypes and phenotypes for the traits of interest to be exploited to test the genotype-phenotype association. The second part of the chapter is dedicated to describe the association analysis itself with two different approaches, firstly using the GrapeReSeq 18K *Vitis* genotyping chip, then with an innovative approach called XP-GWAS (Yang et al., 2015) where pool of individuals displaying extreme phenotypes are whole-genome resequenced and allele frequencies compared to a random pool are screened for enrichment.

Methods

Plant material

The CREA-VIT Conegliano collection (hereafter CCC) is a grapevine germplasm collection comprising more than 2,000 grapevine accessions, among wine, table

cultivars, hybrids and rootstocks. The CCC has been extensively phenotyped for over 50 years for phenology traits (flowering time, veraison time, ripening time) and to a less extent for other various phenotypic traits like cluster architecture and wine acidity. The set of grapevine cultivars representing the object of our work consists in 617 unique genotypes (corresponding to 937 cultivars) for which phenotypic and genotypic data were complete and available. The list of the 617 genotypes is given in Supplementary Table 12.

Genetic data and genetic diversity characterization

The genotypic data provided by our partners consisted in the genetic profiles of the 617 grapevine unique genotypes genotyped with 45 microsatellites (SSR) markers; of these, 32 were already published (Cipriani et al., 2010), while the remaining 13 have been developed and run subsequently. This additional set of microsatellite markers is composed of the 9 SSR markers used internationally for grapevine varietal identification (Maul et al., 2012) plus 4 additional markers developed by the researchers of the CREA-VIT to perform variety identification service (the ISV named markers and the VMCNG4B9). The protocols describing the generation of the SSR data are available from Cipriani. SSR markers were chosen to cover the whole genome of grapevine (19 chromosomes) with at least two markers per chromosome. To give an overview of the genetic diversity of the CCC different indexes commonly used in population genetics, such as expected heterozygosity, were calculated with the software Genalex v6.5.1 (Peakall and Smouse, 2012). Accessions displaying more than 20% of missing data were discarded, so the number of accessions used for the genetic diversity characterization and subsequent analysis was 530.

Population structure analysis

To explore the genetic variability of the collection and the population structure, the first method employed was PCA (principal component analysis) which helps to visualize the entire variability of the data in only two dimensions. PCA was performed on the 530 x 45 data set with the *dudi.pca* function of the *R* package *ade4*, after centring and scaling, and replacing missing values with column mean.

Using this method, the alleles sizes are firstly converted to absence/presence (0/1), so the PCA is not calculated directly on the allele sizes but on allele frequencies. The genetic diversity of the collection represented by the PCA was matched with the geographical origins (each cultivar was classified according to its geographic origin or region of cultivation as reported in the VIVC website <http://www.vivc.de/index.php> or <http://catalogoviti.politicheagricole.it/catalogo.php>) and grapes usage (wine vs table) of the individuals in the collection. The second method employed to explore population structure is the one included in the software STRUCTURE v2.3.4 which uses a Bayesian approach to assign a posterior probability to cluster individuals in sub-populations (Pritchard et al., 2000). Ten independent runs for K values ranging from 1 to 20 were performed with a burn-in length of 1,000,000 followed by 1,500,000 iterations. The admixture model was applied, and no prior population information was used. The best K was chosen based on the estimated membership coefficients (Q) for each individual in each cluster. The optimal subpopulation model was investigated by applying the informal pointers (i.e. the plateau criterion) proposed by Pritchard et al.; individuals with a proportional membership $Q > 0.8$ were considered members of the group, while the remaining were considered admixed individuals. To validate the results from STRUCTURE software a non-parametric clustering approach called DAPC (Discriminant Analysis of Principal Components) implemented in the R package *adegenet 2.0.1* (Jombart and Collins, 2015) was also applied. This non-parametric approach makes different assumptions about the Hardy-Weinberg equilibrium of the genetic loci, so that it can be applied to very different ranges of populations. Prior clusters were identified by a sequential K-means clustering algorithm (*find.clusters* function) after data transformation by PCA. Then, a discriminant analysis (DA) used part of the principal components (PCs) to describe the clusters. K-means was ran with K varying from 1 to 20 and to ensure convergence we increased the number of starting points to 400. The number of clusters was chosen based on the Bayesian Information Criterion (BIC).

Phenotypic data

Phenotypic data consist of the flowering beginning and veraison beginning date in the last 13 years (2004-2016), with the value recorded as Julian day. Flowering beginning corresponds to the phenological stage when 10% of flowerhoods of a cluster have fallen, while veraison beginning corresponds to the stage when 10% of the berries of a cluster changed the colour from green to the particular colour of the cultivar, and this stage is usually considered the beginning of ripening. The interval from flowering to veraison, calculated as the difference between the two traits in number of days, was also included in the analysis. For each accession in the collection five plants are present, and all the plants are grafted on SO4 rootstock. The single phenotypic value per accession per year is obtained as the mean of the five plants. Beside raw data analysis, we also tried to understand the effect of temperature on phenological stages; we thus transformed raw flowering and veraison date values to a new value based on the GDD index. GDD (Growing Degree-Days) is an index used in agriculture that measures the heat accumulation throughout the year. The GDD value was calculated for each day of each year (2004-2016) for the Conegliano region and replaced the raw values (weather data source http://www.arpa.veneto.it/bollettini/storico/Mappa_2019_TEMP.htm). In this way the effect of temperature is normalized among years making the phenotypes more comparable. GDD is calculated as $GDD = \max\left(\frac{T_{max} + T_{min}}{2} - T_{base}, 0\right)$, where temperatures below 10 °C and above 30 °C are set to 10 °C and 30 °C respectively. GDD values were calculated for each day and then summed to obtain a value for each accession. Historical weather data were retrieved from ARPAV website. ARPAV is the regional agency for the environment protection of Veneto region. Data were recorded at a station located in the same area where the experimental vineyard is located. Phenotypic data are recorded every year according to the OIV descriptors. Phenological observations were recorded by visual inspection. All statistical analysis were performed with the statistical programming language *R*, version 3.4.4 (Team and R Development Core Team, 2016).

Retrieval of published SNPchip data

We downloaded genotyping data publicly available from a recent publication (Laucou et al., 2018) from a French grapevine germplasm collection (Vassal collection) to be used as starting point for our GWAS study. Indeed, Laucou et al. released genotyping data for more than 700 grapevine accessions. Among these, 95 were in common, that is they had the same name, with the accessions of the CREA-VIT collection. We obtained these data and explored the genetic diversity of this 95 accessions subset in our collection. More in detail, released data consisted of genotyping data of 10,207 solid SNPs with no missing data, obtained with the GrapeReSeq 18K Vitis genotyping chip.

Core collection construction

Core collections construction was performed using the SSR data (530 accessions by 45 markers) with the software Core Hunter 3 (De Beukelaer et al., 2018). The software can select the smallest number of individuals maximizing different indexes. We applied a strategy of genetic diversity maximization, implemented in the software CoreHunter 3 (De Beukelaer et al., 2018), which allows to maximize allelic diversity of a collection, starting from a number of fixed entries. Core Hunter 3 can construct cores based on genetic marker data, phenotypic traits or precomputed distance matrices, optimizing one of many provided evaluation measures depending on the precise purpose of the core (e.g. high diversity, representativeness, or allelic richness). We decide to perform a maximization using allele coverage, i.e. the percentage of marker alleles observed in the full collection that are retained in the core, keeping as fixed the 95 cultivars in common with the GrapeReSeq dataset (Paslier M-C et al., 2013). Core Hunter was run 100 times to obtain the minimum number of unique individuals maximizing allele coverage. After obtaining this number, the individuals were ranked by occurrence and the most present individuals were selected to constitute the core collection. The R package *poppr* (Kamvar et al., 2014) was used to evaluate allelic diversity of the core and compare it to the entire collection.

Integration of SNPChip data: DNA extraction and SNPchip hybridization

The DNA of the cultivars chosen with the core collection construction method was extracted with Qiagen DNeasy Plant Mini Kit (Qiagen, Hilden, Germany), according to the manufacturer's instructions from frozen leaf tissue. DNA was quantified with a NanoDrop. DNA was purified with Agencourt AMPure XP (Beckman Coulter) and sent for hybridization to Fondazione Edmund Mach. Genotype data were scored and validated from the GrapeReSeq 18K *Vitis* genotyping chip raw data using GenomeStudio Data Analysis v2011.1 (Illumina Inc, San Diego, CA, USA). Genotypes were called and for the subsequent analysis only the 10,207 solid SNPs comprised in the Vassal dataset were kept.

Association analysis SNPchip

The association test was performed on the three phenotypic traits independently, flowering, veraison and flowering-veraison interval, both on mean value across years and on each independent year. Three different software were used: EMMAX (Kang et al., 2010), GAPIT (Lipka et al., 2012) and QTCAT (Klasen et al., 2016). For calculating the association with EMMAX, both no population structure correction and a correction based on kinship were tested, the latter obtained using all the 10K SNPs for the 132 individuals using the command *\$kinship plink -s -v*. Regarding GAPIT, a correction based on population structure was applied; the population structure included this time was the Q-matrix calculated with the 45 SSR markers and the software STRUCTURE. Regarding QTCAT, the software includes a new method that does not need population structure correction, so no other parameters other than genotypes and phenotypes were included. Linkage disequilibrium was evaluated on the 132 cultivars panel using the *R* package *LDcorSV* (Mangin et al., 2012) that takes into account population structure and relatedness. The complete set of 10,207 SNPs was used for the evaluation.

XP-GWAS pool design and DNA extraction

With this approach the panel selected for the association study from a germplasm collection is selected based on the phenotypic and not the genotypic diversity. Indeed, the distribution of the trait of interest was explored and the cultivars displaying extreme phenotypes were selected from the tails of the distribution. The

extreme phenotype GWAS approach (XP-GWAS) (Yang et al., 2015) expects that three different pools of individuals from a germplasm collection or a natural population are created based on the phenotypic distributions of the trait under study. In particular, the more the sample size and the standard deviation of the pools are similar the better. The three pools, hereafter called low, high and random pool, were designed from the flowering-veraison interval trait since it was the trait that displayed a more normal distribution. Starting from the 530 cultivars of the CCC, we sampled 48 and 47 cultivars from the low and high tail of the distribution respectively, and we randomly picked 38 cultivars from the entire collection. The distributions and statistics of the three pools were studied with the software *R 3.4.4*. For each accession of the 3 pools, frozen leaves tissue was grinded and equal amounts of frozen powder were pooled together. DNA was extracted with Qiagen DNeasy Plant Mini Kit (Qiagen, Hilden, Germany), according to the manufacturer's instructions. Extracted DNA was resuspended in water and sent to the genomics facility for quality control and sequencing. Genomic DNA samples were quantified with the Qubit dsDNA HS Assay kit (Life Technologies). DNA purity and integrity were assessed at the Nanodrop 1000 spectrophotometer (Thermo Scientific) and by capillary electrophoresis on a 2200 TapeStation (Agilent Technologies), respectively. For each pool, 500ng DNA was sheared into 350bp fragments by sonication using a S220 Covaris Ultrasonicator. The fragmented DNA was then used for the preparation of Whole Genome libraries following the Kapa Hyper Prep PCR-free workflow (KAPA Biosystems) according to manufacturer's instructions with minor modifications. To avoid index-hopping during sequencing, libraries were treated with Illumina Free Adapter Blocking Reagent (Illumina) prior to further processing. DNaseq libraries were pooled at equimolar concentration and sequenced over 3 lanes of an Illumina HiSeqX sequencer using 150bp paired-end reads.

Results and discussion

CCC genetic diversity characterization and population structure description

The CREA-VIT Conegliano collection (CCC) is a wide grapevine germplasm collection including more than 2,000 grapevine accessions. The cultivars for which

complete phenotypic information on phenology and genotypic information at 45 microsatellite markers was available (Cipriani et al., 2010) were 617. We first used the latter information to study the genetic diversity and the population structure of this collection subset. Full information about country of origin, cultivation, berry colour and usage, retrieved either from <http://www.vivc.de/index.php> or <http://catalogoviti.politicheagricole.it/catalogo.php> are provided in Supplementary Table 11 and Figure 5.

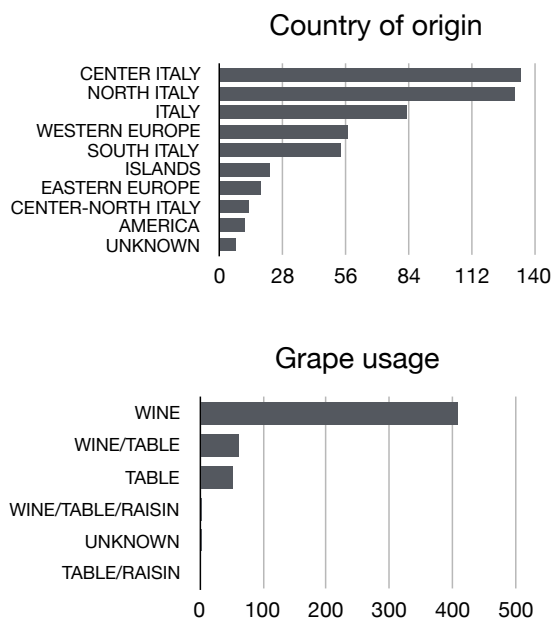


Figure 5. First panel, top: country of origin of the 530 grapevine accessions, when not available, replaced with the area of major cultivation. Second panel, bottom: destination usage of the grape varieties.

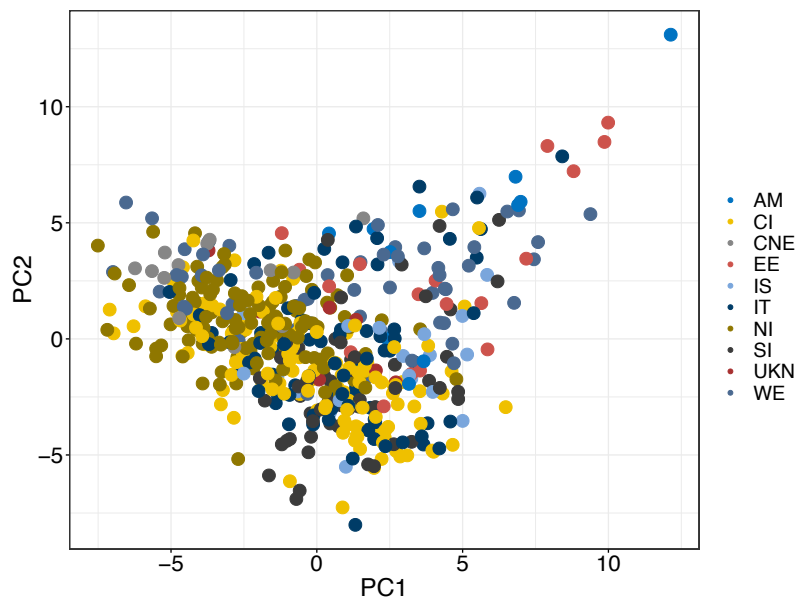
The majority of cultivars of the CCC are of Italian origin, especially from north and centre of Italy, followed by cultivars of western Europe origin. Concerning the destination usage of the grapes, the majority (77 %) are cultivars designated to wine production. The 530 distinct genotypes characterized with 45 SSR markers (Cipriani et al., 2010 and personal communication) revealed a large number of alleles detected (Table 7). The number of different alleles (A) for the SSRs was 369 and ranged from 2 to 16 per locus, with an average of 8.2. The observed (H_o) and

expected heterozygosities (He) were 0.658 and 0.75, respectively, and the former is in line with the value in other grapevine collections (Nicolas et al., 2016).

Table 7. Summary statistics of genetic variation at 45 SSR loci in the 530 germplasm cultivars. In the column locus, in green the previously reported SSR markers (Cipriani et al., 2010), in yellow the new set of markers. *N* (Sample Size), *Na* (No. Alleles), *Ne* (No. Effective Alleles), *I* (Information Index), *Ho* (Observed Heterozygosity), *He* (Expected Heterozygosity), *uHe* (Unbiased Expected Heterozygosity), *F* (Fixation Index).

Locus	N	Na	Ne	I	Ho	He	uHe	F
VChr1a	495	9.000	2.737	1.400	0.655	0.635	0.635	-0.031
VChr1b	526	4.000	2.728	1.156	0.671	0.633	0.634	-0.060
VChr1c	528	3.000	1.973	0.724	0.523	0.493	0.494	-0.060
VChr2a	525	4.000	1.859	0.771	0.520	0.462	0.462	-0.126
VChr2b	497	4.000	1.748	0.772	0.443	0.428	0.428	-0.035
VChr3a	487	12.000	6.275	2.026	0.786	0.841	0.841	0.064
VChr4a	475	6.000	2.448	1.135	0.589	0.592	0.592	0.003
VChr5a	520	11.000	5.149	1.880	0.806	0.806	0.807	0.000
VChr5b	513	9.000	3.704	1.517	0.754	0.730	0.731	-0.033
VChr5c	450	7.000	4.215	1.623	0.760	0.763	0.764	0.004
VChr6a	509	3.000	2.037	0.846	0.417	0.509	0.510	0.182
Vchr7a	524	3.000	1.982	0.723	0.508	0.495	0.496	-0.025
VChr7b	469	4.000	3.287	1.277	0.736	0.696	0.697	-0.057
VChr8a	498	12.000	5.702	1.918	0.588	0.825	0.825	0.287
VChr9a	448	7.000	5.059	1.741	0.850	0.802	0.803	-0.060
VChr9b	395	13.000	4.385	1.760	0.324	0.772	0.773	0.580
Vchr10b	512	4.000	2.831	1.083	0.670	0.647	0.647	-0.036
Vchr11a	511	5.000	2.039	0.955	0.485	0.510	0.510	0.048
Vchr12a	525	8.000	2.566	1.204	0.547	0.610	0.611	0.104
Vchr12b	482	3.000	1.385	0.465	0.295	0.278	0.278	-0.060
Vchr13a	504	7.000	3.281	1.479	0.704	0.695	0.696	-0.013
Vchr13b	511	8.000	2.558	1.342	0.614	0.609	0.610	-0.009
Vchr13c	513	4.000	3.141	1.258	0.700	0.682	0.682	-0.027
Vchr14a	403	5.000	2.294	0.956	0.600	0.564	0.565	-0.065
Vchr15a	511	7.000	3.387	1.455	0.663	0.705	0.705	0.059
Vchr16a	525	8.000	1.507	0.734	0.250	0.336	0.337	0.258
Vchr16b	523	8.000	2.086	1.144	0.530	0.521	0.521	-0.017
Vchr17a	488	2.000	1.781	0.630	0.281	0.439	0.439	0.360
Vchr18a	519	9.000	3.458	1.553	0.570	0.711	0.712	0.198
Vchr18b	529	5.000	2.829	1.146	0.681	0.647	0.647	-0.053
Vchr19a	520	9.000	3.061	1.471	0.673	0.673	0.674	0.000
Vchr19b	523	5.000	3.281	1.306	0.562	0.695	0.696	0.191
VVS2	529	13.000	5.504	1.964	0.822	0.818	0.819	-0.005
VVMD27	529	9.000	5.615	1.827	0.824	0.822	0.823	-0.003
VVMD7	529	14.000	5.320	1.907	0.822	0.812	0.813	-0.013
ISV2	525	16.000	6.641	2.061	0.891	0.849	0.850	-0.049
VrZAG62	530	10.000	6.383	1.979	0.860	0.843	0.844	-0.020
VVMD5	524	10.000	6.098	1.949	0.819	0.836	0.837	0.021
VMCNG4B9	524	15.000	6.231	2.139	0.853	0.840	0.840	-0.016
VrZAG79	527	11.000	5.667	2.018	0.827	0.824	0.824	-0.005
ISV3	488	10.000	3.119	1.361	0.836	0.679	0.680	-0.231
ISV4	520	10.000	4.682	1.693	0.754	0.786	0.787	0.041
VVMD28	526	14.000	7.751	2.207	0.882	0.871	0.872	-0.013
VVMD25	443	14.000	4.434	1.669	0.786	0.774	0.775	-0.014
VVMD32	428	15.000	5.864	1.962	0.862	0.829	0.830	-0.039
Mean	501.8	8.200	3.780	1.426	0.658	0.675	0.676	0.027
SE	5.088	0.580	0.252	0.071	0.026	0.022	0.022	0.020

To explore the genetic variability of the collection and population structure, the first method employed was the PCA. The genetic diversity of the collection represented by the PCA was matched with the geographical origins and grapes usage of the cultivars in the collection. Clustering was weak concerning the geographic subdivision (weak gradient right to left, eastern Europe to north Italy/center-north Europe), while the clustering based on usage was more evident (Figure 6), displaying a sort of gradient from right to left (table to wine cultivars), with the wine/table cultivars in the middle of the distribution, similar to what has been reported before for other collections (Migicovsky et al., 2017).



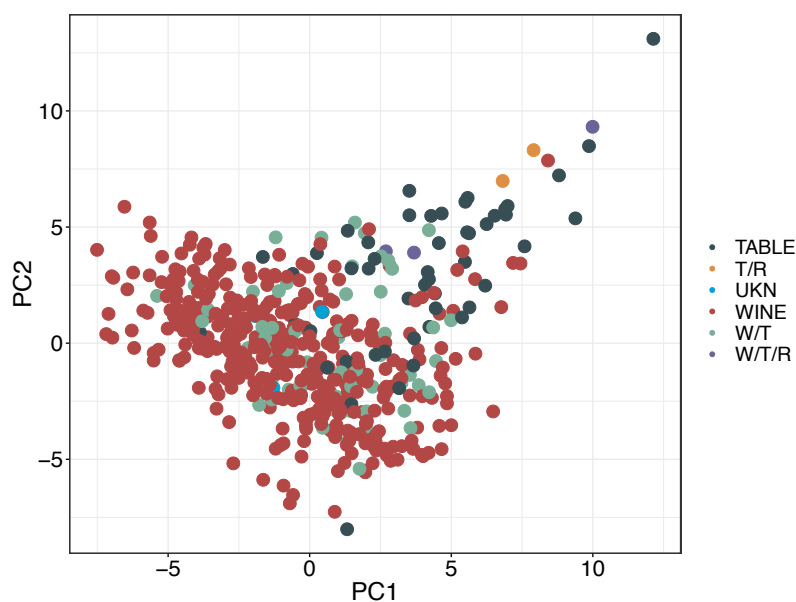


Figure 6. Principal component analysis plots from SSR data. Each dot represents one of the 530 cultivars. Top plot represents geographic origin/cultivation, while bottom is grape usage destination. Top panel abbreviations: AM America, CI Center Italy, CNE Center North Europe, EE Eastern Europe, IS Islands (Sardinia, Sicily), IT Italy, NI North Italy, SI South Italy, UKN Unknown origin, WE Western Europe. Bottom panel abbreviations: T/R Table/Raisin, UKN Unknown origin, W/T Wine/Table, W/T/R Wine/Table/Raisin.

Population structure analysis performed with the software STRUCTURE on the SSR data set suggested as the most likely number of clusters (K), evaluated with the plateau criterion proposed by Pritchard et al. and the ΔK method (Evanno et al., 2005) a maximum probability for $K = 2$ and a smaller probability for $K = 6$. Indeed, the ΔK criterion gave the highest value at $K = 2$, and a small peak at $K = 6$. Instead, the plateau criterion, highlighted by the mean log-likelihood curve, revealed a maximum value with no standard deviation associated at $K = 6$, beyond that, a sort of plateau is reached, and the standard deviations associated with the remaining estimates increase. When the cultivars in the PCA are coloured according to the membership of the groups identified by STRUCTURE, the 2 groups subdivision is very evident (Figure 8). Table 8 gives the genetic diversity statistics associated to each one of the 2 subgroups and the admixed one, compared to the values (already reported in Table 7) obtained considering the entire collection.

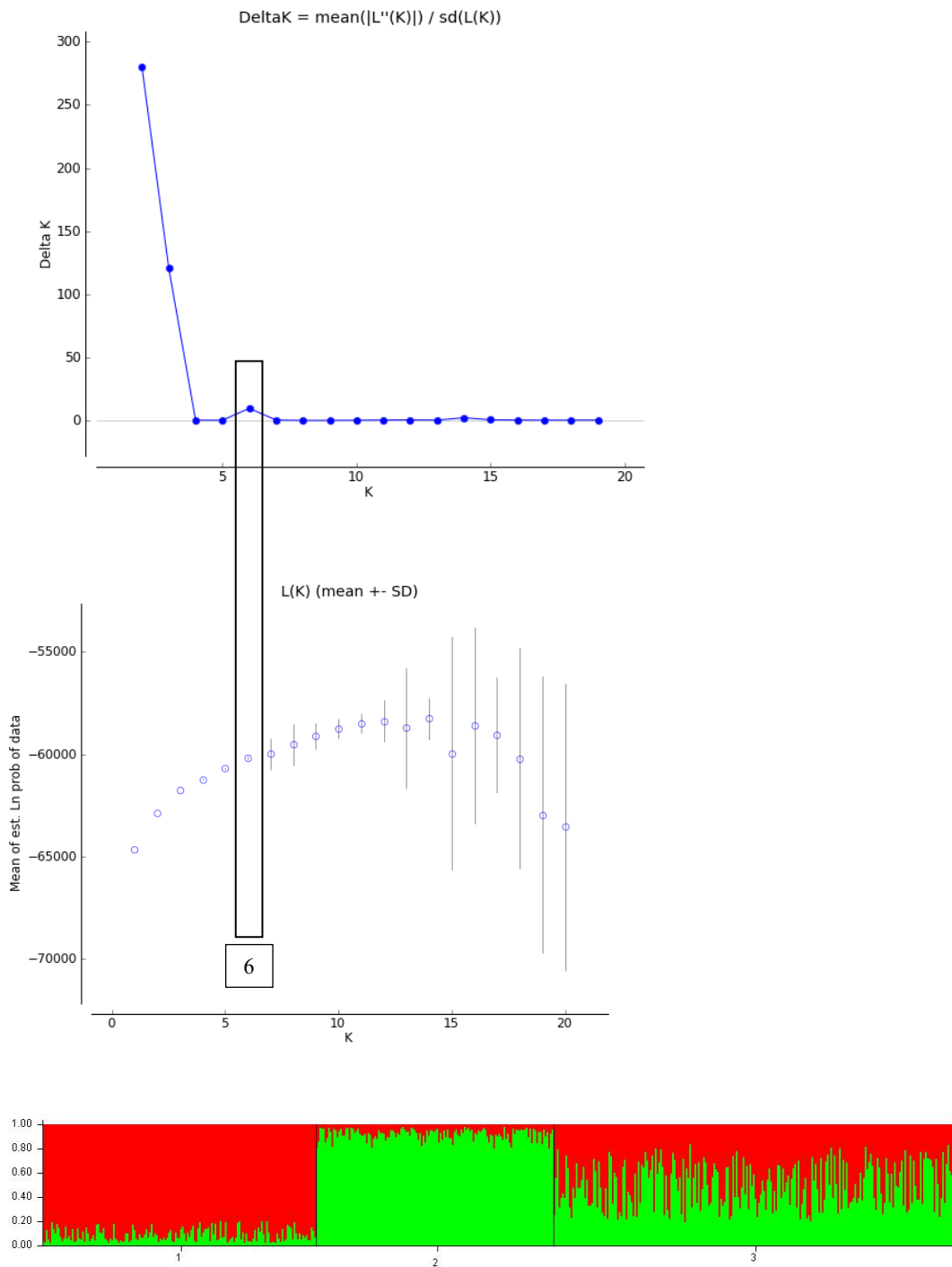


Figure 7. Estimated number of clusters obtained with STRUCTURE for K values from 1 to 20. Graphical representation of its derivative statistics ΔK (top) and estimated mean $L(K)$ (middle). Bottom figure represents plot generated based on the Q -matrix. Each cultivars is represented by a single vertical line, which is divided in coloured segments in proportion to the estimated membership in the two subgroups. On the y-axis is the likelihood of assignment to any given cluster K .

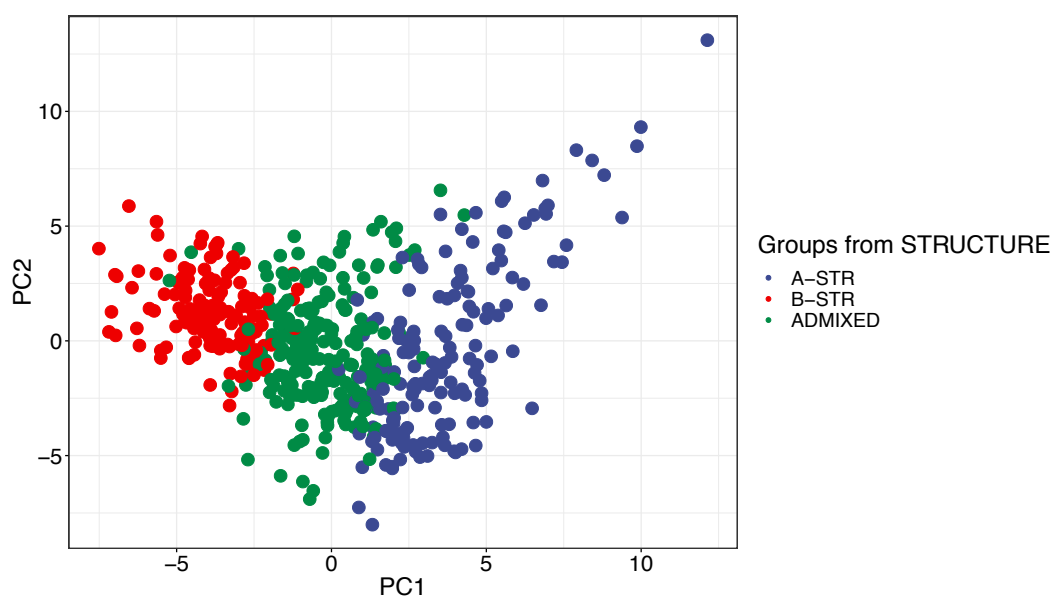


Figure 8. Principal component analysis plot from SSR data. Each dot represents one of the 530 cultivars. The colors represent the 2 groups subdivision identified by STRUCTURE.

Table 8. Summary statistics of genetic variation at 45 SSR loci in the 530 germplasm cultivars, subdivided into 2 groups as identified by STRUCTURE, compared to the values obtained considering the entire collection.

Pop		N	Na	Ne	I	Ho	He	uHe	F
A-STR	Mean	148.778	7.378	3.736	1.409	0.655	0.671	0.673	0.025
	SE	1.925	0.488	0.252	0.070	0.026	0.022	0.023	0.022
B-STR	Mean	131.644	7.378	3.745	1.420	0.663	0.675	0.677	0.017
	SE	1.239	0.501	0.249	0.071	0.026	0.022	0.022	0.020
ADMIXED	Mean	221.356	7.467	3.757	1.419	0.656	0.674	0.676	0.029
	SE	2.027	0.481	0.246	0.070	0.026	0.023	0.023	0.021
CCC	Mean	501.8	8.2	3.78	1.426	0.658	0.675	0.676	0.027
	SE	5.088	0.58	0.252	0.071	0.026	0.022	0.022	0.02

Homogeneity of genetic diversity between the three subgroups is appreciable, and the values are comparable to the ones of the entire collection; however, pairwise F_{ST} values (fixation index or inbreeding coefficient), which describe the genetic differentiation between groups or population, indicates a very low level of differentiation between the three subgroups (0.0026 between A-STR and B-STR, 0.0019 between A-STR and ADMIXED, and 0.0021 between B-STR and

admixed), although very similar to values previously reported separating *sativa* cultivars of among Western, Central and Eastern Europe (Myles et al., 2011). We tried to characterize the subgroups to find specific features of the two, so we looked at enrichment in terms of geographic origins, and found a significative overrepresentation of cultivars from the east (mostly table grapes), the *orientalis* group (*proles*) as defined in the works of Negrul and Troshin (Negrul et al., 1946; Troshin LP et al., 1990), in the group A-STR, and a significant underrepresentation of cultivars from the North Italy group (Table 9). Regarding group B-STR, we found a significant overrepresentation of cultivars belonging to the North Italy group and a slight enrichment for cultivars belonging to the Center-North Europe group ($p = 0.061$ two-tailed, $p = 0.0554$ one-tailed Fisher's Exact Test) comprised in the *pontica occidentalis proles*. On the other hand, in this group we observed very few cultivars belonging to groups overrepresented in group A-STR (AM, EE, IS [2 cultivars]).

Table 9. Composition of the two groups identified by STRUCTURE plus the admixed cultivars. Top table shows contingency table for country of origin, bottom table for colour. In red overrepresented groups, in blue underrepresented ones. In parenthesis, in italics are reported *p*-values from Fisher's Exact Test two-tailed. Abbreviations: AM America, CI Center Italy, CNE Center North Europe, EE Eastern Europe, IS Islands (Sardinia, Sicily), IT Italy, NI North Italy, SI South Italy, UKN Unknown origin, WE Western Europe.

COUNTRY	A-STR	B-STR	ADMIXED	CCC
AM	8 (0.09445)	0	3 (0.5692)	11
CI	42 (0.8417)	34 (I)	58 (I)	134
CNE	0	8 (0.06159)	5 (I)	13
EE	13 (0.0285)	0	5 (0.4912)	18
IS	15 (0.0274)	2 (0.1956)	5 (0.2069)	22
IT	27 (0.7169)	8 (0.006577)	48 (0.1853)	83
NI	6 (3.431e-08)	69 (9.71e-05)	56 (0.9294)	131
SI	20 (0.4707)	0	34 (0.1449)	54
UKN	3 (0.7049)	2 (I)	2 (0.73)	7
WE	25 (0.1696)	15 (I)	17 (0.1862)	57
	159	138	233	530

COLOR	A-STR	B-STR	ADMIXED	CCC
BLANC	86 (0.1308)	38 (0.03239)	100 (0.9427)	224
GRIS	0	0	2	2
NOIR	51 (0.009774)	96 (0.04294)	121 (0.8398)	268
RED	2	0	1	3
ROSE	2	0	1	3
ROUGE	4	3	1	8
UKN	14	1	7	22
	159	138	233	530

When the same reasoning is applied to the colour characteristic, we observe an underrepresentation of black-skinned (noir) cultivars in the A-STR, coupled with an overrepresentation of the same in the B-STR.

To support the results obtained by STRUCTURE we also applied a non-parametric approach called DAPC to the same SSR dataset (530 individuals, 45 SSRs). To identify the optimal number of clusters the Bayesian Information Criterion (BIC) method was employed (Jombart et al., 2010). The greatest delta between two points is found between $K = 1$ and $K = 2$, while the lowest value is reached at $K = 7$. Both K values (2 and 7) were explored and compared to the results obtained previously with STRUCTURE (Figure 9).

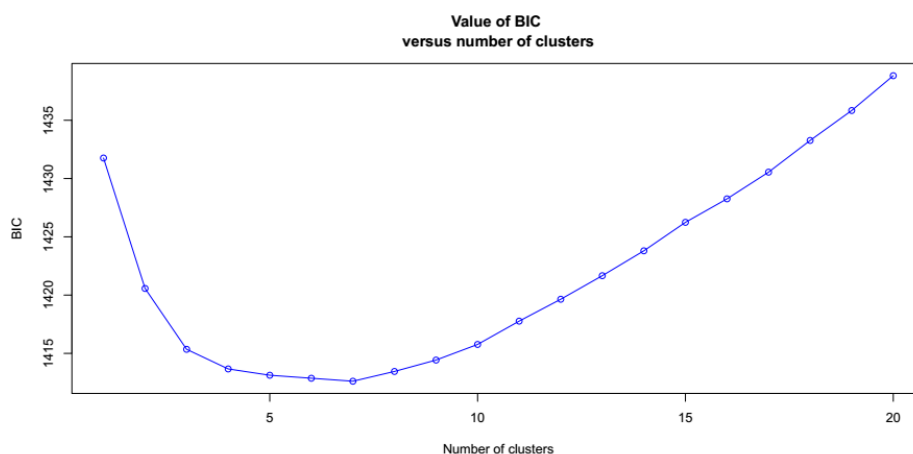


Figure 9. Bayesian Information Criterion (BIC) according to the number of inferred clusters ($K = 0-20$). 300 principal components were kept and the number of starting points was set at 100. Number of iterations was 1000000 and the chosen number of clusters were $K = 2$ and $K = 7$.

When the individuals belonging to the subgroups identified by STRUCTURE are matched with the individuals belonging to the subgroups identified by DAPC there is a perfect match (Figure 10, top). The individuals classified as admixed by STRUCTURE (group c in the figure) are split between the 2 groups identified by DAPC, which usually identifies a very small number of admixed individuals, in this case just 3 (not shown). Moreover, the two DAPC groups separates very good in the PCA plot, meaning that their genetic diversity is high (Figure 10, bottom).

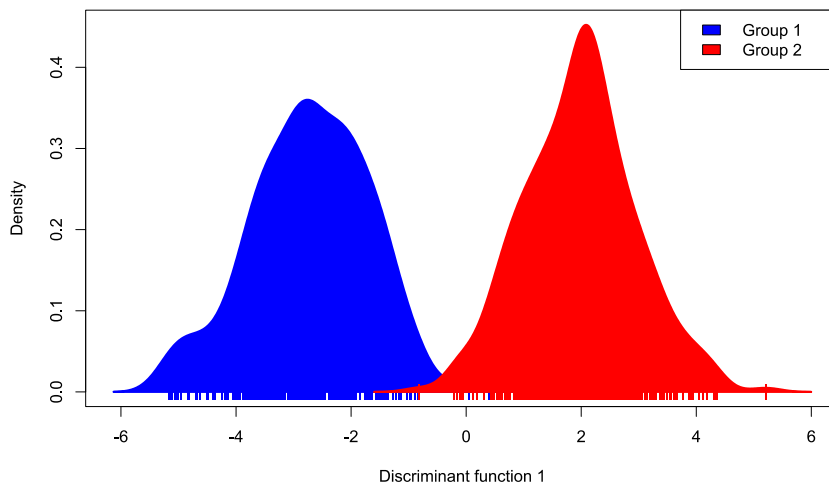
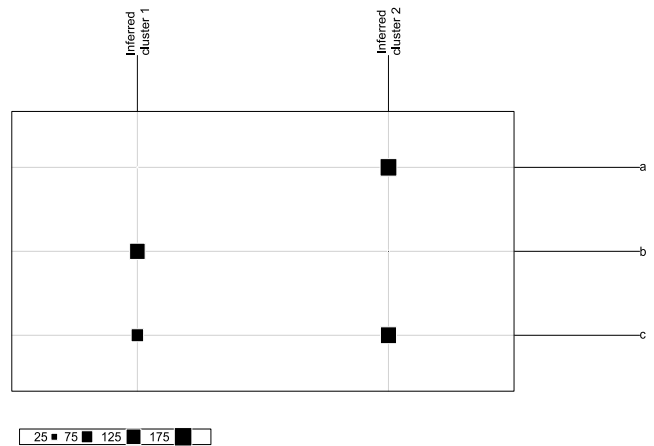
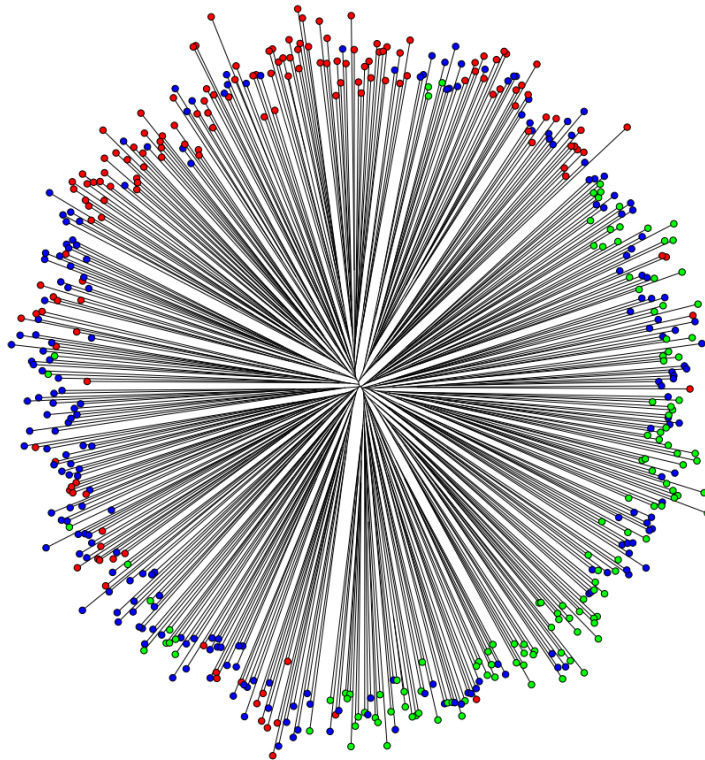


Figure 10. Top figure. Representation of contingency table by square sizes to compare prior group assignments using K-means clustering to the groups identified by STRUCTURE. Group a is A-STR, b is B-STR and c is admixed. Inferred clusters 1 and 2 are the two clusters identified by DAPC approach. Bottom panel is the discriminant analysis component plot for the two inferred clusters by DAPC.

Another way of assessing the results of the clustering method we employed is with phylogenetic trees and dendrograms. Using the R package *phangorn v2.1.1* we built a Neighbour-Joining tree based on Euclidean distances and a dendrogram based on Manhattan distances (Figure 11). In both, the 2 subgroups identified by STRUCTURE and DAPC (data not shown) and the groups found by the trees were in agreement except for few individuals incorrectly placed, thus reinforcing the two groups subdivision identified initially by STRUCTURE.



Three groups from STR - no adm (Manhattan distances/Ward method)

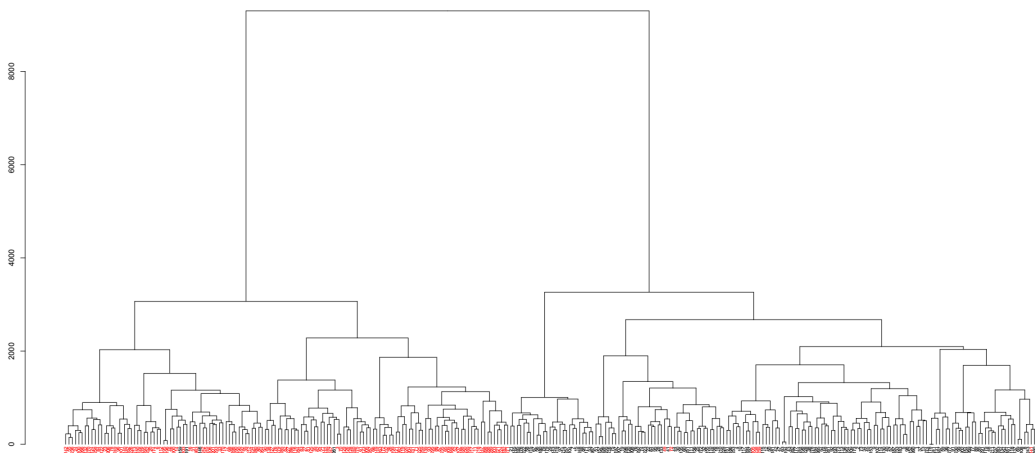


Figure 11. Top panel, Neighbor-joining tree based on euclidean distances. In red, green and blue group A-STR, B-STR and admixed cultivars respectively. Bottom panel, dendrogram based on manhattan distances, Ward method. Red labels represent group A-STR, black labels are cultivars from group B-STR. Admixed individuals are not displayed.

We then tried to explore the additional subdivision of the population in 6 subgroups as previously suggested by STRUCTURE (Figure 7). When the PCA of the 530 cultivars is coloured according to the 6 subgroups (Figure 12), except for groups *d*

and *e*, which are slightly overlapping, the remaining 4 groups are well separated. Admixed cultivars are the majority (316, ~ 60%) and are dispersed all over the points, but mostly concentrate in the middle of the plot. The smallest group is group *c* ($n = 10$), while group *f* is the largest, with 67 cultivars. In Table 10 summary statistics of the genetic diversity of the 6 subgroups are reported. Values are again comparable to each other's and to the entire collection. Pairwise fixation index ranged from 0.019 between *d* and *f* and 0.096 between *b* and *c* subpopulations (Table 11). Considering the small sample size compared to other grapevine germplasm collections (Emanuelli et al., 2013; Nicolas et al., 2016), these values, with an average value of 0.051, may reflect statistically supported subpopulations. Also in this case we tried to characterize the subpopulations from a geographic (Table 12) and grape usage point of view. We notice some over- and underrepresentation: for example group *a* is enriched in cultivars of the *proles orientalis*, very similarly to the previous group A-STR, while at the same time is scarce of cultivars from the north of Italy; group *b* is very small ($n = 12$), but being very close to group *a* is again slightly enriched for cultivars from classified as America (Cardinal, Early Muscat, July Muscat, mainly table grape cultivars). Group *c* is the smallest ($n = 10$) composed only of wine cultivars and not enriched in cultivar from any geographic area; group *d* is composed mainly by wine cultivars and is enriched in cultivars of north Italian origin and, though not significant, the other representatives are only cultivars from centre of Italy. Group *e*, similar to group *d*, is enriched in cultivars of centre-Italy origin (though significant only at one-tail), and even if almost overlapping to group *d*, it also displays overrepresentation of western European cultivars (in particular 7 wine French cultivars: Becuet, Pinot Blanc, Malbec, Merlot, Sauvignon, Semillon, Chenin). Group *f* is significantly enriched for centre and south Italian cultivars, while it comprises only one cultivar classified as North Italian, and, according to the PCA plot, it is the only subgroup with no cultivars overlapping to any other subgroups. By building a Neighbor-joining phylogenetic tree without considering the admixed individuals identified by STRUCTURE, the 6 subgroups identified both by STRUCTURE separates well supporting again the hypothesis of the 6 groups subdivision (Figure 13 B).

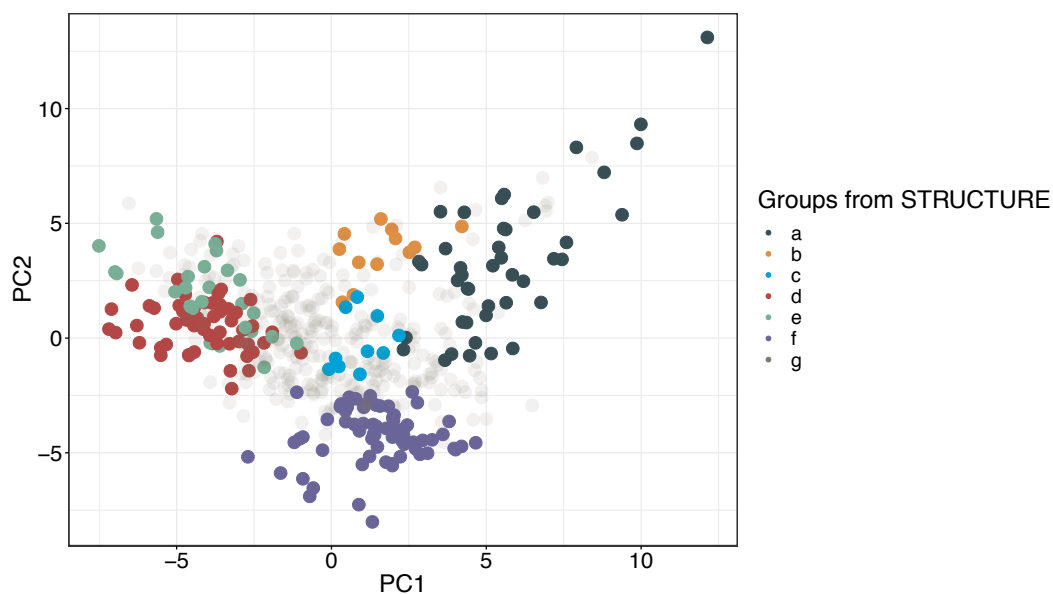


Figure 12. Principal component analysis plot from SSR data. Each dot represents one of the 530 cultivars. The colors represent the 6 groups subdivision identified by STRUCTURE. Group g is admixed cultivars, colored in light grey.

Table 10. Summary statistics of genetic variation at 45 SSR loci in the 530 germplasm cultivars, subdivided into 6 groups as identified by STRUCTURE, compared to the values obtained considering the entire collection. Group g is admixed cultivars.

Pop		N	Na	Ne	I	Ho	He	uHe	F
a	Mean	40.556	6.489	3.649	1.375	0.667	0.661	0.669	-0.009
	SE	0.548	0.434	0.255	0.071	0.026	0.023	0.023	0.023
b	Mean	11.222	4.822	3.421	1.275	0.648	0.653	0.685	0.013
	SE	0.220	0.278	0.220	0.062	0.032	0.022	0.023	0.033
c	Mean	9.400	4.556	3.252	1.230	0.664	0.634	0.670	-0.035
	SE	0.140	0.257	0.197	0.062	0.035	0.023	0.025	0.038
d	Mean	52.511	6.667	3.765	1.404	0.662	0.674	0.680	0.013
	SE	0.564	0.402	0.253	0.069	0.026	0.022	0.023	0.023
e	Mean	23.911	5.844	3.481	1.323	0.618	0.647	0.661	0.046
	SE	0.439	0.358	0.238	0.070	0.032	0.024	0.025	0.034
f	Mean	63.133	6.844	3.719	1.401	0.662	0.672	0.677	0.015
	SE	0.795	0.452	0.248	0.070	0.026	0.022	0.022	0.023
g	Mean	301.044	7.778	3.767	1.425	0.658	0.675	0.676	0.027
	SE	2.664	0.512	0.247	0.070	0.026	0.022	0.023	0.021
CCC	Mean	501.8	8.2	3.78	1.426	0.658	0.675	0.676	0.027
	SE	5.088	0.58	0.252	0.071	0.026	0.022	0.022	0.02

Table 11. Pairwise F_{st} index (calculated as $1 - (H_o / H_e)$) between the six subgroups subdivision as identified by STRUCTURE. Highest and lowest values highlighted in red and blue respectively, excluding admixed individuals.

Pop	a	b	c	d	e	f
b	0.055					
c	0.066	0.096				
d	0.022	0.052	0.055			
e	0.036	0.067	0.081	0.037		
f	0.023	0.045	0.066	0.019	0.037	
g	0.016	0.045	0.060	0.013	0.032	0.010

Table 12. Contingency table of geographic composition of the six groups identified by STRUCTURE plus the admixed cultivars. In red overrepresented groups, in blue underrepresented ones. In parenthesis, in italics are reported *p*-values from Fisher's Exact Test two-tailed.

COUNTRY	STRUCTURE GROUPS						ADMIXED	CCC
	a	b	c	d	e	f	g	
AM	4 (0.025443)	3 (0.004851)	0	0	0	0	4 (0.591)	11
CI	3 (0.02003)	0	1 (0.7025)	20 (0.2324)	0	33 (0.006073)	77 (0.8735)	134
CNE	0	1 (0.2848)	0	0	1 (0.4971)	0	11 (0.4006)	13
EE	8 (0.0007567)	1 (0.3642)	1 (0.3188)	0	0	0	8 (0.5438)	18
IS	6 (0.02024)	0	0	0	1 (1)	3 (0.7538)	12 (0.8585)	22
IT	4 (0.4999)	3 (0.4452)	2 (0.6719)	5 (0.3187)	3 (0.7851)	15 (0.2397)	51 (0.9235)	83
NI	0	2 (1)	4 (0.4957)	30 (0.003079)	13 (0.06351)	1 (1.916e-05)	81 (0.8125)	131
SI	3 (0.7888)	1 (1)	1 (0.4709)	0	0	15 (0.01876)	34 (0.8178)	54
UKN	0	0	0	0	1 (0.3263)	0	6 (0.5692)	7
WE	15 (0.0007697)	1 (1)	1 (1)	1 (0.04942)	7 (0.06835)	0	32 (0.8189)	57
	43	12	10	56	26	67	316	530

Also in this case, to validate STRUCTURE results, we tried the DAPC approach which suggested a possibility having a 7 subgroups subdivision (Figure 9). When we tried to match the composition of individuals identified by both the methods, this time the match is not perfect but is still significant. In particular for groups *a*, *b*, and *e*, the match is almost perfect with DAPC clusters 3, 6 and 7 respectively (Figure 13 C). The plot of the discriminant components based on the DAPC approach shows that not all the 7 groups were clearly separated from each other (Figure 13 D).

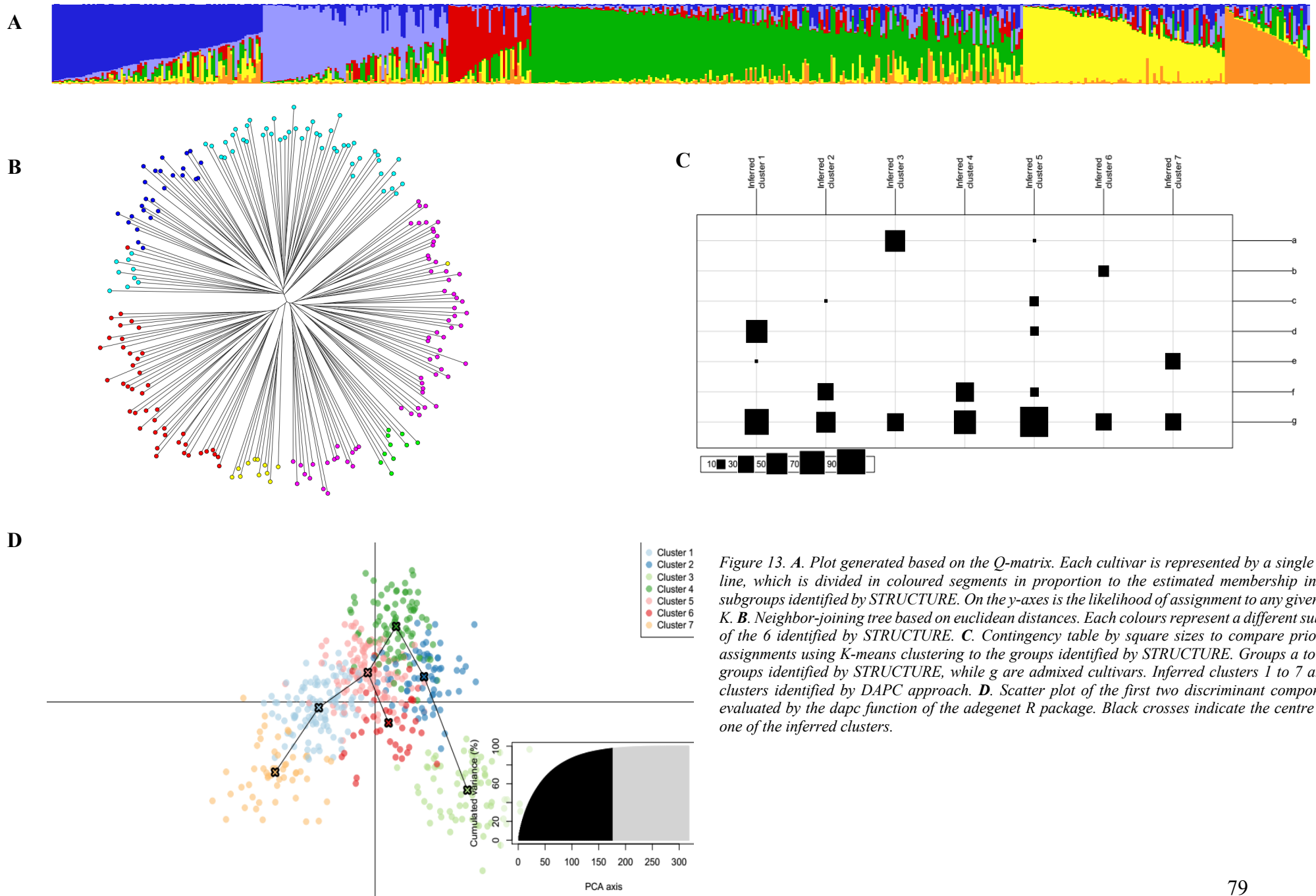


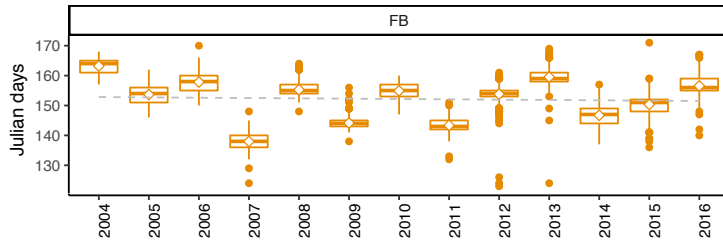
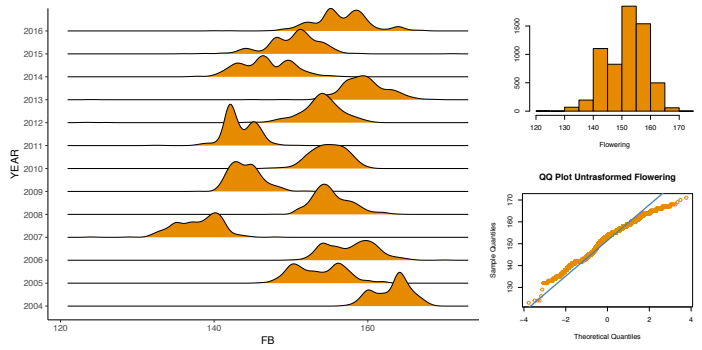
Figure 13. **A.** Plot generated based on the *Q*-matrix. Each cultivar is represented by a single vertical line, which is divided in coloured segments in proportion to the estimated membership in the six subgroups identified by *STRUCTURE*. On the *y*-axis is the likelihood of assignment to any given cluster *K*. **B.** Neighbor-joining tree based on euclidean distances. Each colours represent a different subgroups of the 6 identified by *STRUCTURE*. **C.** Contingency table by square sizes to compare prior group assignments using *K*-means clustering to the groups identified by *STRUCTURE*. Groups *a* to *g* are 6 groups identified by *STRUCTURE*, while *g* are admixed cultivars. Inferred clusters 1 to 7 are the 7 clusters identified by *DAPC* approach. **D.** Scatter plot of the first two discriminant components as evaluated by the *dapc* function of the *adegenet* R package. Black crosses indicate the centre of each one of the inferred clusters.

Phenotypic data

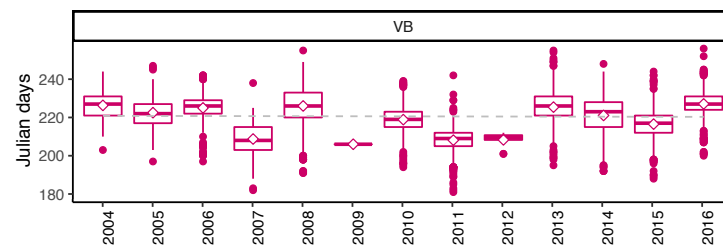
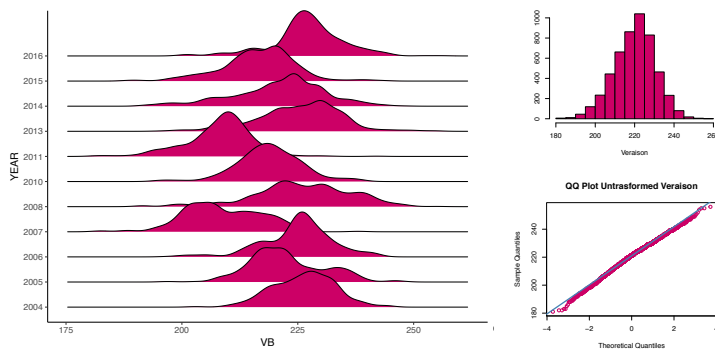
Phenotypic data consisting of Julian days (days from the beginning of the year) for the beginning of flowering (FB) and the beginning of veraison (VB) were recorded for the whole CCC for over 50 years. Flowering-veraison interval trait (F-V) was also considered and obtained as the raw difference between the time of veraison beginning and flowering beginning. We focused our analysis on the data of seasons 2002 to 2016, given the observation (Tomasi et al., 2011) that a significant breakpoint in the grapevine phenology in the Conegliano region occurred around 20 years ago. Complete phenotypic data were available for 13 years for FB trait, while for VB, and consequently also F-V, for 11 years.

When we checked the single years distribution of flowering, many years showed a bimodal distribution, as well as the all-years distribution (Figure 14, Panel 1). We then checked the distribution of the traits with histograms and quantile-quantile plots (QQ plots). Flowering suggests a bimodal distribution while veraison approximates well a normal distribution. Raw phenotypic values were then plotted for each year as boxplot in order to check the variability for the three traits among the 13 years. Variability among years looks greater for flowering than for veraison, though quite significant for both (p -value $\ll 0.01$, ANOVA), showing a slightly decreasing trend over the years. The inter-years variability looks more levelled when the trait flowering-veraison interval is considered, though again still significant when an ANOVA test is performed to compare all the years together (p -value $\ll 0.01$). Since it is important to consider the effect of temperature on phenological stages of plants, and in particular in grapevine (De Cortázar-Atauri et al., 2017; Duchêne et al., 2010; Williams et al., 1985) we wanted to verify the effect of temperature on the two traits, performing a transformation of the raw flowering and veraison date values to a new value based on the GDD index. GDD (Growing Degree-Days) is an index used in agriculture that measures the heat accumulation throughout the year. After plotting the newly GDD- transformed values the distribution of flowering changed from bimodal to a good normal distribution, while the veraison distribution remained unchanged (Figure 14, Panel 2); especially from the QQ plots it can be observed that when using the GDD values almost all

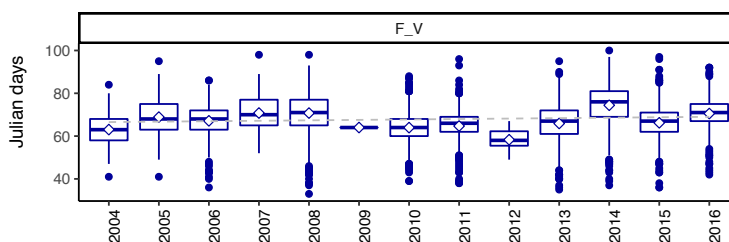
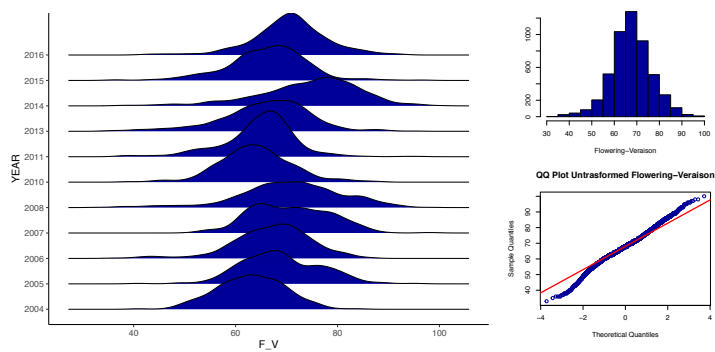
the points fall on the theoretical quantile distribution except for few points at the flowering tails. The same effect can be seen on the flowering-veraison trait, and it can be noted that when considering the GDD values, the entire distribution profile of the F-V interval trait is completely determined by the VB trait profile. Such a decrease in variability among years when using the GDD corrected traits was also confirmed by a comparison of the *p-values* intensities from a pairwise t-test between every year (Figure 15). Overall, the *p-values* of the comparison of the means lose significance when considering GDD values, both for flowering and for veraison. Finally, we plotted the traits (both as raw date and GDD-corrected dates) for each genotype as boxplot (Data not shown) to check the intra- and inter-genotypic variability and could observe that both decreased after the GDD correction for the flowering trait while remained similar for veraison.



Flowering				
YEAR	Count	Mean	Median	SD
2004	263	163.21	164	2.33
2005	268	153.64	154	3.33
2006	368	157.85	158	3.19
2007	288	137.96	138	3.00
2008	564	155.27	155	2.46
2009	506	144.17	144	2.10
2010	570	154.92	155	2.27
2011	506	143.35	143	2.07
2012	526	153.80	154	3.44
2013	595	159.50	159	3.21
2014	568	146.72	147	3.41
2015	583	150.33	151	3.46
2016	524	156.56	156	3.62
ALL	6129	152.08	154	6.999

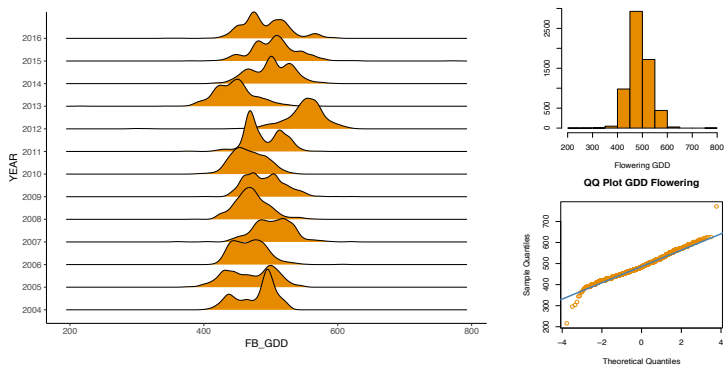


Veraison				
YEAR	Count	Mean	Median	SD
2004	263	226.29	227	6.64
2005	268	222.46	222	8.01
2006	368	224.94	226	7.45
2007	288	208.70	207.5	8.22
2008	564	225.98	226	10.46
2010	570	218.87	219	7.05
2011	506	208.13	209	7.09
2013	595	225.41	226	8.95
2014	568	221.05	223	9.85
2015	583	216.52	217	7.93
2016	524	227.07	227	7.57
ALL	5623	220.52	221	10.42

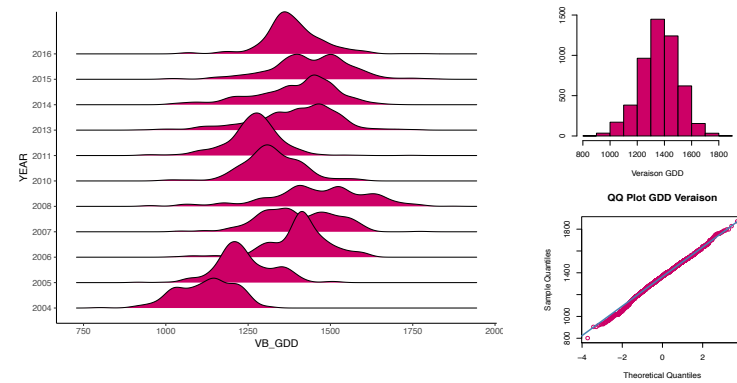
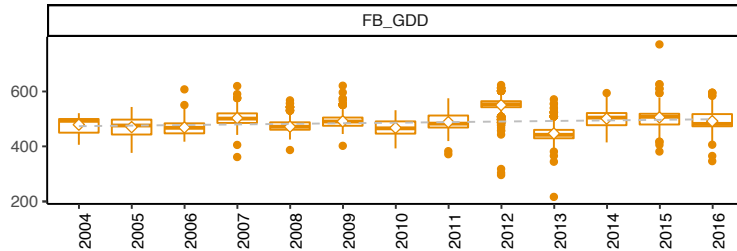


Flowering-Veraison				
YEAR	Count	Mean	Median	SD
2004	263	63	63	6.64
2005	268	68.9	68	7.79
2006	369	67.1	68	7.76
2007	288	70.8	70	7.64
2008	567	70.8	71	10.2
2010	568	64	64	7.16
2011	500	64.7	66	7.17
2013	536	65.9	67	8.75
2014	564	74.4	76	9.95
2015	583	66.2	67	7.86
2016	521	70.5	71	7.37
ALL	5392	67.85	68.27	8.03

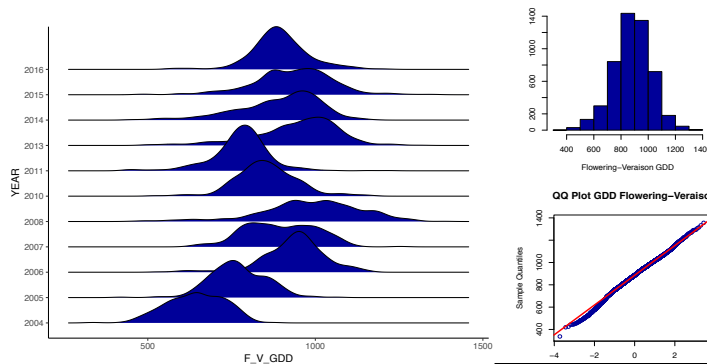
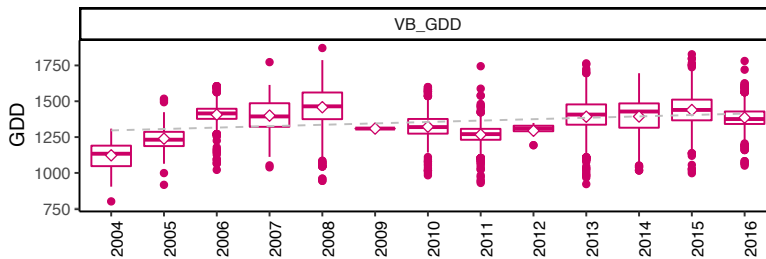
Figure 14. Panel 1. On previous page, panel showing different plots and tables regarding raw phenotypic values; flowering, veraison and flowering-veraison interval in orange, purple and blue respectively. For images, from top left, clockwise: density plots showing trait distribution over different years; histogram of overall distribution across all years; QQ plot across all years; boxplot showing inter-years differences.



Flowering GDD				
YEAR	Count	Mean	Median	SD
2004	263	479	493	28.8
2005	268	470	476	36
2006	371	469	468	25.5
2007	289	503	501	29.9
2008	568	472	472	25
2009	512	491	490	28.8
2010	573	467	466	24.9
2011	500	488	483	27.9
2012	529	550	553	32.8
2013	596	447	442	31.8
2014	570	501	505	30.9
2015	586	506	508	36
2016	527	492	482	34.8
ALL	6152	487.31	487.61	30.24



Veraison GDD				
YEAR	Count	Mean	Median	SD
2004	264	1123	1134	87.3
2005	269	1239	1232	86.3
2006	372	1407	1415	92
2007	289	1400	1394	114
2008	567	1458	1465	153
2010	569	1322	1320	90.9
2011	507	1267	1271	84.9
2013	538	1392	1407	130
2014	565	1394	1428	124
2015	583	1439	1439	121
2016	521	1386	1376	88.8
ALL	5044	1347.91	1352.82	106.6



Flowering-Veraison GDD				
YEAR	Count	Mean	Median	SD
2004	263	643	641	86.3
2005	268	769	762	83.8
2006	371	937	947	92.7
2007	288	897	893	106
2008	567	987	993	149
2010	568	855	851	91.7
2011	500	778	783	86.7
2013	536	945	967	127
2014	564	893	922	123
2015	583	934	943	118
2016	521	894	887	86.1
ALL	5029	866.545	871.727	104.6

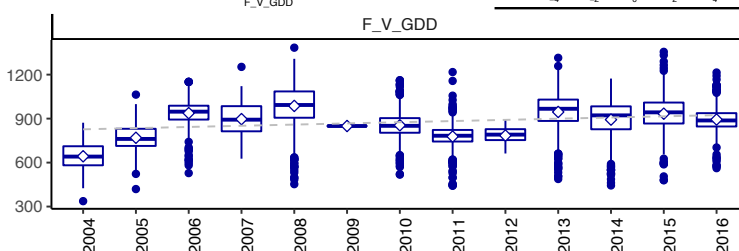
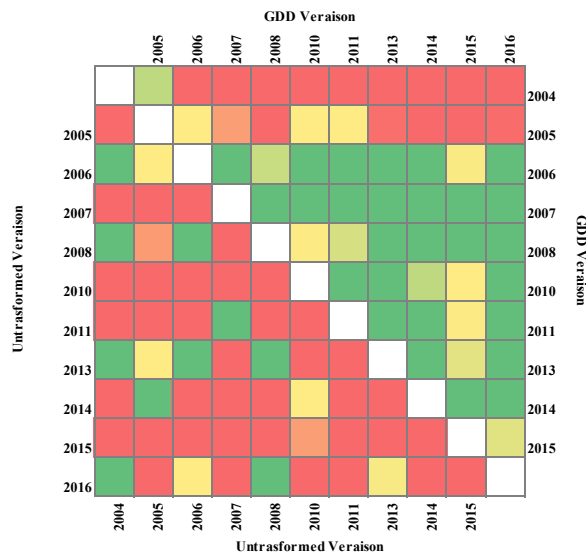
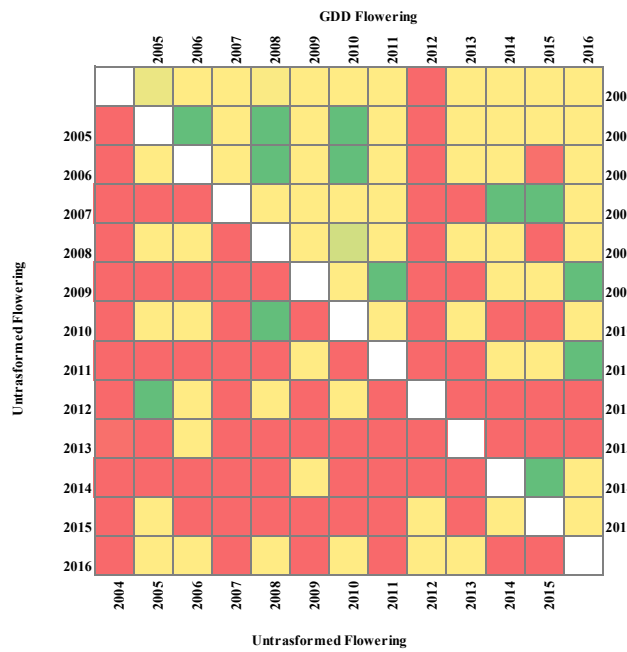


Figure 14. Panel 2. On previous page, panel showing different plots and tables regarding GDD phenotypic values; flowering, veraison and flowering-veraison interval in orange, purple and blue respectively. For images, from top left, clockwise: density plots showing trait distribution over different years; histogram of overall distribution across all years; QQ plot across all years; boxplot showing inter-years differences.



■ ■ $p < 0.001$
■ ■ ■ $0.001 < p < 1$

Figure 15. Pairwise t-test p-values intensity for flowering (upper panel) and veraison (lower panel) traits; in each panel lower triangle is raw values while upper triangle displays values for GDD values. Scales are from red to green, where red values represent more lower p-values while yellow to green values represent higher p-values.

Diversity panel construction

Since our aim was to perform a GWAS on the CCC, we wanted to utilize a subset diversity panel (core collection) representing the entire allelic diversity of the CCC. We downloaded GrapeReSeq 18K *Vitis* genotyping chip data from a recent publication (Laucou et al., 2018) consisting in a matrix of 10,207 SNPs x 783 unique grapevine individuals with no missing values. The number of cultivars in common between the 530 from CCC and the 783 was 95 (Supplementary Table 13). When highlighted in the PCA plot based on SSR data, these 95 cultivars show a sort of good coverage of the entire plot space (Figure 16).

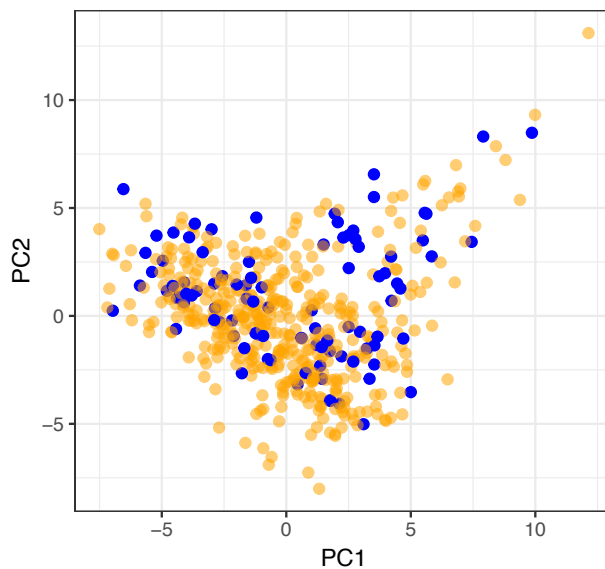


Figure 16. PCA plot based on SSR data of the CCC. In blue, the 95 cultivars in common with the French collection are highlighted. In orange, the rest of the cultivars.

When considering the average number of alleles (allelic diversity) of the 95 cultivars in common between the CCC and the French collection, the value reached is 6.95, compared to the one of the entire CCC which is 8.2. To obtain the minimum number of cultivars covering all the loci of the entire collection, we used the approach of the core collection construction, using the *R* package *corehunter* (De Beukelaer et al., 2018). This software is able to select the minimum number of representatives from larger collection, with least redundancy, while maximizing

different indexes, like allelic diversity or expected heterozygosity. Given as input the SSR genotypic data matrix from the CCC (45 SSR x 530 cultivars), and as main option, to keep the 95 cultivars in common as fixed (that is, always included in the resulting core collection), we evaluated the lowest number of cultivars needed to reach the allelic diversity average value of 8.2. As shown in Table 13, the number of cultivars needed to reach this value is 132, that is, the 95 fixed ones plus 37 additional cultivars from the CCC.

Table 13. Values of allele coverage (CV, i.e. the percentage of marker alleles observed in the full collection that are retained in the core) and allelic diversity (AD) obtained from the software corehunter, starting from the 95 cultivars fixed, adding one cultivar at the time, until reaching the complete coverage of the CCC.

N° of entries	CV	AD
95	0.8482385	6.9555557
96	0.8617886	7.06666652
97	0.8753388	7.17777816
98	0.8834688	7.24444416
99	0.8915989	7.31111098
100	0.899729	7.3777778
101	0.9051491	7.42222262
102	0.9105691	7.46666662
103	0.9159892	7.51111144
104	0.9214092	7.55555544
105	0.9268293	7.60000026
106	0.9295393	7.62222226
107	0.9322493	7.64444426
108	0.9349593	7.66666626
109	0.9376694	7.68888908
110	0.9403794	7.71111108
111	0.9430894	7.73333308
112	0.9457995	7.7555559
113	0.9485095	7.7777779
114	0.9512195	7.7999999
115	0.9539295	7.8222219
116	0.9566396	7.84444472
117	0.9593496	7.86666672
118	0.9620596	7.88888872
119	0.9647696	7.91111072
120	0.9674797	7.93333354
121	0.9701897	7.95555554
122	0.9728997	7.97777754
123	0.9756098	8.00000036
124	0.9783198	8.02222236
125	0.9810298	8.04444436
126	0.9837398	8.06666636
127	0.9864499	8.08888918
128	0.9891599	8.11111118
129	0.9918699	8.13333318
130	0.9945799	8.15555518
131	0.99729	8.177778
132	1	8.2

Since, among the 435 remaining cultivars ($530 - 95 = 435$), the number of possible combinations to choose the 37 additional one was high, we simulated 100 core collections of 132 cultivars, and selected, among the 37, the cultivars that were more present in the 100 simulations. We found 26 cultivars being always present in all the simulations; to choose the remaining 11, we counted the frequency of appearance of the remaining 11 cultivars in all the 100 core collections and selected the most frequent ones. Figure 17 shows the PCA plot where the resulting diversity panel is highlighted. The 37 additional cultivars that resulted necessary to reach the allelic diversity maximization are depicted in red in Figure 17. From their position in the PCA plot, it can be noted that they get to cover quite uniformly the remaining areas that were not fully covered with just the individuals from the French collection (in blue).

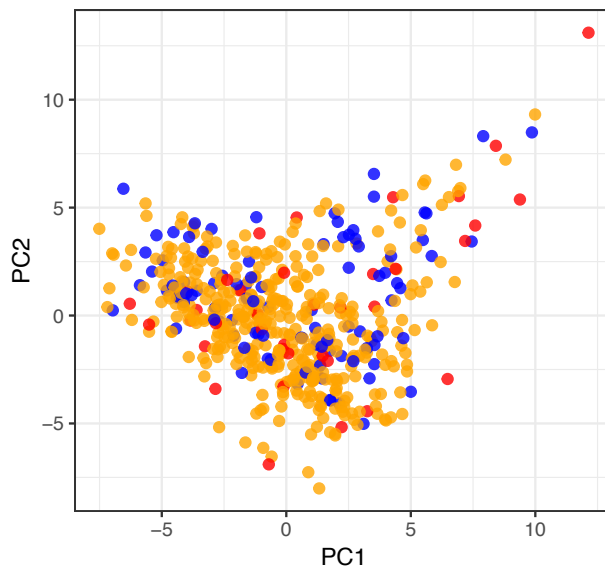


Figure 17. PCA plot based on SSR data of the CCC. In blue, the 95 cultivars in common with the French collection are highlighted. In red, the 37 cultivars that together with the 95, maximize the allelic diversity of the CCC. In orange, the rest of the cultivars.

Summary statistics of the genetic diversity of the core collection compared to the CCC are given in Table 14. The average number of observed alleles is, as requested before, the same of the CCC, while both Shannon diversity Index and expected

heterozygosity are higher than in the CCC. The index of evenness, a measure of the distribution of genotype abundances, is highly comparable between the two.

Table 14. Summary genetic diversity statistics of the core collection and the CCC.

	Na	I	He	Evenness
CORE	8.2	1.4570	0.6842	0.7526
CCC	8.2	1.4264	0.6759	0.7572

When the composition of the diversity panel from the geographical origin point of view is compared with the entire germplasm collection, the unique geographic group that shows an altered composition is the one of the cultivars from western Europe, which is enriched in the core collection compared to the entire collection (Table 15 A). When the same comparisons are made for grapes usage, no enrichment is observed (Table 15 B), and the same can be said regarding the numerosity of the cultivars of the core belonging to the subgroups identified by STRUCTURE, both when considering the 3 and the 6 groups subdivision (Table 15 C and D), suggesting a homogenous composition of the diversity panel from different perspectives. Supplementary table 14 describes the 132 cultivars included in the diversity panel.

Table 15. A. Contingency table of geographic composition of the core collection of 132 cultivars identified with corehunter. B. Contingency table of grapes usage of the core collection. C. Contingency table of the composition of the 2 subgroups subdivision identified by structure compared between the core collection and the CCC. D. Contingency table of the composition of the 6 subgroups subdivision identified by structure compared between the core collection and the CCC. In red overrepresented groups. In parenthesis, in italics are reported p-values from Fisher's Exact Test two-tailed.

A	<u>COUNTRY</u>	<u>CORE</u>	<u>CCC</u>
	AM	6 (0.1296)	11
	CI	31 (0.827)	134
	CNE	4 (0.7583)	13
	EE	9 (0.1397)	18
	IS	5 (1)	22
	IT	14 (0.2171)	83
	NI	24 (0.2142)	131
	SI	12 (0.8714)	54
	UKN	1 (1)	7
	WE	26 (0.0221)	57
		132	530

B	<u>USAGE</u>	<u>CORE</u>	<u>CCC</u>
	TABLE	18 (0.2755)	52
	TABLE/RAISIN	1 (0.4886)	2
	UKN	0	3
	WINE	89 (0.4063)	409
	WINE/TABLE	23 (0.1176)	61
	WINE/TABLE/RAISIN	1 (1)	3
		132	530

C	<u>STR-3</u>	<u>CORE</u>	<u>CCC</u>
	A-STR	49 (0.2816)	159
	B-STR	33 (0.9145)	138
	ADMIXED	50 (0.4713)	233
		132	530

D	<u>STR-6</u>	<u>CORE</u>	<u>ALL</u>
	a	18 (0.0973)	43
	b	5 (0.3576)	12
	c	2 (1)	10
	d	20 (0.2298)	56
	e	3 (0.2404)	26
	f	9 (0.0923)	67
	g (admixed)	75 (0.8099)	316
		132	530

Phenotypic diversity of the 132 cultivars of the GWAS diversity panel

We studied the phenotypic data of the 132 individuals included in the GWAS diversity panel, and compared them to the data of the entire collection, to understand if the approach of maximizing the number of alleles with the minimum number of individuals would retain a phenotypic distribution similar to the CCC one. Figure 16 shows the phenotypic distribution of the cultivars included in the

panel overlaid with the distribution of the entire collection. As can be seen from the density plots, the phenotypic values of the diversity panel precisely reflect the values of the entire collection, except for very few values in the tails.

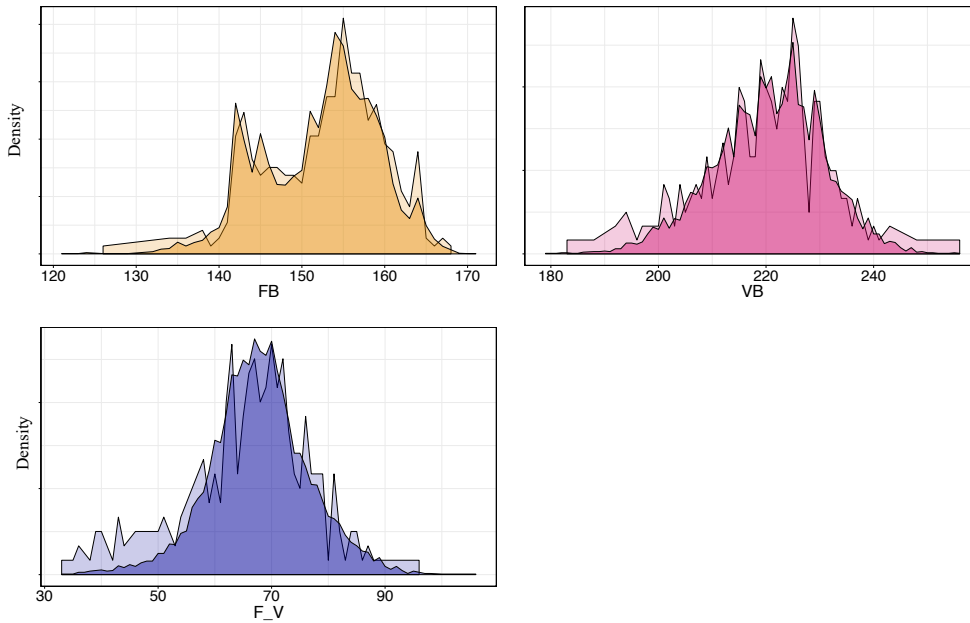


Figure 16. Density plots of the phenotypic traits flowering beginning (FB), veraison beginning (VB) and flowering-veraison interval (F_V) from the diversity panel, transparent colour, and from the entire collection, normal colour. On the x-axis the phenotypic value expressed in days of year. On the y-axis the density distribution.

Integration of published SNPchip data: DNA extraction, hybridization and SNP data extraction

DNA of the 37 additional samples identified to reach the 132 individuals diversity panel was extracted with the Qiagen DNeasy Plant Mini Kit (Qiagen, Hilden, Germany) and quantified with the NanoDrop. Supplementary Table 13 reports the concentration and quality ratio values. Approximately 1 μ L for each sample at a concentration ranging from 40-60 ng/ μ L was used to perform the GrapeReSeq 18K *Vitis* genotyping chip hybridization. Hybridizations evaluation and SNP calling were performed using the standard workflow of GenomeStudio Data Analysis v2011.1 (Illumina Inc, San Diego, CA, USA). After exporting the genotypic matrix for the 37 samples for performing the subsequent GWAS analysis we subset it to the 10,207 solid SNPs identified by Laucou et al. Among these

10,207 SNPs, we found only 97 SNPs that did not meet quality criteria, so that the resulting matrix used for GWAS was 10,110 SNPs x 37 individuals. We then merged the data matrix obtained from Laucou et al. with the data matrix produced by us and checked the consistency of both data sets in terms of genotypes scoring.

Association analysis SNPchip

Before running the association tests, we filtered SNPs having a minor allele frequency less than 0.05 using TASSEL, obtaining 9536 SNPs in total. In order to have a sort of confirmation of the design of our diversity panel, we performed a preliminary association test using the skin colour as phenotype. Using EMMAX (Kang et al., 2010) and running an association test correcting for kinship, inputting a kinship matrix as calculated by EMMAX itself on the same data matrix, we found as the most significant region associated to the colour phenotype, a region on chromosome 2 very close and overlapping to the extensively characterized colour locus (Fournier-Level et al., 2009) (Figure 17).

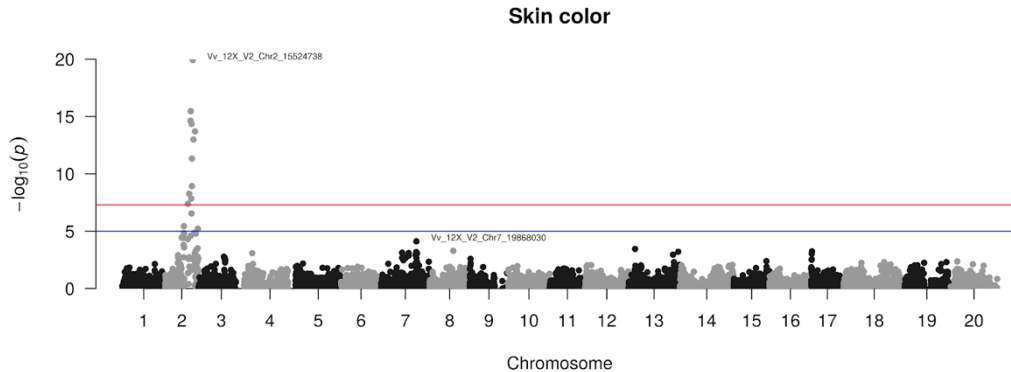


Figure 17. Manhattan plot showing the results of the GWAS association test using grapes skin colour as phenotype. Most significantly associated SNPs reside in the region of chromosome 2 around 15 Mbp. In this case GWAS was performed with EMMAX.

The most significantly associated SNP, *Vv_12X_V2_Chr2_15524738*, is also the same most significantly associated SNP found when the association test is run using QTCAT, in this way giving a significant comparison between the approaches. A

similar test with grape skin colour was performed also by Laucou et al. and they identified the same region as the most significantly associated one.

We then proceeded with performing GWAS association on the phenology phenotypes with three different software, of which, two, use population structure or kinship as factor of correction, EMMAX and Gapit, while QTCAT works without using any other file for correction. Different runs were performed leading to many combinations (Supplementary Table 17), whose most significant results for the phenotypic values averaged across all the years are reported in Table 16. In this case the most significant results come from the raw phenotypic values and not the GDD ones (results not shown). Regarding EMMAX and Gapit, to make the results more comparable, the model used for both was the one corrected only by kinship. No significant results were found for the trait flowering beginning, while different significant SNPs were found for the other 2 traits (Table 16). Regarding veraison beginning, 5 significantly associated SNPs were found but only by the QTCAT approach, that were located respectively on chromosomes 3, 12, 13, 16 and 18. Concerning flowering-veraison interval, the three approaches identified altogether 13 signals of association, located on chromosomes 4, 8, 11, 12, 14, 16 and 18. Importantly 3 SNPs were significantly associated both to the veraison beginning trait and to flowering-veraison interval, thus suggesting a relevance of these regions in controlling grape veraison time and as consequence the flowering-veraison interval length. As far as the use of different software is concerned, QTCAT identified the highest number of significantly associated SNPs (5 for veraison beginning and 10 for flowering-veraison interval) while Gapit identified three SNPs and EMMAX only one. Interestingly two of the three SNPs associated to both traits also emerged by applying different softwares.

*Table 16. The table reports the most significantly associated SNPs for the phenological traits averaged across the years. No significant results were found for the beginning of flowering. * FDR < 0.05; ** FDR < 0.01 as obtained from the approach under which the association was found. For QTCAT, the concept of FDR does not stand, so the stars are given according to the p-value.*

	Trait	Software	Significance	Multiple evidence
<i>Chr3_379409</i>	VB	QTCAT	*	No

<i>Chr4_6106210</i>	F-V	QTCAT	**	No
<i>Chr8_3847595</i>	F-V	Gapit	*	No
<i>Chr8_7340158</i>	F-V	QTCAT	*	No
<i>Chr8_8216855</i>	F-V	Gapit	**	No
<i>Chr11_963022</i>	F-V	QTCAT	*	No
<i>Chr11_1343142</i>	F-V	QTCAT	*	No
<i>Chr12_21100465</i>	VB, F-V	QTCAT, EMMAX	** $, p < 0.1$	Yes
<i>Chr13_26217739</i>	VB	QTCAT	**	No
<i>Chr14_23248717</i>	F-V	QTCAT	**	No
<i>Chr14_29502138</i>	F-V	QTCAT	**	No
<i>Chr16_348557</i>	VB, F-V, F-V	QTCAT, Gapit, QTCAT	** $, *, **$	Yes
<i>Chr16_20303373</i>	F-V	QTCAT	**	No
<i>Chr18_3381571</i>	VB, F-V	QTCAT, QTCAT	** $, **$	Yes
<i>Chr18_22124028</i>	F-V	QTCAT	**	No

For further discussion we decided to focus on the SNPs associated to both traits veraison time and flowering veraison interval. The SNP *Vv_12X_V2_Chr12_21100465* that resulted significant ($p = 0.00162$) with the software QTCAT for the veraison beginning trait, and almost significant for the flowering-veraison interval trait with the software EMMAX (FDR = 0.052). This SNP resides in the coding sequence of the gene VIT_12s0035g00280, that is annotated as an endomembrane protein 70. The second SNP that resulted in common for both traits and was revealed by between more than one approach was *Vv_12X_V2_Chr16_348557*. This SNP resulted significant with the software Gapit for the trait F-V (FDR = 0.044) and with QTCAT both for VB ($p = 0.00226$) and F-V ($p = 0.00356$). This SNP resides in the coding sequence of the gene VIT_16s0039g00700, that is annotated as a maltose transporter (RCP1 in *A. thaliana*), thus a gene involved in the carbohydrate metabolic processes. The third and last SNP pointed out as in common for both traits is *Vv_12X_V2_Chr18_3381571*. This SNP resulted significant only with the software QTCAT but with the two phenotypic traits VB ($p = 0.00318$) and F-V ($p = 0.00294$). Also this SNP resides in the coding sequence of a gene, VIT_18s0001g03540, whose function is described as an auxin transporter protein 4 (LAX2 in *A. thaliana*). Moreover, this same gene is included in a meta-QTL interval that we identified in chapter one, in particular within *pheno_18_1*, a minor meta-QTL originating from

two QTLs, one from a mapped from flowering time trait (Carreño Ruiz, 2012) and the other from veraison time trait (Zyprian et al., 2016).

Table 17. Table listing the upstream and downstream flanking genes to the most significant SNPs associated to VB and F-V traits. In the first column, highlighted in italics and bold are the genes where the significantly associated SNP falls. Only highlighted in italics are the genes considered interesting for explaining the phenotype according to their function.

Flanking genes	Chr	Start	End	Function	Gene Ontology Slim
VIT_12s0035g00200	12	20991910	21013685	Phospholipase D	lipid metabolic process; catabolic process; cellular process
VIT_12s0035g00210	12	21019518	21020261	MAPKKK19	cellular protein modification process
VIT_12s0035g00220	12	21046133	21050594	No hit	
VIT_12s0035g00240	12	21059265	21062347	DAG protein, chloroplast precursor	
VIT_12s0035g00250	12	21064129	21066252	EMB2758	
VIT_12s0035g00260	12	21070623	21081261	Mlo4	response to stress; cell death; response to biotic stimulus
VIT_12s0035g00270	12	21081724	21082383	Ferredoxin, chloroplast (PETF)	generation of precursor metabolites and energy; transport; cellular process; protein metabolic process
<i>VIT_12s0035g00280</i>	12	21083032	21100612	<i>Endomembrane protein 70</i>	
<i>VIT_12s0035g00290</i>	12	21118063	21120870	<i>Sugar transporter ERD6-like 6</i>	
<i>VIT_12s0035g00300</i>	12	21130316	21134875	<i>Carbohydrate transmembrane transporter SFP1</i>	transport; cellular process
VIT_12s0035g00310	12	21148330	21154433	Protein kinase SPK-3 ASK1 (SnRK-6)	cellular protein modification process; response to stress; signal transduction; response to abiotic stimulus; response to endogenous stimulus
VIT_12s0035g00320	12	21159933	21169655	Phosphomethylpyrimidine kinase; thiamin-phosphate pyrophosphorylase	biosynthetic process; cellular process
<i>VIT_16s0039g00570</i>	16	283917	286597	<i>10-deacetylbaocatin III 10-O-acetyltransferase</i>	cellular protein modification process
VIT_16s0039g00610	16	316837	332541	Serine/threonine-protein kinase ppk15	
VIT_16s0039g00660	16	332542	337573	RNA polymerase nonessential primary-like sigma factor SIGA	

VIT_16s0039g00690	16	341722	344560	D111/G-patch domain-containing protein	carbohydrate metabolic process; transport; catabolic process; response to biotic stimulus; cellular process
<i>VIT_16s0039g00700</i>	16	346728	353020	<i>RCPI (root cap 1)</i>	
VIT_16s0039g00720	16	357505	361097	Folate-biopterin transporter	DNA metabolic process; biosynthetic process
VIT_16s0039g00730	16	361349	363172	DNA polymerase delta, subunit D	cellular process; cellular component organization
VIT_16s0039g00740	16	370309	400930	Histone-lysine N-methyltransferase ASHH3	metabolic process
VIT_16s0039g00760	16	401533	403436	CYP89A2	
VIT_18s0001g03390	18	3298924	3306685	S-receptor kinase	carbohydrate metabolic process; cellular protein modification process; biosynthetic process; pollen-pistil interaction; cellular process
VIT_18s0001g03420	18	3307440	3307550	No hit	
<i>VIT_18s0001g03430</i>	18	3309917	3311940	<i>Flavonol synthase</i>	metabolic process; biosynthetic process; cellular process; secondary metabolic process
VIT_18s0001g03440	18	3313991	3315438	No hit	
VIT_18s0001g03450	18	3320975	3328281	Glycine-rich protein	
<i>VIT_18s0001g03470</i>	18	3338337	3340959	<i>Flavonol synthase</i>	metabolic process; biosynthetic process; cellular process; secondary metabolic process

<i>VIT_18s0001g03490</i>	18	3349225	3350592	<i>Flavonol synthase</i>	metabolic process; biosynthetic process; cellular process; secondary metabolic process
<i>VIT_18s0001g03510</i>	18	3354104	3359003	<i>Flavonol synthase XM_002284374.1</i>	metabolic process; biosynthetic process; cellular process; secondary metabolic process
VIT_18s0001g03520	18	3359393	3369207	Camphor resistance CrCB	
<i>VIT_18s0001g03540</i>	18	3380455	3383288	<i>Auxin transporter protein 4</i>	transport; signal transduction; response to endogenous stimulus
VIT_18s0001g03570	18	3387900	3389335	Thaumatococcus ATPase-1	response to stress
VIT_18s0001g03580	18	3389546	3393993	Ubiquitin-fold modifier 1 precursor	
VIT_18s0001g03610	18	3401893	3411144	Auxin-independent growth promoter	
VIT_18s0001g03630	18	3412345	3414417	Pentatricopeptide (PPR) repeat-containing protein	biological process; catabolic process; cellular process
VIT_18s0001g03640	18	3417193	3418012	No hit	
VIT_18s0001g03650	18	3418650	3419295	No hit	
<i>VIT_18s0001g03670</i>	18	3422279	3424214	<i>Zinc finger (C2H2 type) family</i>	
<i>VIT_18s0001g03680</i>	18	3433101	3445210	<i>Protein kinase</i>	cellular protein modification process
VIT_18s0001g03720	18	3445760	3445939	No hit	
VIT_18s0001g03730	18	3445960	3490992	SET Domain group 37	

Since in this diversity panel we estimated a linkage disequilibrium decay at 0.2 of around 77 Kbp (averaged across all the chromosomes and corrected by kinship with the *R* package *LDcorSV*) showed in Supplementary Table 16, it is clear that we reported only the gene closest to the significant SNP but other genes may be linked to the studied trait. Looking at the Manhattan plot and the QQ plot of expected versus observed *p-values* for the F-V GWAS performed with EMMAX, it is clear to observe that, on the contrary with the grapes skin colour phenotype, it is not possible to identify a typical dense column of SNPs with low *p-values* around the most significant one. Indeed, the most significant SNP looks like a false positive, maybe due to population structure stratification, but if we consider that for chromosome 12, LD decay at 0.2 is around 50 Kbp and after filtering the closest downstream and upstream SNPs are 20 Kbp and 48 Kbp away respectively, that does not look so much like a strange signal of association. Considering the other two significantly associated SNPs that we selected, the same idea can be applied, and we see that for SNP *Vv_12X_V2_Chr16_348557*, the closest SNPs are at 25 Kbp (down) and 22 Kbp (up), where LD decay for chromosome 16 is around 37 Kbp. For the SNP identified with QTCAT, this reasoning is more difficult to discuss since the method does not imply any kind of correction and every SNP is tested individually within blocks of similar SNPs.

A complete list of the genes flanking the three most significant selected SNPs, in the range of LD decay for that chromosome, is given in Table 17. Few interesting candidate genes are highlighted and here discussed. On chromosome 12 two downstream genes of *Vv_12X_V2_Chr12_21100465* SNP, that is *VIT_12s0035g00290* and *VIT_12s0035g00300*, appeared as functionally related to the phenotype. The first gene is annotated as a sugar transporter ERD6-like 6, a subgroup of the monosaccharide transporters family firstly described in *Arabidopsis* (Büttner, 2007). ERD stands for early-responsive to dehydration, and the gene is in fact induced upon dehydration (Kiyosue et al., 1998). Interestingly, dehydration is a characteristic step of the berry ripening process after veraison (Keller, 2010), and different transcriptomic studies have previously identified several sugar accumulation related genes as induced after veraison in the grapevine berry (Fasoli et al., 2012, 2018; Fontana et al., 2007; Massonnet et al., 2017;

Palumbo et al., 2014). The other gene is annotated as a carbohydrate transmembrane transporter SFP1, a sugar-porter family protein closely related to ERD6-like genes. SFP1 has a homolog, SFP2, and they are found as tandem genes. SFP1 was shown to be senescence-induced, which is paralleled by an accumulation of monosaccharides in the Arabidopsis leaves (Quirino et al., 2001). Regarding SNP *Vv_12X_V2_Chr16_348557* potential candidates, we highlight the gene VIT_16s0039g00570, annotated as a 10-deacetylbaocatin III 10-O-acetyltransferase, an enzyme belonging to the family of acyltransferases that catalyses the conversion of acetyl-CoA and 10-deacetylbaocatin III to CoA and baocatin III (Walker and Croteau, 2000). This enzyme participates in diterpenoid biosynthesis. Terpenoids are well known as major components for wine flavour and aroma (Lund and Bohlmann, 2006; Martin et al., 2010; Wen et al., 2015), and have been found to accumulate during the last phase of berry development, when most of the secondary metabolites accumulate (Lücker et al., 2004). Different transcriptomic studies have identified diverse genes encoding for enzymes responsible for the biosynthesis of secondary metabolites to increase their expression right before the last of the three steps of berry development (Deluc et al., 2007), but few if none have focused on this specific candidate, making it interesting for further explorations. The last one of the three candidate SNPs, *Vv_12X_V2_Chr18_3381571*, is flanked upstream by a family of flavonol synthase encoding genes. Flavonol synthase, from the family of oxidoreductases, is an enzyme that catalyses the production of flavonol. Flavonols are a predominant class of flavonoids, secondary metabolites widely present in plants, that are involved in different functions like response to biotic and abiotic stresses. In grapevine berries they accumulate in the cell wall and the vacuole of the skin cells and are almost absent in the pulp. Like anthocyanins, the determinants of the red colour in red grapevine cultivars, flavonols are a product of the phenylpropanoid pathway. Regarding the content of flavonols in the berry skin during development, it has been found to start accumulation right after veraison, and then reach a maximum at the initial stage of berry development (Downey et al., 2003). Other genes encoding for flavonol synthase or for different enzymes involved in the phenylpropanoid pathway have been also recently emerged as candidates from few transcriptomics

experiments (Fasoli et al., 2012; Palumbo et al., 2014); even more recently a gene encoding for a 2'-hydroxy isoflavone/dihydroflavonol reductase (from the anthocyanin biosynthesis) has been defined, amongst others, as a marker transition gene, representing a gene that marks the transition to the late ripening stages of the berry, in agreement to the observation on the accumulation of anthocyanins (Downey et al., 2003).

When we looked at the phenotypic differences for the three allelic combinations of each one of the three most interesting SNPs, selected for resulting as significantly associated across more than one trait or more than one software, in almost all cases we observe quite a significant difference between the heterozygotes and the homozygotes cultivars for those SNPs, as shown in Figure 17.

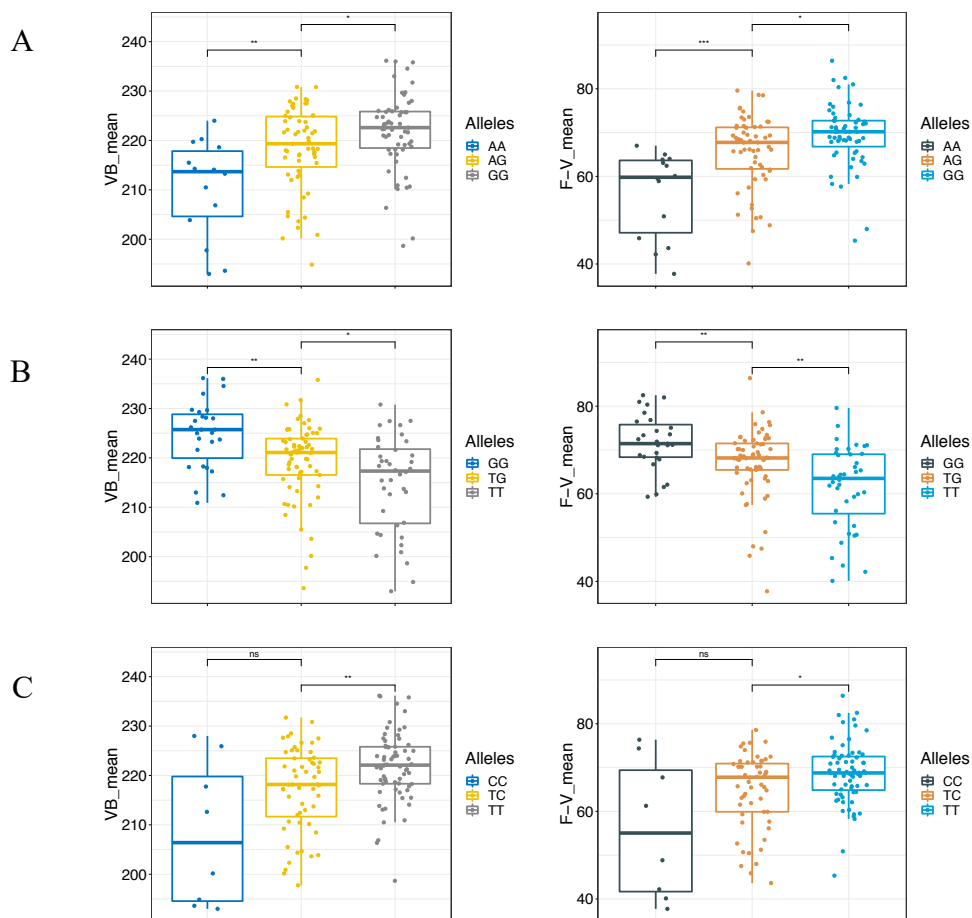


Figure 17. Boxplots showing phenotypic values of veraison beginning and flowering-veraison interval phenotypes against genotypes of the three selected SNPs significantly associated to the traits. The three SNPs *Vv_12X_V2_Chr12_21100465*, *Vv_12X_V2_Chr16_348557* and *Vv_12X_V2_Chr18_3381571* are in A, B and C respectively.

In particular for SNP *Vv_12X_V2_Chr16_348557* where the cultivars seem more equally distributed in the three genotypic classes, the differences are quite significant and an average of around ten days diversity in the veraison date and flowering-veraison time interval is observed between the two homozygotes (Figure 17 B).

Overall, the results suggest that probably a bigger sample size is needed to catch all the rare alleles. Indeed phenology in general, and in particular veraison time, is considered a polygenic complex trait, with many loci contributing to small variations, and many authors have previously failed to identify strong signals of association for such complex traits (Marrano et al., 2018; Migicovsky et al., 2017; Myles et al., 2011). Moreover, the grapevine SNPchip, with its 10K SNPs, may not be an adequate technology to identify all the small variance-contributors loci for such complex traits. In particular because linkage disequilibrium extends longer for regions subject to selection but, on the contrary to berry size or grapes skin colour, which are typical traits selected over many generations, the time of veraison and phenology in general are traits that have not been selected since long times.

To overcome such limitations, we opted for a different experimental design that takes into account the phenotypic diversity of a germplasm collection and measures allele frequencies in the extreme pools, enabling discovery of associations between genetic variants and traits of interest, without testing the association of the single individual to the phenotype. Indeed, the XP-GWAS approach overcome the limitations of a SNPchip GWAS by allowing a bigger sample size at a reduced cost, enriching for rare alleles and augment allele effects via extreme phenotypic selection, and using a whole-genome resequencing approach, opposed to genotyping chip where density of coverage of the genome is way lower than in a resequencing. Moreover, XP-GWAS, by considering the average phenotypic value of a pool of individuals, tolerates a degree of inaccuracy in the phenotyping data, which is desirable for traits difficult to phenotype like flowering and veraison time

or phenology in general, where the trait is not easily quantifiable by human eyes. We created three pools of individuals, named low, high and random pool by observing the distribution of the flowering-veraison interval trait and after DNA pooling, we are currently subjecting them to resequencing.

Conclusions

Grapevine veraison is a stage that is critical for determining the final quality of the grape, and ultimately the wine. The transition from the immature to the mature stage of the grapevine berry has been demonstrated to be a critical point where environmental conditions can impact significantly the entire cycle of formation of the berry and its components. In particular, in a scenario where climate change will impact the temperature with a forecasted increase of around 2 degrees in the next 50 years in many areas including the most famous viticulture area (Jones et al., 2005), this situation may disclose different aspects to be taken into account when considering viticulture and the winemaking process. For example, it has been demonstrated that higher temperatures impact the formation of typical compounds of the grape berry skin, like flavonoids and anthocyanins in particular (Mori et al., 2007; Pastore et al., 2017; Yamane et al., 2006) and this will affect the assembly of other compounds that represent the specificity of a wine, like tannins. The increased temperature of the last years led to and will lead to an advance of the phenological stages (Tomasi et al., 2011), and this advance could bring to a more rapid ripening phase, that when different to a normal maturation is not paralleled by the accumulation of flavour components that require more time to store. In particular, if veraison will occur earlier during the season there will be less time for the pre-veraison production of flavanols that can be assembled into tannins before and during ripening. A possible overcome to this problem is to wait the flavours to assemble and develop but doing so, grapes are harvested with very high sugar concentrations that will result in wines with high alcohol contents. Temperature is not the only factor that can influence phenological stages in grapevine, but also conditions of water deficit, both before and after veraison, can impact the formation of organic compounds in the berry and in particular in the skins (Ojeda et al., 2002). With such a scenario, different approaches may be taken in order to contrast the effect of climate change on grapevine phenology. The genetic approach, that is for example exploiting genetic diversity from the wild or from germplasm collections to integrate rare and natural alleles into existing cultivars, is a long process and it still needs to be addressed carefully in grapevine. The genetics underlying complex traits like phenology is still poorly known. Here, by integrating different genetic

approaches to identify the genetic determinants of grapevine veraison process, we aimed to produce relevant information towards the disclosure of the major loci contributing to the berry ripening process.

In the first chapter we created the first integrated consensus map of grapevine from different individual grapevine genetic maps with the aim to perform the first meta-QTL analysis for grapevine. In detail, we collected genetic maps info from 42 different publications and integrated them with a statistical approach, in order to obtain the most significant and reliable grapevine consensus map that can be used to summarize and integrate different QTL results. We collected all the available QTL information that were produced for grapevine and then we focused on phenological traits. We identified 4 meta-QTLs for the veraison trait that represent the most reliable genomic spots where the most significant QTLs mapped for veraison so far have been identified. One of the main aims was to reduce the number of possible positional candidate genes comprised in the high number of veraison associated QTL present in literature. In performing such meta-analysis, we were able to reduce the number of candidate genes by almost 4-fold. Indeed, one of the main limitations of the QTL approach is the downstream analysis represented by the search of the candidate genes; since the number of genes within the interval of a QTL can be really high, an approach that tries to reduce this number may be eventually useful, especially in situations where the trait studied is a complex trait, and the loci governing the trait are numerous. After performing the meta-analysis of the QTLs, we integrated data from different transcriptomic experiments, given the idea that the genes resulting differentially expressed across veraison time in grapevine berries may be also in common with positional candidate genes deriving from QTL studies. In particular, different previous transcriptomic experiments (Fasoli et al., 2012; Massonnet et al., 2017; Palumbo et al., 2014) have identified a number of candidate genes that are either up or down regulated across the veraison stage of grapevine berries and are considered as master regulators of the transition from the green to the mature stage of the grapevine. For example, some special sets of the genes identified, for example the “switch genes” (Palumbo et al., 2014) characterized with a network analysis as having many significant negative

correlations outside their own group in the network, represent a group of genes, mainly transcription factors, considered as master regulators of the transcriptome remodelling marking the developmental shift from immature to mature growth. We found some of these special master regulators to lie within the meta-QTL intervals, indicating that the integration of different approaches, from summarizing QTL data to integrating existent transcriptomic data, may be helpful to prioritize most significant results, with the final aim of identifying a restricted number of candidate genes to be explored individually.

In the second chapter we studied the genetic diversity of a grapevine germplasm collection, in order to identify the most genetically diverse and representative panel of individuals to be used for genetic association study. Studying the population structure of the collection, we firstly found out that the Conegliano collection is mostly composed by cultivars from Italian origin, and even so, the overall genetic diversity is comparable to the one of other germplasm collection, indicating that among all *Vitis vinifera* cultivars, the overall genetic diversity is easily reached with a small number of alleles. We were able to identify significant genetically distinct subgroups/substructure in the collection, and found that this subgroups resemble the geographical subdivision of the collection. We collected all these information and used them to construct diversity panels to be used for association analysis. Before, we made use of existing genotypic data, with the idea of integrating them with newly generated data. Through the use of the GrapeReseq Vitis Genotyping Chip we genotyped additional cultivars that from the genetic point of view summarize the entire collection, and tested the genotype-phenotype association with an incredible resource of grapevine phenology phenotypic data provided by our CREA-VIT Conegliano partners. Though some limitations due to sample size, genetic architecture of the trait, and not easily scorable phenotypic traits, we identified some significant genomic regions that would represent the most interesting regions linked to veraison time traits. For doing so, we did not only used the classical GWAS approach, but we had the idea of integrating different approaches represented by different software that apply different statistical procedures. Moreover, we integrated the results from the GWAS approach with the

results of the meta-analysis of the QTLs and found that one of the veraison time most significantly associated SNP is located precisely in a meta-QTL interval on chromosome 18.

We have shown that the integration of existing data, also of different sources, is a strategic procedure when the nature of the trait studied is complex and multifaceted. Also with limited resources, the summarization of existing results and the exploration of new results with the aid of reorganized and prioritized information, may disclose novel targets and shed light on the genetic control of complex traits.

Acronyms

CCC CREA-VIT Conegliano Collection

DAPC Discriminant Analysis of Principal Components

FB Flowering beginning

F-V Flowering-Veraison interval

GCM Grapevine Consensus Map

GWAS Genome Wide Association Study

LD Linkage Disequilibrium

PCA Principal Component Analysis

QTL Quantitative Trait Loci

SNP Single Nucleotide Polymorphism

SSR Simple Sequence Repeat

VB Veraison beginning

Bibliography

- Ananiev, E. V., Rafalski, J.-A., Svtashev, S., Niu, X., Tingey, S. V., Sponza, G., et al. (2007). Conserved noncoding genomic sequences associated with a flowering-time quantitative trait locus in maize. *Proc. Natl. Acad. Sci.* 104, 11376–11381. doi:10.1073/pnas.0704145104.
- Bancroft, I., Morgan, C., Meng, J., Jiang, C., Qiu, D., Li, R., et al. (2009). Unraveling the Complex Trait of Crop Yield With Quantitative Trait Loci Mapping in Brassica napus. *Genetics* 182, 851–861. doi:10.1534/genetics.109.101642.
- Bayo Canha, A. (2016). Genetic analysis of traits of interest in *Vitis vinifera* using a progeny of wine grapes: Monastrell x Syrah. Available at: <http://repositorio.upct.es/xmlui/handle/10317/5393?locale-attribute=en> [Accessed October 30, 2017].
- Blasi, P., Blanc, S., Wiedemann-Merdinoglu, S., Prado, E., Rühl, E. H., Mestre, P., et al. (2011). Construction of a reference linkage map of *Vitis amurensis* and genetic mapping of *Rpv8*, a locus conferring resistance to grapevine downy mildew. *Theor. Appl. Genet.* 123, 43–53. doi:10.1007/s00122-011-1565-0.
- Boss, P. K., Buckeridge, E. J., Poole, A., and Thomas, M. R. (2003). New insights into grapevine flowering. *Funct. Plant Biol.* 30, 593. doi:10.1071/FP02112.
- Büttner, M. (2007). The monosaccharide transporter(-like) gene family in Arabidopsis. *FEBS Lett.* 581, 2318–2324. doi:10.1016/J.FEBSLET.2007.03.016.
- Canaguier, A., Grimplet, J., Di Gaspero, G., Scalabrin, S., Duchêne, E., Choisne, N., et al. (2017). A new version of the grapevine reference genome assembly (12X.v2) and of its annotation (VCost.v3). *Genomics Data* 14, 56–62. doi:10.1016/J.GDATA.2017.09.002.
- Carmona, M. J., Chaib, J., Martinez-Zapater, J. M., and Thomas, M. R. (2008). A molecular genetic perspective of reproductive development in grapevine. *J. Exp. Bot.* 59, 2579–2596. doi:10.1093/jxb/ern160.
- Carreño Ruiz, I. (2012). Identificación de regiones cromosómicas implicadas en el control genético de caracteres de interés para la mejora genética de la uva de mesa.

Proy. Investig. Available at: <https://digitum.um.es/xmlui/handle/10201/28936>
[Accessed October 30, 2017].

- Chardon, F., Virlon, B., Moreau, L., Falque, M., Joets, J., Decousset, L., et al. (2004). Genetic architecture of flowering time in maize as inferred from quantitative trait loci meta-analysis and synteny conservation with the rice genome. *Genetics* 168, 2169–2185. doi:10.1534/genetics.104.032375.
- Chin, C.-S., Peluso, P., Sedlazeck, F. J., Nattestad, M., Concepcion, G. T., Clum, A., et al. (2016). Phased diploid genome assembly with single-molecule real-time sequencing. *Nat. Methods* 13, 1050–1054. doi:10.1038/nmeth.4035.
- Christenhusz, M. J. M., and Byng, J. W. (2016). The number of known plants species in the world and its annual increase. *Phytotaxa* 261, 201–217. doi:10.11646/phytotaxa.261.3.1.
- Cipriani, G., Spadotto, A., Jurman, I., Gaspero, G. Di, Crespan, M., Meneghetti, S., et al. (2010). The SSR-based molecular profile of 1005 grapevine (*Vitis vinifera* L.) accessions uncovers new synonymy and parentages, and reveals a large admixture amongst varieties of different geographic origin. *Theor. Appl. Genet.* 121, 1569–1585. doi:10.1007/s00122-010-1411-9.
- Coombe, B., and Bishop, G. (1980). Development of the grape berry. II. Changes in diameter and deformability during veraison. *Aust. J. Agric. Res.* 31, 499. doi:10.1071/AR9800499.
- Coombe, B. G. (1995). Growth Stages of the Grapevine: Adoption of a system for identifying grapevine growth stages. *Aust. J. Grape Wine Res.* 1, 104–110. doi:10.1111/j.1755-0238.1995.tb00086.x.
- Costantini, L., Battilana, J., Lamaj, F., Fanizza, G., and Grando, M. (2008). Berry and phenology-related traits in grapevine (*Vitis vinifera* L.): From Quantitative Trait Loci to underlying genes. *BMC Plant Biol.* 8, 38. doi:10.1186/1471-2229-8-38.
- Danan, S., Veyrieras, J.-B., and Lefebvre, V. (2011). Construction of a potato consensus map and QTL meta-analysis offer new insights into the genetic architecture of late blight resistance and plant maturity traits. *BMC Plant Biol.* 11, 16. doi:10.1186/1471-2229-11-16.

- De Beukelaer, H., Davenport, G. F., and Fack, V. (2018). Core Hunter 3: flexible core subset selection. *BMC Bioinformatics* 19, 203. doi:10.1186/s12859-018-2209-z.
- De Cortázar-Atauri, I. G., Duchêne, É., Destrac-Irvine, A., Barbeau, G., De Rességuier, L., Lacombe, T., et al. (2017). Grapevine phenology in France: From past observations to future evolutions in the context of climate change. *J. Int. des Sci. la Vigne du Vin* 51, 115–126. doi:10.20870/oeno-one.2016.0.0.1622.
- Delrot, S., Duchêne, E., Garcia de Cortazar-Atauri, I., Pieri, P., Bois, B., Bavaresco, L., et al. (2013). Why climate change will not dramatically decrease viticultural suitability in main wine-producing areas by 2050. *Proc. Natl. Acad. Sci.* 110, E3051–E3052. doi:10.1073/pnas.1307927110.
- Deluc, L. G., Grimplet, J., Wheatley, M. D., Tillett, R. L., Quilici, D. R., Osborne, C., et al. (2007). Transcriptomic and metabolite analyses of Cabernet Sauvignon grape berry development. *BMC Genomics* 8, 429. doi:10.1186/1471-2164-8-429.
- Di Matteo, A., Giovane, A., Raiola, A., Camardella, L., Bonivento, D., De Lorenzo, G., et al. (2005). Structural Basis for the Interaction between Pectin Methyltransferase and a Specific Inhibitor Protein. *PLANT CELL ONLINE* 17, 849–858. doi:10.1105/tpc.104.028886.
- Doligez, A., Adam-Blondon, A. F., Cipriani, G., Di Gaspero, G., Laucou, V., Merdinoglu, D., et al. (2006). An integrated SSR map of grapevine based on five mapping populations. *Theor. Appl. Genet.* 113, 369–382. doi:10.1007/s00122-006-0295-1.
- Downey, M. O., Harvey, J. S., and Robinson, S. P. (2003). Analysis of tannins in seeds and skins of Shiraz grapes throughout berry development. *Aust. J. Grape Wine Res.* 9, 15–27. doi:10.1111/j.1755-0238.2003.tb00228.x.
- Duchene, E. (2016). How can grapevine genetics contribute to the adaptation to climate change? *OENO One* 50. doi:10.20870/oeno-one.2016.50.3.98.
- Duchêne, E., Butterlin, G., Claudel, P., Dumas, V., Jaegli, N., and Merdinoglu, D. (2009). A grapevine (*Vitis vinifera* L.) deoxy-d-xylulose synthase gene colocates with a major quantitative trait loci for terpenol content. *Theor. Appl. Genet.* 118, 541–552. doi:10.1007/s00122-008-0919-8.

- Duchêne, E., Butterlin, G., Dumas, V., and Merdinoglu, D. (2012). Towards the adaptation of grapevine varieties to climate change: QTLs and candidate genes for developmental stages. *Theor. Appl. Genet.* 124, 623–635. doi:10.1007/s00122-011-1734-1.
- Duchêne, E., Huard, F., Dumas, V., Schneider, C., and Merdinoglu, D. (2010). The challenge of adapting grapevine varieties to climate change. *Clim. Res.* 41, 193–204. doi:10.3354/cr00850.
- Emanuelli, F., Lorenzi, S., Grzeskowiak, L., Catalano, V., Stefanini, M., Troggio, M., et al. (2013). Genetic diversity and population structure assessed by SSR and SNP markers in a large germplasm collection of grape. *BMC Plant Biol.* 13, 39. doi:10.1186/1471-2229-13-39.
- Evanno, G., Regnaut, S., and Goudet, J. (2005). Detecting the number of clusters of individuals using the software STRUCTURE: A simulation study. *Mol. Ecol.* 14, 2611–2620. doi:10.1111/j.1365-294X.2005.02553.x.
- Fasoli, M., Dal Santo, S., Zenoni, S., Tornielli, G. B., Farina, L., Zamboni, A., et al. (2012). The Grapevine Expression Atlas Reveals a Deep Transcriptome Shift Driving the Entire Plant into a Maturation Program. *Plant Cell* 24, 3489–3505. doi:10.1105/tpc.112.100230.
- Fasoli, M., Richter, C. L., Zenoni, S., Bertini, E., Vitulo, N., Dal Santo, S., et al. (2018). Timing and Order of the Molecular Events Marking the Onset of Berry Ripening in Grapevine. *Plant Physiol.* 178, 1187–1206. doi:10.1104/pp.18.00559.
- Fechter, I., Hausmann, L., Zyprian, E., Daum, M., Holtgräwe, D., Weisshaar, B., et al. (2014). QTL analysis of flowering time and ripening traits suggests an impact of a genomic region on linkage group 1 in *Vitis*. *Theor. Appl. Genet.* 127, 1857–1872. doi:10.1007/s00122-014-2310-2.
- Fennell, A., Clark, L., McKay, S., Mathiason, K., Luby, J., Owens, C., et al. (2019). Mapping of Photoperiod-induced Growth Cessation in the Wild Grape *Vitis riparia*. *J. Am. Soc. Hortic. Sci.* 134, 261–272. doi:10.21273/jashs.134.2.261.
- Fennell, A. Y., Schlauch, K. A., Gouthu, S., Deluc, L. G., Khadka, V., Sreekantan, L., et al. (2015). Short day transcriptomic programming during induction of dormancy in

- grapevine. *Front. Plant Sci.* 6, 834. doi:10.3389/fpls.2015.00834.
- Fischer, B. M., Salakhutdinov, I., Akkurt, M., Eibach, R., Edwards, K. J., Töpfer, R., et al. (2004). Quantitative trait locus analysis of fungal disease resistance factors on a molecular map of grapevine. *Theor. Appl. Genet.* 108, 501–515. doi:10.1007/s00122-003-1445-3.
- Fontana, P., Moser, C., Malossini, A., Viola, R., Cestaro, A., Demattè, L., et al. (2007). Genome-wide transcriptional analysis of grapevine berry ripening reveals a set of genes similarly modulated during three seasons and the occurrence of an oxidative burst at véraison. *BMC Genomics* 8, 428. doi:10.1186/1471-2164-8-428.
- Fournier-Level, A., Le Cunff, L., Gomez, C., Doligez, A., Ageorges, A., Roux, C., et al. (2009). Quantitative genetic bases of anthocyanin variation in grape (*Vitis vinifera* L. ssp. *sativa*) berry: a quantitative trait locus to quantitative trait nucleotide integrated study. *Genetics* 183, 1127–39. doi:10.1534/genetics.109.103929.
- Gambetta, G. A., Wada, H., Matthews, M. A., Cramer, G. R., Peterlunger, E., Castellarin, S. D., et al. (2015). Characterization of major ripening events during softening in grape: turgor, sugar accumulation, abscisic acid metabolism, colour development, and their relationship with growth. *J. Exp. Bot.* 67, 709–722. doi:10.1093/jxb/erv483.
- Giovanelli, G., and Brenna, O. V. (2007). Evolution of some phenolic components, carotenoids and chlorophylls during ripening of three Italian grape varieties. *Eur. Food Res. Technol.* 225, 145–150. doi:10.1007/s00217-006-0436-4.
- Goffinet, B., and Gerber, S. (2000). Quantitative trait loci: A meta-analysis. *Genetics* 155, 463–473.
- Jaillon, O., Aury, J. M., Noel, B., Policriti, A., Clepet, C., Casagrande, A., et al. (2007). The grapevine genome sequence suggests ancestral hexaploidization in major angiosperm phyla. *Nature* 449, 463–467. doi:10.1038/nature06148.
- Jombart, T., and Collins, C. (2015). A tutorial for Discriminant Analysis of Principal Components (DAPC) using adegenet 2.0.0. Available at: <http://adegenet.r-forge.r-project.org/files/tutorial-dapc.pdf> [Accessed August 22, 2017].
- Jombart, T., Devillard, S., and Balloux, F. (2010). Discriminant analysis of principal

- components: a new method for the analysis of genetically structured populations. *BMC Genet.* 11, 94. doi:10.1186/1471-2156-11-94.
- Jones, V. G., White, M. A., Cooper, O. R., and Storchmann, K. (2005). Climate Change and Global Wine Quality. *Clim. Change* 73, 319–343. doi:10.1007/s10584-005-4704-2.
- Kamvar, Z. N., Tabima, J. F., and Grünwald, N. J. (2014). *Poppr* : an R package for genetic analysis of populations with clonal, partially clonal, and/or sexual reproduction. *PeerJ* 2, e281. doi:10.7717/peerj.281.
- Kang, H. M., Sul, J. H., Service, S. K., Zaitlen, N. A., Kong, S., Freimer, N. B., et al. (2010). Variance component model to account for sample structure in genome-wide association studies. *Nat. Genet.* 42, 348–354. doi:10.1038/ng.548.
- Keller, M. (2010). *The science of grapevines - anatomy and physiology*. doi:10.1016/B978-0-12-374881-2.00012-X.
- Keller, M., Tarara, J. M., and Mills, L. J. (2010). Spring temperatures alter reproductive development in grapevines. *Aust. J. Grape Wine Res.* 16, 445–454. doi:10.1111/j.1755-0238.2010.00105.x.
- Khowaja, F. S., Norton, G. J., Courtois, B., and Price, A. H. (2009). Improved resolution in the position of drought-related QTLs in a single mapping population of rice by meta-analysis. *BMC Genomics* 10, 276. doi:10.1186/1471-2164-10-276.
- Kiyosue, T., Abe, H., Yamaguchi-Shinozaki, K., and Shinozaki, K. (1998). ERD6, a cDNA clone for an early dehydration-induced gene of Arabidopsis, encodes a putative sugar transporter. *Biochim. Biophys. Acta - Biomembr.* 1370, 187–191. doi:10.1016/S0005-2736(98)00007-8.
- Klasen, J. R., Barbez, E., Meier, L., Meinshausen, N., Bühlmann, P., Koornneef, M., et al. (2016). A multi-marker association method for genome-wide association studies without the need for population structure correction. *Nat. Commun.* 7. doi:10.1038/ncomms13299.
- Kobayashi, S., Goto-Yamamoto, N., and Hirochika, H. (2004). Retrotransposon-Induced Mutations in Grape Skin Color. *Science (80-.)*. 304, 982. doi:10.1126/science.1095011.

- Laucou, V., Launay, A., Bacilieri, R., Lacombe, T., Adam-Blondon, A.-F., Bérard, A., et al. (2018). Extended diversity analysis of cultivated grapevine *Vitis vinifera* with 10K genome-wide SNPs. *PLoS One* 13, e0192540. doi:10.1371/journal.pone.0192540.
- Lebon, G., Wojnarowicz, G., Holzapfel, B., Fontaine, F., Vaillant-Gaveau, N., and Clement, C. (2008). Sugars and flowering in the grapevine (*Vitis vinifera* L.). *J. Exp. Bot.* 59, 2565–2578. doi:10.1093/jxb/ern135.
- Lionetti, V., Raiola, A., Mattei, B., and Bellincampi, D. (2015). The Grapevine VvPMEI1 Gene Encodes a Novel Functional Pectin Methyltransferase Inhibitor Associated to Grape Berry Development. *PLoS One* 10, e0133810. doi:10.1371/journal.pone.0133810.
- Lipka, A. E., Tian, F., Wang, Q., Peiffer, J., Li, M., Bradbury, P. J., et al. (2012). GAPIT: genome association and prediction integrated tool. *Bioinformatics* 28, 2397–2399. doi:10.1093/bioinformatics/bts444.
- Lorenz, D., Eichhorn, K., Holder, H., Klose, R., Meier, U. C., Weber, E., et al. (1994). Phänologische Entwicklungsstadien der Weinrebe (*Vitis vinifera* L. ssp. *vinifera*). Available at: <https://www.scienceopen.com/document?vid=a6780a45-bc95-4678-96c7-4b66a4f9f6be> [Accessed December 11, 2018].
- Lücker, J., Bowen, P., and Bohlmann, J. (2004). *Vitis vinifera* terpenoid cyclases: functional identification of two sesquiterpene synthase cDNAs encoding (+)-valencene synthase and (–)-germacrene D synthase and expression of mono- and sesquiterpene synthases in grapevine flowers and berries. *Phytochemistry* 65, 2649–2659. doi:10.1016/j.phytochem.2004.08.017.
- Lund, S. T., and Bohlmann, J. (2006). The Molecular Basis for Wine Grape Quality-A Volatile Subject. *Science* (80-.). 311, 804–805. doi:10.1126/science.1118962.
- Mangin, B., Siberchicot, A., Nicolas, S., Doligez, A., This, P., and Cierco-Ayrolles, C. (2012). Novel measures of linkage disequilibrium that correct the bias due to population structure and relatedness. *Heredity (Edinb)*. 108, 285–291. doi:10.1038/hdy.2011.73.
- Marrano, A., Micheletti, D., Lorenzi, S., Neale, D., and Grando, M. S. (2018).

Horticulture Research Genomic signatures of different adaptations to environmental stimuli between wild and cultivated *Vitis vinifera* L. *Hortic. Res.* 5, 34.
doi:10.1038/s41438-018-0041-2.

Martin, D. M., Aubourg, S., Schouwey, M. B., Daviet, L., Schalk, M., Toub, O., et al. (2010). Functional annotation, genome organization and phylogeny of the grapevine (*Vitis vinifera*) terpene synthase gene family based on genome assembly, FLcDNA cloning, and enzyme assays. *BMC Plant Biol.* 10, 226. doi:10.1186/1471-2229-10-226.

Massonnet, M., Fasoli, M., Tornielli, G. B., Altieri, M., Sandri, M., Zuccolotto, P., et al. (2017). Ripening Transcriptomic Program in Red and White Grapevine Varieties Correlates with Berry Skin Anthocyanin Accumulation. *Plant Physiol.* 174, 2376–2396. doi:10.1104/pp.17.00311.

Migicovsky, Z., Sawler, J., Gardner, K. M., Aradhya, M. K., Prins, B. H., Schwaninger, H. R., et al. (2017). Patterns of genomic and phenomic diversity in wine and table grapes. *Hortic. Res.* 4, hortres201735. doi:10.1038/hortres.2017.35.

Mori, K., Goto-Yamamoto, N., Kitayama, M., and Hashizume, K. (2007). Loss of anthocyanins in red-wine grape under high temperature. *J. Exp. Bot.* 58, 1935–1945. doi:10.1093/jxb/erm055.

Mosedale, J. R., Wilson, R. J., and Maclean, I. M. D. (2015). Climate Change and Crop Exposure to Adverse Weather: Changes to Frost Risk and Grapevine Flowering Conditions. *PLoS One* 10, e0141218. doi:10.1371/journal.pone.0141218.

Mullins, M. G., Bouquet, A., and Williams, L. E. (1992). Biology of the grapevine. *Biol. grapevine*. Available at: <https://www.cabdirect.org/cabdirect/abstract/19920316870> [Accessed November 19, 2018].

Myles, S., Boyko, A. R., Owens, C. L., Brown, P. J., Grassi, F., Aradhya, M. K., et al. (2011). Genetic structure and domestication history of the grape. *Proc. Natl. Acad. Sci.* 108, 3530–3535. doi:10.1073/pnas.1009363108.

Negrul, A. M., Baranov, A., Kai, Y., Lazarevski, M., Palibin, T., and Prosmoserdov, N. (1946). “Origin and classification of cultivated grape,” in, 159–216.

Nicolas, S. D., Péros, J.-P., Lacombe, T., Launay, A., Le Paslier, M.-C., Bérard, A., et al.

- (2016). Genetic diversity, linkage disequilibrium and power of a large grapevine (*Vitis vinifera* L) diversity panel newly designed for association studies. *BMC Plant Biol.* 16, 74. doi:10.1186/s12870-016-0754-z.
- Niculcea, M., López, J., Sánchez-Díaz, M., and Carmen Antolín, M. (2014). Involvement of berry hormonal content in the response to pre- and post-veraison water deficit in different grapevine (*Vitis vinifera* L.) cultivars. *Aust. J. Grape Wine Res.* 20, 281–291. doi:10.1111/ajgw.12064.
- Ojeda, H., Andary, C., Kraeva, E., Carbonneau, A., and Deloire, A. (2002). Influence of Pre- and Postveraison Water Deficit on Synthesis and Concentration of Skin Phenolic Compounds during Berry Growth of *Vitis vinifera* cv. Shiraz. *Am. J. Enol. Vitic.* 53, 261–267. Available at: <http://www.ajevonline.org/content/53/4/261.1> [Accessed December 10, 2018].
- Palumbo, M. C., Zenoni, S., Fasoli, M., Massonnet, M., Farina, L., Castiglione, F., et al. (2014). Integrated Network Analysis Identifies Fight-Club Nodes as a Class of Hubs Encompassing Key Putative Switch Genes That Induce Major Transcriptome Reprogramming during Grapevine Development. *Plant Cell Online* 26, 4617–4635. doi:10.1105/tpc.114.133710.
- Paslier M-C, L., Choisne, N., R, B., R, B., Boursiquot, J.-M., D, B., et al. (2013). *The GrapeReSeq 18 k Vitis genotyping chip.*
- Pastore, C., Dal Santo, S., Zenoni, S., Movahed, N., Allegro, G., Valentini, G., et al. (2017). Whole Plant Temperature Manipulation Affects Flavonoid Metabolism and the Transcriptome of Grapevine Berries. *Front. Plant Sci.* 8, 929. doi:10.3389/fpls.2017.00929.
- Peakall, R., and Smouse, P. E. (2012). GenA1Ex 6.5: genetic analysis in Excel. Population genetic software for teaching and research--an update. *Bioinformatics* 28, 2537–2539. doi:10.1093/bioinformatics/bts460.
- Petrie, P. R., and Clingeleffer, P. R. (2005). Effects of temperature and light (before and after budburst) on inflorescence morphology and flower number of Chardonnay grapevines (*Vitis vinifera* L.). *Aust. J. Grape Wine Res.* 11, 59–65. doi:10.1111/j.1755-0238.2005.tb00279.x.

- Pritchard, J. K., Stephens, M., and Donnelly, P. (2000). Inference of population structure using multilocus genotype data. *Genetics* 155, 945–959. Available at: <http://www.ncbi.nlm.nih.gov/pmc/articles/PMC1461096/> [Accessed September 19, 2016].
- Quirino, B. F., Reiter, W.-D., and Amasino, R. D. (2001). One of two tandem Arabidopsis genes homologous to monosaccharide transporters is senescence-associated. *Plant Mol. Biol.* 46, 447–457. doi:10.1023/A:1010639015959.
- Roach, M. J., Johnson, D. L., Bohlmann, J., van Vuuren, H. J. J., Jones, S. J. M., Pretorius, I. S., et al. (2018). Population sequencing reveals clonal diversity and ancestral inbreeding in the grapevine cultivar Chardonnay. *PLOS Genet.* 14, e1007807. doi:10.1371/journal.pgen.1007807.
- Sadras, V. O., and Mccarthy, M. G. (2007). Quantifying the dynamics of sugar concentration in berries of *Vitis vinifera* cv. Shiraz: A novel approach based on allometric analysis. *Aust. J. Grape Wine Res.* 13, 66–71. doi:10.1111/j.1755-0238.2007.tb00236.x.
- Sadras, V. O., and Petrie, P. R. (2011). Climate shifts in south-eastern Australia: Early maturity of Chardonnay, Shiraz and Cabernet Sauvignon is associated with early onset rather than faster ripening. *Aust. J. Grape Wine Res.* 17, 199–205. doi:10.1111/j.1755-0238.2011.00138.x.
- Said, J. I., Song, M., Wang, H., Lin, Z., Zhang, X., Fang, D. D., et al. (2015). A comparative meta-analysis of QTL between intraspecific *Gossypium hirsutum* and interspecific *G. hirsutum* × *G. barbadense* populations. *Mol. Genet. Genomics* 290, 1003–1025. doi:10.1007/s00438-014-0963-9.
- Salvi, S., Corneti, S., Bellotti, M., Carraro, N., Sanguineti, M. C., Castelletti, S., et al. (2011). Genetic dissection of maize phenology using an intraspecific introgression library. *BMC Plant Biol.* 11, 4. doi:10.1186/1471-2229-11-4.
- Sosnowski, O., Charcosset, A., and Joets, J. (2012). Biomeator V3: An upgrade of genetic map compilation and quantitative trait loci meta-analysis algorithms. *Bioinformatics* 28, 2082–2083. doi:10.1093/bioinformatics/bts313.
- Team, R. D. C., and R Development Core Team, R. (2016). R: A Language and

- Environment for Statistical Computing. *R Found. Stat. Comput.* 1, 409.
doi:10.1007/978-3-540-74686-7.
- Terral, J.-F., Tabard, E., Bouby, L., Ivorra, S., Pastor, T., Figueiral, I., et al. (2010). Evolution and history of grapevine (*Vitis vinifera*) under domestication: new morphometric perspectives to understand seed domestication syndrome and reveal origins of ancient European cultivars. *Ann. Bot.* 105, 443–455.
doi:10.1093/aob/mcp298.
- Tomasi, D., Jones, G. V., Giust, M., Lovat, L., and Gaiotti, F. (2011). Grapevine Phenology and Climate Change: Relationships and Trends in the Veneto Region of Italy for 1964-2009. *Am. J. Enol. Vitic.* 62, 329–339. doi:10.5344/ajev.2011.10108.
- Troshin LP, Nedov, P., Litvak, I., and Guzun, N. (1990). Improvement of *Vitis vinifera* sativa DC. taxonomy. *Vitis (special issue) Proc. 5th Int. Symp. Grape Breeding, 1989*, 37–43.
- Uhlig, B. A., and Clingeleffer, P. R. (1998). Ripening Characteristics of the Fruit From *Vitis vinifera* L. Drying Cultivars Sultana and Merbein Seedless Under Furrow Irrigation. *Am. J. Enol. Vitic.* 49, 375–382. Available at:
<http://www.ajevonline.org/content/49/4/375> [Accessed December 11, 2018].
- Vasconcelos, M. C., Greven, M., Winefield, C. S., Trought, M. C. T., and Raw, V. (2009). The Flowering Process of *Vitis vinifera*: A Review. *Am. J. Enol. Vitic.* 30, 312–317. Available at: <http://www.ajevonline.org/content/60/4/411.short> [Accessed January 21, 2019].
- Venuti, S., Copetti, D., Foria, S., Falginella, L., Hoffmann, S., Bellin, D., et al. (2013). Historical Introgression of the Downy Mildew Resistance Gene Rpv12 from the Asian Species *Vitis amurensis* into Grapevine Varieties. *PLoS One* 8, e61228.
doi:10.1371/journal.pone.0061228.
- Veyrieras, J. B., Goffinet, B., and Charcosset, A. (2007). MetaQTL: A package of new computational methods for the meta-analysis of QTL mapping experiments. *BMC Bioinformatics* 8, 49. doi:10.1186/1471-2105-8-49.
- Vitolo, N., Forcato, C., Carpinelli, E., Telatin, A., Campagna, D., D'Angelo, M., et al. (2014). A deep survey of alternative splicing in grape reveals changes in the

- splicing machinery related to tissue, stress condition and genotype. *BMC Plant Biol.* 14, 99. doi:10.1186/1471-2229-14-99.
- Walker, A. R., Lee, E., Bogs, J., McDavid, D. A. J., Thomas, M. R., and Robinson, S. P. (2007). White grapes arose through the mutation of two similar and adjacent regulatory genes. *Plant J.* 49, 772–785. doi:10.1111/j.1365-313X.2006.02997.x.
- Walker, K., and Croteau, R. (2000). Molecular cloning of a 10-deacetylbaocatin III-10-O-acetyl transferase cDNA from *Taxus* and functional expression in *Escherichia coli*. *Proc. Natl. Acad. Sci. U. S. A.* 97, 583–7. Available at: <http://www.ncbi.nlm.nih.gov/pubmed/10639122> [Accessed January 26, 2019].
- Wang, N., Zheng, Y., Xin, H., Fang, L., and Li, S. (2013). Comprehensive analysis of NAC domain transcription factor gene family in *Vitis vinifera*. *Plant Cell Rep.* 32, 61–75. doi:10.1007/s00299-012-1340-y.
- Wen, Y.-Q., Zhong, G.-Y., Gao, Y., Lan, Y.-B., Duan, C.-Q., and Pan, Q.-H. (2015). Using the combined analysis of transcripts and metabolites to propose key genes for differential terpene accumulation across two regions. *BMC Plant Biol.* 15, 240. doi:10.1186/s12870-015-0631-1.
- Williams, D. W., Andris, H. L., Beede, R. H., Luvlsi, D. A., Norton, M. V. K., Williams, L. E., et al. (1985). Validation of a Model for the Growth and Development of the Thompson Seedless Grapevine. II. Phenology. Available at: <http://www.ajevonline.org/content/ajev/36/4/283.full.pdf> [Accessed December 3, 2018].
- Yamane, T., Jeong, S. T., Goto-Yamamoto, N., Koshita, Y., and Kobayashi, S. (2006). Effects of Temperature on Anthocyanin Biosynthesis in Grape Berry Skins. *Am. J. Enol. Vitic.* 53, 171–182. Available at: <http://www.ajevonline.org/content/57/1/54> [Accessed December 10, 2018].
- Yang, J., Jiang, H., Yeh, C.-T., Yu, J., Jeddloh, J. A., Nettleton, D., et al. (2015). Extreme-phenotype genome-wide association study (XP-GWAS): a method for identifying trait-associated variants by sequencing pools of individuals selected from a diversity panel. *Plant J.* 84, 587–596. doi:10.1111/tpj.13029.
- Zyprian, E., Ochßner, I., Schwander, F., Šimon, S., Hausmann, L., Bonow-Rex, M., et al.

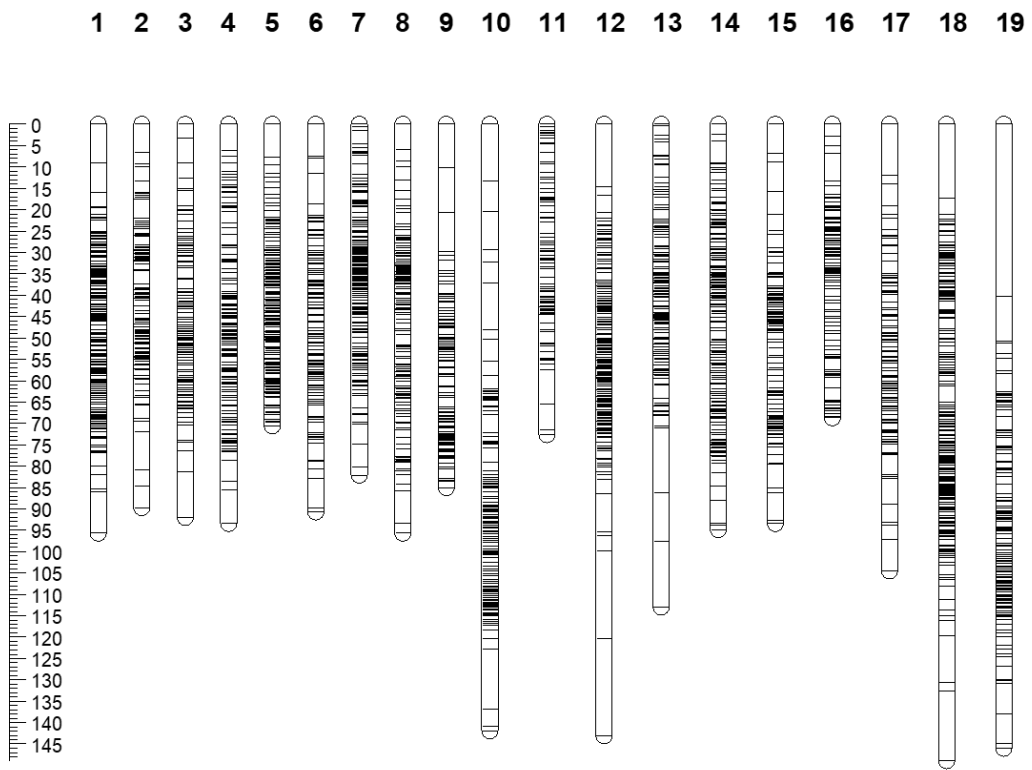
(2016). Quantitative trait loci affecting pathogen resistance and ripening of grapevines. *Mol. Genet. Genomics* 291, 1573–1594. doi:10.1007/s00438-016-1200-5.

Zyprian, E., Trapp, O., Eibach, R., Trapp, O., Schwander, F., and Töpfer, R. (2018). Grapevine breeding under climate change: Applicability of a molecular marker linked to véraison Sensor-assisted phenotyping of grape bunch architecture. *Vitis - J. Grapevine Res.* 57, 119–123. doi:<https://doi.org/10.5073/vitis.2018.57.119-123>.

Appendix

Supplementary Table 1

External file (Available upon request)

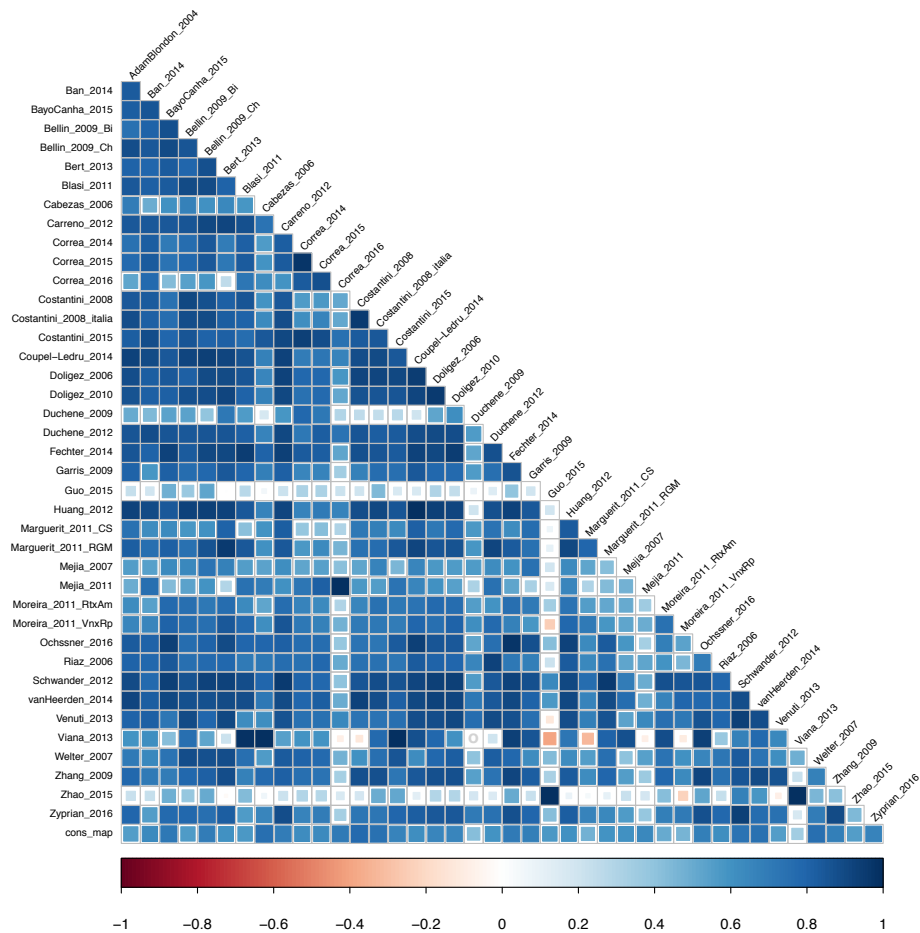


Supplementary Figure 1. The grapevine consensus map

Supplementary Table 2. Contribution of each individual genetic map to the construction of the consensus map.

Reference	I	II	III	IV	V	VI	VII	VIII	IX	X	XI	XII	XIII	XIV	XV	XVI	XVII	XVIII	XIX
<i>Ban et al. 2014</i>	x	x	x	x	x	x	x	x	x	x	x	x	x	x	x	x	x	x	x
<i>Bayo Canha, PhD thesis 2015</i>	x	x	x	x	x	x	x	x	x	x	x	x	x	x	x	x	x	x	x
<i>Bellin et al. 2009 BI</i>	x	x	x	x	x	x	x	x	x	x	x	x	x	x	x	x	x	x	x
<i>Bellin et al. 2009 CH</i>	x	x	x	x	x	x	x	x	x	x	x	x	x	x	x	x	x	x	x
<i>Bert et al. 2013</i>	x	x	x	x	x	x	x	x	x	x	x	x	x	x	x	x	x	x	x
<i>Blasi et al. 2011</i>	x	x	x	x	x	x	x	x	x	x	x	x	x	x	x	x	x	x	x
<i>Cabezas et al. 2006</i>	x	x	x	x	x	x	x	x	x	x	x	x	x	x	x	x	x	x	x
<i>Carreño Ruiz, PhD thesis 2012</i>	x	x	x	x	x	x	x	x	x	x	x	x	x	x	x	x	x	x	x
<i>Correa et al. 2014</i>	x	x	x	x	x	x	x	x	x	x	x	x	x	x	x	x	x	x	x
<i>Correa et al. 2015</i>	x	x	x	x	x	x	x	x	x	x	x	x	x	x	x	x	x	x	x
<i>Correa et al. 2016</i>	x	x	x	x	x	x	x	x	x	x	x	x	x	x	x	x	x	x	x
<i>Costantini et al. 2008 IT</i>	x	x	x	x	x	x	x	x	x	x		x	x	x	x	x	x	x	x
<i>Costantini et al. 2008</i>	x	x	x	x	x	x	x	x	x	x	x	x	x	x	x	x	x	x	x
<i>Costantini et al. 2015</i>	x	x		x	x	x	x			x		x					x	x	
<i>Coupel-Ledru et al. 2014, 2016</i>	x	x	x	x	x	x	x	x	x	x		x	x	x	x	x	x	x	x
<i>Doligez et al. 2006</i>	x	x	x	x	x	x	x	x	x	x	x	x	x	x	x	x	x	x	x
<i>Doligez et al. 2010</i>	x	x	x	x	x	x	x	x	x	x	x	x	x	x	x	x	x	x	x
<i>Duchêne et al. 2009</i>	x	x	x	x	x	x	x	x	x	x	x	x	x	x	x	x	x	x	x
<i>Duchêne et al. 2012</i>	x	x	x	x	x	x	x	x	x	x	x	x	x	x	x	x	x	x	x
<i>Fechter et al. 2014</i>	x	x	x	x	x	x	x	x	x	x	x	x	x	x	x	x	x	x	x
<i>Garris et al. 2009</i>	x	x	x	x	x	x	x	x	x	x	x	x	x	x	x	x	x	x	x
<i>Guo et al. 2015</i>	x	x	x	x	x	x	x	x	x	x		x	x	x	x	x	x	x	x

<i>Huang et al. 2012</i>	x	x	x	x	x	x	x	x	x	x		x	x	x	x	x	x	x	x
<i>Marguerit et al. 2009, 2011 CS</i>	x	x	x	x	x	x	x	x	x	x		x	x	x	x	x	x	x	x
<i>Marguerit et al. 2009, 2011 RGM</i>	x	x	x	x	x	x	x	x	x	x		x	x	x	x	x	x	x	x
<i>Mejía et al. 2007</i>	x	x	x	x	x	x	x	x	x	x		x	x	x	x	x	x	x	x
<i>Mejía et al. 2011</i>	x	x	x	x	x	x	x	x	x	x		x	x	x	x	x	x	x	x
<i>Moreira et al. 2011 RT</i>	x	x	x	x	x	x	x	x	x	x	x	x	x	x	x	x	x	x	x
<i>Moreira et al. 2011 AM</i>	x	x	x	x	x	x	x	x	x	x	x	x	x	x	x	x	x	x	x
<i>Ochssner et al. 2016</i>	x	x	x	x	x	x	x	x	x	x	x	x	x	x	x	x	x	x	x
<i>Schwander et al. 2012</i>	x	x	x	x	x	x	x	x	x	x	x	x	x	x	x	x	x	x	x
<i>Riaz et al. 2006</i>	x	x	x	x	x	x	x	x	x	x	x	x	x	x	x	x	x	x	x
<i>van Heerden et al. 2014</i>	x	x	x	x	x	x	x	x	x	x	x	x	x	x	x	x	x	x	x
<i>Venuti et al. 2013</i>	x	x	x	x	x	x	x	x	x	x	x	x	x	x	x	x	x	x	x
<i>Viana et al. 2013</i>	x	x		x	x					x		x					x	x	
<i>Welter et al. 2007</i>	x	x	x	x	x	x	x	x		x		x	x	x	x		x	x	x
<i>Zhang et al. 2009</i>	x	x	x	x	x	x	x	x		x		x	x	x	x		x	x	x
<i>Zhao et al. 2015</i>	x	x	x	x	x	x	x	x	x	x		x	x	x	x	x	x	x	x
<i>Zyprian et al. 2016</i>	x	x	x	x	x	x	x	x	x	x	x	x	x	x	x	x	x	x	x
Number Of Maps Used To Construct Linkage Group	39	39	37	39	39	38	38	37	35	39	26	39	37	37	37	35	39	39	37



Supplementary Figure 2. Correlation plot displaying Pearson correlation values for each pair of input genetic maps.

Supplementary Table 3

External file (Available upon request)

Supplementary Table 4

External file (Available upon request)

Supplementary Table 5

LG	Meta-QTL	Peak Position (cM)	R ²	Start (cM)	End (cM)	Start (bp)	End (bp)	Candidates	Original QTLs co-located	QTL Studies (Populations)	Reference
II	<i>anthocyanin_2_1</i>	49.04	0.560143	48.72	49.36	8600542	9173540	25	14	5	<i>Carreño Ruiz 2012, Costantini et al. 2015, Azuma et al. 2015, Guo et al. 2015, Bayo Canha PhD thesis 2015</i>
II	<i>anthocyanin_2_2</i>	50.76	0.554231	50.315	51.205	10028560	10710740	22	13	3	<i>Costantini et al. 2015, Azuma et al. 2015, Bayo Canha PhD thesis 2015</i>
II	<i>anthocyanin_2_3</i>	52.4	0.567667	52.17	52.63	11130194	12095023	19	15	3	<i>Costantini et al. 2015, Azuma et al. 2015, Bayo Canha PhD thesis 2015</i>
II	<i>anthocyanin_2_4</i>	52.94	0.563625	52.76	53.12	12753898	14578477	57	16	3	<i>Costantini et al. 2015, Azuma et al. 2015, Bayo Canha PhD thesis 2015</i>
II	<i>anthocyanin_2_5</i>	54.03	0.561125	53.86	54.2	16667197	16683683	1	16	3	<i>Costantini et al. 2015, Azuma et al. 2015, Bayo Canha PhD thesis 2015</i>
II	<i>anthocyanin_2_6</i>	54.4	0.574389	54.4	54.4	16693380	16693380	0	18	3	<i>Costantini et al. 2015, Azuma et al. 2015, Bayo Canha PhD thesis 2015</i>
II	<i>anthocyanin_2_7</i>	56.58	0.588667	56.51	56.65	17799696	17822818	1	12	2	<i>Costantini et al. 2015, Bayo Canha PhD thesis 2015</i>

Supplementary Table 6

Meta-QTL	Gene ID	Chr	Start (bp)	End(bp)	Annotation_V1	
anthocyanin_2_1	VIT_02s0012g01940	2	8639809	8644529	Myb KAN2 (KANADI 2)	
	VIT_02s0012g01950	2	8684996	8685382	Photosystem II protein D1	
	VIT_02s0012g01960	2	8685632	8694337	Transcription factor jumonji (jmj)	
	VIT_02s0012g01970	2	8725299	8725604	No hit	
	VIT_02s0012g01980	2	8737610	8738292	Valyl tRNA synthetase	
	VIT_02s0012g01990	2	8745023	8746458	4-hydroxyphenylpyruvate dioxygenase	
	VIT_02s0012g02000	2	8805267	8815050	Binding	
	VIT_02s0012g02020	2	8846265	8846784	GTP binding protein	
	VIT_02s0012g02030	2	8851816	8858007	Homeobox-7	
	VIT_02s0012g02050	2	8869228	8874707	PAP/fibrillin family	
	VIT_02s0012g02060	2	8876177	8876668	Calmodulin	
	VIT_02s0012g02070	2	8877753	8893038	Dolichol phosphate-mannose biosynthesis regulatory protein	
	VIT_02s0012g02080	2	8903756	8904732	No hit	
	VIT_02s0012g02090	2	8918570	8923074	Unknown protein	
	VIT_02s0012g02110	2	8936032	8953681	No hit	
	VIT_02s0012g02120	2	8961449	8968305	Defender against cell death 1 (DAD1)	
	VIT_02s0012g02130	2	9009706	9010443	Unknown	
	VIT_02s0012g02140	2	9020625	9024203	No hit	
	VIT_02s0012g02150	2	9028389	9028757	Reduced sugar response 4 RSR4	
	VIT_02s0012g02160	2	9055038	9090180	Glycerol-3-phosphate acyltransferase	
	VIT_02s0012g02170	2	9098719	9099667	No hit	
	VIT_02s0012g02180	2	9103155	9107033	Abhydrolase domain-containing protein	
	VIT_02s0012g02190	2	9124133	9129245	Cellulose synthase CSLD2	
	VIT_02s0012g02200	2	9133993	9144207	No hit	
	VIT_02s0012g02210	2	9151187	9151438	No hit	
	anthocyanin_2_2	VIT_02s0012g02520	2	10095290	10107351	Vacuolar protein sorting 25
		VIT_02s0012g02530	2	10144914	10157269	Phosphomevalonate kinase
		VIT_02s0012g02540	2	10157476	10159508	Chlororespiratory reduction 4 (CRR4)
		VIT_02s0012g02560	2	10211013	10211294	No hit
VIT_02s0012g02570		2	10303823	10313431	Guanine nucleotide-binding protein alpha-1 subunit	
VIT_02s0012g02580		2	10333777	10333986	No hit	
VIT_02s0012g02590		2	10333987	10335087	Galacturonosyltransferase 1	
VIT_02s0012g02600		2	10337139	10337655	Octicosapeptide/Phox/Bem1p (PB1) domain-containing protein	
VIT_02s0012g02610		2	10346830	10347282	SAR1 (suppressor of auxin resistance1) (Nup160)	
VIT_02s0012g02620		2	10358627	10359350	PFT1 (phytochrome and flowering time 1) MED25	
VIT_02s0012g02640		2	10371559	10372237	Aspartic-type endopeptidase	
VIT_02s0012g02650		2	10379257	10380646	Purple acid phosphatase 2 PAP2	
VIT_02s0012g02660		2	10381950	10405928	Proteasome 26S regulatory subunit (RPN9)	
VIT_02s0012g02670		2	10482684	10485983	Unknown protein	
VIT_02s0012g02680		2	10538523	10542564	No hit	
VIT_02s0012g02690		2	10556046	10556298	No hit	
VIT_02s0012g02700		2	10603213	10607154	Unknown	
VIT_02s0012g02710		2	10617021	10618719	Unknown	
VIT_02s0012g02720		2	10620819	10623614	RPM1 (resistance to p. syringae pv maculicola 1)	

	VIT_02s0012g02760	2	10685743	10699497	Methionyl-tRNA synthetase
	VIT_02s0012g02770	2	10703356	10703813	ABC transporter g family pleiotropic drug resistance 12 PDR12
	VIT_02s0012g02780	2	10706920	10720569	Cytochrome b5 domain-containing protein
anthocyanin_2_3	VIT_02s0012g02920	2	11133984	11136347	Acyl-CoA oxidase ACX3
	VIT_02s0012g02970	2	11183822	11186832	No hit
	VIT_02s0012g03040	2	11666980	11687641	AAA-type ATPase
	VIT_02s0012g03050	2	11688053	11691156	AAA-type ATPase
	VIT_02s0012g03060	2	11710057	11710461	6-phosphogluconate dehydrogenase, decarboxylating
	VIT_02s0012g03090	2	11751038	11752949	AAA-type ATPase
	VIT_02s0012g03100	2	11771975	11773559	No hit
	VIT_02s0012g03110	2	11774822	11776354	CTV.22
	VIT_02s0012g03130	2	11817589	11831312	No hit
	VIT_02s0012g03140	2	11831313	11832597	Ribosomal protein S7 30S
	VIT_02s0012g03160	2	11840324	11841710	No hit
	VIT_02s0012g03170	2	11873089	11874714	No hit
	VIT_02s0012g03180	2	11879297	11879706	Unknown
	VIT_02s0012g03190	2	11885508	11886222	CTV.22
	VIT_02s0012g03200	2	11893087	11894138	Armadillo/beta-catenin repeat
	VIT_02s0012g03210	2	11897304	11897873	No hit
	VIT_02s0012g03240	2	11947893	11959569	AAA-type ATPase
	VIT_02s0012g03250	2	11959578	11960203	AAA-type ATPase
	VIT_02s0012g03260	2	11987891	11988792	No hit
anthocyanin_2_4	VIT_02s0109g00230	2	12786746	12808921	Early-responsive to dehydration protein / ERD protein
	VIT_02s0109g00240	2	12814813	12815037	No hit
	VIT_02s0109g00250	2	12822109	12827876	4-coumarate-CoA ligase
	VIT_02s0109g00260	2	12868384	12876281	Retrotransposon gag protein
	VIT_02s0109g00280	2	12912306	12929427	No hit
	VIT_02s0109g00290	2	12929477	12929908	CYP76C6
	VIT_02s0109g00300	2	12929909	12931565	CYP76B1
	VIT_02s0109g00310	2	12936238	12938714	flavonoid 3-monooxygenase
	VIT_02s0109g00320	2	12982398	12982920	Translation initiation factor eIF-3 subunit 8
	VIT_02s0109g00350	2	13058347	13059533	Carboxyl-terminal proteinase
	VIT_02s0109g00360	2	13116317	13119876	Translocase of chloroplast 34
	VIT_02s0109g00370	2	13163595	13167989	RNA recognition motif (RRM)-containing protein
	VIT_02s0109g00380	2	13170239	13193614	Stress response suppressor 1
	VIT_02s0109g00390	2	13282201	13282765	N-hydroxycinnamoyl/benzoyltransferase 5
	VIT_02s0109g00400	2	13282778	13283707	Serine-type peptidase SLP3
	VIT_02s0109g00410	2	13308757	13312393	No hit
	VIT_02s0109g00420	2	13341559	13342323	Disease resistance protein (CC-NBS-LRR class)
	VIT_02s0109g00430	2	13347364	13349570	Nitrilase 4 (NIT4)
	VIT_02s0109g00440	2	13353462	13353985	No hit
	VIT_02s0033g00010	2	13457765	13460162	Unknown protein
	VIT_02s0033g00020	2	13460163	13461470	Unknown protein
	VIT_02s0033g00030	2	13506518	13511727	No hit
	VIT_02s0033g00040	2	13512257	13512649	No hit
	VIT_02s0033g00050	2	13518893	13519179	Scarecrow transcription factor 3 (SCL3)
	VIT_02s0033g00060	2	13531787	13538078	DNAJ plastid division protein (ARC6)

VIT_02s0033g00070	2	13568564	13569348	No hit	
VIT_02s0033g00080	2	13590737	13637352	Pleckstrin (PH) domain-containing protein	
VIT_02s0033g00090	2	13639223	13640252	DNA replication licensing factor MCM2	
VIT_02s0033g00120	2	13705067	13785560	Pleckstrin (PH) domain-containing protein	
VIT_02s0033g00130	2	13786111	13787768	Cis-zeatin O-beta-D-glucosyltransferase	
VIT_02s0033g00150	2	13832782	13833455	No hit	
VIT_02s0033g00160	2	13856081	13859536	Pleckstrin (PH) domain-containing protein	
VIT_02s0033g00180	2	13880089	13881941	Phenylpropanoid:glucosyltransferase 2	
VIT_02s0033g00190	2	13884200	13933646	DNA replication licensing factor MCM2	
VIT_02s0033g00230	2	13998724	14007202	Unknown protein	
VIT_02s0033g00240	2	14031671	14033252	Glucosyltransferase twi 1	
VIT_02s0033g00250	2	14051742	14052882	No hit	
VIT_02s0033g00260	2	14104114	14107827	Pinoretinol-laricetin reductase	
VIT_02s0033g00270	2	14123184	14126331	Pinoretinol-laricetin reductase	
VIT_02s0033g00290	2	14139881	14141542	Pinoretinol-laricetin reductase	
VIT_02s0033g00300	2	14144838	14148929	myb family	
VIT_02s0033g00310	2	14158366	14159002	No hit	
VIT_02s0033g00320	2	14159003	14183582	PRLI-interacting factor L	
VIT_02s0033g00350	2	14253249	14254161	No hit	
VIT_02s0033g00360	2	14265226	14266015	Urease	
VIT_02s0033g00370	2	14275372	14275752	myb domain protein 113	
VIT_02s0033g00380	2	14291438	14291683	VvMybA2 (C-term)	
VIT_02s0033g00390	2	14291727	14292732	VvMybA2	
VIT_02s0033g00400	2	14302187	14303282	myb domain protein 113	
VIT_02s0033g00410	2	14351791	14352807	VvMybA1	
VIT_02s0033g00420	2	14386896	14387181	Ribosomal protein S28 (RPS28C) 40S	
VIT_02s0033g00430	2	14392775	14393842	myb domain protein 113	
VIT_02s0033g00440	2	14400037	14401092	Myb VvMYBA1	
VIT_02s0033g00450	2	14420525	14421283	VvMybA3	
VIT_02s0033g00460	2	14425416	14426478	myb domain protein 113	
VIT_02s0033g00480	2	14498732	14499419	No hit	
VIT_02s0033g00490	2	14567216	14568104	No hit	
anthocyanin_2_5	VIT_02s0033g01190	2	16677461	16690102	Unknown protein
anthocyanin_2_6					
anthocyanin_2_7	VIT_02s0087g00390	2	17799720	17825371	Endonuclease

Supplementary Table 7. Description of the phenology meta-QTLs

LG	Meta-QTL	Peak Position (cM)	R ²	Start (cM)	End (cM)	Original QTLs co-located	QTL Studies (Populations)	Traits	Reference
I	<i>ver_1_1</i>	31.29	0.11	29.15	33.43	2	2	VT	<i>Fechter et al 2014, Zyprian et al 2016</i>
	<i>pheno_1_1</i>	30.30	0.15	28.08	32.53	9	5	VT, FBL, FT, FS, RT	<i>Carreño Ruiz 2012, Costantini et al 2008, Fechter et al 2014, Zyprian et al 2016</i>
	<i>pheno_1_2</i>	37.94	0.15	36.68	39.21	9	3	VT, FBL, RT, FS	<i>Carreño Ruiz 2012, Fechter et al 2014, Zyprian et al 2016,</i>
II	<i>ver_2_1</i>	31.34	0.17	28.79	33.89	7	2	VB, Vr	<i>Bayo Canha 2015, Grzeskowiak et al 2013</i>
	<i>ver_2_2</i>	41.55	0.13	40.00	43.30	5	3	Vr, VB, VE, VT	<i>Costantini et al 2008, Bayo Canha 2015, Grzeskowiak et al 2013</i>
	<i>ver_2_3</i>	53.47	0.34	52.88	54.07	5	3	Vr, VE, VP	<i>Costantini et al 2008, Bayo Canha 2015, Grzeskowiak et al 2013</i>
	<i>pheno_2_1</i>	31.22	0.18	30.03	32.42	15	5	Ac, VE, Rp, FT, ssc, VB, VE, V-R, Vr, Vr-Rp	<i>Carreño Ruiz 2012, Costantini et al 2008, Ban et al 2016, Bayo Canha 2015, Grzeskowiak et al 2013</i>
	<i>pheno_2_2</i>	41.58	0.18	40.23	42.94	9	4	Ac, VB, FT, Rp, VE, Vr, Vr-Rp, VT	<i>Carreño Ruiz 2012, Costantini et al 2008, Bayo Canha 2015, Grzeskowiak et al 2013</i>

<i>pheno_2_3</i>	48.83	0.24	46.52	51.14	10	4	Tss/Ac, Vr, Ac, Rp, FT, F-V, Vr-Rp, VE	<i>Carreño Ruiz 2012, Costantini et al 2008, Bayo Canha 2015, Grzeskowiak et al 2013</i>
<i>pheno_2_4</i>	53.60	0.25	53.01	54.19	11	4	Ac,Tss/Ac, F-V, Rp, VE, VP, FT, Vr	<i>Carreño Ruiz 2012, Costantini et al 2008, Bayo Canha 2015, Grzeskowiak et al 2013</i>

Supplementary Table 8

Meta-QTL	Gene ID	Chr	Start (bp)	End(bp)	Annotation V1
<i>ver_1_1</i>	VIT_01s0011g02820	1	2508191	2516979	Unknown protein
	VIT_01s0011g02830	1	2517659	2519101	Signal peptidase I
	VIT_01s0011g02840	1	2525946	2527902	Cytochrome B561
	VIT_01s0011g02850	1	2528541	2534477	Unknown protein
	VIT_01s0011g02860	1	2536230	2541355	CHUP1 (chloroplast unusual positioning 1)
	VIT_01s0011g02870	1	2542304	2545664	Related to Ubiquitin 1 (RUB1)
	VIT_01s0011g02880	1	2546007	2547946	Cationic amino acid transporter 8
	VIT_01s0011g02890	1	2549534	2550146	Unknown protein
	VIT_01s0011g02900	1	2553217	2553958	No hit
	VIT_01s0011g02910	1	2555006	2563359	Coiled-coil domain containing 130
	VIT_01s0011g02920	1	2574244	2575738	TCP family transcription factor DICHOTOMA
	VIT_01s0011g02930	1	2597606	2599224	DNA-binding protein, chloroplast nucleoid
	VIT_01s0011g02940	1	2606154	2608392	basic helix-loop-helix (bHLH) family
	VIT_01s0011g02950	1	2618690	2632669	Zinc finger (C3HC4-type ring finger)
	VIT_01s0011g02960	1	2632786	2636066	leucoanthocyanidin reductase 1 (VvLAR1) [Vitis vinifera] GENE ID: 100232982
	VIT_01s0011g02970	1	2651546	2665672	ILP1 (Increased level of polyploidy1-1d)
	VIT_01s0011g02980	1	2666162	2676144	ILP1 (Increased level of polyploidy1-1d)
	VIT_01s0011g02990	1	2677653	2684941	NAC domain-containing protein (VvNAC12)
	VIT_01s0011g03000	1	2688188	2688578	No hit
	VIT_01s0011g03010	1	2692236	2698927	Serine/threonine-protein kinase SNT7, chloroplast precursor
	VIT_01s0011g03020	1	2699631	2703068	HAK5 (High affinity K+ transporter 5)
	VIT_01s0011g03030	1	2708028	2711823	No hit

VIT_01s0011g03040	1	2714906	2715758	Unknown protein
VIT_01s0011g03050	1	2717642	2719224	Unknown protein
VIT_01s0011g03060	1	2726727	2743646	Symbiosis receptor-like kinase
VIT_01s0011g03070	1	2751566	2753036	ERF/AP2 Gene Family (VvRAV1)
VIT_01s0011g03080	1	2754305	2765766	Methionine aminopeptidase 1B, chloroplast precursor
VIT_01s0011g03090	1	2766597	2767444	Allene oxide cyclase (jasmonates from fatty acids)
VIT_01s0011g03100	1	2770673	2771827	Zinc finger (C2H2 type) protein (WIP6)
VIT_01s0011g03110	1	2781518	2783517	myb family
VIT_01s0011g03120	1	2786238	2790806	Unknown protein
VIT_01s0011g03130	1	2791893	2796533	Unknown protein
VIT_01s0011g03140	1	2806814	2809091	PFT1 (phytochrome and flowering time 1) MED25
VIT_01s0011g03160	1	2819342	2877060	PFT1 (phytochrome and flowering time 1) MED25
VIT_01s0011g03170	1	2877767	2878493	PFT1 (phytochrome and flowering time 1) MED25
VIT_01s0011g03180	1	2879352	2882108	Lysine and histidine specific transporter
VIT_01s0011g03190	1	2886723	2897786	ATP-dependent Clp protease adaptor protein ClpS containing protein
VIT_01s0011g03200	1	2898690	2906357	Transmembrane protein FT27/PFT27
VIT_01s0011g03210	1	2924829	2926924	Aspartic Protease (VvAP1)
VIT_01s0011g03220	1	2928959	2935184	Choline transporter
VIT_01s0011g03230	1	2941266	2946275	Basic Leucine Zipper Transcription Factor (VvbZIP01)
VIT_01s0011g03240	1	2948265	2949046	PGPS/D12
VIT_01s0011g03250	1	2951539	2951847	Fw2.2 ORFX
VIT_01s0011g03260	1	2954243	2955469	Fw2.2 ORFX
VIT_01s0011g03270	1	2958052	2959131	CXE carboxylesterase
VIT_01s0011g03280	1	2967860	2979364	Protein phosphatase 2 regulatory subunit A
VIT_01s0011g03290	1	2981226	2996541	Aluminum-activated malate transporter 9
VIT_01s0011g03300	1	3007049	3007411	Plastid-specific 30S ribosomal protein 3
VIT_01s0011g03310	1	3008153	3011404	Unknown protein
VIT_01s0011g03320	1	3011621	3013806	Arabidopsis histidine phosphotransfer AHP2
VIT_01s0011g03330	1	3014379	3016292	Unknown protein
VIT_01s0011g03340	1	3028681	3030154	No hit
VIT_01s0011g03350	1	3030155	3040612	PRP4 pre-mRNA processing factor 4 homolog B
VIT_01s0011g03360	1	3044557	3045849	Unknown
VIT_01s0011g03370	1	3046873	3051454	Agenet domain-containing protein
VIT_01s0011g03380	1	3061306	3065510	Dihydrolipoamide S-acetyltransferase (LTA2)
VIT_01s0011g03390	1	3065990	3068987	Unknown protein
VIT_01s0011g03400	1	3076982	3080343	Proton-dependent oligopeptide transport (POT) family protein

	VIT_01s0011g03410	1	3084191	3092672	DNA repair protein RAD23
	VIT_01s0011g03420	1	3100807	3101627	Unknown protein
	VIT_01s0011g03430	1	3112762	3113407	No hit
	VIT_01s0011g03440	1	3117073	3117578	DNA mismatch repair protein
	VIT_01s0011g03450	1	3127812	3132261	Alpha-glucosidase
	VIT_01s0011g03460	1	3141923	3142868	No hit
	VIT_01s0011g03470	1	3142869	3144296	ERF/AP2 Gene Family (VvERF122)
	VIT_01s0011g03480	1	3147476	3149151	Cinnamoyl CoA reductase
	VIT_01s0011g03490	1	3167509	3169015	3-ketoacyl-CoA synthase
	VIT_01s0011g03500	1	3175430	3178998	Homocysteine S-methyltransferase 1
	VIT_01s0011g03510	1	3180020	3185492	Protein kinase PKN/PRK1
	VIT_01s0011g03520	1	3190826	3192777	Constans-like 16
	VIT_01s0011g03530	1	3204646	3205573	Lateral organ boundaries protein 41
	VIT_01s0011g03540	1	3210273	3211389	Lateral organ boundaries protein 41
	VIT_01s0011g03550	1	3217781	3218222	Unknown
	VIT_01s0011g03560	1	3223281	3227712	fiber protein Fb34
	VIT_01s0011g03570	1	3232043	3232750	Unknown
	VIT_01s0011g03580	1	3235418	3237772	Unknown protein
	VIT_01s0011g03590	1	3246882	3249663	Ribosomal protein L15, chloroplast (CL15) 50S
	VIT_01s0011g03600	1	3252820	3255824	JAGGED
<i>ver_2_1</i>	VIT_02s0025g04660	2	4037933	4039464	Senescence-inducible chloroplast stay-green protein 1
	VIT_02s0025g04670	2	4043652	4045210	Senescence-inducible chloroplast stay-green protein 2
	VIT_02s0025g04680	2	4047267	4056403	Cell division cycle 20-like protein 1
	VIT_02s0025g04690	2	4059360	4060286	Unknown protein
	VIT_02s0025g04700	2	4061719	4063223	Expansin (VvEXPA2)
	VIT_02s0025g04710	2	4064018	4073343	Unknown protein
	VIT_02s0025g04720	2	4094895	4096363	Leucoanthocyanidin dioxygenase (VvLDOX) [Vitis vinifera]
	VIT_02s0025g04730	2	4100066	4103095	Glyoxylate reductase
	VIT_02s0025g04750	2	4108905	4111169	Glycerate dehydrogenase
	VIT_02s0025g04760	2	4121700	4124366	Splicing factor YT521-B
	VIT_02s0025g04770	2	4135934	4139911	Unknown protein
	VIT_02s0025g04780	2	4141626	4144449	Subtilisin stomatal density and distribution
	VIT_02s0025g04790	2	4145024	4146976	Hydrogenobyric acid a,c-diamide synthase
	VIT_02s0025g04800	2	4149493	4151715	Hydrogenobyric acid a,c-diamide synthase
	VIT_02s0025g04810	2	4153569	4155803	Subtilisin P69F protein
	VIT_02s0025g04820	2	4166469	4168208	Subtilisin P69E protein

VIT_02s0025g04830	2	4169732	4176688	Copper chaperone for superoxide dismutase
VIT_02s0025g04840	2	4177464	4181953	Nudix hydrolase 14
VIT_02s0025g04850	2	4191899	4193146	CYP76B1
VIT_02s0025g04860	2	4193239	4194582	CYP76B1
VIT_02s0025g04870	2	4210862	4211722	No hit
VIT_02s0025g04880	2	4212083	4213721	Geraniol 10-hydroxylase
VIT_02s0025g04890	2	4216365	4217374	CYP76B1
VIT_02s0025g04900	2	4226153	4229768	Phosphoglycerate mutase
VIT_02s0025g04910	2	4233942	4235225	Growth-regulating factor 5
VIT_02s0025g04920	2	4236968	4238438	Phosphate translocator protein2, Plastidic
VIT_02s0025g04930	2	4243946	4246738	CDI3/OZS1/RCD3/SLAC1 (slow anion channel-associated 1)
VIT_02s0025g04940	2	4246754	4248676	Carboxyl-terminal peptidase
VIT_02s0025g04950	2	4251382	4252445	No hit
VIT_02s0025g04960	2	4257725	4263946	Unknown protein
VIT_02s0025g04970	2	4267189	4268564	Subtilisin protease
VIT_02s0025g04980	2	4274342	4280444	1-aminocyclopropane-1-carboxylate synthase
VIT_02s0025g04990	2	4282395	4290690	Unknown protein
VIT_02s0025g05000	2	4300566	4305985	Bile acid:sodium symporter
VIT_02s0025g05010	2	4307128	4313693	Ycf49
VIT_02s0025g05020	2	4313694	4314578	No hit
VIT_02s0025g05030	2	4314983	4315368	Unknown protein
VIT_02s0025g05040	2	4315576	4316706	Nuclear pore complex component
VIT_02s0025g05050	2	4321904	4323519	Zf A20 and AN1 domain-containing stress-associated protein 1
VIT_02s0025g05060	2	4324307	4346662	Microtubule motor PAK (phosphatidic acid kinase) KHC
VIT_02s0025g05070	2	4346663	4347651	Microtubule motor PAK (phosphatidic acid kinase) KHC
VIT_02s0025g05080	2	4348262	4351307	Zf A20 and AN1 domain-containing stress-associated protein 1
VIT_02s0025g05090	2	4356581	4373218	Microtubule motor PAK (phosphatidic acid kinase) KHC
VIT_02s0025g05100	2	4376256	4377810	AT-hook DNA-binding protein
VIT_02s0025g05110	2	4390487	4392478	MATE efflux family protein
VIT_02s0025g05120	2	4410051	4413324	ACT domain-containing protein (ACR8)
VIT_02s0025g05130	2	4421391	4429393	High mobility group HMG-I and HMG-Y, DNA-binding
VIT_02s0025g05140	2	4437507	4440897	ATP-dependent Clp protease proteolytic subunit (ClpP2)
VIT_02s0025g05150	2	4444146	4448453	TFIIH basal transcription factor complex TTD-A subunit
VIT_02s0025g05160	2	4450431	4454056	Cornichon family
VIT_02s0025g05170	2	4454528	4456260	Unknown protein
VIT_00s2563g00010	2	4456792	4458501	Glycogenin glucosyltransferase

VIT_02s0241g00010	2	4481714	4483309	Pentatricopeptide (PPR) repeat-containing protein
VIT_02s0241g00020	2	4486591	4488109	Unknown
VIT_02s0241g00030	2	4497165	4497380	Sterol 4-alpha-methyl-oxidase 1 (SMO1)
VIT_02s0241g00040	2	4500666	4508486	Cyclobutane pyrimidine dimer photolyase
VIT_02s0241g00050	2	4516706	4519215	Unknown protein
VIT_02s0241g00060	2	4528876	4533648	Unknown protein
VIT_02s0241g00070	2	4545465	4546112	Zinc finger (DHHC type)
VIT_02s0241g00080	2	4546113	4551868	Glycine-rich protein-like
VIT_02s0241g00090	2	4553230	4560602	Translation release factor
VIT_02s0241g00100	2	4560763	4561723	Unknown protein
VIT_02s0241g00110	2	4563842	4567239	Aminomethyltransferase
VIT_02s0241g00120	2	4567672	4570586	Receptor protein kinase
VIT_02s0241g00130	2	4572517	4573830	No hit
VIT_02s0241g00140	2	4577280	4577983	Calmodulin (A)
VIT_02s0241g00150	2	4581818	4583479	No hit
VIT_02s0241g00160	2	4583480	4597122	Esterase/lipase/thioesterase family
VIT_02s0241g00170	2	4599598	4602678	Zinc finger (C2H2 type) family
VIT_02s0241g00180	2	4617301	4618383	UDP-D- glucuronate 4-epimerase 5 GAE5
VIT_02s0241g00190	2	4626070	4626875	No hit
VIT_00s0555g00010	2	4641190	4641853	CYP706A12
VIT_00s0555g00020	2	4648183	4650503	flavonoid 3-monooxygenase
VIT_00s0555g00050	2	4665292	4666049	CHCH domain containing protein
VIT_00s0323g00010	2	4668106	4670512	No hit
VIT_00s0323g00020	2	4671193	4672013	HSP associated protein
VIT_00s0323g00030	2	4678930	4682628	HSP associated protein
VIT_00s0323g00040	2	4697703	4701979	Unknown protein
VIT_00s0323g00050	2	4703890	4704749	Invertase/pectin methylesterase inhibitor
VIT_00s0323g00060	2	4707844	4708734	Invertase/pectin methylesterase inhibitor
VIT_00s0323g00070	2	4716445	4717351	Pectin methylesterase inhibitor
VIT_00s0323g00080	2	4728265	4732585	Elongation factor G, chloroplast precursor
VIT_00s0323g00100	2	4758426	4761706	Vacuolar processing enzyme beta
VIT_02s0154g00010	2	4765224	4766070	Auxin-responsive SAUR11
VIT_02s0154g00020	2	4779757	4782259	NAC domain-containing protein (VvNAC02)
VIT_02s0154g00030	2	4784152	4784510	No hit
VIT_02s0154g00040	2	4788746	4794088	Thylakoid luminal protein
VIT_02s0154g00050	2	4794446	4795025	Glycosyl hydrolase family 5

VIT_02s0154g00060	2	4795026	4798608	Thylakoid lumenal protein
VIT_02s0154g00070	2	4804832	4807460	Abnormal floral organs
VIT_02s0154g00080	2	4813347	4818031	Multi-copper oxidase (SKU5)
VIT_02s0154g00090	2	4824906	4827102	Vacuolar invertase 2, GIN2
VIT_02s0154g00100	2	4830177	4840110	Transaldolase totaL2
VIT_02s0154g00110	2	4840895	4843817	Trehalose-6-phosphate phosphatase (AtTPPA)
VIT_02s0154g00120	2	4856955	4857771	Unknown
VIT_02s0154g00130	2	4864567	4866368	Exostosin (Xyloglucan galactosyltransferase KATAMARI 1)
VIT_02s0154g00140	2	4866564	4878108	3-oxoacyl-[acyl-carrier-protein] synthase 3 A, chloroplast precursor
VIT_02s0154g00150	2	4891997	4893321	PLATZ transcription factor
VIT_02s0154g00160	2	4895022	4898791	flavin-containing monooxygenase family protein / FMO family protein
VIT_02s0154g00170	2	4900531	4903560	flavin-containing monooxygenase 3
VIT_02s0154g00180	2	4905399	4908515	flavin-containing monooxygenase 3
VIT_02s0154g00190	2	4917402	4920926	flavin-containing monooxygenase 3
VIT_02s0154g00200	2	4926234	4929441	Unknown protein
VIT_02s0154g00210	2	4932248	4932565	WRKY DNA-binding protein 21
VIT_02s0154g00220	2	4968010	4968965	Zinc finger (C2H2 type) family
VIT_02s0154g00230	2	4979771	4980739	Phosphatidic acid phosphatase / PAP2
VIT_02s0154g00240	2	5005578	5017004	Oxysterol binding protein
VIT_02s0154g00250	2	5021111	5041753	Oxysterol binding protein
VIT_02s0154g00260	2	5048952	5052974	Nitrate transporter
VIT_02s0154g00270	2	5059261	5059470	No hit
VIT_02s0154g00280	2	5063840	5064500	Arachidonic acid-induced DEA1
VIT_02s0154g00290	2	5068196	5068884	Extensin
VIT_02s0154g00300	2	5073755	5074467	Small nuclear ribonucleoprotein Sm D3
VIT_02s0154g00310	2	5077143	5078172	Protease inhibitor/seed storage/lipid transfer protein (LTP)
VIT_02s0154g00320	2	5084359	5085114	Protease inhibitor/seed storage/lipid transfer protein (LTP)
VIT_02s0154g00330	2	5090858	5100329	Unknown protein
VIT_02s0154g00340	2	5100931	5102577	No hit
VIT_02s0154g00350	2	5107218	5109108	L-lactate dehydrogenase A
VIT_02s0154g00360	2	5109216	5109392	No hit
VIT_02s0154g00370	2	5110262	5115144	YbaK/prolyl-tRNA synthetase associated region
VIT_02s0154g00380	2	5117118	5118512	Unknown
VIT_02s0154g00390	2	5127909	5131694	Autophagy 8f (APG8f)
VIT_02s0154g00400	2	5145761	5147651	Scarecrow transcription factor 6 (SCL6)
VIT_02s0154g00410	2	5164705	5167011	Unknown protein

	VIT_02s0154g00420	2	5169940	5170164	No hit
	VIT_02s0154g00430	2	5170165	5170573	Unknown
	VIT_02s0154g00440	2	5170574	5171512	Unknown protein
	VIT_02s0154g00450	2	5174203	5183898	Zinc knuckle
	VIT_02s0154g00460	2	5184751	5188467	Unknown protein
	VIT_02s0154g00470	2	5188779	5190703	No hit
	VIT_02s0154g00480	2	5191329	5192828	Heat shock protein MTSHP
	VIT_02s0154g00490	2	5197928	5198941	Heat shock 22 kDa protein mitochondrial
	VIT_02s0154g00500	2	5201356	5203907	VAP27-1 (VAMP/synaptobrevin-associated protein 27-1)
	VIT_02s0154g00510	2	5205962	5214005	Aspartic Protease (VvAP2)
	VIT_02s0154g00520	2	5216152	5221223	Aspartyl protease
	VIT_02s0154g00530	2	5227339	5229999	Histidine triad nucleotide binding protein 3
	VIT_02s0154g00540	2	5231330	5239367	Protein arginine N-methyltransferase
	VIT_02s0154g00550	2	5239749	5268651	DnaJ homolog, subfamily C, member 11
	VIT_02s0154g00560	2	5280620	5283758	No hit
	VIT_02s0154g00580	2	5295292	5296235	Unknown
	VIT_02s0154g00590	2	5308401	5308985	Unknown
	VIT_02s0154g00600	2	5321389	5323536	Pectinesterase family
	VIT_02s0154g00610	2	5324724	5332701	Pex19 protein
	VIT_02s0154g00620	2	5333217	5334885	Unknown
	VIT_00s1338g00010	2	5339303	5340709	DNA-directed RNA polymerase III subunit C34
	VIT_00s1338g00020	2	5343106	5344525	Protein transport protein Sec61 subunit alpha
	VIT_00s0229g00010	2	5346706	5349092	No hit
ver_2_2	VIT_02s0012g00010	2	5737022	5737770	No hit
	VIT_02s0012g00020	2	5764306	5772117	Glycine-rich protein
	VIT_02s0012g00030	2	5772754	5778969	Unknown
	VIT_02s0012g00040	2	5781659	5781796	No hit
	VIT_02s0012g00050	2	5786859	5796200	Glycine-rich protein
	VIT_02s0012g00060	2	5796703	5801313	Unknown
	VIT_02s0012g00070	2	5801456	5801882	Unknown protein
	VIT_02s0012g00080	2	5804657	5813125	Casein kinase II subunit beta-4
	VIT_02s0012g00090	2	5813865	5826392	Phosphatidylinositol-4-phosphate 5-kinase
	VIT_02s0012g00100	2	5828133	5830613	Ribosomal protein L37a (RPL37aB) 60S
	VIT_02s0012g00110	2	5835376	5837313	Chromatin remodeling 31
	VIT_02s0012g00140	2	5869675	5887801	Novel plant snare 11
	VIT_02s0012g00150	2	5897718	5902809	NAK-type protein kinase

VIT_02s0012g00160	2	5910037	5913981	Unknown
VIT_02s0012g00170	2	5916093	5918986	1,4-alpha-D-glucan maltohydrolase
VIT_02s0012g00180	2	5923457	5932422	Serine protease
VIT_02s0012g00190	2	5938773	5978552	Unknown protein
VIT_02s0012g00240	2	5999054	6002113	Unknown protein
VIT_02s0012g00250	2	6005214	6012306	Vacuolar protein sorting 13C protein
VIT_02s0012g00270	2	6027694	6106280	Pleckstrin (PH) domain-containing protein
VIT_02s0012g00280	2	6111583	6112872	Senescence-associated protein
VIT_02s0012g00290	2	6133593	6135728	S-ribonuclease binding protein SBP1
VIT_02s0012g00300	2	6151132	6189859	Unknown protein
VIT_02s0012g00310	2	6204735	6223899	Lon protease
VIT_02s0012g00320	2	6225175	6226474	Norcochlorine synthase
VIT_02s0012g00350	2	6233046	6236366	Norcochlorine synthase
VIT_02s0012g00360	2	6238852	6242299	1-aminocyclopropane-1-carboxylate oxidase
VIT_02s0012g00370	2	6242887	6258576	No hit
VIT_02s0012g00380	2	6273340	6285802	Norcochlorine synthase
VIT_02s0012g00390	2	6286306	6288341	Norcochlorine synthase
VIT_02s0012g00400	2	6296189	6299377	1-aminocyclopropane-1-carboxylate oxidase
VIT_02s0012g00410	2	6305682	6310741	Naringenin,2-oxoglutarate 3-dioxygenase
VIT_02s0012g00420	2	6311954	6315948	No hit
VIT_02s0012g00430	2	6320484	6320851	Oxidoreductase, 2OG-Fe(II) oxygenase
VIT_02s0012g00440	2	6320999	6321467	Norcochlorine synthase
VIT_02s0012g00450	2	6323850	6325555	1-aminocyclopropane-1-carboxylate oxidase
VIT_02s0012g00460	2	6332076	6381980	Glycine-rich protein
VIT_02s0012g00470	2	6397883	6398726	Unknown
VIT_02s0012g00480	2	6399524	6430074	Regulator of nonsense transcripts 1
VIT_02s0012g00490	2	6446158	6446783	Cytochrome c oxidase subunit 6b
VIT_02s0012g00500	2	6449814	6450360	Invertase/pectin methylesterase inhibitor
VIT_02s0012g00510	2	6455739	6464806	Golgi transport Got1
VIT_02s0012g00530	2	6490169	6496086	Ribose-phosphate pyrophosphokinase 1
VIT_02s0012g00540	2	6516342	6518185	Peroxidase
VIT_02s0012g00550	2	6518911	6526733	Inositol polyphosphate 5-phosphatase II
VIT_02s0012g00560	2	6533749	6545389	Tobamovirus multiplication 2A TOM2A
VIT_02s0012g00570	2	6554241	6560259	Pseudo-response regulator 2 (APRR2) (TOC2)
VIT_02s0012g00580	2	6586031	6594054	Ankyrin protein kinase
VIT_02s0012g00590	2	6600611	6610281	Unknown protein

VIT_02s0012g00600	2	6611782	6615934	Vacuolar protein sorting 55
VIT_02s0012g00610	2	6616375	6616852	Allyl alcohol dehydrogenase
VIT_02s0012g00620	2	6625135	6636514	Phosphoacetylglucosamine mutase
VIT_02s0012g00630	2	6639102	6640237	Myb family
VIT_02s0012g00640	2	6645562	6645999	PBP1 (pinoid-binding protein 1)
VIT_02s0012g00650	2	6653658	6654223	PBP1 (pinoid-binding protein 1)
VIT_02s0012g00660	2	6660229	6660825	Calcium-binding EF-hand
VIT_02s0012g00670	2	6670534	6672390	No hit
VIT_02s0012g00680	2	6682700	6682873	No hit
VIT_02s0012g00690	2	6707170	6707803	No hit
VIT_02s0012g00700	2	6709030	6709203	No hit
VIT_02s0012g00710	2	6733243	6741163	RAB GTPase RAB6
VIT_02s0012g00720	2	6746761	6748648	Unknown
VIT_02s0012g00730	2	6749467	6750865	Purine permease 10 PUP10
VIT_02s0012g00740	2	6758931	6769661	Dynamin-like protein 2b
VIT_02s0012g00750	2	6769877	6773816	Haloacid dehalogenase hydrolase
VIT_02s0012g00760	2	6778127	6782078	Haloacid dehalogenase hydrolase
VIT_02s0012g00770	2	6787173	6789662	No hit
VIT_02s0012g00780	2	6791455	6791610	No hit
VIT_02s0012g00790	2	6792634	6793661	Ras-related protein RAB6A
VIT_02s0012g00800	2	6795685	6795849	No hit
VIT_02s0012g00810	2	6799938	6800021	No hit
VIT_02s0012g00820	2	6804399	6806143	Unknown
VIT_02s0012g00830	2	6817359	6819815	Expansin (VvEXLB1)
VIT_02s0012g00840	2	6820451	6823470	Pentatricopeptide (PPR) repeat-containing protein
VIT_02s0012g00850	2	6823971	6851054	Splicing factor PWI domain-containing protein
VIT_02s0012g00860	2	6855160	6859171	No hit
VIT_02s0012g00870	2	6859219	6873440	RNA-binding protein 10
VIT_02s0012g00880	2	6897090	6898500	AT-hook DNA-binding protein
VIT_02s0012g00890	2	6914782	6915482	Unknown protein
VIT_02s0012g00900	2	6917525	6928933	AT-hook protein 1 (AHP1)
VIT_02s0012g00910	2	6930227	6946661	Adaptor-related protein complex 2, mu 2 subunit
VIT_02s0012g00920	2	6947431	6967357	Conserved oligomeric complex COG6
VIT_02s0012g00930	2	6972956	6979797	Unknown protein
VIT_02s0012g00940	2	6980980	6981681	Late embryogenesis abundant group 1
VIT_02s0012g00950	2	6991276	6991983	H(+)-ATPase 9 AHA9

	VIT_02s0012g00960	2	6993519	6994847	1-deoxy-D-xylulose-5-phosphate synthase
	VIT_02s0012g00970	2	7008648	7012385	Cu ²⁺ -exporting ATPase HMA5 (heavy metal ATPase 5)
	VIT_02s0012g00980	2	7027209	7037654	ferredoxin-6, chloroplast precursor
	VIT_02s0012g00990	2	7043508	7046965	LOL1 (LSD ONE like 1)
	VIT_02s0012g01000	2	7050270	7060977	Protein tyrosine phosphatase
	VIT_02s0012g01010	2	7087110	7089452	Leucine-rich repeat
	VIT_02s0012g01020	2	7092594	7099500	Zinc finger (C3HC4-type ring finger)
	VIT_02s0012g01030	2	7100088	7118988	AL-activated malate transporter 1
	VIT_02s0012g01040	2	7120118	7122681	NAC domain-containing protein (VvNAC13)
	VIT_02s0012g01050	2	7131585	7133584	ABC protein 6 non-intrinsic
	VIT_02s0012g01060	2	7154618	7155584	ABC Transporter (VvNAP3 - VvABC13)
<i>ver_2_3</i>	VIT_02s0109g00420	2	13341559	13342323	Disease resistance protein (CC-NBS-LRR class)
	VIT_02s0109g00430	2	13347364	13349570	Nitrilase 4 (NIT4)
	VIT_02s0109g00440	2	13353462	13353985	No hit
	VIT_02s0033g00010	2	13457765	13460162	Unknown protein
	VIT_02s0033g00020	2	13460163	13461470	Unknown protein
	VIT_02s0033g00030	2	13506518	13511727	No hit
	VIT_02s0033g00040	2	13512257	13512649	No hit
	VIT_02s0033g00050	2	13518893	13519179	Scarecrow transcription factor 3 (SCL3)
	VIT_02s0033g00060	2	13531787	13538078	DNAJ plastid division protein (ARC6)
	VIT_02s0033g00070	2	13568564	13569348	No hit
	VIT_02s0033g00080	2	13590737	13637352	Pleckstrin (PH) domain-containing protein
	VIT_02s0033g00090	2	13639223	13640252	DNA replication licensing factor MCM2
	VIT_02s0033g00120	2	13705067	13785560	Pleckstrin (PH) domain-containing protein
	VIT_02s0033g00130	2	13786111	13787768	Cis-zeatin O-beta-D-glucosyltransferase
	VIT_02s0033g00150	2	13832782	13833455	No hit
	VIT_02s0033g00160	2	13856081	13859536	Pleckstrin (PH) domain-containing protein
	VIT_02s0033g00180	2	13880089	13881941	Phenylpropanoid:glucosyltransferase 2
	VIT_02s0033g00190	2	13884200	13933646	DNA replication licensing factor MCM2
	VIT_02s0033g00230	2	13998724	14007202	Unknown protein
	VIT_02s0033g00240	2	14031671	14033252	Glucosyltransferase twi1
	VIT_02s0033g00250	2	14051742	14052882	No hit
	VIT_02s0033g00260	2	14104114	14107827	Pinoretinol-lariciresinol reductase
	VIT_02s0033g00270	2	14123184	14126331	Pinoretinol-lariciresinol reductase
	VIT_02s0033g00290	2	14139881	14141542	Pinoretinol-lariciresinol reductase
	VIT_02s0033g00300	2	14144838	14148929	myb family

VIT_02s0033g00310	2	14158366	14159002	No hit
VIT_02s0033g00320	2	14159003	14183582	PRLI-interacting factor L
VIT_02s0033g00350	2	14253249	14254161	No hit
VIT_02s0033g00360	2	14265226	14266015	Urease
VIT_02s0033g00370	2	14275372	14275752	myb domain protein 113
VIT_02s0033g00380	2	14291438	14291683	VvMybA2 (C-term)
VIT_02s0033g00390	2	14291727	14292732	VvMybA2
VIT_02s0033g00400	2	14302187	14303282	myb domain protein 113
VIT_02s0033g00410	2	14351791	14352807	VvMybA1
VIT_02s0033g00420	2	14386896	14387181	Ribosomal protein S28 (RPS28C) 40S
VIT_02s0033g00430	2	14392775	14393842	myb domain protein 113
VIT_02s0033g00440	2	14400037	14401092	Myb VvMYBA1
VIT_02s0033g00450	2	14420525	14421283	VvMybA3
VIT_02s0033g00460	2	14425416	14426478	myb domain protein 113
VIT_02s0033g00480	2	14498732	14499419	No hit
VIT_02s0033g00490	2	14567216	14568104	No hit
VIT_02s0033g00500	2	14590818	14592828	No hit
VIT_02s0033g00510	2	14598530	14598698	PBS1 (avrPphB susceptible 1)
VIT_02s0033g00520	2	14670377	14678952	Disease resistance protein (NBS-LRR class)
VIT_02s0033g00530	2	14726996	14728257	N2, N2-dimethylguanosine tRNA methyltransferases-like protein
VIT_02s0033g00540	2	14729299	14732859	No hit
VIT_02s0033g00550	2	14732860	14734074	No hit
VIT_02s0033g00590	2	14932630	14936675	BRXL1 (Brevis radix like 1)
VIT_02s0033g00610	2	15055455	15095871	Chromomethylase 2
VIT_02s0033g00620	2	15151759	15156338	No hit
VIT_02s0033g00630	2	15195006	15198779	Nitrilase
VIT_02s0033g00640	2	15255096	15255623	Octicosapeptide/Phox/Bem1p (PB1) domain-containing protein
VIT_02s0033g00650	2	15322348	15324313	Serine/threonine protein phosphatase 7
VIT_02s0033g00660	2	15362144	15364074	Nitrilase 4B
VIT_02s0033g00670	2	15406882	15408793	Nitrilase 4B
VIT_02s0033g00680	2	15409640	15418937	No hit
VIT_02s0033g00700	2	15436012	15438008	Nitrilase
VIT_02s0033g00710	2	15461213	15462314	No hit
VIT_02s0033g00720	2	15480470	15486817	No hit
VIT_02s0033g00730	2	15493459	15493956	Papain cysteine proteinase isoform I
VIT_02s0033g00740	2	15495048	15496242	Kinesin motor

VIT_02s0033g00750	2	15496243	15499175	Kinesin motor protein
VIT_02s0033g00770	2	15560608	15562469	Nitrilase 4B
VIT_02s0033g00780	2	15573189	15573552	14-3-3 protein GF14 omega (GRF2)
VIT_02s0033g00790	2	15591008	15592898	Nitrilase 4B
VIT_02s0033g00800	2	15606321	15608743	Nitrilase 4 (NIT4)
VIT_02s0033g00810	2	15612721	15613040	No hit
VIT_02s0033g00830	2	15651191	15651721	RAB GTPase RABA4A
VIT_02s0033g00840	2	15659957	15669174	Nitrilase 4B
VIT_02s0033g00850	2	15669871	15671771	Nitrilase
VIT_02s0033g00870	2	15700024	15702438	Nitrilase 4B
VIT_02s0033g00880	2	15714340	15714678	Ribosomal protein L8 (RPL8C) 60S
VIT_02s0033g00900	2	15829983	15834399	Unc51-like kinase
VIT_02s0033g00910	2	15835533	15836148	Kinesin motor protein
VIT_02s0033g00920	2	15921498	15922178	No hit
VIT_02s0033g00930	2	15941055	15952365	Single-strand DNA binding protein
VIT_02s0033g00960	2	15974263	15978140	Zinc-binding protein
VIT_02s0033g00970	2	16053537	16062151	No hit
VIT_02s0033g00980	2	16081574	16084857	NADH-plastoquinone oxidoreductase subunit 2
VIT_02s0033g00990	2	16084858	16085540	Ribosomal protein S7 30S
VIT_02s0033g01000	2	16093114	16095441	Anthraniloyl-CoA: methanol anthraniloyl transferase
VIT_02s0033g01010	2	16152695	16154133	Ribosomal protein S7 30S
VIT_02s0033g01020	2	16190948	16193334	Anthraniloyl-CoA: methanol anthraniloyl transferase
VIT_02s0033g01030	2	16252684	16254941	Anthraniloyl-CoA: methanol anthraniloyl transferase
VIT_02s0033g01050	2	16299329	16301080	Anthraniloyl-CoA: methanol anthraniloyl transferase
VIT_02s0033g01060	2	16349045	16351278	Anthraniloyl-CoA: methanol anthraniloyl transferase
VIT_02s0033g01070	2	16356696	16359431	Anthraniloyl-CoA: methanol anthraniloyl transferase
VIT_02s0033g01100	2	16435669	16439357	No hit
VIT_02s0033g01110	2	16439358	16447346	Male germ cell-associated kinase
VIT_02s0033g01120	2	16515095	16520470	Dehydration-responsive protein
VIT_02s0033g01130	2	16555004	16556115	SAR1 (secretion-associated ras)
VIT_02s0033g01150	2	16602266	16611445	Unknown protein
VIT_02s0033g01160	2	16649637	16654775	Unknown protein
VIT_02s0033g01170	2	16657559	16664675	Replication protein RPA 70kDa subunit

Supplementary Table 9

Meta-QTL	Gene ID	Chr	Start (bp)	End(bp)	Annotation_V1
<i>pheno_3_1</i>	VIT_03s0038g00620	3	547345	562437	Zinc knuckle
	VIT_03s0038g00630	3	565597	568081	Endo-1,4-beta-glucanase
	VIT_03s0038g00640	3	574493	578920	Unknown
	VIT_03s0038g00650	3	579366	583281	Coenzyme Q10 homolog B
	VIT_03s0038g00660	3	584427	587912	Unknown protein
	VIT_03s0038g00670	3	592539	594503	fructose-bisphosphate aldolase, chloroplast precursor
	VIT_03s0038g00690	3	594846	598517	Zinc finger (B-box type)
	VIT_03s0038g00700	3	606114	613813	Kinesin motor protein
	VIT_03s0038g00710	3	614468	614930	Unknown
	VIT_03s0038g00720	3	615777	618174	NADH dehydrogenase (ubiquinone) 1 beta subcomplex 9
	VIT_03s0038g00730	3	623867	624348	No hit
	VIT_03s0038g00740	3	624648	632238	GC1 (GIANT chloroplast 1)
	VIT_03s0038g00750	3	632713	639536	Ubiquitin fusion degradation protein UFD1
	VIT_03s0038g00760	3	644491	647420	Arginine decarboxylase (Fragment)
	VIT_03s0038g00790	3	662174	664796	V-type H ⁺ -transporting ATPase 16kDa proteolipid subunit
	VIT_03s0038g00800	3	666647	670774	NADP-dependent D-sorbitol-6-phosphate dehydrogenase
	VIT_03s0038g00820	3	670775	676616	3-oxo-5-alpha-steroid 4-dehydrogenase, C-terminal
	VIT_03s0038g00840	3	679207	684375	BPC4/BBR/BPC4/BPC4
	VIT_03s0038g00860	3	689247	693308	Basic Leucine Zipper Transcription Factor (VvbZIP05)
	VIT_03s0038g00870	3	694566	700828	Dihydrouridine synthase 3
	VIT_03s0038g00880	3	702486	704460	Amidophosphoribosyltransferase 2
	VIT_03s0038g00890	3	709401	710989	No hit
	VIT_03s0038g00910	3	713857	721463	Ribosome-binding factor A, chloroplast precursor
	VIT_03s0038g00920	3	722303	732914	Carbohydrate kinase, PfkB
	VIT_03s0038g00930	3	736435	737319	Auxin responsive SAUR protein
	VIT_03s0038g00940	3	738127	738887	Auxin-responsive
	VIT_03s0038g00950	3	749716	750398	Auxin-responsive SAUR9
	VIT_03s0038g00960	3	755323	760266	Transcription factor TFIIF
	VIT_03s0038g00980	3	783897	784664	Unknown
	VIT_03s0038g01010	3	799108	799188	No hit

VIT_03s0038g01020	3	815278	815673	Metalloprotease
VIT_03s0038g01060	3	854295	855373	Metalloprotease
VIT_03s0038g01070	3	856872	858394	Pentatricopeptide (PPR) repeat-containing protein
VIT_03s0038g01080	3	858886	859170	Auxin responsive SAUR protein
VIT_03s0038g01090	3	862995	863398	Auxin responsive SAUR protein
VIT_03s0038g01100	3	864608	864876	Auxin responsive SAUR protein
VIT_03s0038g01110	3	866357	866897	Auxin-responsive SAUR31
VIT_03s0038g01120	3	867890	868156	Auxin responsive SAUR protein
VIT_03s0038g01130	3	869586	872380	Auxin-responsive
VIT_03s0038g01140	3	876348	878337	Metalloendoproteinase 1 precursor
VIT_03s0038g01150	3	880653	881315	Auxin-responsive
VIT_03s0038g01160	3	883689	883976	Auxin responsive SAUR protein
VIT_03s0038g01170	3	885397	885684	Auxin responsive SAUR protein
VIT_03s0038g01180	3	888635	888955	Auxin responsive SAUR protein
VIT_03s0038g01190	3	892009	892382	Auxin-induced SAUR
VIT_03s0038g01210	3	894854	895141	Auxin responsive SAUR protein
VIT_03s0038g01220	3	897891	898180	Auxin-induced protein 15A
VIT_03s0038g01230	3	900918	901205	Auxin responsive SAUR protein
VIT_03s0038g01250	3	903282	903569	Auxin responsive SAUR protein
VIT_03s0038g01260	3	905892	906181	Auxin responsive SAUR protein
VIT_03s0038g01270	3	908817	909399	Auxin responsive SAUR protein
VIT_03s0038g01280	3	910867	911175	Auxin responsive SAUR protein
VIT_03s0038g01290	3	915230	915499	Auxin responsive SAUR protein
VIT_03s0038g01300	3	917424	917748	Auxin-induced SAUR
VIT_03s0038g01310	3	921733	927965	Auxin responsive SAUR protein
VIT_03s0038g01320	3	930985	948815	Crp1 protein
VIT_03s0038g01330	3	955035	956506	Anthranilate N-benzoyltransferase protein 1
VIT_03s0038g01360	3	964891	966169	Unknown
VIT_03s0038g01370	3	967748	969830	ABA-responsive protein (HVA22)HVA22H
VIT_03s0038g01380	3	971266	975571	Calcium-binding EF hand
VIT_03s0038g01390	3	976131	977121	Aquaporin TIP3;1
VIT_03s0038g01400	3	978958	982622	R protein PRF disease resistance protein
VIT_03s0038g01410	3	984045	985466	Aquaporin PIP PIP1A
VIT_03s0038g01420	3	991431	993320	Phytochelatin synthetase
VIT_03s0038g01430	3	993344	994100	Phytochelatin synthetase
VIT_03s0038g01440	3	996232	1004637	Adenosylhomocysteine nucleosidase.

VIT_03s0038g01450	3	1004638	1005093	No hit
VIT_03s0038g01460	3	1006320	1009717	Chalcone synthase
VIT_03s0038g01470	3	1009718	1014601	ER lumen protein retaining receptor
VIT_03s0038g01480	3	1015472	1018780	Beta-fructofuranosidase
VIT_03s0038g01490	3	1025473	1040019	Unknown protein
VIT_03s0038g01510	3	1041388	1041967	Unknown protein
VIT_03s0038g01520	3	1044307	1047456	R protein PRF disease resistance protein
VIT_03s0038g01530	3	1050448	1058022	R protein PRF disease resistance protein
VIT_03s0038g01540	3	1062491	1063732	R protein PRF disease resistance protein
VIT_03s0038g01550	3	1066258	1068897	R protein PRF disease resistance protein
VIT_03s0038g01580	3	1077896	1078534	R protein PRF disease resistance protein
VIT_03s0038g01590	3	1082216	1083954	Disease resistance protein (CC-NBS-LRR class)
VIT_03s0038g01610	3	1084197	1085815	R protein PRF disease resistance protein
VIT_03s0038g01620	3	1088445	1096163	R protein MLA10
VIT_03s0038g01630	3	1111137	1113800	R protein PRF disease resistance protein
VIT_03s0038g01670	3	1168819	1177208	R protein PRF disease resistance protein
VIT_03s0038g01740	3	1215576	1222056	Disease resistance RPP8 2
VIT_03s0038g01750	3	1224505	1226936	Disease resistance RPP8 2
VIT_03s0038g01760	3	1231040	1235642	Disease resistance protein (CC-NBS class)
VIT_03s0038g01770	3	1235713	1237448	Disease resistance protein (CC-NBS-LRR class)
VIT_03s0038g01780	3	1238202	1248527	Triosephosphate isomerase, chloroplast precursor
VIT_03s0038g01790	3	1252286	1255340	basic helix-loop-helix (bHLH) family
VIT_03s0038g01810	3	1263090	1274110	XAP5
VIT_03s0038g01820	3	1275024	1279206	Translocon-associated protein alpha TRAP complex
VIT_03s0038g01830	3	1283253	1285733	Proline-rich protein 4
VIT_03s0038g01840	3	1286455	1288037	Proline-rich protein 4
VIT_03s0038g01850	3	1298173	1299515	Proline-rich protein 4
VIT_03s0038g01860	3	1301501	1302939	Proline-rich protein 4
VIT_03s0038g01870	3	1303910	1304387	Nuclear pore complex protein Nup188
VIT_03s0038g01880	3	1313644	1323526	Nuclear pore complex protein Nup188
VIT_03s0038g01920	3	1332326	1347193	Nuclear pore complex protein Nup188
VIT_03s0038g01930	3	1347905	1348611	Peptidyl-prolyl cis-trans isomerase ROC5 (rotamase CYP 5)
VIT_03s0038g01940	3	1349912	1356622	Permease nonimprinted in Prader-Willi/Angelman
VIT_03s0038g01950	3	1357739	1360559	Glycine-rich protein
VIT_03s0038g01960	3	1362167	1363750	Proline-rich family protein
VIT_03s0038g01970	3	1367294	1369340	Amidase

VIT_03s0038g01990	3	1374043	1381233	Amidase
VIT_03s0038g02000	3	1383516	1393182	Amidase
VIT_03s0038g02010	3	1393183	1395922	Amidase
VIT_03s0038g02020	3	1395923	1400744	Amidase
VIT_03s0038g02030	3	1402181	1405517	Amidase
VIT_03s0038g02040	3	1406571	1408542	Amidase
VIT_03s0038g02050	3	1412118	1412819	Dirigent protein pDIR7
VIT_03s0038g02060	3	1415776	1416475	Dirigent protein pDIR7
VIT_03s0038g02070	3	1424949	1429038	TOC132
VIT_03s0038g02080	3	1436852	1438855	Pentatricopeptide (PPR) repeat-containing protein
VIT_03s0038g02090	3	1441262	1442535	Phospholipase C.
VIT_03s0038g02100	3	1443063	1447359	SAM-dependent methyltransferase
VIT_03s0038g02110	3	1449330	1451521	Co-chaperone-curved DNA binding protein A
VIT_03s0038g02120	3	1459580	1461586	Armadillo/beta-catenin repeat
VIT_03s0038g02130	3	1468239	1469371	Cold shock protein-1
VIT_03s0038g02140	3	1472504	1476160	Auxin transporter protein 2
VIT_03s0038g02150	3	1482091	1483271	Unknown
VIT_03s0038g02160	3	1484216	1486196	Thaumatococcus
VIT_03s0038g02170	3	1492918	1494778	Thaumatococcus
VIT_03s0038g02180	3	1497491	1500305	Glycosyl hydrolase family 10 protein
VIT_03s0038g02190	3	1502133	1506299	Nodulin
VIT_03s0038g02200	3	1512323	1518218	Peptidyl-prolyl cis-trans isomerase A (cyclophilin A)
VIT_03s0038g02210	3	1519055	1524015	Choline transporter
VIT_03s0038g02220	3	1528083	1528899	Cofilin
VIT_03s0038g02230	3	1535564	1538193	Subtilisin-like serine protease 2
VIT_03s0038g02240	3	1543645	1546820	Unknown protein
VIT_03s0038g02250	3	1549919	1551865	Pentatricopeptide (PPR) repeat-containing protein
VIT_03s0038g02280	3	1560125	1564783	ERD7 (EARLY-responsive TO dehydration 7)
VIT_03s0038g02290	3	1565250	1567734	Amino acid permease 3
VIT_03s0038g02300	3	1570637	1574913	Proteasome 20S alpha subunit D2 (PAD2) (PRS1) (PRC6)
VIT_03s0038g02310	3	1584039	1585078	myb domain protein 4 (VvMyb4a)
VIT_03s0038g02320	3	1587630	1594603	L-ascorbate peroxidase.
VIT_03s0038g02330	3	1595396	1600087	CLB1 protein
VIT_03s0038g02340	3	1612568	1639214	HECT ubiquitin-protein ligase 3 (KAKTUS protein)
VIT_03s0038g02350	3	1639215	1639769	No hit
VIT_03s0038g02360	3	1640991	1645417	D-galactoside/L-rhamnose binding SUEL lectin

<i>pheno_3_2</i>	VIT_03s0180g00010	3	5934501	5937492	Cysteine proteinase
	VIT_03s0180g00020	3	5941848	5961872	Phosphoric monoester hydrolase
	VIT_03s0180g00030	3	5962649	5966620	Calcium-binding protein
	VIT_03s0180g00040	3	5973785	5975813	Cyclin D3_2
	VIT_03s0180g00050	3	5981525	5989159	DNA-directed RNA polymerase II subunit C
	VIT_03s0180g00060	3	5989504	5993941	Late embryonic abundant protein EMB7
	VIT_03s0180g00070	3	5995174	6000876	Cyclase
	VIT_03s0180g00080	3	6009317	6020720	Cyclase
	VIT_03s0180g00090	3	6023040	6024531	Receptor kinase
	VIT_03s0180g00100	3	6030251	6032840	Unknown protein
	VIT_03s0180g00110	3	6033723	6036694	Stress enhanced protein 1 (SEP1)
	VIT_03s0180g00120	3	6037870	6059709	Sodium hydrogen antiporter NHD1
	VIT_03s0180g00130	3	6060227	6064528	D-3-phosphoglycerate dehydrogenase, chloroplast precursor
	VIT_03s0180g00140	3	6071530	6072486	Acetyl xylan esterase AxeA
	VIT_03s0180g00150	3	6078670	6081676	Receptor protein kinase
	VIT_03s0180g00160	3	6090668	6100225	ATTIC21/CIA5/TIC21 (chloroplast import apparatus 5)
	VIT_03s0180g00170	3	6101310	6105927	Reticulon-like protein B11 RTNLB11
	VIT_03s0180g00180	3	6106602	6118797	Unknown protein
	VIT_03s0180g00190	3	6119889	6124371	No hit
	VIT_03s0180g00200	3	6124465	6126202	Limonoid UDP-glucosyltransferase (VvGT2)
	VIT_03s0180g00210	3	6147352	6148726	Myb domain protein R1
	VIT_03s0180g00230	3	6166608	6177981	UNC-50
	VIT_03s0180g00240	3	6179625	6179759	No hit
	VIT_03s0180g00250	3	6179858	6181360	Cinnamyl alcohol dehydrogenase
	VIT_03s0180g00260	3	6212329	6214039	Cinnamyl alcohol dehydrogenase
	VIT_03s0180g00270	3	6217552	6226884	Pseudouridine synthase
	VIT_03s0180g00280	3	6255489	6257208	Indole-3-acetate beta-glucosyltransferase
	VIT_03s0180g00290	3	6263737	6264635	Gibberellin-regulated protein 4 (GASA4)
	VIT_03s0180g00300	3	6267395	6267971	ABC transporter F member 2
	VIT_03s0180g00310	3	6269156	6269856	ATP-dependent Clp protease ClpB protein
	VIT_03s0180g00320	3	6281986	6283705	indole-3-acetate beta-glucosyltransferase (VvGT3)
	VIT_03s0091g00010	3	6310807	6311602	No hit
	VIT_03s0091g00020	3	6314436	6314606	No hit
	VIT_03s0091g00030	3	6314607	6315780	No hit
	VIT_03s0091g00040	3	6338109	6339850	Limonoid UDP-glucosyltransferase (VvGT1)
	VIT_03s0091g00050	3	6357496	6364352	Triacylglycerol/steryl ester hydrolase

VIT_03s0091g00060	3	6374562	6374820	ACT domain-containing protein (ACR6)
VIT_03s0091g00070	3	6374821	6376254	ACT domain-containing protein (ACR6)
VIT_03s0091g00080	3	6384738	6388178	Methylthioribose kinase
VIT_03s0091g00090	3	6388280	6390379	No hit
VIT_03s0091g00100	3	6391617	6395252	Methylthioribose kinase
VIT_03s0091g00110	3	6395575	6397456	Plant basic secretory protein (BSP) family
VIT_03s0091g00120	3	6398105	6398826	Prp27-like protein
VIT_03s0091g00130	3	6399870	6400567	Prp27
VIT_03s0091g00140	3	6404905	6405345	Plant basic secretory protein (BSP) family
VIT_03s0091g00150	3	6405346	6405711	NtPRp27 secretory protein
VIT_03s0091g00160	3	6406167	6406991	NtPRp27 secretory protein
VIT_03s0091g00180	3	6419877	6420461	Unknown
VIT_03s0091g00190	3	6447349	6451553	WD40
VIT_03s0091g00200	3	6479048	6503929	DNA repair protein REV1
VIT_03s0091g00210	3	6507392	6509263	Ethylene-responsive protein
VIT_03s0091g00220	3	6511172	6511647	Unknown protein
VIT_03s0091g00230	3	6512832	6514492	Unknown protein
VIT_03s0091g00240	3	6521904	6537905	Haloacid dehalogenase hydrolase
VIT_03s0091g00250	3	6538966	6539935	Unknown
VIT_03s0091g00260	3	6548677	6549577	Zinc finger protein 4
VIT_03s0091g00270	3	6551840	6559848	TIP41
VIT_03s0091g00280	3	6566136	6569256	Cyclin A3;4
VIT_03s0091g00290	3	6571900	6589424	Pathogenesis-related homeodomain protein (PRHA)
VIT_03s0091g00300	3	6623124	6623416	B-cell receptor-associated protein 31
VIT_03s0091g00310	3	6633708	6635996	Indole-3-acetic acid-amido synthetase GH3.8
VIT_03s0091g00320	3	6642216	6651075	Ribosomal rna assembly protein mis3
VIT_03s0091g00350	3	6664651	6666079	No hit
VIT_03s0091g00360	3	6668161	6688642	Seed maturation protein PM23
VIT_03s0091g00370	3	6691248	6693137	Pentatricopeptide (PPR) repeat-containing protein
VIT_03s0091g00380	3	6699445	6705656	Thioredoxin domain-containing protein 9
VIT_03s0091g00390	3	6715491	6716068	Snakin-1
VIT_03s0091g00400	3	6717421	6752391	Transducin family protein / WD-40 repeat
VIT_03s0091g00410	3	6773316	6776359	Unknown protein
VIT_03s0091g00420	3	6785458	6787059	No hit
VIT_03s0091g00430	3	6798217	6802152	SWIB complex BAF60b domain-containing protein
VIT_03s0091g00440	3	6804406	6807382	Pentatricopeptide (PPR) repeat-containing protein

VIT_03s0091g00450	3	6811798	6813280	Progesterone 5-beta-reductase
VIT_03s0091g00460	3	6817116	6818768	Unknown protein
VIT_03s0091g00470	3	6846055	6849796	Protein phosphatase 2C
VIT_03s0091g00480	3	6851584	6855075	Zinc finger (C3HC4-type ring finger)
VIT_03s0091g00490	3	6859815	6860409	Unknown protein
VIT_03s0091g00500	3	6871858	6872341	Unknown protein
VIT_03s0091g00510	3	6894959	6895595	Unknown
VIT_03s0091g00520	3	6905764	6914781	Prolyl 4-hydroxylase
VIT_03s0091g00530	3	6917800	6921320	N-acetyltransferase ESCO2
VIT_03s0091g00540	3	6976055	6984113	Prolyl 4-hydroxylase
VIT_03s0091g00550	3	6987237	6990594	Unknown protein
VIT_03s0091g00560	3	6995098	6998522	Leucine-rich repeat protein kinase
VIT_03s0091g00570	3	6998808	6999512	No hit
VIT_03s0091g00580	3	7035451	7039010	Protein Mpv17
VIT_03s0091g00590	3	7040488	7042974	Unknown protein
VIT_03s0091g00600	3	7044909	7047565	Amino acid permease
VIT_03s0091g00610	3	7050934	7055804	Sulfhydryl oxidase Erv1/Alr
VIT_03s0091g00620	3	7055805	7059068	Histone deacetylase HDA6
VIT_03s0091g00630	3	7065044	7065631	YGGT family protein
VIT_03s0091g00640	3	7072474	7073358	Ribosomal protein S29 (RPS29C) 40S
VIT_03s0091g00650	3	7076200	7076677	No hit
VIT_03s0091g00660	3	7082071	7098207	Unknown protein
VIT_03s0091g00670	3	7099015	7099742	Lateral organ boundaries protein 38
VIT_03s0091g00680	3	7103281	7113666	NPY2 (naked pins in yuc mutants 2)
VIT_03s0091g00690	3	7125371	7126295	Salt tolerance zinc finger
VIT_03s0091g00700	3	7137444	7143607	ATP-dependent Clp protease proteolytic subunit (ClpR1) (nClpP5)
VIT_03s0091g00710	3	7149908	7160638	Mitotic checkpoint protein BUB3
VIT_03s0091g00720	3	7168741	7177092	Zinc finger (C3HC4-type ring finger)
VIT_03s0091g00730	3	7192504	7193911	basic helix-loop-helix (bHLH) family
VIT_03s0091g00740	3	7195947	7206249	Vacuolar sorting receptor 3
VIT_03s0091g00750	3	7219508	7223633	Beta-1,4-xylosidase
VIT_03s0091g00760	3	7223730	7230484	Interferon-related developmental regulator family
VIT_03s0091g00770	3	7244888	7245217	No hit
VIT_03s0091g00810	3	7287360	7289100	Beta-1,4-xylosidase
VIT_03s0091g00820	3	7291711	7302903	Radical SAM domain-containing protein
VIT_03s0091g00830	3	7303408	7311191	Cyclin-related

VIT_03s0091g00840	3	7321433	7322062	Porin
VIT_03s0091g00850	3	7323004	7324112	Unknown protein
VIT_03s0091g00860	3	7324113	7339946	DNA polymerase kappa subunit
VIT_03s0091g00870	3	7342165	7357074	Adenylylsulfate kinase 1 (AKN1)
VIT_03s0091g00880	3	7374686	7382483	Endoxylanase
VIT_03s0091g00890	3	7385745	7389061	Endoxylanase
VIT_03s0091g00900	3	7389633	7402240	Endoxylanase
VIT_03s0091g00920	3	7415296	7415826	Zfwd2 protein (ZFWD2)
VIT_03s0091g00930	3	7417454	7418376	GRAM domain-containing protein / ABA-responsive
VIT_03s0091g00940	3	7428322	7430945	Zfwd2 protein (ZFWD2)
VIT_03s0091g00950	3	7441440	7444729	Endoxylanase
VIT_03s0091g00960	3	7446465	7449614	No hit
VIT_03s0091g00970	3	7469828	7484328	ADP-ribosylation factor-like A1D
VIT_03s0091g00990	3	7502149	7502253	Heat shock protein 70
VIT_03s0091g01010	3	7535063	7536574	LIM domain protein WLIM1
VIT_03s0091g01020	3	7537306	7559608	Unknown protein
VIT_03s0091g01030	3	7563890	7582120	Telomere repeat binding factor 1
VIT_03s0091g01040	3	7603310	7604326	No hit
VIT_03s0091g01050	3	7652632	7661288	Nucleobase-ascorbate transporter 4 (NAT4)
VIT_03s0091g01060	3	7673917	7675754	Cyclin delta-2
VIT_03s0091g01080	3	7693399	7695038	l-aminocyclopropane-1-carboxylate oxidase
VIT_03s0091g01090	3	7704746	7705934	Unknown
VIT_03s0091g01100	3	7710736	7711700	Unknown protein
VIT_03s0091g01110	3	7716202	7726782	Meprin and TRAF homology domain-containing protein
VIT_03s0091g01120	3	7739421	7740245	Meprin and TRAF homology domain-containing protein
VIT_03s0091g01130	3	7741682	7743818	Meprin and TRAF homology domain-containing protein
VIT_03s0091g01140	3	7747402	7749276	Meprin and TRAF homology domain-containing protein
VIT_03s0091g01150	3	7759653	7762665	Cleavage and polyadenylation specificity factor
VIT_03s0091g01160	3	7771297	7771879	No hit
VIT_03s0091g01170	3	7813667	7815342	Meprin and TRAF homology domain-containing protein
VIT_03s0091g01180	3	7826669	7826884	No hit
VIT_03s0091g01190	3	7831919	7853120	Magnesium transporter CorA
VIT_03s0091g01200	3	7855565	7861870	Sinapoylglucose:malate sinapoyltransferase (SNG1)
VIT_03s0091g01220	3	7888986	7890085	Enhancer of mRNA-decapping protein 4
VIT_03s0091g01230	3	7890272	7892417	Enhancer of mRNA-decapping protein 4
VIT_03s0091g01240	3	7903958	7907570	Serine carboxypeptidase S10 / Anthocyanin Acyl-transferase

VIT_03s0091g01260	3	7918875	7934080	No hit
VIT_03s0091g01270	3	7935398	7938767	sinapoylglucose-choline O-sinapoyltransferase
VIT_03s0091g01280	3	7942831	7944961	No hit
VIT_03s0091g01290	3	7951175	7955690	Serine carboxypeptidase S10
VIT_03s0088g00010	3	7987351	7989378	Concanavalin A lectin
VIT_03s0088g00030	3	8005949	8006486	Serine carboxypeptidase-like 6
VIT_03s0088g00040	3	8018981	8020373	Concanavalin A lectin
VIT_03s0088g00050	3	8035215	8039037	Serine carboxypeptidase 1
VIT_03s0088g00060	3	8069862	8072808	Isoflavone reductase
VIT_03s0088g00070	3	8084352	8086688	No hit
VIT_03s0088g00100	3	8122234	8124112	Concanavalin A lectin
VIT_03s0088g00110	3	8141417	8145242	Serine carboxypeptidase SCPL17
VIT_03s0088g00140	3	8186019	8188472	Isoflavone reductase protein 2
VIT_03s0088g00150	3	8193838	8194272	Serine carboxypeptidase SCPL17
VIT_03s0088g00160	3	8195668	8197771	Serine carboxypeptidase SCPL17
VIT_03s0088g00170	3	8209417	8210614	Brassinosteroid insensitive 1-associated receptor kinase 1
VIT_03s0088g00180	3	8212188	8213029	No hit
VIT_03s0088g00190	3	8220525	8221777	Brassinosteroid insensitive 1-associated receptor kinase 1
VIT_03s0088g00200	3	8228928	8232449	Unknown
VIT_03s0088g00210	3	8232628	8239401	STT3B (staurosporin and temperature sensitive 3-like B)
VIT_03s0088g00220	3	8240353	8241018	Replication factor A 1, rfa1
VIT_03s0088g00230	3	8241019	8242075	Replication protein A 70 kDa DNA-binding subunit
VIT_03s0088g00240	3	8242076	8244718	Replication protein A 70b
VIT_03s0088g00250	3	8244719	8251952	Isoflavone reductase
VIT_03s0088g00260	3	8252549	8257129	Serine carboxypeptidase S10
VIT_03s0088g00270	3	8267214	8267760	No hit
VIT_03s0088g00280	3	8281268	8302843	Ribosomal RNA small subunit methyltransferase E
VIT_03s0088g00290	3	8315170	8315924	Phytosulfokines PSK2
VIT_03s0088g00300	3	8320984	8322831	Unknown
VIT_03s0088g00310	3	8329921	8335645	No hit
VIT_03s0088g00320	3	8343365	8347681	Peptidase M50
VIT_03s0088g00330	3	8350297	8352177	F-box protein 7
VIT_03s0088g00340	3	8371381	8372242	No hit
VIT_03s0088g00350	3	8374871	8376359	Unknown
VIT_03s0088g00370	3	8403058	8408371	Unknown protein
VIT_03s0088g00380	3	8412010	8414515	Tubulin alpha

VIT_03s0088g00390	3	8414516	8423780	DnaJ homolog, subfamily C, member 17
VIT_03s0088g00400	3	8427000	8430780	Tubulin alpha-6 chain
VIT_03s0088g00410	3	8432142	8436432	Pyruvate kinase isozyme A, chloroplast precursor
VIT_03s0088g00420	3	8443429	8445079	Gag-pol polyprotein
VIT_03s0088g00450	3	8486720	8618518	FKBP12-rapamycin complex-associated protein
VIT_03s0088g00460	3	8630875	8631169	Angustifolia
VIT_03s0088g00470	3	8631326	8631646	Auxin responsive SAUR protein
VIT_03s0088g00490	3	8653859	8658460	Unknown
VIT_03s0088g00500	3	8660759	8679489	TRNA synthetase class II (D, K and N)
VIT_03s0088g00510	3	8696026	8697570	hypothetical MADS-box type 1 alpha 1b (VviMADS1A1b)
VIT_03s0088g00540	3	8736929	8743307	No hit
VIT_03s0088g00550	3	8744237	8744878	putative MADS-box type 1 alpha 1a (VviMADS1A1a)
VIT_03s0088g00560	3	8763759	8765911	Citrate synthase
VIT_03s0088g00570	3	8766129	8766881	Glutamine synthetase B1 GLB1
VIT_03s0088g00590	3	8776002	8776646	hypothetical MADS-box type 1 alpha 1g (VviMADS1A1g)
VIT_03s0088g00600	3	8793246	8793890	putative MADS-box type 1 alpha 1c (VviMADS1A1c)
VIT_03s0088g00610	3	8820035	8820694	hypothetical MADS-box type 1 alpha 1f (VviMADS1A1f)
VIT_03s0088g00620	3	8825504	8827218	Stress-induced
VIT_03s0088g00630	3	8828264	8830122	Unknown protein
VIT_03s0088g00650	3	8842942	8844322	Xyloglucan:xyloglucosyl transferase
VIT_03s0088g00680	3	8883856	8884465	Pathogenesis-related protein 1 precursor (PRP 1)
VIT_03s0088g00690	3	8895244	8909155	Pathogenesis-related protein 1 precursor (PRP 1)
VIT_03s0088g00700	3	8911524	8912111	Pathogenesis related protein 1 precursor (pr1 gene)
VIT_03s0088g00710	3	8916223	8916893	Pathogenesis-related protein 1 precursor (PRP 1)
VIT_03s0088g00720	3	8923838	8924209	Pathogenesis-related protein 1 precursor (PRP 1)
VIT_03s0088g00730	3	8927274	8927983	Methionine sulfoxide reductase
VIT_03s0088g00750	3	8949588	8950233	Pathogenesis related protein 1 precursor [Vitis vinifera]
VIT_03s0088g00760	3	8955534	8962261	No hit
VIT_03s0088g00780	3	8986184	8986955	Pathogenesis-related protein 1 precursor (PRP 1)
VIT_03s0088g00810	3	9044529	9045211	Pathogenesis-related protein 1 precursor (PRP 1)
VIT_03s0088g00820	3	9050245	9055257	Unknown
VIT_03s0088g00840	3	9072903	9073766	No hit
VIT_03s0088g00860	3	9080159	9081145	Lectin-like receptor kinase
VIT_03s0088g00880	3	9083004	9083780	Kinase
VIT_03s0088g00890	3	9101007	9101495	Pathogenesis related protein 1 precursor [Vitis vinifera]
VIT_03s0088g00900	3	9106967	9110222	Pathogenesis-related protein 1B

VIT_03s0088g00910	3	9119915	9130668	Pathogenesis related protein 1 precursor [Vitis vinifera]
VIT_03s0088g00920	3	9145287	9145858	Unknown
VIT_03s0088g00930	3	9146189	9147403	Zinc finger (C3HC4-type ring finger)
VIT_03s0088g00940	3	9150089	9150575	Pathogenesis-related protein 1 precursor (PRP 1)
VIT_03s0088g00950	3	9153293	9162432	Unknown protein
VIT_03s0088g00960	3	9168413	9182543	Unknown protein
VIT_03s0088g00970	3	9190121	9193027	No hit
VIT_03s0088g00980	3	9205881	9213548	Unknown protein
VIT_03s0088g00990	3	9216064	9223316	Metal transporter CNNM4 (Cyclin-M4)
VIT_03s0088g01000	3	9223670	9231652	Unknown protein
VIT_03s0088g01030	3	9249737	9251605	No hit
VIT_03s0088g01040	3	9270928	9285459	Aminotransferase AGD2
VIT_03s0088g01050	3	9286043	9295905	Transposon protein, Mutator sub-class
VIT_03s0088g01060	3	9296849	9309519	Aminotransferase AGD2
VIT_03s0088g01070	3	9310070	9311966	Mutator-like transposase
VIT_03s0088g01080	3	9311967	9314129	No hit
VIT_03s0088g01090	3	9340156	9341562	Zinc finger (C3HC4-type ring finger)
VIT_03s0088g01100	3	9342100	9347312	Leaf senescence related protein-like
VIT_03s0088g01130	3	9373663	9376242	EMB2758 (embryo defective 2758)
VIT_03s0088g01140	3	9385888	9388788	Squalene monooxygenase 2
VIT_03s0088g01150	3	9394421	9397946	Squalene monooxygenase
VIT_03s0088g01160	3	9408764	9412394	Unknown protein
VIT_03s0088g01170	3	9414656	9433536	Proline iminopeptidase
VIT_03s0088g01180	3	9438885	9442060	Proline iminopeptidase
VIT_03s0088g01190	3	9452241	9454982	Malate dehydrogenase, glyoxysomal precursor
VIT_03s0088g01200	3	9455172	9457915	Unknown protein
VIT_03s0088g01220	3	9506440	9508439	Unknown protein
VIT_03s0088g01240	3	9525109	9527109	basic helix-loop-helix (bHLH) family
VIT_03s0088g01250	3	9538993	9552353	D-threo-aldose 1-dehydrogenase
VIT_03s0088g01260	3	9553280	9614184	TIP growth defective 1
VIT_03s0088g01270	3	9672111	9672900	No hit
VIT_03s0088g01280	3	9675335	9678621	No hit
VIT_03s0088g01290	3	9698489	9706945	Inorganic pyrophosphatase
VIT_03s0088g01300	3	9707224	9708876	No hit
VIT_00s0282g00060	3	9723604	9724492	No hit
VIT_00s0282g00050	3	9731330	9732112	Separase

VIT_00s0282g00040	3	9752559	9770979	Major facilitator superfamily protein (MFS) Spinster
VIT_00s0282g00030	3	9781570	9797118	Leaf senescence protein
VIT_00s0282g00020	3	9805549	9820005	K ⁺ efflux antiporter (KEA3)
VIT_00s0282g00010	3	9821313	9827537	Methionine sulfoxide reductase
VIT_03s0097g00010	3	9843656	9843781	No hit
VIT_03s0097g00030	3	9871902	9873992	Concanavalin A lectin
VIT_03s0097g00040	3	9876165	9877081	No hit
VIT_03s0097g00060	3	9887464	9888181	Arginine-tRNA-protein transferase 1
VIT_03s0097g00070	3	9889442	9890273	Lectin protein kinase
VIT_03s0097g00080	3	9894840	9900035	Lectin protein kinase
VIT_03s0097g00090	3	9909044	9909574	Lectin protein kinase
VIT_03s0097g00110	3	9958876	9960414	Concanavalin A lectin
VIT_03s0097g00120	3	9991550	9993565	Concanavalin A lectin
VIT_03s0097g00130	3	10022997	10024832	Concanavalin A lectin
VIT_03s0097g00140	3	10025188	10025953	No hit
VIT_03s0097g00160	3	10121969	10123630	putative MADS-box Agamous-like 17b (VviAGL17b)
VIT_03s0097g00210	3	10224330	10224440	No hit
VIT_03s0097g00220	3	10252090	10253094	1,4-beta-mannan endohydrolase
VIT_03s0097g00230	3	10258196	10258417	No hit
VIT_03s0097g00240	3	10269562	10272060	No hit
VIT_03s0097g00250	3	10282948	10283841	No hit
VIT_03s0097g00280	3	10349623	10350180	Unknown protein
VIT_03s0097g00290	3	10361093	10362571	Unknown
VIT_03s0097g00300	3	10363405	10365027	Myosin-like protein XIK
VIT_03s0097g00330	3	10451345	10452028	No hit
VIT_03s0097g00340	3	10470864	10472031	Monofunctional aspartokinase
VIT_03s0097g00350	3	10472994	10475771	Myosin-like protein XIK
VIT_03s0097g00360	3	10534330	10535472	No hit
VIT_03s0097g00370	3	10558884	10559186	No hit
VIT_03s0097g00380	3	10665097	10666177	Monofunctional aspartokinase
VIT_03s0097g00390	3	10666726	10676862	Unknown protein
VIT_03s0097g00400	3	10714440	10714920	No hit
VIT_03s0097g00410	3	10717626	10717748	No hit
VIT_03s0097g00450	3	10822230	10823579	No hit
VIT_03s0097g00460	3	10833705	10835724	Geraniol 10-hydroxylase
VIT_03s0097g00470	3	10845461	10849526	ATHVA22A (Arabidopsis thaliana HVA22 homologue A)

<i>pheno_5_1</i>	VIT_05s0029g00940	5	16873754	16875673	No hit
	VIT_05s0029g00950	5	16879756	16883457	Tripeptidyl-peptidase 2
	VIT_05s0029g00970	5	16986453	17015689	No hit
	VIT_05s0029g00990	5	17071792	17090213	Tripeptidyl-peptidase 2
	VIT_05s0029g01000	5	17106964	17111001	HcrVf3 protein
	VIT_05s0029g01030	5	17241274	17241571	Aspartate aminotransferase
	VIT_05s0029g01040	5	17241582	17243823	Aspartate aminotransferase
	VIT_05s0029g01050	5	17254865	17255236	No hit
	VIT_05s0029g01060	5	17287266	17288837	ATELC/ELC
	VIT_05s0029g01070	5	17290076	17305071	Ribosome biogenesis protein Bms1
	VIT_05s0029g01080	5	17305146	17321891	Ribosome biogenesis protein Bms1
	VIT_05s0029g01090	5	17330068	17349574	Alpha 1,3-glucosidase
	VIT_05s0029g01100	5	17352483	17364242	RNA recognition motif (RRM)-containing protein
	VIT_05s0029g01110	5	17380653	17382173	Unknown protein
	VIT_05s0029g01120	5	17387012	17388607	WD-repeat protein
	VIT_05s0029g01130	5	17397255	17402916	Pentatricopeptide (PPR) repeat-containing protein
	VIT_05s0029g01140	5	17405622	17411752	Sucrose-phosphate synthase
	VIT_05s0029g01150	5	17421093	17421226	Elongation factor 1-alpha 1
	VIT_05s0029g01160	5	17421227	17421628	Elongation factor 1-alpha 1
	VIT_05s0029g01180	5	17458897	17459835	Unknown
	VIT_05s0029g01200	5	17481773	17510650	Methionyl-tRNA synthetase
	VIT_05s0029g01210	5	17512328	17526686	Alkaline phytoceramidase
	VIT_05s0029g01220	5	17527161	17548530	Unknown protein
	VIT_05s0029g01230	5	17566105	17570227	Unknown protein
	VIT_05s0029g01240	5	17581401	17589938	Unknown protein
	VIT_05s0029g01260	5	17601845	17608169	Unknown protein
	VIT_05s0029g01270	5	17618652	17621736	Unknown protein
	VIT_05s0029g01280	5	17634559	17635294	Unknown protein
	VIT_05s0029g01290	5	17661362	17667411	Aspartic protease
	VIT_05s0029g01300	5	17668812	17672689	MAGE (melanoma antigen-encoding gene)
	VIT_05s0029g01310	5	17672690	17691790	Actin related protein 2/3 complex, subunit 4
	VIT_05s0029g01340	5	17729528	17779782	Auxin-independent growth promoter (axi 1)
	VIT_05s0029g01350	5	17780683	17808865	RabGAP/TBC domain-containing protein
	VIT_05s0029g01360	5	17816849	17817058	No hit
	VIT_05s0029g01370	5	17818237	17852241	Ubiquitin-associated (UBA)
	VIT_05s0029g01380	5	17865450	17890042	UV radiation resistance associated

VIT_05s0029g01390	5	17892783	17894587	No hit
VIT_05s0029g01410	5	17910253	17910654	No hit
VIT_05s0029g01420	5	17958264	17962588	Ankyrin repeat
VIT_05s0029g01430	5	17962589	17980463	Ankyrin
VIT_05s0029g01440	5	17982084	17983215	Protein kinase Xa21
VIT_05s0029g01450	5	17991431	17992219	No hit
VIT_05s0029g01460	5	17997058	18001928	No hit
VIT_05s0029g01470	5	18038062	18038862	Protein kinase Xa21
VIT_05s0029g01480	5	18039108	18041182	Receptor kinase TRKe
VIT_05s0029g01490	5	18051810	18062080	Ankyrin repeat
VIT_05s0029g01500	5	18083541	18084599	Ankyrin repeat protein
VIT_05s0029g01510	5	18145463	18145669	No hit
VIT_05s0029g01520	5	18164134	18166380	Seven in absentia SINA4
VIT_05s0029g01530	5	18176485	18176941	No hit
VIT_05s0029g01540	5	18204070	18207297	Ankyrin repeat
VIT_05s0029g01570	5	18305556	18306917	CTV.20
VIT_05s0029g01580	5	18309911	18310471	Ankyrin repeat protein
VIT_05s0062g00010	5	18385412	18406790	PUMILIO 5 (APUM5)
VIT_05s0062g00020	5	18414218	18419262	F-box family protein
VIT_05s0062g00050	5	18586887	18587566	Protease Do-like 2, chloroplastic DEG2
VIT_05s0062g00060	5	18595309	18596094	Retrotransposon protein
VIT_05s0062g00110	5	18634743	18638371	Unknown protein
VIT_05s0062g00120	5	18674775	18679369	Ribosomal protein S8 (RPS8B) 40S
VIT_05s0062g00130	5	18682670	18707735	Protein transport protein Sec23A
VIT_05s0062g00140	5	18711528	18719113	PRD1
VIT_05s0062g00150	5	18721220	18732785	Pentatricopeptide repeat protein
VIT_05s0062g00160	5	18735084	18743648	No hit
VIT_05s0062g00200	5	18783093	18784137	Pentatricopeptide repeat-containing protein
VIT_05s0062g00210	5	18784791	18791811	Vacuolar ATP synthase subunit F
VIT_05s0062g00220	5	18792041	18801353	Inner membrane import protein Tic22, Chloroplast
VIT_05s0062g00240	5	18818659	18820264	Xyloglucan endotransglucosylase/hydrolase 23
VIT_05s0062g00250	5	18831568	18833016	Xyloglucan endotransglucosylase/hydrolase 15
VIT_05s0062g00260	5	18834498	18839309	Unknown
VIT_05s0062g00270	5	18843664	18845204	UDP-glucose:flavonoid 7-O-glucosyltransferase
VIT_05s0062g00300	5	18872492	18879621	UDP-glucuronosyl/UDP-glucosyl transferase UGT75C1
VIT_05s0062g00310	5	18881653	18883335	UDP-glucuronosyl/UDP-glucosyl transferase UGT75C1

VIT_05s0062g00320	5	18886880	18887014	No hit
VIT_05s0062g00340	5	18889800	18892378	UDP-glucose:flavonoid 7-O-glucosyltransferase
VIT_05s0062g00350	5	18895153	18896550	UDP-glucose:flavonoid 7-O-glucosyltransferase
VIT_05s0062g00360	5	18899918	18901613	UDP-glucose:flavonoid 7-O-glucosyltransferase
VIT_05s0062g00370	5	18920244	18920915	No hit
VIT_05s0062g00400	5	18966256	18968160	Indole-3-acetate beta-glucosyltransferase 1
VIT_05s0062g00410	5	18968252	18970326	No hit
VIT_05s0062g00430	5	18991958	18993513	UDP-glucose:flavonoid 7-O-glucosyltransferase
VIT_05s0062g00450	5	19023771	19025352	No hit
VIT_05s0062g00460	5	19027377	19028774	UDP-glucose:flavonoid 7-O-glucosyltransferase
VIT_05s0062g00470	5	19035904	19037295	UDP-glucose:flavonoid 7-O-glucosyltransferase
VIT_05s0062g00480	5	19056125	19057777	Xyloglucan endo-transglycosylase, C-terminal
VIT_05s0062g00490	5	19060743	19062243	No hit
VIT_05s0062g00500	5	19065380	19066637	No hit
VIT_05s0062g00510	5	19074901	19075119	Unknown
VIT_05s0062g00520	5	19088785	19090792	UDP-glucose:flavonoid 7-O-glucosyltransferase
VIT_05s0062g00560	5	19149824	19158516	No hit
VIT_05s0062g00570	5	19171107	19175569	UDP-glucose:flavonoid 7-O-glucosyltransferase
VIT_05s0062g00590	5	19182683	19184074	UDP-glucose:flavonoid 7-O-glucosyltransferase
VIT_05s0062g00610	5	19193950	19195592	Xyloglucan endotransglucosylase/hydrolase 23
VIT_05s0062g00620	5	19200908	19216029	Unknown
VIT_05s0062g00630	5	19226293	19228218	UDP-glucose transferase (UGT75B2)
VIT_05s0062g00640	5	19275169	19276859	UDP-glucose:flavonoid 7-O-glucosyltransferase
VIT_05s0062g00650	5	19303220	19312340	No hit
VIT_05s0062g00660	5	19312821	19313569	UDP-glucose:flavonoid 7-O-glucosyltransferase
VIT_05s0062g00670	5	19328962	19334904	No hit
VIT_05s0062g00680	5	19337594	19340715	Maturase
VIT_05s0062g00690	5	19347255	19348250	Heat shock protein 81-2 (HSP81-2)
VIT_05s0062g00700	5	19355732	19357242	UDP-glucose:flavonoid 7-O-glucosyltransferase
VIT_05s0062g00710	5	19377833	19379259	UDP-glucose:flavonoid 7-O-glucosyltransferase
VIT_05s0062g00720	5	19413520	19414986	UDP-glucuronosyl/UDP-glucosyl transferase UGT75C1
VIT_05s0062g00730	5	19415117	19418358	No hit
VIT_05s0062g00740	5	19421537	19423163	UDP-glucuronosyl/UDP-glucosyl transferase UGT75C1
VIT_05s0062g00760	5	19469712	19473848	Receptor kinase RHG4
VIT_05s0062g00770	5	19490732	19492576	Beta-1,3-glucanase
VIT_05s0062g00780	5	19498492	19500009	Rho GDP-dissociation inhibitor 2

	VIT_05s0062g00790	5	19501484	19509384	NSL1 (necrotic spotted lesions 1)
	VIT_05s0062g00800	5	19530733	19532850	No hit
	VIT_05s0062g00810	5	19532960	19534168	Lipoprotein
<i>pheno_7_1</i>	VIT_07s0151g00020	7	1111699	1112960	Ankyrin
	VIT_07s0151g00030	7	1116653	1117940	Ankyrin
	VIT_07s0151g00070	7	1121621	1122629	Ankyrin
	VIT_07s0151g00080	7	1124567	1125468	Ankyrin
	VIT_07s0151g00100	7	1127267	1139316	Ankyrin
	VIT_07s0151g00110	7	1143815	1145064	Chlorophyllase 1
	VIT_07s0151g00130	7	1150474	1152362	Chlorophyllase 1
	VIT_07s0151g00150	7	1156509	1163510	Ankyrin
	VIT_07s0151g00170	7	1164369	1165503	Ankyrin
	VIT_07s0151g00180	7	1168055	1169359	Ankyrin
	VIT_07s0151g00190	7	1171172	1172409	Chlorophyllase 1
	VIT_07s0151g00210	7	1176483	1178421	Chlorophyllase 1
	VIT_07s0151g00220	7	1180875	1191846	Ankyrin
	VIT_07s0151g00240	7	1194385	1195514	Ankyrin
	VIT_07s0151g00250	7	1197507	1198777	Chlorophyllase
	VIT_07s0151g00270	7	1206559	1206948	Chlorophyllase 1
	VIT_07s0151g00280	7	1223073	1225810	Bax inhibitor
	VIT_07s0151g00290	7	1226423	1230024	Unknown protein
	VIT_07s0151g00300	7	1231259	1234402	Unknown protein
	VIT_07s0151g00310	7	1234739	1241465	NIMA protein kinase NEK1
	VIT_07s0151g00340	7	1264579	1270254	Sulfate transporter 3.1 (AST12) (AtST1)
	VIT_07s0151g00360	7	1272684	1275182	Unknown protein
	VIT_07s0151g00370	7	1276735	1277605	Kinase interacting
	VIT_07s0151g00390	7	1284716	1284960	Ribosomal protein S14 30S
	VIT_07s0151g00410	7	1288652	1294516	Sulfate transporter 3.1 (AST12) (AtST1)
	VIT_07s0151g00430	7	1295689	1305019	Kinase interacting family protein
	VIT_07s0151g00460	7	1313821	1325350	3-methylcrotonyl-CoA carboxylase
	VIT_07s0151g00500	7	1326958	1332156	MLK/Raf-related protein kinase 1
	VIT_07s0151g00520	7	1334807	1343225	Homocysteine S-methyltransferase 3
	VIT_07s0151g00530	7	1344129	1346891	Unknown protein
	VIT_07s0151g00550	7	1350567	1353627	BUD32 family protein kinase
	VIT_07s0151g00570	7	1356706	1357645	OB-fold nucleic acid binding domain containing protein
	VIT_07s0151g00590	7	1363622	1368249	Inositol-1,4,5-trisphosphate 5-phosphatase CVP2, type I

	VIT_07s0151g00610	7	1386497	1394126	No hit
	VIT_07s0151g00620	7	1402324	1404679	Pentatricopeptide (PPR) repeat-containing protein
	VIT_07s0151g00630	7	1405392	1407468	Globulin-1 S allele precursor
	VIT_07s0151g00640	7	1408097	1410570	Globulin-1 S allele precursor
	VIT_07s0151g00660	7	1411745	1415073	Ribosomal protein L24 (At5g23535) 50S
	VIT_07s0151g00670	7	1415670	1416297	No hit
	VIT_07s0151g00690	7	1417935	1421821	Proteasome 20S beta subunit D (PBD1) (PRGB)
	VIT_07s0151g00700	7	1422111	1423298	EDA4 (embryo sac development arrest 4)
	VIT_07s0151g00720	7	1424054	1424497	Lipid transfer protein
	VIT_07s0151g00730	7	1428488	1429004	Unknown
	VIT_07s0151g00740	7	1430006	1434168	Non-specific lipid-transfer protein
	VIT_07s0151g00760	7	1435365	1436689	Lipid transfer protein
	VIT_07s0151g00770	7	1437817	1442530	Kelch repeat-containing F-box protein
	VIT_07s0151g00790	7	1443772	1448869	Transducin family protein / WD-40 repeat
	VIT_07s0151g00800	7	1454149	1456559	Unknown
	VIT_07s0151g00810	7	1459489	1462135	Unknown protein
	VIT_07s0151g00830	7	1467714	1468455	HSP20 chaperone
	VIT_07s0151g00840	7	1469525	1471546	Late embryogenesis abundant protein D-34 (LEA D-34)
	VIT_07s0151g00850	7	1475572	1476564	Unknown
	VIT_07s0151g00870	7	1478086	1496830	PHD finger transcription factor
	VIT_07s0151g00900	7	1499105	1501968	Ribosomal protein S24 (RPS24A) 40S
	VIT_07s0151g00910	7	1507287	1509238	Unknown
	VIT_07s0151g00930	7	1535022	1535998	Unknown protein
	VIT_07s0151g00950	7	1540668	1543574	Unknown protein
	VIT_07s0151g00960	7	1545126	1547795	WD repeat domain 5
	VIT_07s0151g00970	7	1548436	1560633	F-box protein
<i>pheno_11_1</i>	VIT_11s0016g03590	11	2932300	2940485	Transducin protein
	VIT_11s0016g03600	11	2943205	2945209	Proton-dependent oligopeptide transport (POT) family protein
	VIT_11s0016g03610	11	2948392	2950502	Proton-dependent oligopeptide transport (POT) family protein
	VIT_11s0016g03630	11	2964436	2968009	Peroxiredoxin-5
	VIT_11s0016g03640	11	2972017	2974625	Rac-like GTP-binding protein ARAC7 (GTPase protein ROP9)
	VIT_11s0016g03650	11	2976690	2979682	CDKF;1 (CDK-activating kinase 1A)
	VIT_11s0016g03660	11	2982086	2991775	Glucose transporter 2 plastidic
	VIT_11s0016g03670	11	2994483	3005396	Zinc finger (Ran-binding)
	VIT_11s0016g03680	11	3008220	3017923	Tesmin/TSO1-like CXC domain-containing
	VIT_11s0016g03690	11	3021953	3031545	Peroxisomal fatty acid beta-oxidation multifunctional protein (aim1)

VIT_11s0016g03700	11	3037438	3043744	Pentatricopeptide (PPR) repeat-containing protein
VIT_11s0016g03710	11	3044618	3049139	Abl interactor protein 1 (ABL1)
VIT_11s0016g03720	11	3049799	3055105	Aspartate aminotransferase, cytoplasmic (Transaminase A)
VIT_11s0016g03730	11	3057394	3057525	No hit
VIT_11s0016g03740	11	3057526	3060476	Rho guanyl-nucleotide exchange factor ROPGEF8
VIT_11s0016g03750	11	3061340	3072065	Myb-related protein 3R-1 (Plant c-MYB-like protein 1) MYB3R1
VIT_11s0016g03760	11	3079092	3081830	Unknown protein
VIT_11s0016g03770	11	3082194	3082576	Dynein light chain LC6, flagellar outer arm
VIT_11s0016g03780	11	3088819	3105779	Continuous vascular ring (COV1)
VIT_11s0016g03790	11	3107842	3108617	No hit
VIT_11s0016g03800	11	3108853	3113767	No hit
VIT_11s0016g03810	11	3121899	3123934	Unknown protein
VIT_11s0016g03820	11	3124371	3128849	Signal peptidase I
VIT_11s0016g03830	11	3130738	3133954	Protein kinase
VIT_11s0016g03840	11	3134022	3136115	No hit
VIT_11s0016g03850	11	3138660	3143394	Peroxisomal membrane 22 kDa
VIT_11s0016g03860	11	3143481	3153202	Raspberry3
VIT_11s0016g03870	11	3153879	3162165	Subtilisin
VIT_11s0016g03880	11	3163900	3169609	Receptor protein kinase PERK1
VIT_11s0016g03890	11	3174051	3179257	Short-chain dehydrogenase/reductase (SDR)
VIT_11s0016g03900	11	3182349	3186809	AAA-type ATPase
VIT_11s0016g03910	11	3186960	3190875	Unknown protein
VIT_11s0016g03920	11	3191384	3193086	Polyol transporter 5
VIT_11s0016g03930	11	3213014	3215223	Dimethylaniline monooxygenase, N-oxide-forming
VIT_11s0016g03940	11	3224068	3225265	Heat shock transcription factor C1
VIT_11s0016g03950	11	3234837	3236255	Dehydration-responsive protein (RD22)
VIT_11s0016g03960	11	3236395	3243211	Kinesin family member 2/24
VIT_11s0016g03970	11	3245946	3247926	Ubiquitin-conjugating enzyme E2 D/E
VIT_11s0016g03980	11	3249496	3250787	Unknown protein
VIT_11s0016g03990	11	3251962	3254889	R protein PRF disease resistance protein
VIT_11s0016g04000	11	3255776	3256586	Unknown protein
VIT_11s0016g04010	11	3263191	3268784	Unknown protein
VIT_11s0016g04020	11	3271684	3276160	Ras-related protein Rab-5A
VIT_11s0016g04030	11	3276161	3276314	No hit
VIT_11s0016g04040	11	3289562	3294574	Unknown protein
VIT_11s0016g04050	11	3298356	3299653	No hit

	VIT_11s0016g04060	11	3306255	3323305	MUT9-related serine/threonine protein kinase
	VIT_11s0016g04070	11	3329915	3336836	Hydroxyproline-rich glycoprotein
	VIT_11s0016g04080	11	3340651	3341251	Multiprotein-bridging factor 1c MBF1C
	VIT_11s0016g04090	11	3341776	3358113	DNA repair protein MutS
<i>pheno_12_1</i>	VIT_12s0035g01900	12	23792777	23795385	Pectinesterase family
	VIT_12s0035g01910	12	23795440	23796622	Heat shock protein 18.2 kDa class II
	VIT_12s0035g01920	12	23807633	23823774	Methionine S-methyltransferase
	VIT_12s0035g01930	12	23823775	23826921	No hit
	VIT_12s0035g01940	12	23827787	23828051	Unknown protein
	VIT_12s0035g01950	12	23830296	23836655	4-diphosphocytidyl-2-C-methyl-D-erythritol synthase
	VIT_12s0035g01960	12	23837408	23847527	Stichel
	VIT_12s0035g01970	12	23852741	23854836	Pentatricopeptide (PPR) repeat-containing
	VIT_12s0035g01980	12	23855859	23862754	PHD finger protein alfin
	VIT_12s0035g01990	12	23866171	23877161	Intron maturase, type II
	VIT_12s0035g02000	12	23879356	23879778	Arachidonic acid-induced protein DEA1
	VIT_12s0035g02010	12	23888449	23889619	Ribosomal RNA 23S
	VIT_12s0035g02020	12	23896510	23899220	NAC domain-containing protein (VvNAC40)
	VIT_12s0035g02030	12	23915422	23924545	Unknown protein
	VIT_12s0035g02040	12	23925751	23927332	No hit
	VIT_12s0035g02060	12	23949395	23955283	Methionine S-methyltransferase
	VIT_12s0035g02070	12	23964667	23970073	Cinnamoyl-CoA reductase
	VIT_12s0035g02080	12	23970815	23972655	Unknown protein
	VIT_12s0035g02090	12	23983677	23999372	Leucine-rich repeat family protein
	VIT_12s0035g02100	12	24024790	24027813	Glutathione S-transferase Z1 GSTZ1
	VIT_12s0035g02110	12	24028288	24038974	Glutathione S-transferase Z1 GSTZ1
	VIT_12s0035g02120	12	24046092	24050103	Unknown
	VIT_12s0035g02150	12	24097742	24106206	ferric reduction oxidase 7 FRO7
	VIT_12s0035g02160	12	24122892	24125541	No hit
	VIT_12s0035g02170	12	24125542	24127807	No hit
	VIT_12s0035g02180	12	24145254	24150267	Endo-1,4-beta-glucanase
	VIT_12s0035g02190	12	24151051	24158793	MLO-like protein 13
<i>pheno_14_1</i>	VIT_14s0083g00390	14	22431591	22456772	Calcium exchanger
	VIT_14s0083g00400	14	22465090	22468501	Leaf senescence protein
	VIT_14s0083g00410	14	22474094	22475171	Unknown
	VIT_14s0083g00420	14	22498682	22502947	TRN2 (TORNADO 2)

VIT_14s0083g00430	14	22507642	22508026	No hit
VIT_14s0083g00440	14	22511577	22526125	PHD finger transcription factor
VIT_14s0083g00450	14	22528546	22535692	Protein kinase PKN/PRK1, effector
VIT_14s0083g00460	14	22547153	22550143	Tryptophan synthase beta chain 2
VIT_14s0083g00470	14	22556235	22557761	2,3-biphosphoglycerate-independent phosphoglycerate mutase
VIT_14s0083g00480	14	22557762	22560665	2,3-biphosphoglycerate-independent phosphoglycerate mutase
VIT_14s0083g00490	14	22560666	22560982	Phosphoglycerate mutase
VIT_14s0083g00500	14	22560983	22561672	No hit
VIT_14s0083g00510	14	22562747	22563358	No hit
VIT_14s0083g00520	14	22568746	22570772	Proline oxidase
VIT_14s0083g00530	14	22581005	22585214	Cell division protein FtsH
VIT_14s0083g00540	14	22586239	22598780	Plant adhesion molecule 1 (PAM1)
VIT_14s0083g00550	14	22600241	22604340	Pentatricopeptide (PPR) repeat-containing
VIT_14s0083g00570	14	22609625	22614966	Plant adhesion molecule 1 (PAM1)
VIT_14s0083g00580	14	22620849	22623743	S-adenosyl-L-methionine decarboxylase
VIT_14s0083g00590	14	22625232	22637079	Ribosomal RNA-processing protein 7
VIT_14s0083g00600	14	22639538	22640532	Unknown
VIT_14s0083g00610	14	22649341	22651396	Pentatricopeptide (PPR) repeat-containing protein
VIT_14s0083g00620	14	22672469	22675655	NIK1 (NSP- interacting kinase 1)
VIT_14s0083g00630	14	22677598	22687861	F-box domain containing protein
VIT_14s0083g00640	14	22696160	22698346	Constans 2 (COL2)
VIT_14s0083g00650	14	22700284	22702204	No hit
VIT_14s0083g00660	14	22712276	22717744	Aspartic-type endopeptidase
VIT_14s0083g00670	14	22722348	22722787	No hit
VIT_14s0083g00680	14	22768564	22768923	No hit
VIT_14s0083g00690	14	22797698	22802306	Glycosyl transferase family 8 protein
VIT_14s0083g00700	14	22839619	22840360	Basic Leucine Zipper Transcription Factor (VvbZIP39)
VIT_14s0083g00710	14	22855118	22856402	Zinc finger (C3HC4-type ring finger)
VIT_14s0083g00720	14	22862598	22865888	Pentatricopeptide (PPR) repeat-containing
VIT_14s0083g00730	14	22866088	22869527	Unknown protein
VIT_14s0083g00740	14	22886669	22892408	Amino acid permease
VIT_14s0083g00750	14	22893111	22952397	Unknown protein
VIT_14s0083g00760	14	22952398	22953336	No hit
VIT_14s0083g00770	14	22957850	22959392	Phytoene desaturase
VIT_14s0083g00780	14	22961013	22976952	Anion exchanger adaptor protein Kanadaptn
VIT_14s0083g00790	14	22977589	22994438	DNA-directed RNA polymerase

VIT_14s0083g00800	14	23001150	23005055	Esterase/lipase/thioesterase
VIT_14s0083g00810	14	23017927	23019683	F-box family protein
VIT_14s0083g00820	14	23022233	23026183	Lipase GDSL 7
VIT_14s0083g00830	14	23043321	23046274	Lipase GDSL 7
VIT_14s0083g00840	14	23047679	23050334	Lipase GDSL 7
VIT_14s0083g00850	14	23056787	23058566	Lipase GDSL 7
VIT_14s0083g00870	14	23073964	23082418	Nodulation receptor kinase
VIT_14s0083g00880	14	23082779	23088930	Phosphatidylinositol 4-kinase type-II
VIT_14s0083g00890	14	23094965	23095719	Transport inhibitor response 1 protein
VIT_14s0083g00900	14	23095736	23096308	Aspartate aminotransferase
VIT_14s0083g00910	14	23106621	23115040	Auxin-independent growth promoter
VIT_14s0083g00920	14	23121142	23123350	No hit
VIT_14s0083g00930	14	23125718	23136127	BIM2 (BES1-interacting Myc-like protein 2)
VIT_14s0083g00940	14	23137130	23143930	Auxin-independent growth promoter
VIT_14s0083g00950	14	23153810	23160185	U3 small nucleolar RNA-associated protein IMP3
VIT_14s0083g00960	14	23160685	23194222	Auxin transport protein (BIG)
VIT_14s0083g00970	14	23215781	23219760	Ribosomal protein L7A (RPL7aB) 60S
VIT_14s0083g00980	14	23255198	23256315	Pollen Ole e 1 allergen and extensin
VIT_14s0083g00990	14	23257443	23277391	IMP dehydrogenase
VIT_14s0083g01000	14	23286167	23293023	Zinc finger (C3HC4-type ring finger)
VIT_14s0083g01010	14	23295051	23298839	Protein disulfide oxidoreductase DSBA oxidoreductase
VIT_14s0083g01020	14	23306141	23319918	Regulator of chromosome condensation (RCC1)
VIT_14s0083g01030	14	23320331	23341036	putative MADS-box Fruitfull 2 (VviFUL2)
VIT_14s0083g01050	14	23363261	23379498	putative MADS-box sepallata 1 (VviSEP1)
VIT_14s0083g01060	14	23384136	23385107	myb domain protein 121
VIT_14s0083g01070	14	23391103	23396928	No hit
VIT_14s0083g01090	14	23416450	23425111	N2,N2-dimethylguanosine tRNA methyltransferase
VIT_14s0083g01100	14	23425741	23428785	Alpha-1,4-glucan-protein synthase 1
VIT_14s0083g01110	14	23435436	23438457	Brassinosteroid-6-oxidase
VIT_14s0083g01120	14	23456752	23469960	MAP3K-like protein kinase, putative, expressed
VIT_14s0083g01130	14	23470715	23473749	MAP3K-like protein kinase, putative, expressed
VIT_14s0083g01140	14	23478460	23480345	B12D
VIT_14s0083g01150	14	23524839	23527545	COBRA protein
VIT_14s0083g01160	14	23527926	23532692	COBRA protein
VIT_14s0083g01170	14	23552658	23569757	Mitochondrial substrate carrier family protein
VIT_14s0083g01180	14	23573219	23576042	Unknown protein

VIT_14s0083g01190	14	23585947	23586226
VIT_14s0083g01200	14	23603520	23606026
VIT_14s0083g01210	14	23631468	23634185
VIT_14s0083g01220	14	23647671	23648618
VIT_14s0083g01230	14	23687371	23687925
VIT_14s0068g00010	14	23691896	23694505
VIT_14s0068g00020	14	23702632	23703602
VIT_14s0068g00030	14	23710282	23713253
VIT_14s0068g00040	14	23730955	23731566
VIT_14s0068g00050	14	23741203	23741804
VIT_14s0068g00060	14	23761143	23763198
VIT_14s0068g00070	14	23763889	23765688
VIT_14s0068g00080	14	23790042	23793197
VIT_14s0068g00090	14	23793482	23796203
VIT_14s0068g00100	14	23804737	23805618
VIT_14s0068g00110	14	23806944	23824202
VIT_14s0068g00120	14	23824203	23824397
VIT_14s0068g00130	14	23824529	23825866
VIT_14s0068g00140	14	23848301	23848892
VIT_14s0068g00150	14	23858719	23859396
VIT_14s0068g00160	14	23866963	23867506
VIT_14s0068g00170	14	23880217	23880588
VIT_14s0068g00190	14	23901133	23901667
VIT_14s0068g00200	14	23903015	23903642
VIT_14s0068g00210	14	23920911	23938861
VIT_14s0068g00220	14	23939286	23945038
VIT_14s0068g00230	14	23946758	23949751
VIT_14s0068g00240	14	23956348	23964987
VIT_14s0068g00250	14	23967557	23970244
VIT_14s0068g00260	14	23972158	23975509
VIT_14s0068g00270	14	23981569	23982426
VIT_14s0068g00280	14	23982459	23984970
VIT_14s0068g00290	14	23993049	23996736
VIT_14s0068g00300	14	23997514	24000870
VIT_14s0068g00310	14	24001531	24018716
VIT_14s0068g00320	14	24031909	24031947

S-adenosylmethionine synthetase 1 (SAM1)
Nitrilase
feronia receptor-like kinase
feronia receptor-like kinase
Heat shock protein 81-4 (HSP81-4)
feronia receptor-like kinase
No hit
feronia receptor-like kinase
No hit
No hit
No hit
feronia receptor-like kinase
Non-symbiotic hemoglobin class 1
feronia receptor-like kinase
feronia receptor-like kinase
feronia receptor-like kinase
feronia receptor-like kinase
feronia receptor-like kinase
No hit
No hit
No hit
No hit
No hit
No hit
No hit
ABC Transporter (VvMDR16 - VvABCB16)
Proteasome
Spiral 1 like 2
Rough sheath2-interacting KH-domain protein
Exocyst subunit EXO70 E1
Serine carboxypeptidase S10
Hydroxyproline-rich glycoprotein
Unknown protein
RPK1 (receptor-like protein kinase 1)
ABRC5
Nuclear transport factor 2 (NTF2)
No hit

VIT_14s0068g00330	14	24046880	24048369	PTF1 (plastid transcription factor 1) TCP13
VIT_14s0068g00340	14	24058921	24060831	Transcription initiation factor TFIIID subunit 8
VIT_14s0068g00360	14	24075902	24080124	LNG1 (LONGIFOLIA1)
VIT_14s0068g00370	14	24080150	24081477	No hit
VIT_14s0068g00380	14	24088765	24091151	NLI interacting factor (NIF) family protein
VIT_14s0068g00390	14	24101322	24107332	Esterase PIR7B
VIT_14s0068g00400	14	24127197	24145861	Hydrolase, alpha/beta fold family
VIT_14s0068g00410	14	24150294	24158106	Transducin family protein / WD-40 repeat
VIT_14s0068g00420	14	24160652	24204411	Alpha-amylase isozyme C2 precursor
VIT_14s0068g00430	14	24208142	24215337	Dentin sialophosphoprotein
VIT_14s0068g00440	14	24220054	24221587	UDP-glucosyl transferase
VIT_14s0068g00450	14	24222577	24224432	UDP-glucuronosyl/UDP-glucosyl transferase
VIT_14s0068g00460	14	24225718	24227484	UDP-glucosyl transferase
VIT_14s0068g00470	14	24232271	24232869	UDP-glucosyl transferase
VIT_14s0068g00480	14	24235845	24236264	UDP-glucosyl transferase
VIT_14s0068g00490	14	24236265	24240475	UDP-glucuronosyl/UDP-glucosyltransferase
VIT_14s0068g00500	14	24240476	24246281	Indole-3-acetate beta-glucosyltransferase
VIT_14s0068g00510	14	24246986	24247718	Unknown
VIT_14s0068g00520	14	24253217	24259740	F-box domain containing protein
VIT_14s0068g00600	14	24335233	24336088	Expansin (VvEXPA15)
VIT_14s0068g00630	14	24364739	24437849	Importin
VIT_14s0068g00640	14	24438706	24450994	Acetyl-CoA synthetase
VIT_14s0068g00650	14	24461539	24463112	Unknown
VIT_14s0068g00660	14	24473597	24477950	ATAN11 (ANTHOCYANIN11) (VvWDR2)
VIT_14s0068g00670	14	24478682	24479739	Heavy-metal-associated domain-containing protein
VIT_14s0068g00680	14	24482406	24484689	Glyceraldehyde-3-phosphate dehydrogenase A, chloroplast precursor
VIT_14s0068g00690	14	24485059	24492325	OTU cysteine protease
VIT_14s0068g00700	14	24492483	24497875	EMB1895
VIT_14s0068g00710	14	24498868	24504221	DEAD/DEAH box helicase
VIT_14s0068g00720	14	24509679	24524403	Tudor domain protein 4SNc
VIT_14s0068g00730	14	24525207	24525867	Unknown protein
VIT_14s0068g00740	14	24532101	24533135	Avr9/Cf-9 rapidly elicited protein 146
VIT_14s0068g00750	14	24534760	24535908	C2 domain-containing protein
VIT_14s0068g00760	14	24536260	24538272	Pentatricopeptide (PPR) repeat-containing
VIT_14s0068g00770	14	24540054	24544838	FAR1-related sequence 5
VIT_14s0068g00780	14	24545158	24555142	Nematode chemoreceptor

	VIT_14s0068g00790	14	24569502	24570830	Unknown protein
	VIT_14s0068g00800	14	24574332	24590300	Syntaxin 7
	VIT_14s0068g00810	14	24592155	24604605	Helicase
	VIT_14s0068g00820	14	24605414	24606138	Lipid transfer protein
	VIT_14s0068g00830	14	24606690	24609786	2,3,4,5-tetrahydropyridine-2,6-dicarboxylate N-succinyltransferase
	VIT_14s0068g00840	14	24612133	24616683	RBR1 (retinoblastoma-related 1)
	VIT_14s0068g00850	14	24616889	24623539	Potassium transporter (KUP3)
	VIT_14s0068g00860	14	24626255	24627037	ERF/AP2 Gene Family (VvERF070)
	VIT_14s0068g00870	14	24631161	24634996	Nudix hydrolase 13
<i>pheno_16_1</i>	VIT_16s0022g00940	16	14019798	14021005	Pectinesterase PME3
	VIT_16s0022g00950	16	14025273	14027095	No hit
	VIT_16s0022g00960	16	14028716	14029381	Invertase/pectin methylesterase inhibitor
	VIT_16s0022g00970	16	14044085	14045832	Pentatricopeptide (PPR) repeat-containing protein
	VIT_16s0022g00980	16	14047757	14059196	Adenylate kinase
	VIT_16s0022g00990	16	14066536	14067062	Acetolactate synthase SuRB
	VIT_16s0022g01000	16	14102897	14103279	Chalcone synthase [Vitis vinifera]
	VIT_16s0022g01010	16	14114761	14116548	Acetohydroxyacid synthase
	VIT_16s0022g01020	16	14148552	14149551	Chalcone synthase [Vitis vinifera]
	VIT_16s0022g01030	16	14158599	14160569	Acetolactate synthase SuRB
	VIT_16s0022g01040	16	14229326	14229815	Acetolactate synthase SuRB
	VIT_16s0022g01050	16	14229816	14231180	Acetolactate synthase 1, chloroplast precursor
	VIT_16s0022g01070	16	14274118	14275623	Chalcone synthase [Vitis vinifera]
	VIT_16s0022g01080	16	14288985	14290858	Acetolactate synthase 1, chloroplast precursor
	VIT_16s0022g01100	16	14353302	14354444	Acetohydroxyacid synthase 1
	VIT_16s0022g01110	16	14354445	14355089	Acetohydroxyacid synthase 1
	VIT_16s0022g01120	16	14397803	14399181	Acyl-CoA oxidase ACX3
	VIT_16s0022g01130	16	14433197	14459122	No hit
	VIT_16s0022g01140	16	14459402	14460328	Chalcone synthase [Vitis vinifera]
	VIT_16s0022g01150	16	14470887	14471577	Acyl-CoA oxidase ACX3
	VIT_16s0022g01160	16	14471578	14472628	Acyl-CoA oxidase ACX3
	VIT_16s0022g01190	16	14557320	14558246	Chalcone synthase [Vitis vinifera]
	VIT_16s0022g01210	16	14618249	14620000	myb domain protein 85
	VIT_16s0022g01240	16	14679983	14700893	IRE (incomplete root hair elongation)
	VIT_16s0022g01250	16	14701443	14723650	Unknown protein
	VIT_16s0022g01260	16	14727207	14745148	Metalloendopeptidase
	VIT_16s0022g01280	16	14750817	14755409	Metalloendopeptidase

VIT_16s0022g01290	16	14759440	14760595	SDG29 (SET Domain group 29)
VIT_16s0022g01310	16	14770899	14792137	Hydroxymethylglutaryl coenzyme A synthase
VIT_16s0022g01330	16	14814938	14816839	R protein PRF disease resistance protein
VIT_16s0022g01340	16	14821502	14838464	Deoxyribodipyrimidine photolyase
VIT_16s0022g01350	16	14853500	14855350	No hit
VIT_16s0022g01360	16	14864130	14864695	Unknown
VIT_16s0022g01370	16	14864696	14869194	No hit
VIT_16s0022g01380	16	14886712	14887520	No hit
VIT_16s0022g01390	16	14889269	14893469	flavonoid 3-monooxygenase
VIT_16s0022g01400	16	14900577	14901340	Cellulose synthase CSLD5
VIT_16s0022g01410	16	14908101	14910093	No hit
VIT_16s0022g01420	16	14911334	14916210	Unknown protein
VIT_16s0022g01430	16	14922690	14923901	Phosphate-induced protein 1
VIT_16s0022g01440	16	14962050	14966011	Transketolase, chloroplast precursor
VIT_16s0022g01450	16	14979177	14980434	UDP-D- glucuronate 4-epimerase 2 GAE2
VIT_16s0022g01460	16	14983070	14985988	Ribosomal protein S20 (RPS20A) 40S
VIT_16s0022g01480	16	15008412	15027993	No hit
VIT_16s0022g01490	16	15030595	15031594	4,5-DOPA dioxygenase extradiol
VIT_16s0022g01500	16	15042831	15045000	flavonoid 3',5'-hydroxylase -like protein
VIT_16s0022g01510	16	15060339	15093178	flavonoid 3',5'-hydroxylase -like protein
VIT_16s0022g01520	16	15117078	15117831	4,5-DOPA dioxygenase extradiol
VIT_16s0022g01540	16	15129838	15131081	Flavonoid 3',5'-hydroxylase
VIT_16s0022g01560	16	15152968	15157791	Nucleotide-sensitive chloride conductance regulator (ICln)
VIT_16s0022g01570	16	15160352	15162044	3-ketoacyl-CoA synthase
VIT_16s0022g01580	16	15171729	15173776	3-ketoacyl-CoA synthase
VIT_16s0022g01590	16	15178350	15181780	Ribosomal protein S13 (RPS13A) 40S
VIT_16s0022g01610	16	15216222	15218944	No hit
VIT_16s0022g01620	16	15219297	15223055	Receptor protein kinase
VIT_16s0022g01630	16	15226817	15227624	Unknown protein
VIT_16s0022g01640	16	15237111	15238586	Receptor serine/threonine kinase
VIT_16s0022g01650	16	15243820	15246842	Receptor serine/threonine kinase PR5K
VIT_16s0022g01660	16	15252302	15254570	Receptor kinase homolog LRK10
VIT_16s0022g01670	16	15264752	15268846	Receptor kinase LRK10
VIT_16s0022g01680	16	15283774	15285675	Zinc finger (AN1-like)
VIT_16s0022g01690	16	15290134	15296405	Band 7 family
VIT_16s0022g01700	16	15327451	15327663	No hit

VIT_16s0022g01710	16	15328128	15330621	Ser/Thr receptor-like kinase1
VIT_16s0022g01720	16	15331961	15333786	Receptor kinase homolog LRK10
VIT_16s0022g01730	16	15347338	15347814	6-phosphogluconate dehydrogenase
VIT_16s0022g01740	16	15361931	15364513	Unknown protein
VIT_16s0022g01760	16	15447369	15466229	FK506-binding protein genes family (VvFKBP43-1)
VIT_16s0022g01770	16	15467138	15473529	Phosphopyruvate hydratase.
VIT_16s0022g01780	16	15489281	15497566	Pentatricopeptide (PPR) repeat-containing protein
VIT_16s0022g01790	16	15503664	15504109	Histone deacetylase complex, SIN3 component -like 2 SNL2
VIT_16s0022g01800	16	15512356	15514461	RRNA-processing protein EBP2
VIT_16s0022g01810	16	15518994	15527030	AT-hook protein 1
VIT_16s0022g01820	16	15528278	15533919	Microtubule associated protein (MAP65/ASE1) pleiade
VIT_16s0022g01830	16	15540620	15546227	YLS7 (yellow-leaf-specific gene 7)
VIT_16s0022g01840	16	15565361	15572463	Clp amino terminal domain-containing protein
VIT_16s0022g01850	16	15594331	15596264	No hit
VIT_16s0022g01860	16	15611019	15730450	Cleavage and polyadenylation specificity factor subunit 1
VIT_16s0022g01870	16	15736355	15738229	Unknown protein
VIT_16s0022g01880	16	15741012	15741260	No hit
VIT_16s0022g01890	16	15742832	15752020	GTP-binding protein engA
VIT_16s0022g01900	16	15757973	15758305	Pentatricopeptide (PPR) repeat
VIT_16s0022g01910	16	15758306	15759314	Pentatricopeptide (PPR) repeat
VIT_16s0022g01920	16	15760945	15763090	Pentatricopeptide (PPR) repeat-containing protein
VIT_16s0022g01960	16	15771659	15773575	ATP-dependent Clp protease ATP-binding subunit ClpX1 (CLPX)
VIT_16s0022g01970	16	15780583	15782142	Anthocyanidin 3-O-glucosyltransferase
VIT_16s0022g01980	16	15810041	15810499	Zf A20 and AN1 domain-containing stress-associated protein 1
VIT_16s0022g01990	16	15812472	15812931	Unknown
VIT_16s0022g02000	16	15813047	15813946	Unknown
VIT_16s0022g02010	16	15813947	15818102	1-aminocyclopropane-1-carboxylate synthase
VIT_16s0022g02020	16	15847600	15848975	No hit
VIT_16s0022g02030	16	15855594	15861902	ERL1 (ERECTA 1)
VIT_16s0022g02040	16	15888563	15895646	PBS2 (PPHB susceptible 2)
VIT_16s0022g02050	16	15931002	15931871	Lateral organ boundaries domain gene 36
VIT_16s0022g02060	16	15955898	15988486	K ⁺ efflux antiporter (KEA5)
VIT_16s0022g02070	16	16032507	16033281	Unknown protein
VIT_16s0022g02080	16	16041486	16043235	Exostosin family protein
VIT_16s0022g02090	16	16055649	16056600	Embryo-specific 3
VIT_16s0022g02100	16	16060136	16061359	Embryo-specific 3

VIT_16s0022g02110	16	16067495	16075144	DEAD box RNA helicase (PRH75)
VIT_16s0022g02120	16	16078156	16082489	Metalloendopeptidase OMA1
VIT_16s0022g02130	16	16084547	16085104	No hit
VIT_16s0022g02140	16	16087685	16102990	CYP704A2
VIT_16s0022g02150	16	16103565	16105639	Lectin
VIT_16s0022g02170	16	16130501	16143461	Alpha-L-fucosidase
VIT_16s0022g02190	16	16182278	16183814	Chalcone and stilbene synthases
VIT_16s0022g02200	16	16203664	16206181	Subtilase
VIT_16s0022g02210	16	16215979	16220680	Protein phosphatase 2CA AHG1 PP2CA (VvPP2C-8)
VIT_16s0022g02220	16	16230501	16231445	Receptor Like Protein 48 RLP48
VIT_16s0022g02230	16	16240572	16248680	Leucine-rich repeat receptor protein kinase EXS
VIT_16s0022g02240	16	16255908	16257035	basic helix-loop-helix (bHLH) family
VIT_16s0022g02250	16	16266462	16267491	basic helix-loop-helix (bHLH) family
VIT_16s0022g02270	16	16287811	16288987	basic helix-loop-helix (bHLH) family
VIT_16s0022g02280	16	16301165	16302698	Receptor protein kinase PERK1
VIT_16s0022g02290	16	16334395	16337736	Unknown
VIT_16s0022g02300	16	16350758	16351750	CXE carboxylesterase CXE20
VIT_16s0022g02310	16	16372484	16374087	Gibberellin 3-beta-dioxygenase.
VIT_16s0022g02320	16	16388979	16407441	Phosphoglucomutase chloroplast precursor
VIT_16s0022g02330	16	16451140	16466299	putative MADS-box Agamous-like 6b (VviAGL6b)
VIT_16s0022g02340	16	16470141	16475595	fructokinase-2
VIT_16s0022g02350	16	16481981	16491201	ACI13
VIT_16s0022g02370	16	16500433	16503019	Unknown protein
<i>pheno_16_2</i> VIT_16s0022g02380	16	16506566	16519567	putative MADS-box Suppressor of Constans overexpression 1b (VviSOC1b)
VIT_16s0022g02400	16	16529521	16544563	MADS-box agamous-like 42
VIT_16s0022g02410	16	16558074	16566697	Oxidoreductase
VIT_16s0022g02420	16	16568466	16571206	Subtilisin protease C1
VIT_16s0022g02430	16	16590597	16591356	Carboxylesterase 20 CXE20
VIT_16s0022g02440	16	16658913	16659634	Carboxylesterase 20 CXE20
VIT_16s0022g02450	16	16672729	16677077	Subtilisin protease C1
VIT_16s0022g02460	16	16707603	16710429	Subtilisin protease C1
VIT_16s0022g02470	16	16715289	16716489	Cationic peroxidase
VIT_16s0022g02480	16	16721578	16723006	TCP family transcription factor TCP9
VIT_16s0022g02490	16	16725022	16732924	Hydroxymethylglutaryl coenzyme A synthase
VIT_16s0022g02500	16	16753448	16753788	No hit
VIT_16s0022g02510	16	16758120	16758664	Protein phosphatase 2C

VIT_16s0022g02520	16	16783470	16784544	ZFWD1 (zinc finger WD40 repeat protein 1)
VIT_16s0022g02530	16	16784545	16787333	ZFWD1 (zinc finger WD40 repeat protein 1)
VIT_16s0022g02540	16	16787851	16788601	No hit
VIT_16s0100g00010	16	16802160	16803228	Carboxyesterase 20 CXE20
VIT_16s0100g00030	16	16818864	16821466	Cucumisin precursor
VIT_16s0100g00040	16	16831329	16832283	No hit
VIT_16s0100g00050	16	16833888	16834887	Protein kinase
VIT_16s0100g00060	16	16867556	16872590	Subtilisin protease C1
VIT_16s0100g00070	16	16882780	16883663	Prohibitin 1
VIT_16s0100g00080	16	16889920	16890662	Subtilisin serine protease
VIT_16s0100g00090	16	16896246	16897439	Cationic peroxidase
VIT_16s0100g00110	16	16928141	16929702	Hydroxymethylglutaryl coenzyme A synthase
VIT_16s0100g00120	16	16951370	16951710	No hit
VIT_16s0100g00130	16	16955981	16956564	Protein phosphatase 2C / PP2C
VIT_16s0100g00140	16	16974820	16975365	Protein phosphatase 2C / PP2C
VIT_16s0100g00150	16	16977103	16977433	COP9 signalosome complex subunit 5
VIT_16s0100g00160	16	16987602	16993787	HMG-CoA synthase 2
VIT_16s0100g00170	16	17000645	17002770	Xyloglucan endotransglucosylase/hydrolaseXTR2
VIT_16s0100g00180	16	17071017	17071584	ATP-dependent Clp protease ClpB protein
VIT_16s0100g00190	16	17115669	17121681	Pentatricopeptide (PPR) repeat-containing protein
VIT_16s0100g00200	16	17122769	17124779	Unknown protein
VIT_16s0100g00210	16	17124780	17125575	No hit
VIT_16s0100g00220	16	17132026	17132339	No hit
VIT_16s0100g00230	16	17132553	17134891	Glucose-methanol-choline (GMC) oxidoreductase family protein
VIT_16s0100g00240	16	17134892	17139634	Mandelonitrile lyase-like protein
VIT_16s0100g00250	16	17139635	17141094	Mandelonitrile lyase-like protein
VIT_16s0100g00260	16	17149698	17150478	No hit
VIT_16s0100g00270	16	17150479	17150928	Peptidoglycan-binding LysM domain-containing protein
VIT_16s0100g00280	16	17157127	17161415	EMB2758 (embryo defective 2758)
VIT_16s0100g00290	16	17162424	17180217	L-idonate dehydrogenase
VIT_16s0100g00300	16	17186416	17190028	Sorbitol dehydrogenase
VIT_16s0100g00310	16	17196699	17198841	Unknown protein
VIT_16s0100g00320	16	17225835	17233936	Zfwd2 protein (ZFWD2)
VIT_16s0100g00330	16	17237416	17238326	Unknown protein
VIT_16s0100g00340	16	17239840	17244491	CDPK
VIT_16s0100g00350	16	17248816	17261155	ABC Transporter (VvTAP3 - VvABC23)

	VIT_16s0100g00360	16	17265204	17272005	Per1
	VIT_16s0100g00370	16	17274084	17324348	Valyl-tRNA synthetase
<i>pheno_17_1</i>	VIT_17s0000g04630	17	4965012	5015746	Phenylalanyl-tRNA synthetase beta chain
	VIT_17s0000g04640	17	5017391	5020555	H/ACA ribonucleoprotein complex subunit 2
	VIT_17s0000g04650	17	5021431	5035538	Phosphoribulokinase/uridine kinase
	VIT_17s0000g04660	17	5042400	5052215	Agmatine deiminase
	VIT_17s0000g04670	17	5052921	5063485	Serine/threonine protein kinase ATPK3
	VIT_17s0000g04680	17	5090954	5095558	Signal peptide peptidase SPPA
	VIT_17s0000g04690	17	5096080	5107168	Protease SppA
	VIT_17s0000g04700	17	5145018	5145988	Protease SppA
	VIT_17s0000g04710	17	5236137	5239225	Pentatricopeptide (PPR) repeat-containing protein
	VIT_17s0000g04720	17	5241247	5243311	No hit
	VIT_17s0000g04730	17	5257791	5259482	Zinc finger (C3HC4-type ring finger)
	VIT_17s0000g04740	17	5261337	5267944	Transducin family protein / WD-40 repeat
	VIT_17s0000g04750	17	5279676	5281368	UDP-glycosyltransferase 89B2
	VIT_17s0000g04760	17	5281484	5283173	UDP-glycosyltransferase 89B2
	VIT_17s0000g04770	17	5286031	5291504	PHD finger transcription factor
	VIT_17s0000g04780	17	5292045	5296110	Phosphatidylinositol 4-kinase type-II
	VIT_17s0000g04790	17	5309123	5318428	BIM1 (BES1-interacting Myc-like protein 1)
	VIT_17s0000g04800	17	5318431	5318559	No hit
	VIT_17s0000g04810	17	5321964	5325762	Auxin-independent growth promoter
	VIT_17s0000g04820	17	5331026	5337299	BSD domain-containing protein
	VIT_17s0000g04830	17	5338567	5345150	DNA Polymerase epsilon, subunit B
	VIT_17s0000g04840	17	5357937	5362286	Sterile alpha motif (SAM) domain-containing
	VIT_17s0000g04850	17	5372091	5373566	OBF binding protein 4
	VIT_17s0000g04860	17	5375984	5380301	Unknown
	VIT_17s0000g04870	17	5390557	5401864	Microtubule-associated protein MBP2C
	VIT_17s0000g04880	17	5408698	5409427	Dirigent protein
	VIT_17s0000g04890	17	5409996	5423899	D-aminoacyl-tRNA deacylase GEKO1
	VIT_17s0000g04900	17	5426843	5441775	ATP-dependent RNA helicase
	VIT_17s0000g04910	17	5446682	5449753	L-asparaginase
	VIT_17s0000g04920	17	5486192	5489071	Histidine kinase (AHK3)
	VIT_17s0000g04930	17	5507759	5509033	Desulfo-glucosinolate sulfotransferase 18
	VIT_17s0000g04940	17	5525332	5525670	Brassinosteroid sulfotransferase ST4A
	VIT_17s0000g04950	17	5528234	5529544	Steroid sulfotransferase
	VIT_17s0000g04960	17	5531301	5546181	Polygalacturonate 4-alpha-galacturonosyltransferase GAUT11

VIT_17s0000g04970	17	5551329	5561922	ADP, ATP carrier protein
VIT_17s0000g04980	17	5562484	5563956	Universal stress protein (USP) family protein
VIT_17s0000g04990	17	5565646	5584353	putative MADS-box Fruitfull 1 (VviFUL1)
VIT_17s0000g05000	17	5589362	5596096	putative MADS-box sepallata 2 (VviSEP2)
VIT_17s0000g05010	17	5614348	5626304	Unknown
VIT_17s0000g05020	17	5637669	5644801	Squamosa promoter-binding protein 6 (SPL6)
VIT_17s0000g05030	17	5645732	5648492	Alpha-1,4-glucan-protein synthase 1
VIT_17s0000g05040	17	5654593	5656105	No hit
VIT_17s0000g05050	17	5659282	5660704	COBRA-like protein 4
VIT_17s0000g05060	17	5661333	5676012	Phytochelatin synthetase
VIT_17s0000g05070	17	5676169	5679862	Phytochelatin synthetase
VIT_17s0000g05080	17	5690884	5710034	Cleavage stimulation factor subunit 1
VIT_17s0000g05090	17	5710035	5711791	Pentatricopeptide (PPR) repeat-containing protein
VIT_17s0000g05100	17	5723289	5730063	No hit
VIT_17s0000g05110	17	5731853	5734268	CYP78A4
VIT_17s0000g05120	17	5751736	5758856	ABC Transporter (VvTAP2 - VvABC22)
VIT_17s0000g05130	17	5759551	5761024	Transcription termination factor mitochondrial mTERF
VIT_17s0000g05140	17	5763617	5769816	Rhomboid
VIT_17s0000g05150	17	5773018	5780793	Enoyl-CoA hydratase
VIT_17s0000g05160	17	5783842	5789162	SP1L2 (SPIRAL2)
VIT_17s0000g05170	17	5793575	5794544	No hit
VIT_17s0000g05180	17	5794802	5795725	Unknown
VIT_17s0000g05190	17	5801569	5810790	Unknown protein
VIT_17s0000g05200	17	5819731	5826246	NLI interacting factor (NIF) family protein
VIT_17s0000g05210	17	5832003	5838142	LNG1 (LONGIFOLIA1)
VIT_17s0000g05220	17	5845847	5850744	TCP family transcription factor TCP5
VIT_17s0000g05230	17	5851190	5861913	Unknown protein
VIT_17s0000g05240	17	5869290	5885095	Nuclear transport factor 2 (NTF2)
VIT_17s0000g05250	17	5885327	5886300	Unknown protein
VIT_17s0000g05260	17	5886472	5890773	Unknown protein
VIT_17s0000g05270	17	5892658	5896385	Unknown protein
VIT_17s0000g05280	17	5898984	5902122	UPF0737 protein AFP3
VIT_17s0000g05290	17	5924194	5926786	Pre-mRNA cleavage complex II protein Clp1
VIT_17s0000g05300	17	5926787	5928753	Pre-mRNA cleavage complex II protein Clp1
VIT_17s0000g05310	17	5933739	5939818	Pre-mRNA cleavage complex II protein Clp1
VIT_17s0000g05320	17	5940805	5944765	IFA binding protein

VIT_17s0000g05330	17	5946645	5949934	Serine/threonine protein phosphatase PP2A-5 catalytic subunit (PP2A5)
VIT_17s0000g05350	17	5958587	5963699	5-formyltetrahydrofolate cycloligase
VIT_17s0000g05360	17	5965138	5966181	Germin
VIT_17s0000g05370	17	5966462	5970848	MYC ZCW32 (bigpetal, bigpetalub)
VIT_17s0000g05380	17	5975939	5976998	Dynein light chain LC8-type
VIT_17s0000g05390	17	5978634	5988830	Unknown protein
VIT_17s0000g05400	17	5992385	5993924	myb domain protein 35
VIT_17s0000g05410	17	5997792	6001685	Galactosyltransferase
VIT_17s0000g05420	17	6003755	6005138	AAA-type ATPase family
VIT_17s0000g05430	17	6005483	6026193	Aminoacyl-tRNA synthetase
VIT_17s0000g05440	17	6061730	6069222	Unknown protein
VIT_17s0000g05450	17	6070433	6082026	ELF5 (early flowering 5)
VIT_17s0000g05460	17	6088077	6090457	Nodulin
VIT_17s0000g05470	17	6090728	6093181	Nodulin
VIT_17s0000g05480	17	6100712	6112781	EMB2454 (embryo defective 2454)
VIT_17s0000g05490	17	6117662	6118846	Lateral organ boundaries domain family protein (LBD27)
VIT_17s0000g05500	17	6120295	6131114	Cysteine endopeptidase
VIT_17s0000g05510	17	6132145	6137273	Pentatricopeptide (PPR) repeat-containing protein
VIT_17s0000g05520	17	6144571	6153251	Calcium Dependent Protein Kinase (VvCPK14)
VIT_17s0000g05530	17	6153633	6161033	DnaJ homolog, subfamily B, member 4
VIT_17s0000g05540	17	6174485	6182145	H(+)-ATPase 11 AHA11
VIT_17s0000g05550	17	6183508	6195130	Proton-dependent oligopeptide transport (POT) family protein
VIT_17s0000g05560	17	6199502	6202250	Proton-dependent oligopeptide transport (POT) family protein
VIT_17s0000g05570	17	6207677	6212987	Receptor protein kinase
VIT_17s0000g05580	17	6213229	6221132	Isopiperitenol dehydrogenase
VIT_17s0000g05600	17	6255629	6256773	(-)-isopiperitenol dehydrogenase
VIT_17s0000g05610	17	6257443	6258438	Isopiperitenol dehydrogenase
VIT_17s0000g05620	17	6259762	6262348	Integral membrane HPP family protein
VIT_17s0000g05630	17	6265801	6268050	Homeodomain leucine zipper protein HB-1
VIT_17s0000g05640	17	6276619	6279624	Nitrate transporter 1:2
VIT_17s0000g05650	17	6279745	6280799	Unknown protein
VIT_17s0000g05660	17	6282923	6285609	Polygalacturonase GH28
VIT_17s0000g05670	17	6286277	6288346	Polygalacturonase GH28
VIT_17s0000g05680	17	6293644	6298086	Band 7 family
VIT_17s0000g05690	17	6299282	6301763	Isochorismate synthase 1, chloroplast precursor
VIT_17s0000g05700	17	6304590	6308202	Phosphoribosylanthranilate transferase

	VIT_17s0000g05710	17	6312022	6312896	Unknown
	VIT_17s0000g05720	17	6319018	6320270	No hit
	VIT_17s0000g05730	17	6343021	6345217	No hit
	VIT_17s0000g05740	17	6347635	6349215	Pectate lyase, N-terminal
	VIT_17s0000g05750	17	6350085	6359530	Isochorismate synthase
	VIT_17s0000g05760	17	6361704	6385247	Nuclear protein ZAP
	VIT_17s0000g05770	17	6397487	6410902	Nuclear ribonuclease Z
<i>pheno_17_2</i>	VIT_17s0000g07830	17	8918616	8923034	Asp/Glu racemase; Tetratricopeptide helical
	VIT_17s0000g07840	17	8924188	8925529	Unknown protein
	VIT_17s0000g07850	17	8931341	8937870	Nucleobase-ascorbate transporter 6 (NAT6)
	VIT_17s0000g07870	17	8950730	8962366	Ribosomal protein L29
	VIT_17s0000g07880	17	8963993	8974679	Bromo-adjacency (BAH) domain-containing protein
	VIT_17s0000g07890	17	8976835	8985225	Rac-like GTP-binding protein ARAC10 (GTPase protein ROP10)
	VIT_17s0000g07900	17	9005528	9011550	Protease Do 9
	VIT_17s0000g07910	17	9011840	9014726	Nodulin MtN21 family
	VIT_17s0000g07920	17	9030527	9032996	Hypoxia-responsive
	VIT_17s0000g07930	17	9034815	9036877	Nodulin MtN21 family
	VIT_17s0000g07940	17	9041797	9042384	ERF/AP2 Gene Family (VvERF024)
	VIT_17s0000g07950	17	9054392	9056553	Unknown protein
<i>pheno_18_1</i>	VIT_18s0001g01250	18	1835240	1837419	Senescence-inducible chloroplast stay-green protein 2
	VIT_18s0001g01270	18	1856972	1863925	Ankyrin
	VIT_18s0001g01300	18	1877353	1877899	Wall-associated receptor kinase 5
	VIT_18s0001g01310	18	1877900	1880259	Wall-associated receptor kinase 5
	VIT_18s0001g01320	18	1885028	1894797	Wall-associated receptor kinase 5
	VIT_18s0001g01350	18	1897393	1914523	Toprim domain-containing protein
	VIT_18s0001g01360	18	1934332	1948604	Toprim domain-containing protein
	VIT_18s0001g01370	18	1952680	1968096	Wall-associated receptor kinase 5
	VIT_18s0001g01390	18	1982983	1985445	GA 20-oxidase
	VIT_18s0001g01410	18	1996714	1997619	Unknown
	VIT_18s0001g01440	18	2005999	2006364	No hit
	VIT_18s0001g01460	18	2028167	2028620	No hit
	VIT_18s0001g01470	18	2040472	2040960	No hit
	VIT_18s0001g01480	18	2050288	2050581	No hit
	VIT_18s0001g01500	18	2060078	2060598	No hit
	VIT_18s0001g01510	18	2075169	2084464	No hit

VIT_18s0001g01530	18	2086640	2087608	No hit
VIT_18s0001g01550	18	2123749	2127932	No hit
VIT_18s0001g01560	18	2130873	2138916	Tetratricopeptide repeat protein 33
VIT_18s0001g01580	18	2149563	2165796	PHD finger transcription factor
VIT_18s0001g01590	18	2174967	2177070	BTB/POZ domain-containing protein
VIT_18s0001g01600	18	2177493	2197513	Ankyrin
VIT_18s0001g01630	18	2200625	2201333	Calcium-binding protein CML
VIT_18s0001g01640	18	2203044	2218030	UDP-sugar pyrophosphorylase
VIT_18s0001g01650	18	2222531	2227556	Unknown
VIT_18s0001g01660	18	2227558	2229622	NADH dehydrogenase I subunit M
VIT_18s0001g01670	18	2231148	2244524	Zinc finger (CCCH-type) family protein
VIT_18s0001g01680	18	2245944	2250220	Protein kinase
VIT_18s0001g01690	18	2256608	2258038	glutathione transferase 5 GSTF5
VIT_18s0001g01700	18	2259998	2279932	Histone-lysine N-methyltransferase ASHH2 EFS (early flowering in short days)
VIT_18s0001g01740	18	2281218	2286726	Histone-lysine N-methyltransferase ASHH2 EFS (Early flowering in short days)
VIT_18s0001g01760	18	2291789	2294046	putative MADS-box Pistillata (VviPI)
VIT_18s0001g01770	18	2299018	2303152	PTAC6 (plastid transcriptionally active6)
VIT_18s0001g01780	18	2306657	2322950	Wound-responsive protein
VIT_18s0001g01810	18	2324024	2335447	MEI1 (meiosis defective 1)
VIT_18s0001g01830	18	2336971	2345138	ATP-NAD kinase
VIT_18s0001g01840	18	2347198	2348370	l-aminocyclopropane-1-carboxylate oxidase
VIT_18s0001g01850	18	2352063	2359939	Amino acid permease
VIT_18s0001g01860	18	2359940	2405390	Preprotein translocase secA
VIT_18s0001g01930	18	2406583	2411640	Preprotein translocase secA
VIT_18s0001g01950	18	2413199	2414815	Pentatricopeptide (PPR) repeat-containing protein
VIT_18s0001g01960	18	2415255	2417215	RKF3 (receptor-like kinase IN in flowers 3)
VIT_18s0001g01980	18	2418945	2426660	Auxilin
VIT_18s0001g02000	18	2438485	2442668	Zinc finger (C2H2 type) family
VIT_18s0001g02010	18	2442718	2443387	No hit
VIT_18s0001g02020	18	2450437	2453364	Amino acid permease 3
VIT_18s0001g02030	18	2460774	2467119	Signal peptidase 1
VIT_18s0001g02050	18	2477226	2479822	TolB protein-related
VIT_18s0001g02060	18	2479868	2484109	Cyclin A1
VIT_18s0001g02080	18	2485740	2489654	Cyclin A
VIT_18s0001g02090	18	2496692	2503378	DNA replication factor C complex subunit 4
VIT_18s0001g02100	18	2504341	2505039	Unknown protein

VIT_18s0001g02120	18	2513739	2517442	Metal transporter Nramp6
VIT_18s0001g02130	18	2519567	2521025	Metal transporter Nramp6
VIT_18s0001g02140	18	2521402	2529629	Metal transporter Nramp1
VIT_18s0001g02160	18	2543141	2554330	Switching protein 3C ATSWI3C
VIT_18s0001g02190	18	2564080	2567938	Switching protein 3C ATSWI3C
VIT_18s0001g02200	18	2573308	2584831	8-oxoguanine-DNA glycosylase (OGG1)
VIT_18s0001g02220	18	2592072	2601990	Beta-galactosidase / lactase
VIT_18s0001g02230	18	2604468	2613076	Beta-galactosidase / lactase
VIT_18s0001g02260	18	2618439	2626112	Proteasome 20S beta subunit C1 (PBC1) (PRCT)
VIT_18s0001g02270	18	2627885	2629132	Unknown
VIT_18s0001g02280	18	2629486	2630245	Zinc finger (C3HC4-type ring finger) family protein
VIT_18s0001g02300	18	2643266	2645234	NAC domain-containing protein (VvNAC08)
VIT_18s0001g02340	18	2663270	2675579	Armadillo/beta-catenin repeat
VIT_18s0001g02370	18	2677244	2684335	DNA replication factor C complex subunit 5
VIT_18s0001g02380	18	2688559	2734881	Kinesin protein (MKRP1)
VIT_18s0001g02420	18	2734882	2737586	Aspartic Protease (VvAP40)
VIT_18s0001g02440	18	2745381	2754460	Aldehyde Dehydrogenase (VvALDH3H1)
VIT_18s0001g02470	18	2761252	2772231	L-ascorbate peroxidase, thylakoid-bound (tAPX)
VIT_18s0001g02480	18	2777880	2785087	Unknown protein
VIT_18s0001g02510	18	2791934	2798318	Protein disulfide-isomerase A1
VIT_18s0001g02540	18	2802829	2805078	ARR9 typeA
VIT_18s0001g02550	18	2813209	2821688	Delta-aminolevulinic acid dehydratase, chloroplast precursor
VIT_18s0001g02570	18	2822064	2827157	IAA-amino acid hydrolase 6
VIT_18s0001g02610	18	2845415	2847110	Caffeic acid methyltransferase
VIT_18s0001g02630	18	2855229	2860609	F-box only protein 9
VIT_18s0001g02640	18	2861119	2864695	Unknown protein
VIT_18s0001g02650	18	2866342	2870749	V-type H ⁺ -transporting ATPase 16kDa proteolipid subunit
VIT_18s0001g02670	18	2875900	2876019	No hit
VIT_18s0001g02680	18	2877451	2880061	BTB/POZ domain-containing protein
VIT_18s0001g02690	18	2881165	2881615	Unknown protein
VIT_18s0001g02700	18	2881700	2884919	Chlorophyll a oxygenase (CAO)
VIT_18s0001g02710	18	2885819	2894159	Unknown protein
VIT_18s0001g02730	18	2898842	2905274	Unknown
VIT_18s0001g02740	18	2905882	2907423	Photosystem II 22 kDa protein PSBS
VIT_18s0001g02750	18	2909150	2910927	Unknown protein
VIT_18s0001g02760	18	2910928	2914749	Lipase GDSL

VIT_18s0001g02770	18	2914955	2920663	Alpha-L-fucosidase 2 precursor
VIT_18s0001g02780	18	2921245	2922708	Lipase GDSL
VIT_18s0001g02790	18	2925094	2926968	Unknown protein
VIT_18s0001g02810	18	2929082	2940502	Acyl-CoA synthetase long-chain member 9
VIT_18s0001g02820	18	2950570	2959607	Transducin protein
VIT_18s0001g02830	18	2960201	2973823	Binding
VIT_18s0001g02860	18	2987834	2994441	Binding
VIT_18s0001g02950	18	3042485	3045575	Unknown protein
VIT_18s0001g02970	18	3057427	3063862	Glucose-6-phosphate/phosphate translocator related
VIT_18s0001g03000	18	3064354	3065865	Universal stress protein (USP) family protein
VIT_18s0001g03020	18	3069509	3079236	Nucleoside-triphosphatase
VIT_18s0001g03060	18	3084053	3095775	Nucleoside-triphosphatase
VIT_18s0001g03080	18	3098022	3101041	Chitin elicitor-binding CEBIP LysM domain-containing
VIT_18s0001g03090	18	3102029	3103369	Aspartic Protease (VvAP41)
VIT_18s0001g03100	18	3109637	3133804	Transcription initiation factor TFIIH subunit H3
VIT_18s0001g03110	18	3134535	3146362	Unknown protein
VIT_18s0001g03130	18	3149249	3169173	Unknown protein
VIT_18s0001g03150	18	3170440	3174962	Cation transport protein chaC
VIT_18s0001g03160	18	3176998	3180139	Nodulin MtN21 family
VIT_18s0001g03170	18	3180624	3188491	Nodulin MtN21 family
VIT_18s0001g03180	18	3190049	3192531	Nodulin MtN21 family
VIT_18s0001g03190	18	3197133	3198315	Glutaredoxin 2
VIT_18s0001g03200	18	3198754	3201304	Emp24/gp25L/p24
VIT_18s0001g03220	18	3206237	3206969	Translation initiation factor eIF-1A
VIT_18s0001g03230	18	3208995	3214247	Aminoacylase/ metalloproteinase
VIT_18s0001g03240	18	3219544	3220699	ERF/AP2 Gene Family (VvERF008),Dehydration Responsive Element-Binding Transcription Factor (VvDREB26)
VIT_18s0001g03250	18	3222134	3232291	Unknown protein
VIT_18s0001g03270	18	3233803	3234804	Zinc finger (C3HC4-type ring finger)
VIT_18s0001g03290	18	3244469	3246948	1-phosphatidylinositol-4-phosphate 5-kinase
VIT_18s0001g03300	18	3249246	3253146	1-aminocyclopropane-1-carboxylate synthase
VIT_18s0001g03310	18	3254531	3256064	Scarecrow transcription factor family
VIT_18s0001g03330	18	3261422	3268381	Unknown protein
VIT_18s0001g03370	18	3282634	3291512	Ribonuclease II family protein
VIT_18s0001g03390	18	3298924	3306685	S-receptor kinase
VIT_18s0001g03420	18	3307440	3307550	No hit
VIT_18s0001g03430	18	3309917	3311940	Flavonol synthase

VIT_18s0001g03440	18	3313991	3315438	No hit
VIT_18s0001g03450	18	3320975	3328281	Glycine-rich protein
VIT_18s0001g03470	18	3338337	3340959	Flavonol synthase
VIT_18s0001g03490	18	3349225	3350592	Flavonol synthase
VIT_18s0001g03510	18	3354104	3359003	flavonol synthase XM_002284374.1
VIT_18s0001g03520	18	3359393	3369207	Camphor resistance CrcB
VIT_18s0001g03540	18	3380455	3383288	Auxin transporter protein 4
VIT_18s0001g03570	18	3387900	3389335	Thaumatococcus ATLP-1
VIT_18s0001g03580	18	3389546	3393993	Ubiquitin-fold modifier 1 precursor
VIT_18s0001g03610	18	3401893	3411144	Auxin-independent growth promoter
VIT_18s0001g03630	18	3412345	3414417	Pentatricopeptide (PPR) repeat-containing protein
VIT_18s0001g03640	18	3417193	3418012	No hit
VIT_18s0001g03650	18	3418650	3419295	No hit
VIT_18s0001g03670	18	3422279	3424214	Zinc finger (C2H2 type) family
VIT_18s0001g03680	18	3433101	3445210	Protein kinase
VIT_18s0001g03720	18	3445760	3445939	No hit
VIT_18s0001g03730	18	3445960	3490992	SET Domain group 37
VIT_18s0001g03760	18	3492878	3505322	Holocarboxylase synthetase 1 (HCS1)
VIT_18s0001g03790	18	3515123	3530220	Oxysterol binding protein
VIT_18s0001g03820	18	3536802	3542078	Phosphatidylinositol-4-phosphate 5-kinase 1
VIT_18s0001g03840	18	3555522	3560233	TEL2 (Terminal EAR1-like 2)
VIT_18s0001g03850	18	3562597	3563546	Ribosomal protein S10 30S
VIT_18s0001g03870	18	3564229	3564690	No hit
VIT_18s0001g03880	18	3565751	3567556	Polcalcin
VIT_18s0001g03910	18	3577992	3582255	Nitrate reductase 2 (NR2)
VIT_18s0001g03930	18	3585471	3585895	No hit
VIT_18s0001g03940	18	3586978	3587567	No hit
VIT_18s0001g03950	18	3587990	3596239	Pm27 protein
VIT_18s0001g03960	18	3596240	3606771	Mekk1
VIT_18s0001g03990	18	3638981	3646405	Stearoyl-ACP desaturase
VIT_18s0001g04010	18	3648331	3660863	Salt tolerant protein
VIT_18s0001g04040	18	3668613	3697492	PHD finger transcription factor
VIT_18s0001g04100	18	3700504	3718045	Histone acetyl transferase HAM1
VIT_18s0001g04130	18	3720073	3720771	Unknown
VIT_18s0001g04140	18	3725171	3732449	Vacuolar protein sorting 9 (VPS9)
VIT_18s0001g04150	18	3732776	3738425	Avr9 elicitor response protein

VIT_18s0001g04160	18	3741241	3745559	Translation initiation factor eIF-5
VIT_18s0001g04180	18	3749619	3757678	Auxin response factor ARF17
VIT_18s0001g04190	18	3759293	3763520	Co-chaperone grpE
VIT_18s0001g04270	18	3791368	3794765	Pentatricopeptide (PPR) repeat-containing
VIT_18s0001g04290	18	3798810	3805936	No hit
VIT_18s0001g04340	18	3822948	3829597	Glycine hydroxymethyltransferase
VIT_18s0001g04380	18	3831159	3832784	Unknown protein
VIT_18s0001g04400	18	3842548	3845101	Rhomboid family KOM (kompeito)
VIT_18s0001g04420	18	3846995	3851906	Phosphopantothenate--cysteine ligase
VIT_18s0001g04440	18	3852065	3861217	Co-chaperone protein DnaJ
VIT_18s0001g04470	18	3861987	3867762	Basic Leucine Zipper Transcription Factor (VvbZIP42)
VIT_18s0001g04500	18	3875315	3878509	Enhanced EM level EEL (VvABF-2), Basic Leucine Zipper Transcription Factor (VvbZIP43)
VIT_18s0001g04520	18	3879307	3882849	No hit
VIT_18s0001g04540	18	3883733	3898683	Unknown protein
VIT_18s0001g04580	18	3900400	3905806	Unknown protein
VIT_18s0001g04590	18	3906073	3907918	Binding
VIT_18s0001g04600	18	3913481	3917327	Glutaredoxin
VIT_18s0001g04610	18	3918203	3923636	Unknown protein
VIT_18s0001g04630	18	3924182	3930381	Aspartate aminotransferase
VIT_18s0001g04640	18	3931182	3931761	No hit
VIT_18s0001g04660	18	3935472	3935878	No hit
VIT_18s0001g04680	18	3938582	3956444	RPG related protein 1 RR1
VIT_18s0001g04700	18	3956796	3960644	GP5 ubiquitin-like
VIT_18s0001g04730	18	3963413	3965554	Kelch repeat-containing F-box protein
VIT_18s0001g04750	18	3967437	3969192	Acetylcholinesterase
VIT_18s0001g04760	18	3976114	3980165	Ribosomal protein L30 (RPL30B) 60S
VIT_18s0001g04770	18	3980567	3987316	Apoptotic chromatin condensation inducer 1 ACIN1
VIT_18s0001g04790	18	3994178	4000375	Aspartic Protease (VvAP42)
VIT_18s0001g04800	18	4003656	4004282	Hyperosmotically inducible periplasmic protein
VIT_18s0001g04810	18	4014840	4015257	putative MADS-box type delta 1b (VviMADSD1b)
VIT_18s0001g04850	18	4033185	4034494	Unknown
VIT_18s0001g04860	18	4035264	4040608	Aspartate transaminase.
VIT_18s0001g04880	18	4041678	4046983	Unknown protein
VIT_18s0001g04890	18	4048925	4052950	Low affinity sulphate transporter
VIT_18s0001g04910	18	4062087	4068935	Sulfate transporter 1.3
VIT_18s0001g04920	18	4068936	4069711	No hit

VIT_18s0001g04930	18	4070013	4071952	Sulfate transporter 1.3
VIT_18s0001g04940	18	4072111	4072857	No hit
VIT_18s0001g04960	18	4076661	4078865	Sulfate transporter 1.2
VIT_18s0001g04970	18	4087210	4096302	TRNA modification GTPase trmE
VIT_18s0001g04980	18	4097931	4113803	Acetyl-CoA carboxylase 2 (ACC2)
VIT_18s0001g05020	18	4122072	4123281	Senescence-associated protein
VIT_18s0001g05030	18	4130541	4134290	Glucan 1,3-beta-glucosidase precursor
VIT_18s0001g05040	18	4138118	4140727	Pollen Ole e 1 allergen and extensin
VIT_18s0001g05060	18	4143615	4147853	2,3-bisphosphoglycerate-dependent phosphoglycerate mutase
VIT_18s0001g05080	18	4148968	4155129	SEC14 cytosolic factor, putative
VIT_18s0001g05100	18	4156671	4159130	No hit
VIT_18s0001g05110	18	4159695	4167493	DNA2-NAM7 helicase
VIT_18s0001g05130	18	4176691	4179995	Unknown protein
VIT_18s0001g05160	18	4181102	4184913	Glycosyl hydrolase family 3 protein
VIT_18s0001g05180	18	4185500	4189977	Beta-D-xylosidase
VIT_18s0001g05220	18	4205002	4212978	WD-40 repeat
VIT_18s0001g05250	18	4220268	4222313	Dehydration Responsive Element-Binding Transcription Factor (VvDREB27)
VIT_18s0001g05270	18	4225485	4241449	ERGIC and golgi 3
VIT_18s0001g05300	18	4254678	4257480	Trehalose-6-phosphate phosphatase
VIT_18s0001g05310	18	4268207	4269413	F-box domain containing protein
VIT_18s0001g05330	18	4272391	4273949	No hit
VIT_18s0001g05340	18	4274062	4275436	Transcription termination factor mitochondrial mTERF
VIT_18s0001g05370	18	4279252	4280705	Unknown protein
VIT_18s0001g05380	18	4284177	4287720	TTL1 (tetratricopeptide-repeat thioredoxin-like 1)
VIT_18s0001g05400	18	4299165	4300807	Unknown
VIT_18s0001g05420	18	4306846	4309947	UNE2 (unfertilized embryo sac 2); carbohydrate transporter
VIT_18s0001g05440	18	4310333	4319306	Methyltransferase type 11
VIT_18s0001g05480	18	4326127	4329358	Unknown protein
VIT_18s0001g05490	18	4329359	4329584	No hit
VIT_18s0001g05500	18	4331692	4337441	PUMILIO 7 (APUM7)
VIT_18s0001g05530	18	4338743	4341637	Annexin 1 (ANN1)
VIT_18s0001g05550	18	4349906	4352613	Splicing factor, arginine/serine-rich 2
VIT_18s0001g05570	18	4363673	4368991	Hexose transporter HT2
VIT_18s0001g05580	18	4373859	4374826	Unknown protein
VIT_18s0001g05590	18	4377588	4386070	CCR4-NOT transcription complex subunit 6
VIT_18s0001g05600	18	4390485	4398813	Synaptonemal complex protein 1 (ZYP1A)

VIT_18s0001g05620	18	4399508	4405646	Carrier protein, Mitochondrial
VIT_18s0001g05640	18	4407516	4416666	Unknown protein
VIT_18s0001g05670	18	4425461	4426613	myb domain protein 93
VIT_18s0001g05680	18	4433417	4440032	Cryptochrome 1
VIT_18s0001g05690	18	4442502	4445540	Protein phosphatase 2C
VIT_18s0001g05710	18	4445541	4452656	Hydrolase, alpha/beta fold
VIT_18s0001g05720	18	4453327	4457820	14-3-3 protein GF14 epsilon (GRF10)
VIT_18s0001g05730	18	4458540	4462662	Adenosine 5'-phosphosulfate reductase 3
VIT_18s0001g05740	18	4465943	4475083	DNA-binding protein
VIT_18s0001g05780	18	4483440	4486850	Leucine-rich repeat family protein
VIT_18s0001g05790	18	4491794	4493362	Unknown protein
VIT_18s0001g05800	18	4494490	4503957	Dehydration-responsive protein
VIT_18s0001g05840	18	4520619	4529938	RNA recognition motif (RRM)-containing protein
VIT_18s0001g05860	18	4531169	4532101	Transparent testa 1
VIT_18s0001g05870	18	4535173	4537082	WPP domain-associated protein
VIT_18s0001g05900	18	4544137	4544831	No hit
VIT_18s0001g05910	18	4550436	4552401	Cis-zeatin O-beta-D-glucosyltransferase
VIT_18s0001g05950	18	4564102	4565743	Cis-zeatin O-beta-D-glucosyltransferase
VIT_18s0001g05970	18	4566745	4574723	No hit
VIT_18s0001g05990	18	4574889	4586041	UDP-glycosyltransferase 85A1
VIT_18s0001g06000	18	4586571	4589855	No hit
VIT_18s0001g06020	18	4594155	4595268	Phosphate-induced protein 1
VIT_18s0001g06030	18	4597940	4599044	Erg-1
VIT_18s0001g06040	18	4600121	4600746	Phosphotyrosyl phosphatase activator PTPA (GB:X73478)
VIT_18s0001g06050	18	4600747	4602556	Phosphotyrosyl phosphatase activator PTPA (GB:X73478)
VIT_18s0001g06060	18	4605365	4607009	UDP-glycosyltransferase 85A1
VIT_18s0001g06080	18	4610459	4612060	UDP-glycosyltransferase 85A1
VIT_18s0001g06090	18	4613633	4615316	Cis-zeatin O-beta-D-glucosyltransferase
VIT_18s0001g06120	18	4629508	4631173	Cis-zeatin O-beta-D-glucosyltransferase
VIT_18s0001g06130	18	4631192	4631628	No hit
VIT_18s0001g06140	18	4643431	4644462	Phosphate-induced protein 1
VIT_18s0001g06150	18	4652464	4653648	Phosphate-induced protein 1
VIT_18s0001g06170	18	4658419	4659571	Phosphate-induced protein 1
VIT_18s0001g06180	18	4659693	4663192	Phosphate-induced protein 1
VIT_18s0001g06200	18	4674500	4678247	Phosphotyrosyl phosphatase activator (PTPA)
VIT_18s0001g06220	18	4684266	4686537	F-box protein (FBW2)

VIT_18s0001g06250	18	4700787	4704775	3-deoxy-D-arabino-heptulosonate 7-phosphate synthase
VIT_18s0001g06270	18	4705961	4722205	Transcription factor jumonji (jmjC) domain-containing protein
VIT_18s0001g06290	18	4724387	4727239	Ribosomal protein S6 (RPS6B) 40S
VIT_18s0001g06300	18	4728333	4729667	Purine permease 1 PUP1
VIT_18s0001g06310	18	4733340	4737514	SnRK2-8
VIT_18s0001g06320	18	4738323	4739992	Cupin, RmlC-type
VIT_18s0001g06330	18	4742712	4744730	14-3-3 protein GF14 omega (GRF2)
VIT_18s0001g06350	18	4751168	4752609	VQ motif-containing protein
VIT_18s0001g06360	18	4760150	4762878	Alcohol dehydrogenase
VIT_18s0001g06370	18	4765814	4772318	L-ascorbate peroxidase, chloroplast
VIT_18s0001g06390	18	4773069	4780063	Auxin-independent growth promoter
VIT_18s0001g06400	18	4788251	4789021	No hit
VIT_18s0001g06410	18	4791622	4794578	Ribosomal protein 60S
VIT_18s0001g06420	18	4796509	4805339	No hit
VIT_18s0001g06430	18	4806981	4808947	Homeobox-leucine zipper protein ATHB-6
VIT_18s0001g06440	18	4810193	4815522	No hit
VIT_18s0001g06460	18	4815751	4855137	Queuine tRNA-ribosyltransferase
VIT_18s0001g06500	18	4859577	4898877	Unknown protein
VIT_18s0001g06520	18	4900037	4954270	Isoamylase protein.
VIT_18s0001g06560	18	4962807	4963515	No hit
VIT_18s0001g06580	18	4966021	4966915	Plastocyanin domain-containing protein
VIT_18s0001g06590	18	4970021	4973908	Pigment defective 322
VIT_18s0001g06600	18	4974906	4979125	Unknown protein
VIT_18s0001g06610	18	4982073	4983574	Plastid-targeted protein 2
VIT_18s0001g06630	18	4993758	4999430	No hit
VIT_18s0001g06640	18	5000284	5003505	Zinc finger (C3HC4-type ring finger)
VIT_18s0001g06650	18	5009725	5011125	basic helix-loop-helix (bHLH) family
VIT_18s0001g06670	18	5020431	5021751	Ring-H2 finger protein ATL1N
VIT_18s0001g06690	18	5029717	5032277	Gibberellin 20 oxidase 2
VIT_18s0001g06710	18	5035063	5039911	Oxidoreductase, 2OG-Fe(II) oxygenase
VIT_18s0001g06760	18	5054380	5055720	Clathrin assembly protein 16
VIT_18s0001g06770	18	5058487	5059001	No hit
VIT_18s0001g06790	18	5062066	5066242	Protein TRANSPARENT TESTA 12 (DDTFR18)
VIT_18s0001g06820	18	5077418	5081480	MATE efflux family protein ripening responsive
VIT_18s0001g06840	18	5092164	5094226	Peroxidase GvPx2b class III
VIT_18s0001g06850	18	5102796	5105019	Peroxidase GvPx2b class III

	VIT_18s0001g06890	18	5121954	5123595	Peroxidase GvPx2b, class III [Vitis vinifera]
	VIT_18s0001g06910	18	5139237	5140617	Purine permease 1 PUP1
	VIT_18s0001g06940	18	5163243	5164681	Purine permease 1 (PUP1)
	VIT_18s0001g06950	18	5169728	5171215	Purine permease 1 (PUP1)
	VIT_18s0001g06970	18	5184425	5218375	DnaJ homolog, subfamily A, member 3
	VIT_18s0001g06980	18	5220072	5221115	Pentatricopeptide repeat-containing protein
	VIT_18s0001g07000	18	5240693	5244484	Pentatricopeptide (PPR) repeat-containing protein
	VIT_18s0001g07010	18	5244635	5245588	GLUTATHIONE S-TRANSFERASE TAU 8
	VIT_18s0001g07020	18	5247639	5250783	No hit
	VIT_18s0001g07060	18	5256010	5263653	Phosphoribosylaminoimidazole-succinocarboxamide synthase.
	VIT_18s0001g07070	18	5266578	5271872	Phosphoenolpyruvate carboxylase kinase 2 (PEPKR2)
	VIT_18s0001g07080	18	5275135	5280005	Protein transport protein SFT1
	VIT_18s0001g07090	18	5290562	5293561	Unknown protein
	VIT_18s0001g07100	18	5294004	5304799	Pyridoxamine 5'-phosphate oxidase
	VIT_18s0001g07110	18	5310450	5311506	No hit
	VIT_18s0001g07120	18	5311507	5314031	Transport inhibitor response 1 protein
	VIT_18s0001g07130	18	5323899	5335911	GEM-like 1
	VIT_18s0001g07140	18	5343590	5344691	Zinc Finger Homeodomain Transcription Factor (VvZHD10)
<i>pheno_18_2</i>	VIT_18s0001g12820	18	10924591	10933193	Dihydroflavonol 4-reductase
	VIT_18s0001g12830	18	10937041	10940329	1,4-beta-mannan endohydrolase
	VIT_18s0001g12840	18	10940330	10945165	ADP-glucose pyrophosphorylase large subunit CagpL2
	VIT_18s0001g12850	18	10951026	10951788	Ribosomal protein L31
	VIT_18s0001g12860	18	10961548	10963014	Unknown protein
	VIT_18s0001g12870	18	10968173	10971522	CYP722A1
	VIT_18s0001g12880	18	10974280	10990318	Jasmonate O-methyltransferase
	VIT_18s0001g12890	18	10990319	10995000	Jasmonate O-methyltransferase
	VIT_18s0001g12900	18	10999096	11003121	S-adenosyl-L-methionine:salicylic acid carboxyl methyltransferase
	VIT_18s0001g12910	18	11011979	11016761	Inositol-pentakisphosphate 2-kinase 1 ATIPK1
	VIT_18s0001g12920	18	11018628	11019094	No hit
	VIT_18s0001g12930	18	11019643	11020221	Heavy-metal-associated domain-containing protein
	VIT_18s0001g12940	18	11025678	11029403	Dihydrofolate reductase-thymidylate synthase
	VIT_18s0001g12950	18	11035878	11042058	SEC14 cytosolic factor
	VIT_18s0001g12960	18	11043696	11049454	Wound-responsive protein
	VIT_18s0001g12970	18	11056806	11060964	Ethylene-responsive protein
	VIT_18s0001g12980	18	11070674	11090733	Cyclin-dependent protein kinase CYCT1;4
	VIT_18s0001g12990	18	11099778	11102242	Anthranilate N-benzoyltransferase protein 1

VIT_18s0001g13000	18	11105764	11116980	Adaptor-related protein complex AP-4, mu 1
VIT_18s0001g13010	18	11126023	11129236	Mitogen-activated Protein Kinase (VvMPK11)
VIT_18s0001g13020	18	11137583	11137919	No hit
VIT_18s0001g13030	18	11137920	11138195	No hit
VIT_18s0001g13040	18	11138196	11139020	Basic Leucine Zipper Transcription Factor (VvbZIP47)
VIT_18s0001g13050	18	11143793	11148102	Protein translocase Tic20
VIT_18s0001g13060	18	11153980	11161250	C3H2C3 ring-finger protein
VIT_18s0001g13070	18	11161718	11165469	NAD-dependent epimerase/dehydratase
VIT_18s0001g13080	18	11166531	11167946	Unknown protein
VIT_18s0001g13090	18	11169585	11174073	Proteasome 26S AAA-ATPase subunit (RPT4)
VIT_18s0001g13100	18	11175122	11179283	Glycosyl transferase family 1 protein
VIT_18s0001g13110	18	11184119	11185662	Peroxidase
VIT_18s0001g13120	18	11188323	11195903	GTP-binding protein hflX
VIT_18s0001g13130	18	11196526	11198302	BEL1-like homeodomain 10
VIT_18s0001g13140	18	11199295	11200843	No hit
VIT_18s0001g13150	18	11201495	11206144	BEL1 homeotic protein 3
VIT_18s0001g13160	18	11209086	11221435	Tetrapyrrole methylase
VIT_18s0001g13180	18	11241300	11245481	Ubiquitin-conjugating enzyme E2 W
VIT_18s0001g13190	18	11247397	11252857	MAPK (MPK9)
VIT_18s0001g13200	18	11256653	11261569	Cytokinin dehydrogenase 5 precursor
VIT_18s0001g13210	18	11268578	11271421	Lectin jacalin
VIT_18s0001g13220	18	11275604	11278396	Pentatricopeptide (PPR) repeat-containing protein
VIT_18s0001g13230	18	11286706	11293739	Beta-galactosidase BG1 [Vitis vinifera]
VIT_18s0001g13240	18	11293740	11296751	Thioredoxin H-type 1
VIT_18s0001g13250	18	11297040	11299715	Thioredoxin H-type 1
VIT_18s0001g13260	18	11307834	11309051	ATP-dependent protease La (LON) domain-containing protein
VIT_18s0001g13270	18	11311350	11316053	Papain cysteine peptidase XBPC3
VIT_18s0001g13280	18	11318782	11330916	RanBPM
VIT_18s0001g13290	18	11331768	11334686	GTP1/OBG family
VIT_18s0001g13300	18	11335834	11336703	Unknown
VIT_18s0001g13310	18	11338330	11346082	GTP1/OBG family protein
VIT_18s0001g13320	18	11347342	11348103	ERF/AP2 Gene Family (VvERF039),Dehydration Responsive Element-Binding Transcription Factor (VvDREB29)
VIT_18s0001g13330	18	11348587	11353628	Purple acid phosphatase 32- ATPAP32/PAP32
VIT_18s0001g13340	18	11355046	11359625	Purple acid phosphatase 32- ATPAP32/PAP32
VIT_18s0001g13350	18	11374221	11381621	Proton-dependent oligopeptide transport (POT) family protein
VIT_18s0001g13360	18	11384285	11387145	Nodulin MtN21 family

VIT_18s0001g13370	18	11397795	11406180	Transcription initiation factor TFIIF beta subunit (TFIIF-beta)
VIT_18s0001g13380	18	11409762	11411534	Papain cysteine proteinase isoform I
VIT_18s0001g13390	18	11419071	11420557	Papain cysteine proteinase isoform II
VIT_18s0001g13400	18	11425591	11427332	Papain cysteine proteinase isoform I
VIT_18s0001g13410	18	11429258	11475180	V-type H+-transporting ATPase subunit I
VIT_18s0001g13420	18	11486984	11488357	SHI-related sequence 5
VIT_18s0001g13430	18	11496666	11502715	Coatomer alpha subunit
VIT_18s0001g13440	18	11503598	11504539	SLAH1 (SLAC1 homologue 1)
VIT_18s0001g13450	18	11505093	11505323	SLAH1 (SLAC1 homologue 1)
VIT_18s0001g13460	18	11506606	11512370	putative MADS-box Apetala 3a (VviAP3a)
VIT_18s0001g13490	18	11525758	11527691	Maturase K
VIT_18s0001g13500	18	11528060	11539323	forkhead-associated domain-containing protein
VIT_18s0001g13510	18	11539928	11541250	Hcr2-p6
VIT_18s0001g13520	18	11546677	11548061	Zinc finger (B-box type)
VIT_18s0001g13530	18	11552151	11558455	SH3 domain-containing protein 2
VIT_18s0001g13540	18	11559472	11560071	Glycine-rich protein
VIT_18s0001g13550	18	11561321	11567816	Zinc knuckle (CCHC-type) family
VIT_18s0001g13560	18	11577367	11581885	Unknown protein
VIT_18s0001g13570	18	11584918	11587466	Calcium ion binding protein
VIT_18s0001g13580	18	11600569	11607735	Kinesin motor protein
VIT_18s0001g13590	18	11608623	11612061	Leucine-rich repeat protein kinase
VIT_18s0001g13600	18	11612878	11613828	No hit
VIT_18s0001g13610	18	11613829	11620092	Abhydrolase domain-containing protein 5
VIT_18s0001g13620	18	11630815	11630958	No hit
VIT_18s0001g13630	18	11631001	11633191	V-type H+-transporting ATPase 16kDa proteolipid subunit
VIT_18s0001g13640	18	11636802	11640737	Amine oxidase
VIT_18s0001g13650	18	11640899	11647357	Amine oxidase
VIT_18s0001g13660	18	11656750	11691457	EMB2757/TAN (embryo defective 2757)
VIT_18s0001g13670	18	11698060	11699721	Glyoxal oxidase-related
VIT_18s0001g13680	18	11710329	11711606	Histone H3
VIT_18s0001g13690	18	11723026	11723485	No hit
VIT_18s0001g13700	18	11726587	11729541	Cell growth defect factor -2
VIT_18s0001g13710	18	11729964	11734394	BPC6/BBR/BPC6/BPC6
VIT_18s0001g13720	18	11734395	11741936	BPC6/BBR/BPC6/BPC6
VIT_18s0001g13730	18	11741937	11743502	BPC6/BBR/BPC6/BPC6
VIT_18s0001g13740	18	11745491	11746246	Basic Leucine Zipper Transcription Factor (VvbZIP48)

VIT_18s0001g13750	18	11750154	11761059	Regulator of chromosome condensation (RCC1)
VIT_18s0001g13760	18	11761760	11763067	CYP71AT2v2
VIT_18s0001g13770	18	11767560	11769317	Cytochrome P450, family 83, subfamily B, polypeptide 1
VIT_18s0001g13780	18	11774368	11775896	Cytochrome P450, family 83, subfamily B, polypeptide 1
VIT_18s0001g13790	18	11779263	11781156	Cytochrome P450, family 83, subfamily B, polypeptide 1
VIT_18s0001g13800	18	11784344	11786071	CYP71AT2v2
VIT_18s0001g13810	18	11789356	11791909	Heat shock protein-related
VIT_18s0001g13820	18	11794593	11796161	Cytochrome P450, family 83, subfamily B, polypeptide 1
VIT_18s0001g13830	18	11801940	11803508	Cytochrome P450, family 83, subfamily B, polypeptide 1
VIT_18s0001g13850	18	11832431	11833905	Cytochrome P450, family 83, subfamily B, polypeptide 1
VIT_18s0001g13870	18	11862607	11871541	Calmodulin binding protein
VIT_18s0001g13880	18	11876078	11892231	Zinc finger (CCCH-type) family protein
VIT_18s0001g13890	18	11893711	11897887	Unknown protein
VIT_18s0001g13900	18	11898378	11909253	Unknown protein
VIT_18s0001g13910	18	11909699	11914734	Unknown protein
VIT_18s0001g13920	18	11917645	11919060	Unknown protein
VIT_18s0001g13930	18	11920505	11928962	Auxin response factor 5 (Transcription factor MONOPTEROS)
VIT_18s0001g13940	18	11933806	11936210	Pentatricopeptide (PPR) repeat-containing
VIT_18s0001g13950	18	11940712	11949407	RNA polymerase Rpa43 subunit
VIT_18s0001g13960	18	11959623	11960345	SAUR_E
VIT_18s0001g13970	18	11974983	11980862	Myosin-related
VIT_18s0001g13980	18	11987475	11987922	Auxin responsive SAUR protein
VIT_18s0001g13990	18	11989161	11997757	No hit
VIT_18s0001g14000	18	12002927	12003389	Auxin-induced SAUR
VIT_18s0001g14010	18	12004532	12014082	Sulfate adenylyltransferase
VIT_18s0001g14020	18	12032185	12069047	5'-3' exoribonuclease 2
VIT_18s0001g14030	18	12073618	12075722	Lysine decarboxylase
VIT_18s0001g14040	18	12086327	12090970	Endo-1,4-beta-glucanase
VIT_18s0001g14060	18	12117278	12118772	Transposon protein, CACTA, En/Spm sub-class
VIT_18s0001g14070	18	12133743	12135762	Unknown
VIT_18s0001g14080	18	12136487	12140512	Diphthine synthase (DPH5)
VIT_18s0001g14090	18	12141515	12144267	Molecular chaperone DnaJ
VIT_18s0001g14100	18	12146146	12150550	ABA-responsive protein (HVA22)HVA22H
VIT_18s0001g14110	18	12151849	12158339	Transcription factor E2F/dimerisation partner (TDP) E2F2
VIT_18s0001g14120	18	12160472	12174229	Translation initiation factor eIF-3 subunit 3
VIT_18s0001g14130	18	12179540	12181647	Zinc finger (C2H2 type) family

VIT_18s0001g14140	18	12191289	12193271	No hit
VIT_18s0001g14150	18	12197073	12197669	No hit
VIT_18s0001g14160	18	12205115	12205631	Heat-and acid-stable phosphoprotein
VIT_18s0001g14170	18	12212398	12215228	Cyclin-dependent protein kinase regulator CYCB2_4
VIT_18s0001g14180	18	12216225	12219253	Armadillo/beta-catenin repeat family protein
VIT_18s0001g14190	18	12223875	12228196	Unknown
VIT_18s0001g14200	18	12229450	12229914	No hit
VIT_18s0001g14210	18	12230572	12231893	Unknown protein
VIT_18s0001g14230	18	12252526	12257027	Hexokinase
VIT_18s0001g14240	18	12257459	12261168	Adaptor-related protein complex 2, sigma 1 sub
VIT_18s0001g14250	18	12262636	12268135	Unknown protein
VIT_18s0001g14260	18	12273788	12276090	No hit
VIT_18s0001g14270	18	12276091	12276597	Gibberellin-regulated protein 1 (GASA1)
VIT_18s0001g14280	18	12281671	12286855	ER lumen protein retaining receptor
VIT_18s0001g14290	18	12292329	12294516	Invertase-like protein
VIT_18s0001g14300	18	12299065	12301674	Cytomatrix protein
VIT_18s0001g14310	18	12303077	12305027	flavanone-3-hydroxylase 2 (F3H2) [Vitis vinifera]
VIT_18s0001g14320	18	12306644	12309420	Unknown protein
VIT_18s0001g14330	18	12310077	12311494	No hit
VIT_18s0001g14340	18	12313857	12316276	No hit
VIT_18s0001g14350	18	12335581	12336788	No hit
VIT_18s0001g14360	18	12337145	12340985	Tubulin beta-1 chain
VIT_18s0001g14370	18	12341546	12342790	No hit
VIT_18s0001g14380	18	12343090	12350501	Brain and reproductive organ-expressed protein
VIT_18s0001g14390	18	12362497	12370721	Transducin protein
VIT_18s0001g14400	18	12377314	12378089	Peptidyl-prolyl cis-trans isomerase ROC5 (rotamase CYP 5)
VIT_18s0001g14410	18	12383680	12402362	Unknown protein
VIT_18s0001g14420	18	12403268	12404144	Unknown
VIT_18s0001g14430	18	12431386	12431715	Unknown
VIT_18s0001g14440	18	12432955	12439459	Molecular chaperone DnaJ
VIT_18s0001g14450	18	12453766	12456583	Ferredoxin:nadp+ Oxidoreductase PETH
VIT_18s0001g14460	18	12457152	12463238	Unknown protein
VIT_18s0001g14470	18	12465257	12466480	No hit
VIT_18s0001g14480	18	12468330	12470542	Thaumatococcus SCUTL1
VIT_18s0001g14490	18	12488747	12490747	Thaumatococcus
VIT_18s0001g14500	18	12501841	12507813	SHD (shepherd)

VIT_18s0001g14510	18	12509258	12513293	Ribosomal protein L28
VIT_18s0001g14520	18	12526253	12526939	Unknown protein
VIT_18s0001g14530	18	12533609	12536412	Ubiquitin-protein ligase CIP8 (COPI1-interacting protein 8)
VIT_18s0001g14540	18	12545280	12566106	DEAD-box ATP-dependent RNA helicase 28
VIT_18s0001g14550	18	12579175	12591899	Unknown protein
VIT_18s0001g14560	18	12608249	12608970	Unknown
VIT_18s0001g14580	18	12620422	12628019	Kinesin family member 18/19
VIT_18s0001g14590	18	12634521	12635111	ATSYTC/NTMC2T1.3/NTMC2TYPE1.3/SYTC
VIT_18s0001g14600	18	12645229	12650755	Pentatricopeptide (PPR) repeat-containing protein
VIT_18s0001g14610	18	12668387	12671744	Clavata1 receptor kinase (CLV1)
VIT_18s0001g14620	18	12678950	12679433	Ribosomal protein S16
VIT_18s0001g14630	18	12682841	12691610	ATSYTB/NTMC2T1.2/NTMC2TYPE1.2/SYTB
VIT_18s0001g14640	18	12698089	12699502	No hit
VIT_18s0001g14650	18	12699590	12707069	DNA-directed RNA polymerase I subunit A12
VIT_18s0001g14660	18	12710695	12716340	ABC Transporter (VvMDR3 - VvABCB3)
VIT_18s0001g14670	18	12719099	12724188	Rac-like GTP-binding protein RAC1
VIT_18s0001g14680	18	12725219	12753021	Vacuolar protein sorting 35
VIT_18s0001g14690	18	12763424	12766855	Protein kinase
VIT_18s0001g14700	18	12767403	12770616	Unknown
VIT_18s0001g14710	18	12772148	12773056	Ketol-acid reductoisomerase precursor
VIT_18s0001g14720	18	12773057	12773368	Ankyrin repeat family protein
VIT_18s0001g14730	18	12776655	12781411	Glutaredoxin
VIT_18s0001g14740	18	12783608	12784580	Protein binding
VIT_18s0001g14750	18	12787199	12809768	Zinc finger (FYVE type) VPS19
VIT_18s0001g14760	18	12821158	12822999	Lipase 3 (EXL3) family II extracellular
VIT_18s0001g14770	18	12823491	12840711	Lipase 3 (EXL3) family II extracellular
VIT_18s0001g14780	18	12841218	12848820	Lipase 3 (EXL3) family II extracellular
VIT_18s0001g14790	18	12853195	12855945	Lipase 3 (EXL3) family II extracellular
VIT_18s0001g14800	18	12859139	12862545	Lipase 3 (EXL3) family II extracellular
VIT_18s0001g14810	18	12863066	12871408	Lipase 3 (EXL3) family II extracellular
VIT_18s0001g14840	18	12887405	12890179	Nickel ion transporter
VIT_18s0001g14850	18	12893670	12898347	Unknown protein
VIT_18s0001g14860	18	12900823	12904890	SKP1
VIT_18s0001g14870	18	12908766	12912392	Subtilisin-type protease precursor
VIT_18s0001g14880	18	12914221	12923327	Unknown protein
VIT_18s0001g14890	18	12936974	12937903	ABA-responsive element-binding protein 3 (AREB3), Basic Leucine Zipper Transcription Factor (VvbZIP49)

VIT_18s0001g14900	18	12941612	12948377	La domain-containing protein
VIT_18s0001g14910	18	12954423	12956365	Mannitol dehydrogenase
VIT_18s0001g14920	18	12959804	12961455	Unknown protein
VIT_18s0001g14930	18	12964045	12967757	Unknown protein
VIT_18s0001g14940	18	12969264	12971832	Pentatricopeptide (PPR) repeat-containing
VIT_18s0001g14950	18	12978238	12979279	EMB2170 (embryo defective 2170)
VIT_18s0001g14960	18	12980373	12984313	Pentatricopeptide (PPR) repeat-containing
VIT_18s0001g14970	18	12985919	12987853	Pentatricopeptide (PPR) repeat-containing
VIT_18s0001g14980	18	12992480	12996562	3-methyl-2-oxobutanoate dehydrogenase
VIT_18s0001g14990	18	12997417	13013251	Dual-specific kinase DSK1
VIT_18s0001g15000	18	13026931	13036065	ACT domain containing protein (ACR4)
VIT_18s0001g15010	18	13037311	13042185	F-box and leucine-rich repeat protein 1
VIT_18s0001g15020	18	13043063	13050564	DnaJ homolog, subfamily A, member 4
VIT_18s0001g15050	18	13073854	13087034	Protein phosphatase 2C
VIT_18s0001g15060	18	13104442	13105749	No hit
VIT_18s0001g15070	18	13107851	13109297	No hit
VIT_18s0001g15080	18	13112575	13112793	No hit
VIT_18s0001g15090	18	13133931	13152578	RAB GTPase RAB18
VIT_18s0001g15100	18	13176556	13178357	flavin-containing monooxygenase, putative
VIT_18s0001g15110	18	13195418	13195879	Flavin-containing monooxygenases
VIT_18s0001g15120	18	13199060	13200303	Unknown protein
VIT_18s0001g15130	18	13201886	13203120	WD40 repeat protein
VIT_18s0001g15140	18	13208994	13210315	Unknown
VIT_18s0001g15150	18	13231125	13232440	Unknown protein
VIT_18s0001g15160	18	13277786	13278346	S-adenosylmethionine sythetase 2
VIT_18s0001g15170	18	13278347	13278514	S-adenosylmethionine sythetase 2
VIT_18s0001g15180	18	13279241	13280607	No hit
VIT_18s0001g15190	18	13303082	13304738	flavin-containing monooxygenase, putative
VIT_18s0001g15200	18	13306083	13306887	SIK1 (serine/threonine kinase 1)
VIT_18s0001g15220	18	13312158	13313392	Unknown protein
VIT_18s0001g15230	18	13322054	13323283	Unknown
VIT_18s0001g15240	18	13365469	13366663	Blue (type 1) copper domain
VIT_18s0001g15250	18	13389043	13389957	Unknown
VIT_18s0001g15260	18	13397962	13399162	myb domain protein 52
VIT_18s0001g15270	18	13408234	13413047	SCL1 (scarecrow-like 1)
VIT_18s0001g15280	18	13418393	13429810	RNA exonuclease 1

VIT_18s0001g15290	18	13430862	13443967	Ribosome maturation protein SDO1
VIT_18s0001g15300	18	13444139	13444288	No hit
VIT_18s0001g15310	18	13444700	13445878	Thioredoxin M-type
VIT_18s0001g15320	18	13446395	13458670	SEU3B protein
VIT_18s0001g15330	18	13476403	13478586	Nodulin MtN3 family
VIT_18s0001g15340	18	13488810	13490580	Pentatricopeptide (PPR) repeat-containing protein
VIT_18s0001g15350	18	13493089	13494429	Pentatricopeptide (PPR) repeat-containing protein
VIT_18s0001g15360	18	13495083	13497819	Thylakoid lumenal 29.8 kDa protein
VIT_18s0001g15370	18	13498468	13504540	Exostosin family protein
VIT_18s0001g15380	18	13511653	13519868	No hit
VIT_18s0001g15390	18	13521135	13522636	Gaiacol peroxidase
VIT_18s0001g15400	18	13526007	13535458	KOW domain-containing transcription factor family protein
VIT_18s0001g15410	18	13539135	13541625	Alcohol dehydrogenase 1
VIT_18s0001g15420	18	13551359	13554243	Auxin efflux carrier protein 6
VIT_18s0001g15430	18	13563113	13563819	Alliin lyase
VIT_18s0001g15450	18	13581959	13584888	Alcohol dehydrogenase 3
VIT_18s0001g15460	18	13616618	13618309	Stearyl acyl carrier protein desaturase
VIT_18s0001g15470	18	13620924	13622663	Leaf senescence related protein-like
VIT_18s0001g15510	18	13646454	13647443	Unknown
VIT_18s0001g15520	18	13650247	13655312	Leaf senescence protein
VIT_18s0001g15530	18	13662369	13665624	Pentatricopeptide (PPR) repeat-containing
VIT_18s0001g15540	18	13666500	13667021	No hit
VIT_18s0001g15550	18	13667832	13671220	Serine carboxypeptidase II
VIT_18s0001g15560	18	13676072	13681500	Unknown protein
VIT_18s0001g15570	18	13682439	13700040	Zinc finger (CCCH-type) family protein
VIT_18s0001g15580	18	13701036	13706265	Glycogenin glucosyltransferase (glycogenin)
VIT_18s0001g15600	18	13720692	13730593	Vacuolar protein sorting 45
VIT_18s0001g15610	18	13733152	13734200	Unknown
VIT_18s0001g15620	18	13735971	13739523	Receptor kinase TRKe
VIT_18s0001g15630	18	13793649	13799974	MAP kinase activating protein
VIT_18s0001g15640	18	13803789	13805200	Pathogenesis-related
VIT_18s0001g15650	18	13805201	13806648	Pathogenesis related protein
VIT_18s0001g15660	18	13810659	13811793	Pathogen-related
VIT_18s0001g15670	18	13812058	13816979	Cytoplasm protein
VIT_18s0001g15680	18	13833441	13835421	Cellulase
VIT_18s0001g15690	18	13835422	13835790	Endo-1,4-beta-glucanase

VIT_18s0001g15700	18	13836500	13838302	GLTP3 (glycolipid transfer protein 3)
VIT_18s0001g15710	18	13848186	13855092	Electron carrier/ oxidoreductase
VIT_18s0001g15720	18	13856940	13861020	Leucine Rich Repeat receptor-like kinase
VIT_18s0001g15730	18	13865318	13866466	Dof zinc finger protein DOF3.5
VIT_18s0001g15740	18	13869407	13877879	No hit
VIT_18s0001g15750	18	13901947	13917102	Protein kinase Xa21
VIT_18s0001g15760	18	13920267	13920719	Copine BON3 (BONZAI 3)
VIT_18s0001g15790	18	13930846	13931145	V-type H ⁺ -transporting ATPase 16kDa proteolipid subunit
VIT_18s0001g15800	18	13945801	13947522	Protein kinase Xa21
VIT_18s0166g00010	18	13949617	13952330	Protein kinase Xa21
VIT_18s0166g00020	18	13966224	13967049	RWP-RK domain-containing protein
VIT_18s0166g00030	18	13981658	13985444	No hit
VIT_18s0166g00040	18	13989688	13993683	Protein kinase Xa21
VIT_18s0166g00050	18	13995521	14000593	EFR (EF-TU receptor)
VIT_18s0166g00060	18	14002147	14002275	No hit
VIT_18s0166g00070	18	14002488	14002937	No hit
VIT_18s0166g00080	18	14023042	14027197	ABC Transporter (VvWBC1 - VvABCG1)
VIT_18s0166g00090	18	14033533	14034350	VQ motif-containing protein
VIT_18s0166g00100	18	14041093	14041505	No hit
VIT_18s0166g00110	18	14041566	14042290	E4/E8 binding protein-1
VIT_18s0166g00120	18	14071620	14072689	Concanavalin A lectin
VIT_18s0166g00130	18	14076141	14077530	Substrate carrier, Mitochondrial
VIT_18s0166g00140	18	14096408	14097042	Oligopeptidase A
VIT_18s0166g00150	18	14109274	14109357	No hit
VIT_18s0166g00160	18	14116931	14117425	No hit
VIT_18s0166g00170	18	14122252	14123294	Unknown
VIT_18s0166g00180	18	14130785	14134673	Zinc finger protein ATRZ-1A
VIT_18s0166g00190	18	14139015	14140400	U-box domain-containing protein
VIT_18s0166g00210	18	14160272	14171887	Regulator of chromosome condensation (RCC1)
VIT_18s0166g00220	18	14204751	14205007	No hit
VIT_18s0166g00230	18	14207946	14210222	S-receptor kinase
VIT_18s0166g00240	18	14210516	14228120	RNA recognition motif (RRM)-containing protein
VIT_18s0166g00250	18	14230226	14231594	No hit
VIT_18s0166g00260	18	14233967	14234837	No hit
VIT_18s0166g00270	18	14276150	14276380	Mutator-like transposase-like protein
VIT_18s0166g00280	18	14293747	14294440	Transcription factor related

VIT_18s0166g00290	18	14296029	14329589	Protein kinase
VIT_18s0166g00300	18	14365849	14379716	Histidinol dehydrogenase, chloroplast precursor
VIT_18s0166g00310	18	14379717	14382427	ABC transporter F member 4
VIT_18s0166g00320	18	14382428	14384232	ABC Transporter (VvGCN1 - VvABCF1)
VIT_18s0076g00380	18	14405761	14410018	ABC Transporter (VvGCN5 - VvABCF5)
VIT_18s0076g00370	18	14415354	14416016	Ribosomal protein P2 (RPP2A) acidic 60S
VIT_18s0076g00360	18	14424417	14427563	EMB1075 (embryo defective 1075) carboxy-lyase
VIT_18s0076g00350	18	14479728	14481025	F-box protein (FBX3)
VIT_18s0076g00340	18	14491505	14493905	CYP707A3
VIT_18s0076g00330	18	14494814	14503181	Basic Leucine Zipper Transcription Factor (VvbZIP50)
VIT_18s0076g00320	18	14527632	14528344	Nodulin
VIT_18s0076g00310	18	14550818	14563944	Translation initiation factor eIF-5B
VIT_18s0076g00300	18	14575052	14575648	Hexokinase-like protein
VIT_18s0076g00290	18	14619070	14619498	No hit
VIT_18s0076g00280	18	14659006	14685257	Protein tyrosine phosphatase
VIT_18s0076g00270	18	14725759	14726714	No hit
VIT_18s0076g00260	18	14726740	14745454	Unknown protein
VIT_18s0076g00250	18	14786911	14789327	Sucrose-proton symporter 2 SUC2 (SUT2-2)
VIT_18s0076g00240	18	14807850	14815102	Preprotein translocase SecY subunit
VIT_18s0076g00230	18	14827587	14833371	No hit
VIT_18s0076g00220	18	14843815	14846194	Sucrose-proton symporter 2 SUC2 (SUT2-3)
VIT_18s0076g00210	18	14868749	14920388	Alpha/beta hydrolase fold
VIT_18s0076g00200	18	14926786	14927997	DELLA protein RGL2 (RGA-like protein 2)
VIT_18s0076g00190	18	14937941	14939662	No hit

Supplementary Table 10. Definition of “molecular veraison”. Number of modulated genes ($|\log_2FC| > 2$), in red, across the time points during berry development. In black the number of days before phenological veraison.

	Days	t0		t1		t2		t3		t4		t5
2012		-36	27	-28	0	-18	127	-9	4	0	0	
2013		-20	11	-14	52	-7	26	0	0		0	
2014		-20	6	-14	38	-6	58	0	0		0	

Supplementary Table 11

Meta-QTL	Gene ID	Chr	Start (bp)	End(bp)	Annotation_V1	Transcriptomic candidates
<i>pheno_3_1</i>	VIT_03s0038g00670	3	592539	594503	fructose-bisphosphate aldolase, chloroplast precursor	<i>Palumbo et al 2014, Massonet et al 2017</i>
	VIT_03s0038g00760	3	644491	647420	Arginine decarboxylase (Fragment)	<i>Fasoli et al 2018</i>
	VIT_03s0038g00860	3	689247	693308	Basic Leucine Zipper Transcription Factor (VvbZIP05)	<i>Fasoli et al 2018</i>
	VIT_03s0038g01090	3	862995	863398	Auxin responsive SAUR protein	<i>Palumbo et al 2014, Massonet et al 2017</i>
	VIT_03s0038g01110	3	866357	866897	Auxin-responsive SAUR31	<i>Palumbo et al 2014, Massonet et al 2017</i>
	VIT_03s0038g01310	3	921733	927965	Auxin responsive SAUR protein	<i>Fasoli et al 2018</i>
	VIT_03s0038g01380	3	971266	975571	Calcium-binding EF hand	<i>Palumbo et al 2014, Massonet et al 2017, Fasoli et al 2018</i>
	VIT_03s0038g01410	3	984045	985466	Aquaporin PIP PIP1A	<i>Palumbo et al 2014, Massonet et al 2017, Fasoli et al 2018</i>
	VIT_03s0038g01510	3	1041388	1041967	Unknown protein	<i>Fasoli et al 2018</i>
	VIT_03s0038g01830	3	1283253	1285733	Proline-rich protein 4	<i>Palumbo et al 2014, Massonet et al 2017, Fasoli et al 2018</i>

	VIT_03s0038g02050	3	1412118	1412819	Dirigent protein pDIR7	<i>Palumbo et al 2014, Massonet et al 2017</i>
	VIT_03s0038g02090	3	1441262	1442535	Phospholipase C.	<i>Palumbo et al 2014, Massonet et al 2017, Fasoli et al 2018</i>
	VIT_03s0038g02110	3	1449330	1451521	Co-chaperone-curved DNA binding protein A	<i>Fasoli et al 2018</i>
	VIT_03s0038g02130	3	1468239	1469371	Cold shock protein-1	<i>Fasoli et al 2018</i>
	VIT_03s0038g02150	3	1482091	1483271	Unknown	<i>Palumbo et al 2014, Massonet et al 2017</i>
	VIT_03s0038g02170	3	1492918	1494778	Thaumatococin	<i>Palumbo et al 2014, Massonet et al 2017, Fasoli et al 2018</i>
	VIT_03s0038g02190	3	1502133	1506299	Nodulin	<i>Fasoli et al 2018</i>
	VIT_03s0038g02220	3	1528083	1528899	Cofilin	<i>Palumbo et al 2014, Massonet et al 2017</i>
	VIT_03s0038g02230	3	1535564	1538193	Subtilisin-like serine protease 2	<i>Palumbo et al 2014, Massonet et al 2017</i>
<i>pheno_3_2</i>	VIT_03s0180g00010	3	5934501	5937492	Cysteine proteinase	<i>Fasoli et al 2018</i>
	VIT_03s0180g00040	3	5973785	5975813	Cyclin D3_2	<i>Fasoli et al 2018</i>
	VIT_03s0180g00090	3	6023040	6024531	Receptor kinase	<i>Fasoli et al 2018</i>

VIT_03s0180g00200	3	6124465	6126202	Limonoind UDP-glucosyltransferase (VvGT2)	<i>Palumbo et al 2014, Massonet et al 2017, Fasoli et al 2018</i>
VIT_03s0180g00280	3	6255489	6257208	Indole-3-acetate beta-glucosyltransferase	<i>Fasoli et al 2018</i>
VIT_03s0180g00320	3	6281986	6283705	indole-3-acetate beta-glucosyltransferase (VvGT3)	<i>Palumbo et al 2014, Massonet et al 2017</i>
VIT_03s0091g00210	3	6507392	6509263	Ethylene-responsive protein	<i>Palumbo et al 2014, Massonet et al 2017</i>
VIT_03s0091g00240	3	6521904	6537905	Haloacid dehalogenase hydrolase	<i>Fasoli et al 2018</i>
VIT_03s0091g00260	3	6548677	6549577	Zinc finger protein 4	<i>Palumbo et al 2014, Massonet et al 2017, Fasoli et al 2018</i>
VIT_03s0091g00420	3	6785458	6787059	No hit	<i>Palumbo et al 2014, Massonet et al 2017, Fasoli et al 2018</i>
VIT_03s0091g00450	3	6811798	6813280	Progesterone 5-beta-reductase	<i>Palumbo et al 2014, Massonet et al 2017</i>
VIT_03s0091g00490	3	6859815	6860409	Unknown protein	<i>Palumbo et al 2014, Massonet et al 2017</i>
VIT_03s0091g00500	3	6871858	6872341	Unknown protein	<i>Palumbo et al 2014, Massonet et al 2017</i>
VIT_03s0091g00580	3	7035451	7039010	Protein Mpv17	<i>Fasoli et al 2018</i>

VIT_03s0091g00670	3	7099015	7099742	Lateral organ boundaries protein 38	<i>Palumbo et al 2014, Massonet et al 2017, Fasoli et al 2018</i>
VIT_03s0091g00680	3	7103281	7113666	NPY2 (naked pins in yuc mutants 2)	<i>Fasoli et al 2018</i>
VIT_03s0091g00870	3	7342165	7357074	Adenylylsulfate kinase 1 (AKN1)	<i>Fasoli et al 2018</i>
VIT_03s0091g01010	3	7535063	7536574	LIM domain protein WLIM1	<i>Palumbo et al 2014, Massonet et al 2017, Fasoli et al 2018</i>
VIT_03s0091g01060	3	7673917	7675754	Cyclin delta-2	<i>Fasoli et al 2018</i>
VIT_03s0091g01130	3	7741682	7743818	Meprin and TRAF homology domain-containing protein	<i>Palumbo et al 2014, Massonet et al 2017</i>
VIT_03s0091g01240	3	7903958	7907570	Serine carboxypeptidase S10 / Anthocyanin Acyl-transferase	<i>Palumbo et al 2014, Massonet et al 2017, Fasoli et al 2018</i>
VIT_03s0091g01290	3	7951175	7955690	Serine carboxypeptidase S10	<i>Palumbo et al 2014, Massonet et al 2017</i>
VIT_03s0088g00050	3	8035215	8039037	Serine carboxypeptitase 1	<i>Palumbo et al 2014, Massonet et al 2017</i>
VIT_03s0088g00290	3	8315170	8315924	Phytosulfokines PSK2	<i>Palumbo et al 2014, Massonet et al 2017</i>
VIT_03s0088g00320	3	8343365	8347681	Peptidase M50	<i>Palumbo et al 2014, Massonet et al 2017</i>

	VIT_03s0088g00710	3	8916223	8916893	Pathogenesis-related protein 1 precursor (PRP 1)	<i>Palumbo et al 2014, Massonet et al 2017</i>
	VIT_03s0088g00810	3	9044529	9045211	Pathogenesis-related protein 1 precursor (PRP 1)	<i>Palumbo et al 2014, Massonet et al 2017</i>
	VIT_03s0088g01180	3	9438885	9442060	Proline iminopeptidase	<i>Fasoli et al 2018</i>
	VIT_03s0088g01250	3	9538993	9552353	D-threo-aldose 1-dehydrogenase	<i>Palumbo et al 2014, Massonet et al 2017</i>
<i>pheno_5_1</i>	VIT_05s0029g01140	5	17405622	17411752	Sucrose-phosphate synthase	<i>Palumbo et al 2014, Massonet et al 2017, Fasoli et al 2018</i>
	VIT_05s0062g00240	5	18818659	18820264	Xyloglucan endotransglucosylase/hydrolase 23	<i>Palumbo et al 2014, Massonet et al 2017</i>
	VIT_05s0062g00250	5	18831568	18833016	Xyloglucan endotransglucosylase/hydrolase 15	<i>Palumbo et al 2014, Massonet et al 2017</i>
	VIT_05s0062g00270	5	18843664	18845204	UDP-glucose:flavonoid 7-O-glucosyltransferase	<i>Fasoli et al 2018</i>
	VIT_05s0062g00430	5	18991958	18993513	UDP-glucose:flavonoid 7-O-glucosyltransferase	<i>Palumbo et al 2014, Massonet et al 2017</i>
	VIT_05s0062g00480	5	19056125	19057777	Xyloglucan endo-transglycosylase, C-terminal	<i>Palumbo et al 2014, Massonet et al 2017, Fasoli et al 2018</i>
	VIT_05s0062g00520	5	19088785	19090792	UDP-glucose:flavonoid 7-O-glucosyltransferase	<i>Palumbo et al 2014, Massonet et al 2017</i>

	VIT_05s0062g00610	5	19193950	19195592	Xyloglucan endotransglucosylase/hydrolase 23	<i>Palumbo et al 2014, Massonet et al 2017, Fasoli et al 2018</i>
	VIT_05s0062g00630	5	19226293	19228218	UDP-glucose transferase (UGT75B2)	<i>Palumbo et al 2014, Massonet et al 2017</i>
	VIT_05s0062g00760	5	19469712	19473848	Receptor kinase RHG4	<i>Fasoli et al 2018</i>
<i>pheno_7_1</i>	VIT_07s0151g00340	7	1264579	1270254	Sulfate transporter 3.1 (AST12) (AtST1)	<i>Palumbo et al 2014, Massonet et al 2017</i>
	VIT_07s0151g00520	7	1334807	1343225	Homocysteine S-methyltransferase 3	<i>Palumbo et al 2014, Massonet et al 2017</i>
	VIT_07s0151g00800	7	1454149	1456559	Unknown	<i>Fasoli et al 2018</i>
<i>pheno_11_1</i>	VIT_11s0016g03590	11	2932300	2940485	Transducin protein	<i>Fasoli et al 2018</i>
	VIT_11s0016g03630	11	2964436	2968009	Peroxiredoxin-5	<i>Fasoli et al 2018</i>
	VIT_11s0016g03640	11	2972017	2974625	Rac-like GTP-binding protein ARAC7 (GTPase protein ROP9)	<i>Palumbo et al 2014, Massonet et al 2017</i>
	VIT_11s0016g03650	11	2976690	2979682	CDKF;1 (CDK-activating kinase 1A)	<i>Fasoli et al 2018</i>
	VIT_11s0016g03660	11	2982086	2991775	Glucose transporter 2 plastidic	<i>Fasoli et al 2018</i>
	VIT_11s0016g03760	11	3079092	3081830	Unknown protein	<i>Fasoli et al 2018</i>
	VIT_11s0016g03880	11	3163900	3169609	Receptor protein kinase PERK1	<i>Fasoli et al 2018</i>
	VIT_11s0016g03890	11	3174051	3179257	Short-chain dehydrogenase/reductase (SDR)	<i>Fasoli et al 2018</i>
	VIT_11s0016g03900	11	3182349	3186809	AAA-type ATPase	<i>Fasoli et al 2018</i>
	VIT_11s0016g03920	11	3191384	3193086	Polyol transporter 5	<i>Fasoli et al 2018</i>

	VIT_11s0016g03940	11	3224068	3225265	Heat shock transcription factor C1	<i>Palumbo et al 2014, Massonet et al 2017</i>
	VIT_11s0016g03980	11	3249496	3250787	Unknown protein	<i>Fasoli et al 2018</i>
<i>pheno_12_1</i>	VIT_12s0035g02080	12	23970815	23972655	Unknown protein	<i>Fasoli et al 2018</i>
	VIT_12s0035g02090	12	23983677	23999372	Leucine-rich repeat family protein	<i>Fasoli et al 2018</i>
	VIT_12s0035g02120	12	24046092	24050103	Unknown	<i>Fasoli et al 2018</i>
	VIT_12s0035g02150	12	24097742	24106206	ferric reduction oxidase 7 FRO7	<i>Palumbo et al 2014, Massonet et al 2017, Fasoli et al 2018</i>
<i>pheno_14_1</i>	VIT_14s0083g00580	14	22620849	22623743	S-adenosyl-L-methionine decarboxylase	<i>Fasoli et al 2018</i>
	VIT_14s0083g00620	14	22672469	22675655	NIK1 (NSP- interacting kinase 1)	<i>Palumbo et al 2014, Massonet et al 2017</i>
	VIT_14s0083g00640	14	22696160	22698346	Constans 2 (COL2)	<i>Palumbo et al 2014, Massonet et al 2017</i>
	VIT_14s0083g00910	14	23106621	23115040	Auxin-independent growth promoter	<i>Fasoli et al 2018</i>
	VIT_14s0083g00940	14	23137130	23143930	Auxin-independent growth promoter	<i>Palumbo et al 2014, Massonet et al 2017, Fasoli et al 2018</i>
	VIT_14s0083g01030	14	23320331	23341036	putative MADS-box Fruitfull 2 (VviFUL2)	<i>Palumbo et al 2014, Massonet et al 2017, Fasoli et al 2018</i>

VIT_14s0083g01100	14	23425741	23428785	Alpha-1,4-glucan-protein synthase 1	<i>Palumbo et al 2014, Massonet et al 2017</i>
VIT_14s0083g01110	14	23435436	23438457	Brassinosteroid-6-oxidase	<i>Palumbo et al 2014, Massonet et al 2017</i>
VIT_14s0083g01140	14	23478460	23480345	B12D	<i>Palumbo et al 2014, Massonet et al 2017</i>
VIT_14s0083g01160	14	23527926	23532692	COBRA protein	<i>Fasoli et al 2018</i>
VIT_14s0083g01170	14	23552658	23569757	Mitochondrial substrate carrier family protein	<i>Fasoli et al 2018</i>
VIT_14s0083g01210	14	23631468	23634185	feronia receptor-like kinase	<i>Palumbo et al 2014, Massonet et al 2017</i>
VIT_14s0083g01220	14	23647671	23648618	feronia receptor-like kinase	<i>Palumbo et al 2014, Massonet et al 2017</i>
VIT_14s0068g00010	14	23691896	23694505	feronia receptor-like kinase	<i>Palumbo et al 2014, Massonet et al 2017</i>
VIT_14s0068g00030	14	23710282	23713253	feronia receptor-like kinase	<i>Palumbo et al 2014, Massonet et al 2017</i>
VIT_14s0068g00040	14	23730955	23731566	No hit	<i>Palumbo et al 2014, Massonet et al 2017</i>
VIT_14s0068g00050	14	23741203	23741804	No hit	<i>Palumbo et al 2014, Massonet et al 2017</i>

	VIT_14s0068g00140	14	23848301	23848892	No hit	<i>Palumbo et al 2014, Massonet et al 2017</i>
	VIT_14s0068g00160	14	23866963	23867506	No hit	<i>Palumbo et al 2014, Massonet et al 2017, Fasoli et al 2018</i>
	VIT_14s0068g00250	14	23967557	23970244	Exocyst subunit EXO70 E1	<i>Fasoli et al 2018</i>
	VIT_14s0068g00300	14	23997514	24000870	ABRC5	<i>Fasoli et al 2018</i>
	VIT_14s0068g00330	14	24046880	24048369	PTF1 (plastid transcription factor 1) TCP13	<i>Palumbo et al 2014, Massonet et al 2017</i>
	VIT_14s0068g00400	14	24127197	24145861	Hydrolase, alpha/beta fold family	<i>Fasoli et al 2018</i>
	VIT_14s0068g00510	14	24246986	24247718	Unknown	<i>Fasoli et al 2018</i>
	VIT_14s0068g00520	14	24253217	24259740	F-box domain containing protein	<i>Fasoli et al 2018</i>
	VIT_14s0068g00640	14	24438706	24450994	Acetyl-CoA synthetase	<i>Fasoli et al 2018</i>
	VIT_14s0068g00830	14	24606690	24609786	2,3,4,5-tetrahydropyridine-2,6-dicarboxylate N-succinyltransferase	<i>Fasoli et al 2018</i>
<i>pheno_16_1</i>	VIT_16s0022g00960	16	14028716	14029381	Invertase/pectin methylesterase inhibitor	<i>Palumbo et al 2014, Massonet et al 2017, Fasoli et al 2018</i>
	VIT_16s0022g01430	16	14922690	14923901	Phosphate-induced protein 1	<i>Palumbo et al 2014, Massonet et al 2017</i>
	VIT_16s0022g01440	16	14962050	14966011	Transketolase, chloroplast precursor	<i>Fasoli et al 2018</i>
	VIT_16s0022g01650	16	15243820	15246842	Receptor serine/threonine kinase PR5K	<i>Fasoli et al 2018</i>

	VIT_16s0022g01770	16	15467138	15473529	Phosphopyruvate hydratase.	<i>Palumbo et al 2014, Massonet et al 2017, Fasoli et al 2018</i>
	VIT_16s0022g01870	16	15736355	15738229	Unknown protein	<i>Fasoli et al 2018</i>
	VIT_16s0022g02080	16	16041486	16043235	Exostosin family protein	<i>Fasoli et al 2018</i>
	VIT_16s0022g02100	16	16060136	16061359	Embryo-specific 3	<i>Fasoli et al 2018</i>
	VIT_16s0022g02200	16	16203664	16206181	Subtilase	<i>Palumbo et al 2014, Massonet et al 2017</i>
	VIT_16s0022g02230	16	16240572	16248680	Leucine-rich repeat receptor protein kinase EXS	<i>Fasoli et al 2018</i>
	VIT_16s0022g02340	16	16470141	16475595	fructokinase-2	<i>Fasoli et al 2018</i>
pheno_16_2	VIT_16s0100g00220	16	17132026	17132339	No hit	<i>Fasoli et al 2018</i>
	VIT_16s0100g00270	16	17150479	17150928	Peptidoglycan-binding LysM domain-containing protein	<i>Palumbo et al 2014, Massonet et al 2017</i>
	VIT_16s0100g00290	16	17162424	17180217	L-idonate dehydrogenase	<i>Palumbo et al 2014, Massonet et al 2017</i>
	VIT_16s0100g00350	16	17248816	17261155	ABC Transporter (VvTAP3 - VvABCB23)	<i>Fasoli et al 2018</i>
pheno_17_1	VIT_17s0000g04750	17	5279676	5281368	UDP-glycosyltransferase 89B2	<i>Fasoli et al 2018</i>
	VIT_17s0000g04840	17	5357937	5362286	Sterile alpha motif (SAM) domain-containing	<i>Palumbo et al 2014, Massonet et al 2017</i>
	VIT_17s0000g04890	17	5409996	5423899	D-aminoacyl-tRNA deacylase GEKO1	<i>Fasoli et al 2018</i>
	VIT_17s0000g05020	17	5637669	5644801	Squamosa promoter-binding protein 6 (SPL6)	<i>Palumbo et al 2014, Massonet et al 2017</i>

VIT_17s0000g05030	17	5645732	5648492	Alpha-1,4-glucan-protein synthase 1	<i>Fasoli et al 2018</i>
VIT_17s0000g05040	17	5654593	5656105	No hit	<i>Fasoli et al 2018</i>
VIT_17s0000g05050	17	5659282	5660704	COBRA-like protein 4	<i>Fasoli et al 2018</i>
VIT_17s0000g05070	17	5676169	5679862	Phytochelatase	<i>Palumbo et al 2014, Massonet et al 2017, Fasoli et al 2018</i>
VIT_17s0000g05110	17	5731853	5734268	CYP78A4	<i>Palumbo et al 2014, Massonet et al 2017</i>
VIT_17s0000g05240	17	5869290	5885095	Nuclear transport factor 2 (NTF2)	<i>Fasoli et al 2018</i>
VIT_17s0000g05250	17	5885327	5886300	Unknown protein	<i>Palumbo et al 2014, Massonet et al 2017</i>
VIT_17s0000g05460	17	6088077	6090457	Nodulin	<i>Palumbo et al 2014, Massonet et al 2017</i>
VIT_17s0000g05550	17	6183508	6195130	Proton-dependent oligopeptide transport (POT) family protein	<i>Palumbo et al 2014, Massonet et al 2017</i>
VIT_17s0000g05580	17	6213229	6221132	Isopiperitenol dehydrogenase	<i>Palumbo et al 2014, Massonet et al 2017, Fasoli et al 2018</i>
VIT_17s0000g05600	17	6255629	6256773	(-)-isopiperitenol dehydrogenase	<i>Fasoli et al 2018</i>
VIT_17s0000g05610	17	6257443	6258438	Isopiperitenol dehydrogenase	<i>Fasoli et al 2018</i>

	VIT_17s0000g05650	17	6279745	6280799	Unknown protein	<i>Palumbo et al 2014, Massonet et al 2017, Fasoli et al 2018</i>
<i>pheno_17_2</i>	VIT_17s0000g07920	17	9030527	9032996	Hypoxia-responsive	<i>Fasoli et al 2018</i>
<i>pheno_18_1</i>	VIT_18s0001g02000	18	2438485	2442668	Zinc finger (C2H2 type) family	<i>Palumbo et al 2014, Massonet et al 2017, Fasoli et al 2018</i>
	VIT_18s0001g02010	18	2442718	2443387	No hit	<i>Palumbo et al 2014, Massonet et al 2017, Fasoli et al 2018</i>
	VIT_18s0001g02540	18	2802829	2805078	ARR9 typeA	<i>Palumbo et al 2014, Massonet et al 2017</i>
	VIT_18s0001g02550	18	2813209	2821688	Delta-aminolevulinic acid dehydratase, chloroplast precursor	<i>Fasoli et al 2018</i>
	VIT_18s0001g02690	18	2881165	2881615	Unknown protein	<i>Fasoli et al 2018</i>
	VIT_18s0001g02770	18	2914955	2920663	Alpha-L-fucosidase 2 precursor	<i>Palumbo et al 2014, Massonet et al 2017</i>
	VIT_18s0001g02790	18	2925094	2926968	Unknown protein	<i>Palumbo et al 2014, Massonet et al 2017, Fasoli et al 2018</i>
	VIT_18s0001g02810	18	2929082	2940502	Acyl-CoA synthetase long-chain member 9	<i>Fasoli et al 2018</i>
	VIT_18s0001g03200	18	3198754	3201304	Emp24/gp25L/p24	<i>Fasoli et al 2018</i>
	VIT_18s0001g03230	18	3208995	3214247	Aminoacylase/ metalloproteinase	<i>Fasoli et al 2018</i>
	VIT_18s0001g03580	18	3389546	3393993	Ubiquitin-fold modifier 1 precursor	<i>Fasoli et al 2018</i>

VIT_18s0001g03610	18	3401893	3411144	Auxin-independent growth promoter	<i>Palumbo et al 2014, Massonet et al 2017</i>
VIT_18s0001g03670	18	3422279	3424214	Zinc finger (C2H2 type) family	<i>Palumbo et al 2014, Massonet et al 2017</i>
VIT_18s0001g03880	18	3565751	3567556	Polcalcain	<i>Fasoli et al 2018</i>
VIT_18s0001g04150	18	3732776	3738425	Avr9 elicitor response protein	<i>Fasoli et al 2018</i>
VIT_18s0001g04340	18	3822948	3829597	Glycine hydroxymethyltransferase	<i>Fasoli et al 2018</i>
VIT_18s0001g04680	18	3938582	3956444	RPG related protein 1 RR1	<i>Palumbo et al 2014, Massonet et al 2017</i>
VIT_18s0001g04790	18	3994178	4000375	Aspartic Protease (VvAP42)	<i>Palumbo et al 2014, Massonet et al 2017</i>
VIT_18s0001g04920	18	4068936	4069711	No hit	<i>Palumbo et al 2014, Massonet et al 2017</i>
VIT_18s0001g04930	18	4070013	4071952	Sulfate transporter 1.3	<i>Palumbo et al 2014, Massonet et al 2017</i>
VIT_18s0001g05020	18	4122072	4123281	Senescence-associated protein	<i>Palumbo et al 2014, Massonet et al 2017</i>
VIT_18s0001g05040	18	4138118	4140727	Pollen Ole e 1 allergen and extensin	<i>Palumbo et al 2014, Massonet et al 2017</i>
VIT_18s0001g05180	18	4185500	4189977	Beta-D-xylosidase	<i>Palumbo et al 2014, Massonet et al 2017, Fasoli et al 2018</i>

VIT_18s0001g05220	18	4205002	4212978	WD-40 repeat	<i>Fasoli et al 2018</i>
VIT_18s0001g05300	18	4254678	4257480	Trehalose-6-phosphate phosphatase	<i>Fasoli et al 2018</i>
VIT_18s0001g05570	18	4363673	4368991	Hexose transporter HT2	<i>Fasoli et al 2018</i>
VIT_18s0001g05910	18	4550436	4552401	Cis-zeatin O-beta-D-glucosyltransferase	<i>Palumbo et al 2014, Massonet et al 2017</i>
VIT_18s0001g05990	18	4574889	4586041	UDP-glycosyltransferase 85A1	<i>Palumbo et al 2014, Massonet et al 2017</i>
VIT_18s0001g06060	18	4605365	4607009	UDP-glycosyltransferase 85A1	<i>Palumbo et al 2014, Massonet et al 2017, Fasoli et al 2018</i>
VIT_18s0001g06180	18	4659693	4663192	Phosphate-induced protein 1	<i>Palumbo et al 2014, Massonet et al 2017</i>
VIT_18s0001g06220	18	4684266	4686537	F-box protein (FBW2)	<i>Palumbo et al 2014, Massonet et al 2017</i>
VIT_18s0001g06370	18	4765814	4772318	L-ascorbate peroxidase, chloroplast	<i>Palumbo et al 2014, Massonet et al 2017</i>
VIT_18s0001g06430	18	4806981	4808947	Homeobox-leucine zipper protein ATHB-6	<i>Palumbo et al 2014, Massonet et al 2017, Fasoli et al 2018</i>
VIT_18s0001g06580	18	4966021	4966915	Plastocyanin domain-containing protein	<i>Palumbo et al 2014, Massonet et al 2017</i>

	VIT_18s0001g06690	18	5029717	5032277	Gibberellin 20 oxidase 2	<i>Palumbo et al 2014, Massonet et al 2017</i>
	VIT_18s0001g06820	18	5077418	5081480	MATE efflux family protein ripening responsive	<i>Fasoli et al 2018</i>
	VIT_18s0001g07090	18	5290562	5293561	Unknown protein	<i>Fasoli et al 2018</i>
pheno_18_2	VIT_18s0001g12830	18	10937041	10940329	1,4-beta-mannan endohydrolase	<i>Palumbo et al 2014, Massonet et al 2017, Fasoli et al 2018</i>
	VIT_18s0001g12840	18	10940330	10945165	ADP-glucose pyrophosphorylase large subunit CagpL2	<i>Fasoli et al 2018</i>
	VIT_18s0001g12960	18	11043696	11049454	Wound-responsive protein	<i>Fasoli et al 2018</i>
	VIT_18s0001g12990	18	11099778	11102242	Anthranilate N-benzoyltransferase protein 1	<i>Fasoli et al 2018</i>
	VIT_18s0001g13010	18	11126023	11129236	Mitogen-activated Protein Kinase (VvMPK11)	<i>Fasoli et al 2018</i>
	VIT_18s0001g13200	18	11256653	11261569	Cytokinin dehydrogenase 5 precursor	<i>Palumbo et al 2014, Massonet et al 2017</i>
	VIT_18s0001g13230	18	11286706	11293739	Beta-galactosidase BG1 [<i>Vitis vinifera</i>]	<i>Palumbo et al 2014, Massonet et al 2017</i>
	VIT_18s0001g13360	18	11384285	11387145	Nodulin MtN21 family	<i>Palumbo et al 2014, Massonet et al 2017</i>
	VIT_18s0001g13610	18	11613829	11620092	Abhydrolase domain-containing protein 5	<i>Fasoli et al 2018</i>
	VIT_18s0001g13770	18	11767560	11769317	Cytochrome P450, family 83, subfamily B, polypeptide 1	<i>Fasoli et al 2018</i>
	VIT_18s0001g13780	18	11774368	11775896	Cytochrome P450, family 83, subfamily B, polypeptide 1	<i>Fasoli et al 2018</i>
	VIT_18s0001g13790	18	11779263	11781156	Cytochrome P450, family 83, subfamily B, polypeptide 1	<i>Fasoli et al 2018</i>

VIT_18s0001g13970	18	11974983	11980862	Myosin-related	<i>Palumbo et al 2014, Massonet et al 2017, Fasoli et al 2018</i>
VIT_18s0001g14040	18	12086327	12090970	Endo-1,4-beta-glucanase	<i>Palumbo et al 2014, Massonet et al 2017</i>
VIT_18s0001g14130	18	12179540	12181647	Zinc finger (C2H2 type) family	<i>Palumbo et al 2014, Massonet et al 2017</i>
VIT_18s0001g14260	18	12273788	12276090	No hit	<i>Palumbo et al 2014, Massonet et al 2017, Fasoli et al 2018</i>
VIT_18s0001g14270	18	12276091	12276597	Gibberellin-regulated protein 1 (GASA1)	<i>Palumbo et al 2014, Massonet et al 2017, Fasoli et al 2018</i>
VIT_18s0001g14360	18	12337145	12340985	Tubulin beta-1 chain	<i>Palumbo et al 2014, Massonet et al 2017</i>
VIT_18s0001g14440	18	12432955	12439459	Molecular chaperone DnaJ	<i>Palumbo et al 2014, Massonet et al 2017</i>
VIT_18s0001g14450	18	12453766	12456583	Ferredoxin:nadp+ Oxidoreductase PETH	<i>Palumbo et al 2014, Massonet et al 2017</i>
VIT_18s0001g14640	18	12698089	12699502	No hit	<i>Fasoli et al 2018</i>
VIT_18s0001g14780	18	12841218	12848820	Lipase 3 (EXL3) family II extracellular	<i>Fasoli et al 2018</i>

VIT_18s0001g14980	18	12992480	12996562	3-methyl-2-oxobutanoate dehydrogenase	<i>Palumbo et al 2014, Massonet et al 2017</i>
VIT_18s0001g15000	18	13026931	13036065	ACT domain containing protein (ACR4)	<i>Palumbo et al 2014, Massonet et al 2017, Fasoli et al 2018</i>
VIT_18s0001g15120	18	13199060	13200303	Unknown protein	<i>Palumbo et al 2014, Massonet et al 2017, Fasoli et al 2018</i>
VIT_18s0001g15360	18	13495083	13497819	Thylakoid lumenal 29.8 kDa protein	<i>Fasoli et al 2018</i>
VIT_18s0001g15390	18	13521135	13522636	Gaiacol peroxidase	<i>Fasoli et al 2018</i>
VIT_18s0001g15410	18	13539135	13541625	Alcohol dehydrogenase 1	<i>Palumbo et al 2014, Massonet et al 2017, Fasoli et al 2018</i>
VIT_18s0001g15460	18	13616618	13618309	Stearyl acyl carrier protein desaturase	<i>Palumbo et al 2014, Massonet et al 2017</i>
VIT_18s0001g15520	18	13650247	13655312	Leaf senescence protein	<i>Palumbo et al 2014, Massonet et al 2017, Fasoli et al 2018</i>
VIT_18s0001g15720	18	13856940	13861020	Leucine Rich Repeat receptor-like kinase	<i>Palumbo et al 2014, Massonet et al 2017, Fasoli et al 2018</i>
VIT_18s0001g15730	18	13865318	13866466	Dof zinc finger protein DOF3.5	<i>Fasoli et al 2018</i>
VIT_18s0166g00250	18	14230226	14231594	No hit	<i>Fasoli et al 2018</i>

VIT_18s0076g00330	18	14494814	14503181	Basic Leucine Zipper Transcription Factor (VvbZIP50)	<i>Fasoli et al 2018</i>
VIT_18s0076g00310	18	14550818	14563944	Translation initiation factor eIF-5B	<i>Fasoli et al 2018</i>
VIT_18s0076g00250	18	14786911	14789327	Sucrose-proton symporter 2 SUC2 (SUT2-2)	<i>Palumbo et al 2014, Massonet et al 2017</i>
VIT_18s0076g00210	18	14868749	14920388	Alpha/beta hydrolase fold	<i>Palumbo et al 2014, Massonet et al 2017</i>

Supplementary Table 12

NAME	COD E	NAME	COD E	NAME	COD E	NAME	COD E
ABBOTTABOTTI	943	BERLA_GROSA	1069	CAPIBIANCHI	1159	CORNIOLA	1103
ABBUOTO	1	BERTINORA	1030	CAPOBIANCO_BIANCO	507	CORSO_BIANCO	1046
ABELLO	677	BERZAMINO	692	CAPOBIANCO_NERO	508	CORVINA	82
ABRUSCO	2	BIANCHETTA_DI_BACEDASC O	693	CAPOLONGO_1	1045	CORVINA_ASOLO	624
AGHEDENE	678	BIANCHETTA_DI_DIOLO	694	CAPOLUNGO	509	CORVINONE	83
AGLIANICO	3	BIANCHETTA_TREVIGIANA	32	CAPRETTA	510	COVE	84
AGLIANICO_GRANA_GROSSA	944	BIANCO_DALESSANO	33	CAPRUGNONE	1160	CREPALLOCCHI	722
AHMEUR_MONARDE	1146	BIANCOLELLA	34	CARDINAL	433	CROATINA	85
AIREN	676	BIANCONE	37	CARICAGIOLA	66	CROVASSA	86
ALBANA	6	BIANCONE_DELLANTELLA	1034	CARIGNANO	67	CUNEUTE	723
ALBANA_BORDINI	1061	BIANCUZZO	695	CARMENERE	50	DALL	724
ALBANA_DEL_PANIERE	679	BICANE	424	CARRICANTE	68	DAMASCHINO	87
ALBANELLO	7	BIGOLONA	696	CASAVECCHIA	366	DAMIANO	726
ALBARANZEULI_BIANCO	10	BLANC_DE_MORGEX	35	CASENTINO	1161	DANUTA	484

ALBAROLA	30	BOGGIONE_NERO	1151	CASSETTA	362	DATTIER_DE_BEYROUTH	431
ALBAROSSA	8	BOGGIONE_ROSSO	698	CATALANESCA_BIANCA	425	DELIGHT	493
ALEANTE_RIVALTO	690	BOMBINO_BIANCO	38	CATARRATTO_BIANCO_COMUNE	70	DIAMANT	1113
ALEATICO	11	BOMBINO_NERO	39	CATARRATTONE	1093	DIMIAT	1105
ALICANTE_BOUSCHET	12	BONAMICO	48	CAVECIA	710	DINDARELLA	88
ALIONZA	16	BONARDA	40	CAVRARA_NERA	1068	DIOLINOIR	89
ALPHONSE_LAVALLEE	430	BONDA	41	CENERENTE	512	DOLCIAME	91
AMERICA	984	BORBOTTONE	700	CENTESIMINO	299	DON_MARIANO	435
ANCELOTTA	17	BOSCHERA	42	CERASOLO	712	DOUX_DHENRY	92
ANSONICA	18	BOSCO	43	CESANESE_DEI_CASTELLI_ROMA NI	513	DURAPECCIO_DI_SLORENZO	729
ANTINELLO	979	BOVALE	45	CHARDONNAY	244	DURELLA	93
APIRENA_BRUNI	495	BRACCIOLA_NERA	46	CHASSELAS_BLANC	426	EARLY_MUSCAT	479
APRILLA	946	BRACHETTO	47	CHENIN	298	EMERALD_RIESLING	667
ARAMONE	703	BRAMBANA	701	CIAVARELLA_FRANCESE	514	EMPEROR	1107
ARGUMANNU	684	BRESSANA	502	CICCHIOLA	986	ERBALUCE	94
ARIS	641	BRUGNOLA	503	CICINESE_GROSSO	715	ERBISEDDA	521
ARNEIS	19	BRUGNOLINO	1037	CILIEGIOLO	74	ERVI	95
ARSILICO	685	BUBBIA	702	CIMINNITA	429	FALANGHINA	96
ARVESINIADU	20	BURGHESANA	1067	CLAIRETTE	75	FERTILIA	97
AURORA_2	1116	BUSSANELLO	49	CLARETTE	1071	FIANO_ROSA_LOCOROTONDO_2	1013
AVANA	22	CABERNET_FRANC	51	CLOTILDE_PROSPERI	449	FLAVIS	99
AVARENGO	23	CABERNET_SAUVIGNON	52	COCCIATOSTA	716	FOGARINA	731
AXINA_DE_FRANCIA	687	CACCIADEBITI	705	COCOCCIOLA	76	FOGLIA_TONDA	100
AXINA_DE_TRES_BIAS	688	CACCIO_DI_FERMO_1	951	CODA_DI_VOLPE_BIANCA	77	FOGLIONA	1076
BACCHUS	642	CADDIU	57	CODELUNGHE	717	FORASTERA	101
BARBERA	24	CAGNULARI	58	COLOMBANA_NERA	78	FORCELLA	1042

BARBERA_BIANCA	25	CALABRESE	59	COLORINO_FORTE	1167	FORCESE_DASCOLI	1043
BARBERA_SELVATICO	1150	CALAMARO	708	COPETA	985	FORGIARIN	102
BARESANA	422	CALORIA	60	CORBINELLA_PADOVANA	518	FORSELLINA	103
BARSAGLINA	27	CANAIOLO_NERO	62	CORBINONA_13_GT	1074	FORTANA	104
BECUET	290	CANINA_1_1	1157	CORINTO_BIANCO	477	FOSCA	732
BEGUGNOL	689	CANINA_NERA	64	CORINTO_NERO	488	FRACIDELLA	733
BELLINO	432	CANNAMELE	709	CORNACCHIA	1170	FRANCONIA	106
BELLISE	1029	CANNER_SEEDLESS	483	CORNALLIN	79	FRAPPATO	107
BELLONE	28	CAPENA	506	CORNAREA	80	FREISA	108
NAME	COD E	NAME	COD E	NAME	COD E	NAME	COD E
FRENCH_COLOMBARD	1025	INCTERZI_N1	134	MALVASIA_DI_CANDIA_AROMATICA	160	MOSCATO_DADDA	443
FUBIANO	109	INVERNENGA	135	MALVASIA_DI_CASORZO	161	MOSCATO_DAMBURGO	444
FULIGNO	738	INVERNESCA	455	MALVASIA_DI_SCHIERANO	164	MOSCATO_DI_SCANZO	185
FUMIN	110	INZOLIA_IMPERIALE	471	MALVASIA_FINA	666	MOSCATO_DI_SPAGNA	1183
FURMINT	647	INZOLIA_PARCHITANA	1110	MALVASIA_FURMHANN	547	MOSCATO_DI_TERRACINA	460
GABBA_VOLPE	525	ITALIA	473	MALVASIA_ISTRIANA	165	MOSCATO_GIALLO	186
GAGLIOPPO	111	ITALICA	136	MALVASIA_NERA_DI_BRINDISI_1	166	MOSCATO_NERO	559
GALLICO	966	JULY_MUSCAT	472	MALVASIA_NERA_LUNGA	368	MOSCATO_NERO_D'_ACQUI	187
GAMARET	112	JUVARELLO	542	MAMMOLETTA	1178	MOSCATO_ROSA_2	188
GAMAY	243	KADARKA	674	MAMMOLO	169	MOSCATO_VIOLETTO	557
GAMBUGLIANA	739	KALILI	486	MANTONICO_BIANCO	978	MULLER_THURGAU	197
GARANOIR	115	KERNER	137	MANTONICONE	977	MUSCAT_OTTONEL	637
GAROFANA	747	KINGS_RUBY	481	MANZONI_BIANCO	170	NASCETTA	367
GATTA	740	LACRIMA	138	MANZONI_MOSCATO	292	NASCO	198
GERUSALEMME	1094	LACRIMA_DI_MARIA	456	MANZONI_ROSA	293	NEBBIERA	199

GIRO	114	LAGREIN	139	MARCHIONE_2	987	NEBBIOLO	200
GIUSTOLISI	742	LAMBRUSCA_DI_ALESSANDRIA	140	MARCONI	545	NEGRETTO	202
GOLDRIESLING	651	LAMBRUSCO_A_FOGLIA_FRAST	141	MARSANNE	171	NEGRETTO_DI_SALUZZO	778
GOLDTRAMINER	365	LAMBRUSCO_DI_SORBARA	142	MARSIGLIANA_NERA_1	440	NEGRO_AMARO	204
GORGOTTESCO	1176	LAMBRUSCO_GRASPAROSSA	143	MARUGA	758	NER_DALA	209
GOSEN	364	LAMBRUSCO_MAESTRI	144	MARUGGIO_1	548	NERA_GROSSA	569
GRAPPI_DE_LA_BORDOGNE	629	LAMBRUSCO_MARANI	145	MARZEMINA_2	1052	NERELLO_MASCALESE	205
GRAY_RIESLING	668	LAMBRUSCO_MONTERICCO	146	MARZEMINO	174	NERETTA_CUNESE	206
GRECHETTO_DI_TODI	1048	LAMBRUSCO_OLIVA	149	MATILDE	421	NERETTO_DI_BAIRO	207
GRECO_DI_TUFO	120	LAMBRUSCO_SALAMINO	147	MATURANO	549	NERO_DI_VASCA	572
GRECO_NERO_1	122	LAMBRUSCO_VIADANESE	148	MAYOLET	175	NERONA	1181
GRENACHE_NOIR	654	LATTUARIO_NERO	437	MAZZESE	176	NEYRET	210
GRIGNOLINO	123	LICRONAXIU	1051	MEDRULINU	770	NIBIO	779
GRILLO	124	LINNEO_NERO	439	MELARA_1	177	NIEDDERA	211
GRILLONE	746	LIVORNESE_BIANCA	289	MERERA	769	NIEDDU_MANNU_1	212
GROPPELLA	1078	LUGLIOLA_ROSSA	753	MERLOT	54	NIGRA	213
GROPPELLO_DI_MOCASINA	125	LUGLIOLA_ROSSA	753	MICHELE_PALIERI	441	NOCCHIANELLO_DI_GAZZARETTO_1	780
GROPPELLO_DI_REVO	291	LUMASSINA	150	MINNELLA_BIANCA_2	178	NOCCHIANELLO_NERO	781
GROPPELLO_GENTILE	127	LUPECCIO_(pisa)	634	MOLINARA	179	NOCCHIANELLO_PELOSO	782
GROS_BOUSCHET	530	MACERATINO	151	MOLINELLI	768	NOCERA	214
GROSPARIOL	745	MADALONA	754	MONDEUSE	1014	NOCERONE_DI_MILAZZO_1	445
GROSSOLANO	751	MADDALENA_BRUNI	457	MONICA	180	NOSIOLA	215
GUARDAVALLE	128	MAGLIOCCO_CANINO_2	152	MONICA_BIANCA	553	NOTARDOMENICO_2	216
HARSLEVELU	636	MAGLIOCCO_DOLCE	970	MONTE_MADONNA_1_GT	772	NURAGUS	217
IMPIGNO	130	MAIOLICA_2	153	MONTEPULCIANO	181	OLIVELLA_NERA_2	1095

INC_BRUNI_185	535	MALBECH	53	MONTONICO_BIANCO	182	OLIVETTA_BIANCA	1111
INC_MALVASIA_X_TREBBIANO_TOSCANO	537	MALBO_GENTILE	154	MONTONICO_NERO	998	OLIVETTA_VIBONESE	1109
INC_MANZONI_2_14	538	MALIGIA_1	544	MONTONICO_PINTO	1009	ORA	485
INCBIANCO_FEDIT_51_C_S_G	131	MALVASIA	155	MONTU	194	ORSINA	574
INCBRUNI_54	132	MALVASIA_BIANCA_2	156	MONUKKA	1097	ORTRUGO	219
INCMANZONI_2_15	133	MALVASIA_BIANCA_DI_CANDIA	157	MORELLINO	774	OSELETA	220
INCMATHIASZ_210	423	MALVASIA_BIANCA_LUNGA	158	MOSCATO	1081	OSERIE_DU_FARODE	786
INCOGNITA	541	MALVASIA_DEL_LAZIO	159	MOSCATO_BCASALESE	565	OTTAVIANELLO	221
INCIROVANO_105_VOLTA	1090	MALVASIA DELLE_LIPARI	162	MOSCATO_BIANCO	184	PALLAGRELLO_BIANCO	189
NAME	COD E	NAME	COD E	NAME	COD E	NAME	COD E
PALLAGRELLO_NERO	190	PRECOCISSIMA_MALIANI	807	SANTA_MARIA	283	TINTILIA	191
PALOMBA	787	PRIE_ROUGE	252	SANTO_STEFANO_BIANCO	1193	TINTORIA_2	833
PALOMINO	1024	PRIMITIVO	253	SAUVIGNON	300	TOCAI_FRIULANO	301
PAMPANARO_GRANDE	1060	PRIMITIVO_31_Pr	1012	SAUVIGNON_GROS	829	TORBATO	318
PANFINONE	788	PRODEST	254	SAUVIGNON_VERT	672	TRAMINER_AROMATICO	319
PANSE_BLANCHE	462	PROSECCO	255	SCACCIADEBITI	706	TREBBIANO_ABRUZZESE_(biotipo_Sbagarina)	320
PANSE_PRECOCE	463	PROSECCO_LUNGO	256	SCACCO	830	TREBBIANO_ABRUZZESE_(biotipo_Svagarina)	321
PANSE_ROSA_DIMALAGA	1102	PRUNESTA	258	SCHIAVA	284	TREBBIANO_GIALLO	322
PASCALE	223	PRUNESTA_BIANCA	1112	SCHIAVA_GENTILE	285	TREBBIANO_MODENESE	323
PASSAU	224	PRUNESTA_ROSSO_VIOLACEA	475	SCHIAVA_GRIGIA	286	TREBBIANO_ROMAGNOLO	324
PATTARESCO	783	QUAGLIANO	259	SCHIAVA_GROSSA	287	TREBBIANO_SPOLETINO	325
PAVANA	226	QUEEN	451	SCHIAVOTTO	594	TREBBIANO_TOSCANO	326
PECHINO	789	RABOSO_PIAVE	580	SCHIOCCOLETTO	1194	TREVISANA_NERA	328
PECORELLO	227	RABOSO_VERONESE	260	SCHIOPPETTINO	302	TROISCINA	1020
PECORINO	228	RAGUSANO	982	SCIAGLIN	303	TUCCANESE	992

PEDEVENDA	229	RAMONDA	1190	SCIASCINOSO	304	TURCA	329
PEDICELLO_ROSSO	575	REBO	261	SCIASCINOSO	304	UCELUT	330
PEDRO_XIMENES	1027	RECANTINA	590	SCIMISCIATA_1	295	ULIVELLO	1084
PELAVERGA	230	RED_GLOBE_1	480	SCONOSCIUTA_MARTINETTI	1126	UNKNOWN	823
PELAVERGA_PICCOLO	231	RED_OHANEZ	1115	SELEZIONE_BRUNI_54	596	UNKNOWN	534
PELAVERGA_S_GRATO	577	REFOSCO_DAL_PEDROSSO	262	SEMIDANO	305	UNKNOWN	183
PENSICATO	792	REFOSCO_DI_RAUSCEDO	1015	SEMILLON	306	UVA_ACETO	839
PERERA	232	REFOSCO_NOSTRANO	263	SENNEN	363	UVA_CARNE	841
PERGOLESE_DI_TIVOLI	447	REGINA_DEI_VIGNETI	468	SGAVETTA	307	UVA_CARRIERI	842
PERLA_DI_CSABA	464	RETAGLIADO_BIANCO	264	SGIUSEPPE_BIANCO	591	UVA_DEI_VECCHI	844
PERLETTE	494	RIBOLLA_GIALLA	265	SGIUSEPPE_NERO	277	UVA_DI_COLOGNE	845
PERLONA	436	RIESLING	266	SILA	962	UVA_DI_CRIMEA	846
PERRICONE	233	RIESLING_BLAU	675	SIRIO	308	UVA_DI_MORNICO	837
PETIT_ROUGE	234	RIESLING_ITALICO	267	SLORENZO	593	UVA_DI_TROIA	332
PETIT_VERDOT	55	RIMINESE	810	SLUNARDO	278	UVA_GATTA	849
PETITE_ARVINE	235	ROIETTO_GRISO	815	SMARTINO	279	UVA_LONGANESI	331
PICCOLA_NERA	236	RONDINELLA	269	SMICHELE	280	UVA_MELONA	459
PICOLIT	237	ROSA_TARDIVA	816	SOMARELLO_ROSSO	598	UVA_POLCE	1139
PICULIT_NERI	238	ROSETTA	1191	SOPERGA	309	UVA_PRUGNA	868
PIEDIROSSO	239	ROSSA_DI_BITONTO	452	SPAGNA_BIANCA	836	UVA_RARA	333
PIGNOLA	240	ROSSESE	271	SULTANA	1099	UVA_REALE	613
PIGNOLO	241	ROSSESE_BIANCO	294	SULTANINA_BIANCA	1098	UVA_TOSCA	334
PINELLA	242	ROSSIGNOLA	272	SURBANO	820	UVALINO	361
PINOT_BIANCO	245	ROSSO_DI_LECCE	993	SUSUMANIELLO	310	VALENTINO	335
PIZZUTELLO_BIANCO	465	ROSSOLA_NERA	273	SYLVANER_VERDE	311	VECCIUTELLO	616
PIZZUTELLO_NERO	448	ROUSSIN	275	TAGLIAFERRO	601	VEGA	336

PLASSA	249	RUBI_RED	454	TANNAT	312	VELTLINER	337
PLISSONA	803	RUCHE	276	TAZZELENICHE	313	VELTLINER_ROSSO_PRECOCE	1086
POLLERA_NERA	250	S_ANNA_DI_LIPSIA	469	TEMPRANILLO	314	VERANO	618
POLLINO	804	S. TERESA	995	TERBASCI_cp2	602	VERDACCHIO	858
POLOGHELLO	581	SAGRANTINO	281	TEROLDEGO	315	VERDANA_BIANCA	975
PORCINA	582	SAN_PIETRO	827	TERRANO	316	VERDANE	1141
PORCINA_BIANCA	805	SANGIOVESE	119	TIMORASSO	317	VERDEA	338
PORTOGHESE	251	SANGIOVESE_DEL_VERRUCC HIO	592	TINTIGLIA	603	VERDECA	339
NAME	COD E						
VERDELLO_DI_BRACCIANO	859						
VERDESE	341						
VERDICCHIO_BIANCO	342						
VERDISO	344						
VERDUSCHIA	345						
VERDUZZO_FRIULANO	346						
VERDUZZO_TREVIGIANO	347						
VERMENTINO	350						
VERMENTINO_NERO	351						
VERNACCIA_DI_ORISTANO	352						
VERNACCIA_DI_SGIMIGNANO	353						
VERNACCIA_NERA	354						
VESPAIOLA	355						
VESPOLINA	356						
VESPRINO	963						
VICTORIA	458						

VIEN_DE_NUS	357
VIOGNIER	1021
VITOUSKA	358
VUILLERMIN	359
WILDBACHER	360
WURZER	645
ZAPPOLINO	862
ZELEN	1144
ZIBIBBO	470
ZIMAVACCA	1096
ZINGARELLO	622
ZIZAK	964
ZUCCACCIO	864

Supplementary Table 13. Country of origin, skin colour and usage of the 530 accessions used for the genetic characterization.

NAME	ORIGIN	COLOUR	USAGE	NAME	ORIGIN	COLOUR	USAGE	NAME	ORIGIN	COLOUR	USAGE
ABBOTTABOTTI	CI	blanc	wine	BIANCUZZO	IT	blanc	wine	CATARRATTO_BIANCO_COMUNE	IS	blanc	wine
ABBUOTO	CI	noir	w/t	BICANE	WE	blanc	w/t	CATARRATTONE	IS	blanc	table
ABELLO	CI	blanc	wine	BIGOLONA	IT	blanc	wine	CAVECIA	NI	blanc	wine
ABRUSCO	CI	noir	wine	BLANC_DE_MORGEX	NI	blanc	wine	CAVRARA_NERA	NI	noir	wine
AGHEDENE	IT	blanc	wine	BOGGIONE_NERO	IT	noir	w/t	CENERENTE	CI	noir	wine
AGLIANICO	CI	noir	wine	BOGGIONE_ROSSO	IT	noir	wine	CESANESE_DEI_CASTELLI_ROMANI	CI	noir	wine
AGLIANICO_GRANA_GROSSA	SI	noir	wine	BOMBINO_BIANCO	CI	blanc	wine	CHARDONNAY	WE	blanc	wine
AHMEUR_MONARDE	WE	rose/noir	table	BOMBINO_NERO	SI	noir	w/t	CHASSELAS_BLANC	WE	blanc	w/t
ALBANA	CI	blanc	wine	BONAMICO	CI	noir	wine	CHENIN	WE	blanc	wine
ALBANA_BORDINI	CI	noir	wine	BONARDA	CI	noir	wine	CICINESE_GROSSO	CI	noir	wine
ALBANA_DEL_PANIERE	CI	blanc	wine	BONDA	NI	noir	wine	CILIEGIOLO	IT	noir	w/t
ALBANELLO	IS	blanc	wine	BORBOTTONE	IT	blanc	wine	CIMINNITA	WE	blanc	w/t/r

ALBARANZEULI_BIANCO	IS	blanc	wine	BOSCHERA	NI	blanc	wine	CLAIRETTE	WE	blanc	w/t
ALBAROLA	CI	blanc	w/t	BOSCO	NI	blanc	w/t	CLOTILDE_PROSPERI	IT	blanc	table
ALBAROSSA	NI	noir	wine	BOVALE	WE	noir	wine	COCCIATOSTA	IT	blanc	wine
ALEANTE_RIVALTO	CI	noir	wine	BRACCIOLA_NERA	CI	noir	wine	COCOCCIOLA	CI	blanc	w/t
ALEATICO	CI	noir	w/t	BRACHETTO	NI	noir	wine	CODA_DI_VOLPE_BIANCA	SI	blanc	w/t
ALICANTE_BOUSCHET	WE	noir	wine	BRAMBANA	IT	noir	wine	CODELUNGHE	IT	noir	wine
ALIONZA	CI	blanc	w/t	BUBBIA	IT	noir	w/t	COPETA	SI	noir	w/t
ALPHONSE_LAVALLEE	WE	noir	w/t/r	BURGHESANA	IT	noir	wine	CORBINELLA_PADOVANA	NI	noir	wine
AMERICA	AM	noir/blanc	wine	BUSSANELLO	NI	blanc	wine	CORBINONA_13_GT	NI	noir	wine
ANCELOTTA	CI	noir	wine	CABERNET_FRANC	WE	noir	wine	CORINTO_BIANCO	EE	blanc	table
ANSONICA	CI	blanc	w/t	CABERNET_SAUVIGNON	WE	noir	wine	CORINTO_NERO	EE	noir	table
ANTINELLO	SI	blanc	wine	CACCIADIBITI	CI	blanc	wine	CORNACCHIA	CI	noir	wine
APRILLA	IT	noir	wine	CACCIO_DI_FERMO_1	CI	blanc/noir	wine	CORNALLIN	NI	noir	wine
ARGUMANNU	IS	blanc	wine	CADDIU	IS	noir	w/t	CORNAREA	NI	noir	wine
ARNEIS	NI	blanc	wine	CAGNULARI	WE	noir	wine	CORNIOLA	IT	blanc	table
ARSILICO	CI	noir	wine	CALABRESE	SI	noir	wine	CORVINA	NI	noir	wine
ARVESINIADU	IS	blanc	w/t	CALAMARO	IT	noir	wine	CORVINA_ASOLO	NI	noir	wine
AVANA	NI	noir	w/t	CALORIA	CI	noir	wine	CORVINONE	NI	noir	wine
AVARENGO	NI	noir	w/t	CANAIOLO_NERO	CI	noir	wine	COVE	NI	blanc	wine
AXINA_DE_FRANCIA	IS	noir	wine	CANINA_1_1	CI	noir	wine	CREPALLOCCHI	CI	noir	wine
AXINA_DE_TRES_BIAS	IT	noir	wine	CANNAMELE	SI	noir	wine	CROATINA	NI	noir	wine
BARBERA	NI	noir	wine	CANNER_SEEDLESS	AM	blanc	table	CROVASSA	NI	noir	wine
BARBERA_BIANCA	NI	blanc	wine	CAPENA	CI	blanc	wine	CUNEUTE	CI	noir	wine
BARESANA	IT	blanc	table	CAPIBIANCHI	CI	noir/blanc	wine	DALL	UKN	ukn	ukn
BARSAGLINA	CI	noir	wine	CAPOBIANCO_BIANCO	CI	blanc	wine	DAMASCHINO	EE	blanc	wine
BECUET	WE	noir	wine	CAPOBIANCO_NERO	CI	noir	wine	DAMIANO	IT	blanc	wine
BEGUGNOL	UKN	blanc	wine	CAPOLONGO_1	CI	blanc	wine	DATTIER_DE_BEYROUGH	WE	blanc	table
BELLINO	WE	noir	w/t	CAPOLUNGO	CI	blanc	wine	DELIGHT	AM	blanc	table
BELLONE	CI	blanc	wine	CAPRETTA	SI	blanc	wine	DIAMANT	EE	blanc	table
BERTINORA	IT	blanc	wine	CARDINAL	AM	rouge/noir	w/t	DIMIAT	WE	blanc	w/t
BERZAMINO	IT	noir	wine	CARICAGIOLA	IS	noir	wine	DINDARELLA	NI	noir	wine
BIANCHETTA_DI_BACEDASCO	CI	blanc	wine	CARIGNANO	CI	noir	wine	DIOLINOIR	CNE	noir	wine
BIANCHETTA_DI_DIOLO	CI	blanc	wine	CARMENERE	WE	noir	wine	DOLCIAME	IT	blanc	wine
BIANCHETTA_TREVIGIANA	NI	blanc	wine	CARRICANTE	IS	blanc	wine	DON_MARIANO	WE	noir	table
BIANCO_DALESSANO	SI	noir	wine	CASAVECCHIA	SI	noir	wine	DOUX_DHENRY	WE	noir	w/t
BIANCOLELLA	SI	blanc	wine	CASENTINO	CI	noir	wine	DURAPECCIO_DI_SLORENZO	IT	blanc	wine

BIANCONE	CI	blanc	wine	CASSETTA	NI	noir	wine	DURELLA	CI	blanc	wine
BIANCONE_DELLANTELLA	CI	blanc	wine	CATALANESCA_BIANCA	SI	blanc	w/t	EARLY_MUSCAT	AM	blanc	w/t

NAME	ORIGIN	COLOUR	USAGE	NAME	ORIGIN	COLOUR	USAGE
ERBALUCE	NI	blanc	w/t	INC_MALVASIA_X_TREBBIANO_TOSCANO	CI	blanc	wine
FALANGHINA	SI	blanc	wine	INC_MANZONI_2_14	NI	noir	wine
FERTILIA	NI	noir	wine	INCBIANCO_FEDIT_51_C_S_G	CI	blanc	wine
FIANO_ROSA_LOCOROTONDO_2	SI	blanc	wine	INCBRUNI_54	CI	blanc	w/t
FLAVIS	NI	blanc	wine	INCMANZONI_2_15	NI	noir	wine
FOGARINA	CI	noir	wine	INCMATHIASZ_210	EE	blanc	table
FOGLIA_TONDA	CI	noir	wine	INCTERZI_N1	NI	noir	wine
FOGLIONA	IT	blanc	w/t	INVERNENGA	WE	blanc	w/t
FORASTERA	WE	blanc	wine	INVERNESCA	IT	blanc	table
FORCESE_DASCOLI	CI	blanc	wine	INZOLIA_IMPERIALE	WE	noir	table
FORGIARIN	NI	noir	wine	INZOLIA_PARCHITANA	WE	blanc	table
FORSELLINA	NI	noir	wine	ITALIA	IT	blanc	table
FORTANA	CI	noir	wine	ITALICA	NI	blanc	wine
FOSCA	CI	blanc	wine	JULY_MUSCAT	AM	blanc	w/t
FRACIDELLA	CI	blanc	wine	KADARKA	EE	noir	wine
FRANCONIA	WE	noir	wine	KALILI	WE	blanc	table
FRAPPATO	IS	noir	wine	KERNER	CNE	blanc	wine
FREISA	NI	noir	wine	LACRIMA	CI	noir	wine
FUBIANO	NI	blanc	wine	LACRIMA_DI_MARIA	SI	blanc	table
FULIGNO	CI	noir	wine	LAGREIN	NI	noir	wine
FUMIN	NI	noir	wine	LAMBRUSCA_DI_ALESSANDRIA	NI	noir	wine
GABBA_VOLPE	UKN	blanc	wine	LAMBRUSCO_A_FOGLIA_FRAST	CI	noir	wine
GAGLIOPPO	SI	noir	wine	LAMBRUSCO_DI_SORBARA	CI	noir	wine
GALLICO	IT	ukn	wine	LAMBRUSCO_GRASPAROSSA	CI	noir	wine
GAMARET	WE	noir	wine	LAMBRUSCO_MAESTRI	CI	noir	wine
GAMAY	WE	noir	wine	LAMBRUSCO_MARANI	CI	noir	wine
GAROFANA	CI	noir	wine	LAMBRUSCO_MONTERICCO	CI	noir	wine
GATTA	IT	blanc/noir	wine	LAMBRUSCO_OLIVA	CI	noir	wine
GERUSALEMME	IT	blanc	table	LAMBRUSCO_SALAMINO	CI	noir	wine

GIRO	WE	blanc/noir/rouge	wine	LAMBRUSCO_VIADANESE	CI	noir	wine
GIUSTOLISI	IT	blanc	wine	LATTUARIO_NERO	EE	noir	table
GOLDTRAMINER	NI	blanc	wine	LINNEO_NERO	IT	noir	table
GOSEN	NI	noir	wine	LIVORNESE_BIANCA	CI	blanc	wine
GRANOIR	CNE	noir	wine	LUGLIOLA_ROSSA	CI	noir	wine
GRECHETTO_DI_TODI	CI	blanc	wine	LUMASSINA	NI	blanc	wine
GRECO_DI_TUFO	SI	blanc	w/t	MACERATINO	CI	blanc	w/t
GRECO_NERO_1	SI	noir	w/t	MADALONA	IT	noir	wine
GRENACHE_NOIR	WE	noir	wine	MADDALENA_BRUNI	IT	blanc	table
GRIGNOLINO	NI	noir	wine	MAGLIOCCO_CANINO_2	SI	noir	wine
GRILLO	SI	blanc	wine	MAGLIOCCO_DOLCE	SI	noir	wine
GRILLONE	IT	noir	wine	MAIOLICA_2	CI	noir	wine
GROPPELLA	NI	noir	wine	MALBECH	WE	noir	wine
GROPPELLO_DI_MOCASINA	NI	noir	wine	MALBO_GENTILE	CI	noir	wine
GROPPELLO_DI_REVO	NI	noir	wine	MALIGIA_1	UKN	blanc	wine
GROPPELLO_GENTILE	CI	noir	wine	MALVASIA	WE	blanc	wine
GROS_BOUSCHET	WE	noir	wine	MALVASIA_BIANCA_2	SI	blanc	w/t
GROSPARIOL	IT	blanc	wine	MALVASIA_BIANCA_DI_CANDIA	CI	blanc	wine
GUARDAVALLE	SI	blanc	wine	MALVASIA_BIANCA_LUNGA	CI	blanc	wine
HARSLEVELU	EE	blanc	w/t	MALVASIA_DEL_LAZIO	CI	blanc	wine
IMPIGNO	SI	blanc	wine	MALVASIA DELLE LIPARI	SI	blanc	wine

NAME	ORIGIN	COLOUR	USAGE	NAME	ORIGIN	COLOUR	USAGE
MALVASIA_DI_CANDIA_AROMATICA	CI	blanc	w/t	MULLER_THURGAU	CNE	blanc	wine
MALVASIA_DI_CASORZO	NI	noir	wine	NASCETTA	NI	blanc	wine
MALVASIA_DI_SCHIERANO	NI	noir	wine	NASCO	IS	blanc	wine
MALVASIA_FURMHANN	CI	blanc	wine	NEBBIERA	NI	noir	wine
MALVASIA_ISTRIANA	EE	blanc	wine	NEBBIOLO	NI	noir	wine
MALVASIA_NERA_DI_BRINDISI_1	CI	noir	w/t	NEGRETTO	CI	noir	wine
MALVASIA_NERA_LUNGA	NI	noir	wine	NEGRETTO_DI_SALUZZO	NI	noir	w/t
MAMMOLETTA	CI	noir	w/t	NEGRO_AMARO	SI	noir	wine
MAMMOLO	CI	noir	wine	NER_DALA	NI	noir	wine
MANTONICO_BIANCO	SI	blanc	wine	NERELLO_MASCALESE	SI	noir	wine

MANTONICONE	SI	noir	wine	NERETTA_CUNESE	NI	noir	wine
MANZONI_BIANCO	NI	blanc	wine	NERETTO_DI_BAIRO	NI	noir	wine
MANZONI_MOSCATO	NI	noir	wine	NERO_DI_VASCA	CI	noir	wine
MANZONI_ROSA	NI	rouge	wine	NEYRET	NI	noir	wine
MARCHIONE_2	SI	blanc	wine	NIBIO	IT	noir	wine
MARSANNE	WE	blanc	wine	NIEDDERA	IS	noir	wine
MARUGA	CI	noir	wine	NIEDDU_MANNU_1	IS	noir	wine
MARUGGIO_1	UKN	blanc	wine	NIGRA	NI	noir	wine
MARZEMINA_2	NI	noir	wine	NOCCHIANELLO_DI_GAZZARETTO_1	IT	blanc	wine
MARZEMINO	CI	noir	w/t	NOCCHIANELLO_NERO	IT	noir	wine
MATILDE	IT	blanc	table	NOCCHIANELLO_PELOSO	IT	blanc	wine
MATURANO	UKN	blanc	wine	NOCERA	SI	noir	w/t
MAYOLET	NI	rouge	wine	NOCERONE_DI_MILAZZO_1	SI	noir	table
MAZZESE	CI	noir	wine	NOSIOLA	NI	blanc	wine
MELARA_1	CI	blanc	wine	NOTARDOMENICO_2	SI	noir	w/t
MERERA	IT	noir	wine	NURAGUS	IS	blanc	wine
MERLOT	WE	noir	wine	OLIVELLA_NERA_1	CI	noir	wine
MICHELE_PALIERI	IT	noir	table	OLIVELLA_NERA_2	CI	noir	wine
MINNELLA_BIANCA_2	IS	blanc	wine	OLIVETTA_BIANCA	CI	blanc	table
MOLINARA	NI	noir	wine	OLIVETTA_VIBONESE	CI	noir	table
MONICA	WE	noir	wine	ORA	WE	blanc	table
MONTE_MADONNA_1_GT	IT	blanc	wine	ORTRUGO	CI	blanc	wine
MONTEPULCIANO	IT	noir	wine	OSELETA	NI	noir	wine
MONTONICO_BIANCO	SI	blanc	w/t	OSERIE_DU_FARODE	WE	rose	wine
MONTONICO_NERO	IT	noir	wine	OTTAVIANELLO	SI	noir	wine
MONTONICO_PINTO	IT	noir	wine	PALLAGRELLO_BIANCO	SI	blanc	wine
MONTU	CI	ukn	ukn	PALLAGRELLO_NERO	SI	noir	wine
MONUKKA	EE	blanc/noir	t/r	PALOMBA	IT	noir	wine
MORELLINO	CI	noir	wine	PALOMINO	WE	noir/blanc	wine
MOSCATO_BCASALESE	NI	blanc	wine	PAMPANARO_GRANDE	CI	blanc	wine
MOSCATO_BIANCO	IT	blanc	wine	PANFINONE	CI	blanc	wine
MOSCATO_DADDA	IT	noir	table	PANSE_BLANCHE	WE	blanc	table
MOSCATO_DAMBURGO	CNE	noir	w/t	PANSE_PRECOCE	WE	blanc	w/t
MOSCATO_DI_SCANZO	NI	noir	wine	PANSE_ROSA_DIMALAGA	WE	rose	table
MOSCATO_DI_TERRACINA	CI	blanc	w/t	PASCALE	IS	noir	w/t
MOSCATO_GIALLO	IT	blanc	w/t	PASSAU	NI	noir	wine

MOSCATO_NERO	NI	noir	wine	PATTARESCO	IT	noir	wine
MOSCATO_NERO_D'_ACQUI	NI	noir	wine	PAVANA	NI	noir	wine
MOSCATO_ROSA_2	NI	rouge	wine	PECHINO	IT	blanc	wine
MOSCATO_VIOLETTO	NI	noir	wine	PECORELLO	SI	blanc	wine

NAME	ORIGIN	COLOUR	USAGE	NAME	ORIGIN	COLOUR	USAGE
PEDEVENDA	NI	blanc	wine	REFOSCO_NOSTRANO	NI	noir	wine
PEDICELLO_ROSSO	CI	noir	wine	REGINA_DEI_VIGNETI	EE	blanc	table
PEDRO_XIMENES	WE	blanc	wine	RETAGLIADO_BIANCO	IS	blanc	w/t
PELAVERGA	NI	noir	table	RIBOLLA_GIALLA	NI	blanc	w/t
PELAVERGA_PICCOLO	NI	noir	wine	RIESLING	CNE	blanc	wine
PELAVERGA_S_GRATO	NI	noir	wine	RIESLING_ITALICO	IT	blanc	wine
PERERA	NI	blanc	wine	ROIETTO_GRISO	IT	gris	table
PERLA_DI_CSABA	EE	blanc	w/t	RONDINELLA	NI	noir	wine
PERLETTE	AM	blanc	t/r	ROSA_TARDIVA	IT	noir	table
PERLONA	IT	blanc	table	ROSSA_DI_BITONTO	SI	rose	table
PERRICONE	IS	noir	wine	ROSSESE	NI	noir	wine
PETIT_ROUGE	NI	noir	wine	ROSSESE_BIANCO	NI	blanc	wine
PETIT_VERDOT	WE	noir	wine	ROSSIGNOLA	NI	noir	wine
PETITE_ARVINE	CNE	blanc	wine	ROSSO_DI_LECCE	SI	red	wine
PICCOLA_NERA	NI	noir	wine	ROSSOLA_NERA	NI	noir	wine
PICOLIT	NI	blanc	wine	ROUSSIN	CNE	noir	wine
PICULIT_NERI	NI	noir	wine	RUBI_RED	AM	rouge	table
PIEDIROSSO	SI	noir	wine	RUCHE	NI	noir	wine
PIGNOLA	NI	noir	wine	S_ANNA_DI_LIPSIA	IT	blanc	table
PIGNOLO	NI	noir	wine	SAGRANTINO	CI	noir	wine
PINELLA	NI	blanc	wine	SALVATICO	CI	noir	w/t
PINOT_BIANCO	WE	blanc	wine	SAN_PIETRO	WE	blanc	wine
PIZZUTELLO_BIANCO	IT	blanc	table	SANGIOVESE	NI	noir	wine
PIZZUTELLO_NERO	WE	noir	table	SANGIOVESE_DEL_VERRUCCHIO	IT	noir	wine
PLASSA	NI	noir	wine	SANTA_MARIA	CI	blanc	wine
PLISSONA	IT	noir	wine	SAUVIGNON	WE	blanc	wine
POLLERA_NERA	CI	noir	wine	SAUVIGNON_GROS	WE	gris	wine

POLLINO	IT	blanc	wine	SCACCIADEBITI	CI	blanc	wine
POLOGHELLO	CI	blanc	wine	SCACCO	IT	blanc	wine
PORCINA_BIANCA	IT	blanc	wine	SCHIAVA	NI	noir	wine
PORTOGHESE	CNE	ukn	wine	SCHIAVA_GENTILE	CI	noir	wine
PRECOCISSIMA_MALIANI	IT	noir	wine	SCHIAVA_GRIGIA	NI	noir	wine
PRIE_ROUGE	NI	rouge	wine	SCHIAVA_GROSSA	NI	noir	w/t
PRIMITIVO	CI	noir	wine	SCHIOPPETTINO	NI	noir	wine
PRODEST	NI	noir	wine	SCIAGLIN	NI	blanc	wine
PROSECCO	NI	blanc	wine	SCIASCINOSO	CI	noir	wine
PROSECCO_LUNGO	NI	blanc	wine	SCIMISCIATA_1	NI	blanc	wine
PRUNESTA	SI	noir	w/t	SELEZIONE_BRUNI_54	NI	blanc	wine
PRUNESTA_BIANCA	SI	blanc	w/t	SEMIDANO	IS	blanc	wine
PRUNESTA_ROSSO_VIOLACEA	SI	noir	table	SEMILLON	WE	blanc	wine
QUAGLIANO	NI	noir	table	SENNEN	NI	noir	wine
QUEEN	AM	noir	table	SGAVETTA	CI	noir	wine
RABOSO_PIAVE	NI	noir	wine	SGIUSEPPE_NERO	IT	noir	wine
RABOSO_VERONESE	CI	noir	wine	SILA	SI	blanc	wine
RAGUSANO	SI	blanc	wine	SIRIO	NI	blanc	wine
REBO	CI	noir	wine	SLORENZO	IT	noir	wine
RECANTINA	NI	noir	wine	SLUNARDO	SI	blanc	wine
RED_GLOBE_1	AM	rouge	table	SMARTINO	IT	noir	wine
RED_OHANEZ	AM	red	table	SMICHELE	IT	noir	wine
REFOSCO_DAL_PEDROSSO	IT	noir	wine	SOMARELLO_ROSSO	SI	blanc	wine

NAME	ORIGIN	COLOUR	USAGE	NAME	ORIGIN	COLOUR	USAGE
SOPERGA	NI	noir	wine	VELTLINER	CNE	blanc	wine
SPAGNA_BIANCA	WE	blanc	wine	VERANO	CI	red	wine
STERESA	IT	blanc	w/t	VERDACCHIO	IT	blanc	wine
SULTANA	EE	blanc	table	VERDANA_BIANCA	IT	blanc	wine
SULTANINA_BIANCA	EE	blanc	w/t/r	VERDEA	CI	blanc	w/t
SURBANO	UKN	ukn	ukn	VERDECA	SI	blanc	wine
SUSUMANIELLO	SI	noir	wine	VERDELLO_DI_BRACCIANO	CI	blanc	wine
SYLVANER_VERDE	CNE	blanc	wine	VERDICCHIO_BIANCO	IT	blanc	wine

TAGLIAFERRO	CI	noir	wine	VERDISO	NI	blanc	w/t
TANNAT	WE	noir	wine	VERDUSCHIA	CI	blanc	wine
TAZZELENICHE	NI	noir	wine	VERDUZZO_FRIULANO	NI	blanc	wine
TEMPRANILLO	WE	noir	wine	VERDUZZO_TREVIGIANO	NI	blanc	wine
TERBASI_cp2	EE	noir	wine	VERMENTINO	CI	blanc	wine
TEROLDEGO	NI	noir	wine	VERMENTINO_NERO	CI	noir	wine
TERRANO	CI	noir	wine	VERNACCIA_DI_ORISTANO	IS	blanc	wine
TIMORASSO	NI	blanc	wine	VERNACCIA_DI_SGIMIGNANO	CI	blanc	wine
TINTILIA	SI	noir	wine	VERNACCIA_NERA	CI	noir	wine
TINTORIA_2	WE	noir	wine	VESPAIOLA	NI	blanc	wine
TOCAI_FRIULANO	NI	blanc	wine	VESPOLINA	NI	noir	wine
TORBATO	WE	blanc	wine	VERPRINO	IT	blanc	wine
TRAMINER_AROMATICO	NI	rouge	wine	VICTORIA	EE	blanc	table
TREBBIANO_ABRUZZESE_1	CI	blanc	wine	VIEN_DE_NUS	WE	noir	wine
TREBBIANO_ABRUZZESE_2	CI	blanc	wine	VITOUSKA	EE	blanc	wine
TREBBIANO_GIALLO	CI	blanc	wine	VUILLERMIN	CNE	noir	wine
TREBBIANO_MODENESE	CI	blanc	wine	WILDBACHER	CNE	noir	wine
TREBBIANO_SPOLETINO	CI	blanc	wine	ZAPPOLINO	IT	noir	wine
TREBBIANO_TOSCANO	IT	blanc	wine	ZELEN	EE	blanc	wine
TREVISANA_NERA	NI	noir	w/t	ZIBIBBO	SI	blanc	w/t
TROISCINA	IT	ukn	wine	ZIMAVACCA	CI	blanc	table
TUCCANESE	SI	noir	wine	ZINGARELLO	CI	noir	wine
TURCA	NI	noir	wine				
UCELUT	NI	blanc	wine				
ULIVELLO	CI	noir	wine				
UVA_ACETO	IT	blanc	wine				
UVA_CARNE	IT	noir/rouge	wine				
UVA_CARRIERI	IT	blanc	wine				
UVA_DEI_VECCHI	CI	blanc	wine				
UVA_DI_COLOGNE	WE	blanc	wine				
UVA_DI_CRIMEA	IT	noir	wine				
UVA_DI_TROIA	SI	noir	wine				
UVA_GATTA	IT	noir	wine				
UVA_LONGANESI	CI	noir	wine				
UVA_MELONA	IS	rouge	table				
UVA_PRUGNA	IT	blanc/noir	table				

UVA_RARA	NI	noir	wine
UVA_REALE	CI	blanc	wine
UVA_TOSCA	CI	noir	wine
UVALINO	NI	noir	wine
VALENTINO	NI	noir	wine
VECCIUTELLO	CI	noir	wine

Supplementary Table 14. Description of the 132 cultivars included in the GWAS diversity panel.

NAME	Genotyped by	Country	Color	Usage	STR-3	STR-6
AHMEUR_MONARDE	CCC	WE	rose/noir	table	A-STR	a
ALBANA	CCC	CI	blanc	wine	ADMIXED	g
ALBARANZEULI_BIANCO	Laucou	IS	blanc	wine	A-STR	a
ALEANTE_RIVALTO	CCC	CI	noir	wine	A-STR	g
ALEATICO	Laucou	CI	noir	w/t	A-STR	g
ALICANTE_BOUSCHET	Laucou	WE	noir	wine	A-STR	g
ALPHONSE_LAVALLEE	Laucou	WE	noir	w/t/r	ADMIXED	b
ANCELOTTA	Laucou	CI	noir	wine	B-STR	d
ANSONICA	Laucou	CI	blanc	w/t	A-STR	g
BELLONE	Laucou	CI	blanc	wine	A-STR	f
AXINA_DE_TRES_BIAS	CCC	IT	noir	wine	A-STR	g
BARBERA_BIANCA	CCC	NI	blanc	wine	A-STR	g
BARESANA	Laucou	IT	noir/rose	table	A-STR	a
CREPALLOCCHI	CCC	CI	noir	wine	B-STR	d
BIANCO_DALESSANO	Laucou	SI	noir	wine	A-STR	g
BOMBINO_BIANCO	Laucou	CI	blanc	wine	A-STR	f
BICANE	Laucou	WE	blanc	w/t	ADMIXED	g
BONAMICO	Laucou	CI	noir	wine	ADMIXED	g
BRACHETTO	Laucou	NI	noir	wine	ADMIXED	g
CABERNET_FRANC	Laucou	WE	noir	wine	ADMIXED	g
CAGNULARI	CCC	WE	noir	wine	ADMIXED	g
CALABRESE	Laucou	SI	noir	wine	ADMIXED	g
CANNER_SEEDLESS	CCC	AM	blanc	table	A-STR	a
CARDINAL	Laucou	AM	rouge/noir	w/t	ADMIXED	b
CARIGNANO	Laucou	CI	noir	wine	A-STR	g
FORTANA	CCC	CI	noir	wine	ADMIXED	d
CATALANESCA_BIANCA	Laucou	SI	blanc	w/t	A-STR	a
INC_MALVASIA_X_TREBBIANO_TOSCANO	CCC	CI	ukn	wine	A-STR	f
LAMBRUSCO_A_FOGLIA_FRAST	CCC	CI	noir	wine	B-STR	d
CHARDONNAY	Laucou	WE	blanc	wine	ADMIXED	g
CHASSELAS_BLANC	Laucou	WE	blanc	w/t	B-STR	g
CILIEGIOLO	Laucou	IT	noir	w/t	ADMIXED	g
CLAIRETTE	Laucou	WE	blanc	w/t	ADMIXED	g

COCOCCIOLA	Laucou	CI	blanc	w/t	A-STR	g
LAMBRUSCO_DI_SORBARA	Laucou	CI	noir	wine	B-STR	d
CORINTO_NERO	CCC	EE	noir	table	A-STR	g
LAMBRUSCO_MAESTRI	Laucou	CI	noir	wine	B-STR	d
LAMBRUSCO_MARANI	Laucou	CI	noir	wine	B-STR	d
CORNIOLA	Laucou	IT	blanc/noir	table	A-STR	a
LAMBRUSCO_SALAMINO	Laucou	CI	noir	wine	B-STR	d
CROATINA	Laucou	NI	noir	wine	ADMIXED	g
CROVASSA	CCC	NI	noir	wine	ADMIXED	g
DATTIER_DE_BEYROUTH	Laucou	WE	blanc	table	A-STR	a
DIMIAT	Laucou	WE	blanc	w/t	A-STR	g
DON_MARIANO	Laucou	WE	noir	table	A-STR	a
EARLY_MUSCAT	CCC	AM	blanc	w/t	ADMIXED	b
FALANGHINA	Laucou	SI	blanc	wine	ADMIXED	g
FLAVIS	CCC	NI	blanc	wine	B-STR	g
FORASTERA	Laucou	WE	blanc	wine	ADMIXED	g
GAMARET	Laucou	WE	noir	wine	B-STR	g
GAMAY	Laucou	WE	noir	wine	ADMIXED	g
GIUSTOLISI	Laucou	IT	blanc	wine	A-STR	g
GRECO_DI_TUFO	Laucou	SI	blanc	w/t	ADMIXED	g
GRILLO	Laucou	SI	blanc	wine	A-STR	g
GROSPARIOL	CCC	IT	blanc	wine	B-STR	d
HARSLEVELU	Laucou	EE	blanc	w/t	A-STR	g
IMPIGNO	Laucou	SI	blanc	wine	A-STR	g
INZOLIA_IMPERIALE	CCC	WE	noir	table	A-STR	a
ITALIA	Laucou	IT	blanc	table	ADMIXED	g
JULY_MUSCAT	Laucou	AM	blanc	w/t	ADMIXED	b
KADARKA	Laucou	EE	blanc/noir/gris/rose	wine	A-STR	g
KALILI	CCC	WE	ukn	table	A-STR	g
KERNER	Laucou	CNE	blanc	wine	B-STR	g
LAGREIN	Laucou	NI	noir	wine	B-STR	g
LAMBRUSCA_DI_ALESSANDRIA	CCC	NI	noir	wine	ADMIXED	g
ARNEIS	Laucou	NI	blanc	wine	B-STR	d
AVARENGO	Laucou	NI	noir	w/t	B-STR	d
CASSETTA	Laucou	NI	noir	wine	B-STR	d
LAMBRUSCO_VIADANESE	CCC	CI	noir	wine	ADMIXED	g

LUMASSINA	Laucou	NI	blanc	wine	ADMIXED	g
MALBO_GENTILE	CCC	CI	noir	wine	ADMIXED	g
MALIGIA_1	CCC	UKN	blanc	wine	ADMIXED	g
MALVASIA_FURMHANN	CCC	CI	blanc	wine	ADMIXED	c
MALVASIA_ISTRIANA	Laucou	EE	blanc	wine	ADMIXED	c
MAMMOLETTA	CCC	CI	noir	w/t	ADMIXED	g
CATARRATTO_BIANCO_COMUNE	Laucou	IS	blanc	wine	ADMIXED	f
PERRICONE	Laucou	IS	noir	wine	A-STR	f
MATILDE	Laucou	IT	blanc	table	ADMIXED	b
MONTONICO_NERO	CCC	IT	noir	wine	ADMIXED	g
MONUKKA	Laucou	EE	blanc/noir	t/r	A-STR	a
MOSCATO_DI_TERRACINA	Laucou	CI	blanc	w/t	A-STR	g
MOSCATO_GIALLO	Laucou	IT	blanc	w/t	A-STR	g
MULLER_THURGAU	Laucou	CNE	blanc	wine	B-STR	g
FORSELLINA	CCC	NI	noir	wine	B-STR	d
MONTEPULCIANO	Laucou	IT	noir	wine	A-STR	f
FREISA	Laucou	NI	noir	wine	B-STR	d
NIBIO	Laucou	IT	noir	wine	ADMIXED	g
NIEDDERA	Laucou	IS	noir	wine	ADMIXED	g
OLIVETTA_BIANCA	Laucou	CI	blanc	table	A-STR	a
OLIVETTA_VIBONESE	CCC	CI	noir	table	ADMIXED	a
ORA	Laucou	WE	blanc	table	A-STR	g
FUMIN	Laucou	NI	noir	wine	B-STR	d
PANSE_PRECOCE	Laucou	WE	blanc	w/t	A-STR	g
GRIGNOLINO	Laucou	NI	noir	wine	B-STR	d
PEDRO_XIMENES	Laucou	WE	blanc	wine	A-STR	a
PERLA_DI_CSABA	Laucou	EE	blanc	w/t	ADMIXED	g
PETIT_VERDOT	Laucou	WE	noir	wine	B-STR	g
PIEDIROSSO	Laucou	SI	noir	wine	ADMIXED	g
PRIMITIVO	Laucou	CI	noir	wine	ADMIXED	g
PICOLIT	Laucou	NI	blanc	wine	B-STR	d
RED_GLOBE_1	Laucou	AM	rouge	table	A-STR	a
RED_OHANEZ	Laucou	AM	red	table	A-STR	a
RIESLING	Laucou	CNE	blanc	wine	B-STR	g
RIESLING_ITALICO	Laucou	IT	blanc	wine	B-STR	g
ROSSIGNOLA	Laucou	NI	noir	wine	ADMIXED	g

PIGNOLO	CCC	NI	noir	wine	B-STR	d
SAGRANTINO	Laucou	CI	noir	wine	ADMIXED	g
CODA_DI_VOLPE_BIANCA	Laucou	SI	blanc	w/t	ADMIXED	f
SCHIAVA_GRIGIA	CCC	NI	noir	wine	ADMIXED	g
RABOSO_PIAVE	Laucou	NI	noir	wine	B-STR	d
SCIMISCIA_1	CCC	NI	blanc	wine	B-STR	g
SELEZIONE_BRUNI_54	CCC	NI	blanc	wine	A-STR	g
SEMIDANO	Laucou	IS	blanc	wine	A-STR	g
MERLOT	Laucou	WE	noir	wine	B-STR	e
SULTANA	Laucou	EE	blanc	table	A-STR	a
TEMPRANILLO	Laucou	WE	noir	wine	A-STR	g
TERBASCI_cp2	CCC	EE	noir	wine	A-STR	a
TORBATO	CCC	WE	blanc	wine	A-STR	a
SEMILLON	Laucou	WE	blanc	wine	B-STR	e
TREBBIANO_SPOLETINO	Laucou	CI	blanc	wine	ADMIXED	g
CHENIN	Laucou	WE	blanc	wine	B-STR	e
UVA_DI_TROIA	Laucou	SI	noir	wine	A-STR	g
RAGUSANO	CCC	SI	blanc	wine	A-STR	f
VELTLINER	CCC	CNE	blanc	wine	ADMIXED	g
TINTILIA	CCC	SI	noir	wine	ADMIXED	f
VERDEA	Laucou	CI	blanc	w/t	ADMIXED	g
VERDISO	Laucou	NI	blanc	w/t	B-STR	d
VERDUZZO_FRIULANO	Laucou	NI	blanc	wine	B-STR	g
VERMENTINO_NERO	Laucou	CI	noir	wine	ADMIXED	g
VERNACCIA_DI_SGIMIGNANO	Laucou	CI	blanc	wine	ADMIXED	g
VICTORIA	Laucou	EE	blanc	table	A-STR	g
ZAPPOLINO	CCC	IT	noir	wine	ADMIXED	g

Supplementary Table 15. Concentration and quality ratio as estimated with the Nanodrop of the 37 additional samples of the CCC used to reach the 132 for the diversity panel.

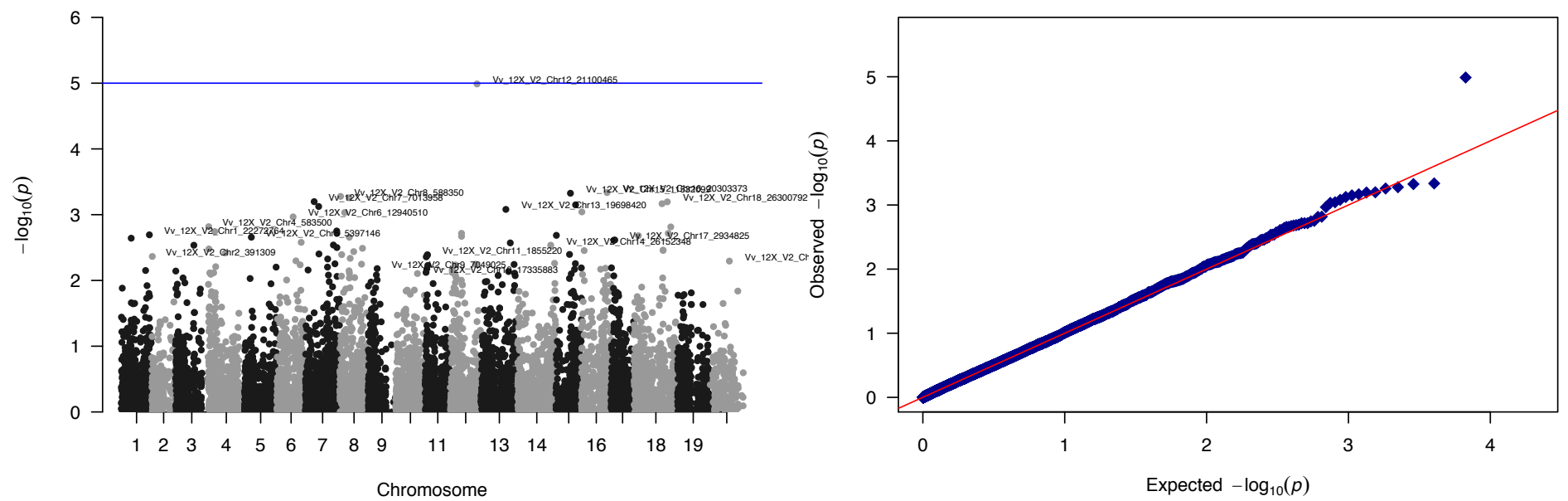
NAME	Concentration (ng/ul)	A260/A280	A260/A230
ALBANA	36.42	1.813	1.472
BARBERA_BIANCA	18.69	1.827	1.296
CAGNULARI	12.62	1.742	0.869
CROVASSA	17.40	1.862	1.857
FLAVIS	26.10	1.749	1.175
FORSELLINA	34.12	1.808	1.770
FORTANA	7.30	1.537	0.342
LAMBRUSCA_DI_ALESSANDRIA	8.74	1.710	0.736
LAMBRUSCO_A_FOGLIA_FRAST	16.60	1.726	1.219
LAMBRUSCO_VIADANESE	18.67	1.804	1.530
MALBO_GENTILE	10.91	1.761	0.991
TINTILIA	32.32	1.792	1.450
PIGNOLO	25.51	1.789	1.179
SCHIAVA_GRIGIA	27.59	1.695	0.758
SCIMISCIA_1	16.83	1.666	1.075
TORBATO	21.46	1.657	0.689
VELTLINER	18.54	1.773	1.188
INZOLIA_IMPERIALE	28.85	1.777	1.460
EARLY_MUSCAT	9.49	1.615	0.522
CANNER_SEEDLESS	26.32	1.743	1.137
KALILI	54.39	NA	NA
CORINTO_NERO	39.41	NA	NA
INC_MALVASIA_X_TREBBIANO_TOSCANO	8.14	1.763	0.876
MALIGIA_1	33.03	1.803	1.623
MALVASIA_FURMHANN	16.55	1.797	1.101
SELEZIONE_BRUNI_54	12.84	1.674	0.706
TERBASCI_cp2	11.54	1.602	0.532
AXINA_DE_TRES_BIAS	26.89	1.777	1.084
ALEANTE_RIVALTO	13.19	1.600	0.642
CREPALLOCCHI	24.79	1.782	1.299
GROSPARIOL	15.14	1.810	1.420
ZAPPOLINO	13.90	1.669	0.711
RAGUSANO	8.56	1.492	0.349
MONTONICO_NERO	17.07	1.709	0.896
OLIVETTA_VIBONESE	16.30	1.774	0.984
AHMEUR_MONARDE	7.00	1.577	0.453
MAMMOLETTA	10.20	1.726	1.005

Supplementary Table 16. Decay of linkage disequilibrium at 0.2 estimated with the 10K SNPs on the diversity panel and corrected by kinship using the package LDcorSV (Mangin et al., 2012).

Chromosome	bp
1	85845
2	124009
3	73080
4	122093
5	82377
6	85783
7	63387
8	84859
9	53133
10	45839
11	68616
12	53121
13	62514
14	81352
15	63304
16	37407
17	104773
18	107425
19	77366
Mean	77699

Supplementary Table 17. Results of GWAS run on each year independently. No significant results were found with QTCAT software. In red are highlighted SNPs that are common between either two approaches or two traits within the same approach. * FDR < 0.05; ** FDR < 0.01 as obtained from the approach under which the association was found.

	Emmax	Gapit
FB 2008	<i>Chr5_2541834 *</i>	<i>Chr5_2541834 **</i>
	<i>Chr5_4058168 *</i>	<i>Chr5_4058168 *</i>
	<i>Chr5_4194452 *</i>	<i>Chr5_4194452 **</i>
2011	<i>Chr5_1134974 *</i>	
	<i>Chr5_2541834 **</i>	
2012	<i>Chr7_10408692 **</i>	
	<i>Chr15_9638997 **</i>	
	<i>Chr15_10198185 **</i>	
2013	<i>Chr16_2792486 *</i>	
VB 2010		<i>Chr15_15612783 *</i>
2013		<i>Chr18_29062596 **</i>
F-V 2013		<i>Chr12_7294026 *</i>
		<i>Chr12_4097019 *</i>
		<i>Chr17_2824109 *</i>
		<i>Chr17_2677298 *</i>
		<i>Chr18_29062596 **</i>



Supplementary Figure 3. On the left, manhattan plot showing the results of the GWAS association test using flowering-veraison interval (F-V) as phenotype. Most significantly associated SNP reside on chromosome 12, Vv_12X_V2_Ch12_21100465. The threshold is set at $p\text{-value} = 0.00001$. On the right, QQ plot of expected versus observed p -values. In this case GWAS was performed with EMMAX.

Acknowledgements

We are very grateful to our partners in CREA-VIT of Conegliano, in particular to Dr. Manna Crespan, Dr. Massimo Gardiman, Dr. Mirella Giust, Dr. Diego Tomasi and Dr. Riccardo Velasco, for providing data, materials and assistance.

Acknowledgments goes to Prof. Silvio Salvi for providing code to produce circo plots.

Thanks to the people that helped me in the lab: Bitu, Riccardo, Luca, Matteo.

Thanks to Prof. Diana Bellin for the opportunity to conduct a research project under her supervision.

Thanks to Dr. Sara Zenoni and Prof. Giampa Tornielli.

Thanks to the awesome #rstats community from Twitter and the StackOverflow users for providing assistance for any kind of *R*/statistics/computer science related problem.